NUMERICAL SOLUTIONS TO PROBLEMS OF NONLINEAR FLOW THROUGH POROUS MATERIALS

by

RAYMOND EDWARD VOLKER

Thesis presented in fulfilment of the requirements for the Degree of

Doctor of Philosophy

in the University of Queensland

Department of Engineering,
University College of Townsville.

March, 1969

SYNOPSIS

Two commonly suggested forms of the equation linking head loss and velocity for flow of water through coarse granular media are the Forchheimer and exponential relations. These have been combined with the continuity expression to give the differential equations applicable, within the limits of validity of the parent relations, to actual regions of flow. The resultant nonlinear elliptic partial differential equations have been solved by numerical methods including the direct finite difference and finite element methods.

Experimental results and associated analytical work were carried out to determine the accuracy of the nonlinear relations as compared to the linear Darcy Law, when applied over an extended Reynolds number range. Solutions have been obtained for some examples of unconfined flow with boundary conditions similar to those likely to be encountered in practical applications. The experimental work in a circular tank and an open flume has shown that good agreement between observed and calculated values of discharge and piezometric head can be obtained when the coefficients in the nonlinear head loss equations are accurately known. The results indicate that while the flow patterns from the Darcy and the nonlinear solutions

are only significantly different for a high degree of curvature of the phreatic line, a nonlinear solution will usually be necessary for accurate predictions of discharge.

CONTENTS

LIST OF FIGURES

LIST OF TABLES

NOTATION

Symbol	Meaning
a, b	= coefficients in the Forchheimer head loss relation.
a_I, b_I, c_I	= constants associated with node I in the representation of the piezometric head function within the element IJM.
c	= coefficient in the exponential head loss relation.
d	= average particle diameter (Chapter 2).
d	= grid length in finite difference formulation (Chapter 4).
f	= friction factor.
$f(\|i\|)$	= a function of the magnitude of the hydraulic gradient $\|i\|$ (Chapter 2).
$f(h_s)$	= a function of the total head gradient (Chapter 4).
$f(r,h)$	= a function used in the approximate Runge-Kutta numerical solution for unconfined Forchheimer flow (Chapter 6).
g	= acceleration due to gravity.
h	= piezometric head = $\frac{p}{\gamma}+y$.
$h_s = \frac{\partial h}{\partial s}$; $h_x = \frac{\partial h}{\partial x}$; $h_y = \frac{\partial h}{\partial y}$	
$h_{xx} = \frac{\partial^2 h}{\partial x^2}$; $h_{yy} = \frac{\partial^2 h}{\partial y^2}$; $h_{xy} = \frac{\partial^2 h}{\partial x \partial y}$	
h_w	= height of water level (in ft.) in the well above impermeable base.
h_e	= height of water level in ft. at the radius of influence of a well.
h_d	= depth of water in ft. on the downstream side of a permeable wall.
h_u	= depth of water in ft. on the upstream side of a permeable wall.
$h_o, h_1, \ldots$ etc	= piezometric head values at points o, 1, ... etc of the finite difference grid.

Symbol	Meaning
h_{ox}, h_{oxx}	$= \frac{\partial h}{\partial x}$ and $\frac{\partial^2 h}{\partial x^2}$ respectively at point o of the finite difference grid.
hs	= height to top of seepage face above impermeable base at a well or at the downstream face of a permeable wall.
h^e	= the piezometric head function associated with a particular element in the finite element field.
h_I	= the value of piezometric head at node I of the finite element field.
i	= negative total head gradient or hydraulic gradient.
$\underline{i}$, $\underline{j}$	= unit vectors in the x and y directions respectively.
k	= coefficient of permeability (ft/sec).
k_s	= specific permeability (ft^2).
ln	= natural logarithm.
m	= coefficient in the exponential head loss relation.
n	= direction of the normal to the free surface at any point (Chapter 4).
n	= total number of permeameter results employed in curve fitting analysis.
p	= pressure at any point in a fluid.
r	= radial cylindrical co-ordinate direction.
r_w	= radius of well in ft.
r_e	= radius of influence of well in ft.
s	= distance measured in direction of the velocity of flow at any point.
$\underline{s}$	= a unit vector in the s direction.
t	= time.
u,v,w	= velocity components in the x, y and z directions respectively.
x,y,z	= co-ordinate directions.

Symbol	Meaning
A	= a factor associated with each element in the formation of the [S] matrix for nonlinear finite element solutions.
B	= thickness of permeable stratum of a confined aquifer.
B_i	= body force in the i direction.
C	= a dimensionless constant (Chapter 2).
C_1	= a constant depending on the properties of the fluid and medium (Chapter 2).
C_1	= a constant used in developing the finite element theory (Chapter 4).
C_D	= coefficient of drag.
DH	= finite difference solution for piezometric head at a point for Darcy flow.
DHC	= piezometric head at a point for confined Darcy flow.
E	= an integral function of h to be minimised over the area of flow in the finite element analysis.
E^e	= the integral function of h associated with one particular element.
EH	= initial value of piezometric head at a point for exponential finite difference solutions.
EHC	= piezometric head at a point for confined exponential flow.
F_p	= resistance of a particle.
F(|V|)	= a function of the velocity magnitude.
FACT	= a term used in the finite difference derivation for Forchheimer flow $\left[\frac{f}{h_{os}} \frac{b}{2} \left(\frac{a^2}{4} + bh_s\right)^{-\frac{1}{2}}\right]$
FH	= initial value of piezometric head at a point for Forchheimer finite difference solutions.
FHC	= piezometric head at a point for confined Forchheimer flow.

Symbol	Meaning
G	= a function of h and its derivatives which is integrated over the area of flow to form the integral E in the finite element formulation.
G_1	= shortened grid length ratio for horizontal grid lines.
G_2	= shortened grid length ratio for vertical grid lines.
H	= total fluid head at a point.
I,J,M	= nodes of the triangular element IJM.
$K_1, K_2, \ldots K_5$	= functions in the approximate Runge-Kutta numerical solution for unconfined Forchheimer flow.
L	= length dimension (Chapter 2).
L'	= distance between grains of medium (Chapter 2).
L	= a function of h (Chapter 4).
M	= $\frac{1-m}{m}$.
O_k	= observed hydraulic gradient in curve fitting analysis for flow No. k.
P	= porosity (Chapter 2).
Q	= discharge.
QE	= discharge for exponential flow in a confined aquifer with the same drawdown as the unconfined flow.
QF	= discharge for Forchheimer flow in a confined aquifer with the same drawdown as the unconfined flow.
Q(CALC)	= discharge from finite difference solution.
Q(EXP)	= experimental discharge value.
RN	= Reynolds number ($= \frac{Vd\rho}{\mu}$).
S	= specific surface = surface area per unit volume (Chapter 2).
S	= storage coefficient of an aquifer (Chapter 3).
[S]	= the S matrix in the finite element analysis (Chapter 4).

Symbol	Meaning
S	= function to be minimised in curve fitting analysis (Chapter 6).
SE	= standard error of estimate of curves fitted to permeameter results.
T	= transmissivity coefficient of an aquifer (Chapter 3).
T_k	= theoretical hydraulic gradient in curve fitting analysis for flow No. k.
V	= superficial velocity.
$\underline{V}$	= vector velocity.
$\|V\|$	= magnitude of the vector $\underline{V}$.
V_k	= velocity for k^{th} flow in curve fitting analysis (Chapter 6).
W	= over relaxation factor in numerical analysis.
α, β	= experimental constants (Chapter 2).
α_1	= area shape factor (Chapter 2).
$\alpha, \beta, \delta, \lambda$	= coefficients in the equation for the natural boundary condition in the variational formulation of a problem.
γ	= specific weight of a fluid.
η	= an auxiliary independent variable in the differential equation of flow (Chapter 2).
θ	= angle of the velocity direction to the x axis.
μ	= dynamic viscosity coefficient of a fluid.
ξ	= an auxiliary independent variable in the differential equation of flow (Chapter 2).
ρ	= density of fluid.
ψ	= a streamline function for linear laminar flow.
ϕ	= a potential function for linear laminar flow (Chapter 4).
$\phi(V)$	= a function of velocity (Chapter 2).
Δ	= the area of a triangular element.

CHAPTER 1

INTRODUCTION

1.1 Background to the Problem

The traditional approach to problems of seepage in saturated porous media has been based on the assumption of Darcy's linear relation between head loss and velocity (Darcy, 1856):

$$V = - k \frac{\partial H}{\partial s}$$

or $$V = ki \qquad \ldots\ldots 1.1\text{-}1$$

in which V is the superficial or average seepage velocity; k is the coefficient of permeability of the medium in the direction s; H is the total fluid head; s is the distance measured in the direction of the resultant velocity at the point under consideration; i is the negative total head gradient $- \frac{\partial H}{\partial s}$, and is sometimes called the hydraulic gradient.

Equation 1.1-1 satisfactorily describes the flow conditions provided velocities are small. It is usually considered that Darcy's Law is applicable for so-called "creeping flows". For many flow conditions met in practice, the grain size of the medium is small enough or the velocity of the fluid low enough, for Darcy's Law to give satisfactory results.

However, since the last century (Slichter, 1897), it has been realized that Darcy's Law fails to hold for high velocities of flow. This realization of the limited validity of Darcy's Law led to the suggestion of relations that would be accurate over all flow ranges encountered.

Forchheimer (1901) introduced the nonlinear equation:

$$i = aV + bV^2 \qquad \text{.... 1.1-2}$$

in which a and b are constants determined by the properties of the fluid and medium. Although Forchheimer later added a third order term cV^3 to make the equation fit experimental results more accurately, his original expression (1.1-2), has become known as the Forchheimer relation and herein will be referred to as such.

Missbach (1937) postulated an equation of the general form:

$$i = cV^m \qquad \text{.... 1.1-3}$$

in which c is a constant determined by the properties of the fluid and medium; m is an exponent lying between 1 and 2. This expression is exponential in form and will be referred to as the exponential relation. White (1935) had previously shown that his experimental results satisfied an equation of this type and other investigators have since used the equation specifying different values

of c and m to fit their experimental results.

While many of the practical problems of flow through porous materials can be accurately solved on the assumption of Darcy's Law, there have arisen various situations where a more accurate relation between head loss and velocity must be employed to obtain realistic solutions. Such situations include flow in the area adjacent to a pumping well in a coarse grained aquifer and flow through rockfill dams and banks.

1.2 Regions of Interest

Flow through porous media is of fundamental importance to a wide range of disciplines including civil engineering, hydrology, chemical engineering, nuclear physics and textile technology. The flow conditions actually considered in this thesis are allied to civil engineering but the methods outlined should be applicable to most nonlinear flows through porous materials.

One of the most important problems facing a community today is the provision of adequate water supplies. At the present time, much of the water used by man is derived from surface storage reservoirs, although actually less than 3 percent of the fluid fresh water available at any given moment on this planet occurs in streams and lakes (Johnson, 1966). The remainder is

underground and although not all of it is recoverable from the water bearing formations in which it is found, subsurface water is destined to play an ever increasing role in satisfying man's demand for this important quantity.

In addition to providing a source of water, permeable underground formations may be used more widely as storage reservoirs. Such formations have the advantage that evaporation losses are negligible and this is of extreme importance in hot arid climates where the effective capacity of surface storage reservoirs is significantly reduced by evaporation. Of course, underground water has provided water supplies in some areas for hundreds of years while aquifer systems are at present used as effective storage systems, but this development is likely to become more important as man uses up his available supply of surface run-off.

For seepage through fine grained sediments the analytical methods based on Darcy's Law are sufficiently accurate for practical purposes. However, in coarse-grained sand or gravel formations, the high velocities which occur in the region adjacent to a pumping well may necessitate the use of a nonlinear head loss relation in an analysis. It is also feasible that gravel beds

may become important in recharge and discharge areas in finer grained sand formations and the availability of an analytical approach incorporating nonlinear equations would then be essential. Filter beds of coarse material have widespread applications and, as they are subjected to nonlinear flows, a better understanding of the flow patterns involved would help in formulating improved design practices.

Improved economics of surface storage reservoirs have been possible by utilising porous rockfill in constructions associated with the formation of the impounding wall. Earth and rockfill dams have been widely used throughout the world. In recent years rockfill dams with inbuilt spillways have been utilised. Wilkins (1956) proposed such a dam where the overflow passes through the rockfill itself so that the need for a costly spillway structure is obviated. Subsequently, Parkin (1963a, 1963b) carried out a detailed experimental investigation of such dams and formulated methods for discharge and stability calculations.

Experience in practice, however, indicates that the functioning of the inbuilt spillway is inhibited due to debris accumulation and to siltation. This reduces the amount of discharge which can be passed through the

rockfill and even with clean rockfill the discharge is considerably smaller than that which could flow unimpeded over an open spillway.

An important development in dam construction methods has taken place in recent decades with the introduction of the technique of passing flood flows over partly completed earth and rockfill dams. Weiss (1951) described actual applications of the technique in the construction of a number of dams in Mexico. The dams considered were conventional rockfill dams, earthfill dams and mixed earth and rockfill dams. Weiss outlined the problems encountered but showed that considerable economic benefits could be obtained by alleviating the need to construct coffer dams. It is also possible to construct coffer dams of earth or rockfill and with suitable protection, allow these to be overtopped in times of high flood.

The increasing use of the technique of passing floods over partly completed dams has stimulated basic research on flow over and through rockfill banks and this will be referred to in a later chapter.

1.3 Formulation of the Problem

In an isotropic homogeneous saturated medium, for continuous steady flow satisfying Darcy's Law, it can be

readily shown that application of the continuity relation results in a Laplace differential equation:

$$\frac{\partial^2 H}{\partial x^2} + \frac{\partial^2 H}{\partial y^2} = 0 \qquad \text{.... 1.3-1}$$

The total fluid head H is equal to the sum of the pressure, static and velocity heads:

$$H = \frac{p}{\gamma} + y + \frac{v^2}{2g} \qquad \text{.... 1.3-2}$$

in which p is the pressure at a point in the fluid; y is the distance above a datum to that point; γ is the specific weight of water; g is the acceleration due to gravity. The sum of the pressure and static heads is called the piezometric head h:

$$h = \frac{p}{\gamma} + y \qquad \text{.... 1.3-3}$$

Since velocity heads are negligible in Darcy flow, the total head H can be replaced by the piezometric head h so that equation 1.3-1 becomes:

$$\frac{\partial^2 h}{\partial x^2} + \frac{\partial^2 h}{\partial y^2} = 0 \qquad \text{.... 1.3-4}$$

The solution of this equation for various boundary conditions has been well treated in the literature. Analytic solutions are available for many common problems, for example as outlined by Polubarinova-Kochina (1962)

and Harr (1962). Numerical finite difference solutions to various problems including "free surface" flows are also well documented (Shaw and Southwell, 1941; Thom and Apelt, 1961; Boulton, 1951; Jeppson, 1968a, 1968b).

More recently the method of finite elements has been applied to the solution of seepage problems (Zienkiewicz, Mayer and Cheung, 1966) and has advantages in dealing with complex boundary shapes and in allowing for anisotropy and non-homogeneity of the media. This method has also been applied to the analysis of "free surface" problems including two-dimensional flow (Finn, 1967) and axisymmetric flow (Taylor and Brown, 1967).

However, until recent years, the analysis of practical field problems involving nonlinear flow equations has been largely neglected probably because, prior to the introduction of high speed digital computing systems, the complex differential equations involved have been too difficult to handle by analytical mathematics. In view of the importance of situations where nonlinear flow occurs, it is desirable to be able to analyse nonlinear flows in porous media. The advent of high speed computers and the advancement in numerical analysis theory now allows the analyst to obtain numerical solutions to a great variety of problems once

considered too difficult to be handled by conventional mathematical methods.

The investigation in this thesis concerns the application of numerical methods to obtain solutions to problems of nonlinear flow through porous materials. To check the accuracy of the numerical analyses and to determine where nonlinear solutions are necessary, corresponding experimental investigations were carried out with coarse grained aggregates.

In developing the mathematical theory for nonlinear flow, the form of the equation linking head loss and velocity must be known and, in view of the diversity of head loss relations that have been suggested in the literature, a careful consideration of these relations was first carried out. Two of the most common nonlinear relations have already been given as equations 1.1-2 and 1.1-3 and these have been used in the analyses.

These equations are empirical when applied to actual media because the coefficients have to be determined experimentally. However, even Darcy's Law remains essentially empirical in application as values of permeability must usually be obtained from experiment. Thus, although it is realised that a complete understanding of the problems associated with seepage beyond the

range of application of Darcy's Law has not been evolved, it has been shown by numerous experimental investigations reported in the literature, that equations of types 1.1-2 and 1.1-3 can adequately express the relation between head loss and velocity at least over limited ranges of flow.

The object of the thesis has been to apply these equations to analyses of nonlinear flows and, by carrying out associated experimental work, to determine if such analyses can adequately predict the experimental results. In this way the range of application of the equations in actual flow situations can be assessed. An indication can also be obtained of whether or not variations in the values of the coefficients in the equations need be incorporated. As a result of these investigations it is hoped that a clearer understanding of nonlinear porous media flow may be developed with relevant applications to practical flow problems.

1.4 Scope of the Investigation

The investigation carried out was fundamental in that it was concerned with the application of nonlinear head loss equations to analyse some specific flows in porous materials and involved associated experimental work to check the accuracy of the analysis. However,

the types of flow considered were aligned to situations of likely practical importance as far as possible.

Flows to a well in a confined and an unconfined aquifer were investigated. In actual aquifers, although the permeable material is usually fine-grained compared to rockfill material, it is still probable that substantial nonlinear effects may occur, for example in coarse sand aquifers, in the area adjacent to a pumping well. These effects may need to be considered in an analysis because of the great variation in velocities from the radius of influence of the well to the radius of the well itself.

The experimental work was carried out in a 'porous media tank' of 20 feet diameter and involved flows through the complete circle of material as well as through a sector of material. Although the analysis of steady confined flow could be carried out easily, the unconfined flow situation was analysed by numerical methods and was more complicated as it involved the solution of a free streamline problem.

Flows through gravel banks were investigated in an open flume to simulate flows through rockfill dams and banks. The work included consideration of dams with an impervious cut-off wall as well as 'straight through' flows on

a horizontal impermeable base. In the numerical analysis it was again necessary to account for a free streamline problem. No consideration of stability aspects of the banks was contemplated although the values of piezometric head, obtained from the solutions, would be applicable in stability analyses within the limits of accuracy of the solutions.

Application of the nonlinear head loss relations results in nonlinear elliptic partial differential equations. As the majority of the analytical work was undertaken on the Townsville University College's IBM 1620, the computer time involved in the numerical solution of these equations was considerable especially as most of the situations investigated were of a free streamline type. The analysis of such problems virtually involves a number of solutions of the partial differential equations as the correct position of the free surface has to be determined by successive approximations as well as the correct distribution of piezometric head under the free surface.

It was therefore not possible, nor was it considered necessary, to analyse all flows for both the nonlinear head loss equations 1.1-2 and 1.1-3. In view of the fact that theoretical work (Irmay, 1958; Stark and Volker, 1967)

has shown that the Forchheimer equation has a rational basis, the numerical solutions were carried out chiefly using equation 1.1-2. Corresponding solutions for some particular flows were then carried out using the exponential relation (equation 1.1-3) for comparison purposes.

Two techniques commonly applied to the numerical solution of elliptic partial differential equations are the finite difference method and the finite element method. Both approaches have been applied in the solutions carried out in this thesis. For a given amount of computer time and a fixed number of memory locations it is usually possible to employ a finer grid of points with the finite difference method provided boundary conditions are relatively simple. Thus the finite difference method was used in the analysis of the well flow problem because the boundary of the flow field was conveniently shaped, having vertical sides and a horizontal base. In addition, a fine grid was required to obtain an accurate solution to the radial flow equations in the vicinity of the well where the drawdown curve is steeper and the velocities of flow larger.

The finite element method is, however, more readily adaptable to complex boundary shapes and was used in most

analyses of flow through dams and banks. It was particularly convenient when considering flows with the complex lower impervious boundary caused by the inclusion of a cut-off wall in dams. The availability of a method of solution by finite elements will be important in practical considerations where irregularly shaped dams and banks of rockfill often occur.

In summary, having established the merit of the Forchheimer relation, a series of computer solutions and experimental tests were undertaken to investigate the accuracy of numerical analyses of the resultant partial differential equation for actual flow fields. Considerable work has previously been carried out on the application of the exponential relation to problems of nonlinear flow, including a substantial amount at the University of Melbourne on flow through rockfill, as will be evidenced by references in later chapters. Moreover Engelund (1953), using a method of solution by series, obtained results for some problems of Forchheimer flow, with simplified boundary conditions.

However, the development presented in this thesis extends the analysis of the Forchheimer field equation to a series of problems with practical applications, by using the finite difference and finite element techniques

of numerical solution. Treatment of the exponential relation is incorporated for some examples, so that the limitations and advantages could be evaluated for different approaches to the solution of problems of nonlinear flow in porous media.

CHAPTER 2

FUNDAMENTALS OF FLOW THROUGH POROUS MEDIA

2.1 Regimes of Flow in Porous Media

It has been postulated that there are three regimes of incompressible continuous flow in porous media; these are:

(i) the linear laminar regime;

(ii) the nonlinear laminar regime;

(iii) the nonlinear turbulent regime.

The existence of a prelinear regime has also been suggested by Dudgeon (1964) and Gheorghitza (1964). In this regime velocities may be so low that water ceases to act as a Newtonian fluid. Bondarenko and Nerpin (1965) discussed the reasons for deviations from Darcy's Law in terms of the rheological properties of water at low hydraulic gradients, and Mencl, Bobkova and Hanzlova (1965) showed how the permeabilities of sand and clay were affected at small hydraulic gradients. However, the problems studied in this thesis deal with deviations from Darcy's Law due to high velocities so that the prelinear regime is not of interest and will not be considered further.

The fundamental equations governing fluid flow, the Navier-Stokes equations, are applicable to the fluid flowing between the grains of a porous medium. For the flow

of an incompressible constant viscosity fluid, the Navier-Stokes equations may be written in tensor form as:-

$$\rho \frac{du_i}{dt} = - \frac{\partial p}{\partial x_i} + B_i + \mu \frac{\partial^2 u_i}{\partial x_j \partial x_j} \qquad \ldots\ 2.1\text{-}1$$

or writing the acceleration $\frac{du_i}{dt}$ in terms of its partial derivatives:

$$\rho \frac{\partial u_i}{\partial t} + \rho u_j \frac{\partial u_i}{\partial x_j} = - \frac{\partial p}{\partial x_i} + B_i + \mu \frac{\partial^2 u_i}{\partial x_j \partial x_j} \ldots\ 2.1\text{-}2$$

in which ρ is the density of the fluid; u_i is the component of velocity in the i direction; t is time; x_j is the co-ordinate in the j direction; B_i is the body force in the i direction; μ is the coefficient of viscosity.

These equations hold on a microscopic scale; that is, for any given element of fluid at any instant of time. A macroscopic solution to a problem can only be obtained by solving the equations for the relevant boundary conditions. Their complexity, however, renders them intractable to an exact solution except for a few relatively simple boundary conditions, although some solutions have been obtained in recent years by numerical methods (Thom and Apelt, 1961; Fromm, 1963; Stark, 1968). Nevertheless, a consideration of the basic equations does allow a better understanding of the factors causing the changes in regimes of flow.

The effects associated with each term of equation 2.1-2 can be nominated as:

$\rho \frac{\partial u_i}{\partial t}$ - unsteady effects or local acceleration forces;

$\rho u_j \frac{\partial u_i}{\partial x_j}$ - convective inertia forces;

$-\frac{\partial p}{\partial x_i}$ - pressure forces;

B_i - body forces;

$\mu \frac{\partial^2 u_i}{\partial x_j \partial x_j}$ - viscous forces.

The regimes of flow in porous media can now be considered with regard to these components of the Navier-Stokes equations.

2.1.1 The linear laminar regime

This is simply the regime where Darcy's Law can be considered to apply with sufficient accuracy. It is the most widely studied and the best understood since the great majority of analytical work in porous media has been undertaken for flows in this regime. Virtually all of the solutions for problems of seepage of water and other fluids through the strata of the earth's crust, for example, have assumed the validity of Darcy's Law. Because the acceptance

of this law allows the flow to be treated by potential theory, problems are amenable to solution by analogies; these include the electric analogue plotter, the Hele-Shaw model and others. Mathematical treatments are also facilitated since complex potential functions can be employed.

Muskat (1946) discussed the basic Navier-Stokes equations with respect to flow in porous media and showed that, from dimensional considerations, Darcy's Law implied that the inertial forces are neglected. Hubbert (1956) showed theoretically that Darcy's Law is valid only for velocities such that inertial forces are negligible compared with those due to viscosity. Irmay (1958) derived the linear Darcy Law by neglecting the inertia terms in the Navier-Stokes equations, but proved that for higher velocities a nonlinear relation would be necessary to link head loss with velocity.

It appears therefore, that in the linear laminar regime, the term $\frac{du_i}{dt}$ must be negligible. For steady flow, which is the case considered here, the unsteady component of this term, $\frac{\partial u}{\partial t}$ is negligible. The convective inertia components $u_j \frac{\partial u_i}{\partial x_j}$ are only zero in straight, parallel laminar flow. In the curved and tortuous paths of a porous medium these components will only be negligible

for very small velocities encountered in "creeping motions". Thus, the linear laminar regime can be considered as the one in which all flows are "creeping flows".

At higher velocities a nonlinear relation will be required because of the increasing importance of the convective inertia terms. Many investigators have therefore attempted to distinguish between the linear laminar regime and the remaining ones by defining a critical Reynolds number at which Darcy's Law is said to break down. Scheidegger (1960a), for example, quotes values of Reynolds number (RN) ranging from 0.1 to 75, above which different authors have stated Darcy's Law becomes invalid. One of the reasons for this wide range in values is the as yet unsolved problem of defining a suitable representative length dimension for Reynolds number for actual porous media. Stark (1968) has shown that Reynolds number can be used as an exact comparison criterion for flows in different media, only if the arrangement of particles is geometrically similar or if the length dimension can statistically account for variations in geometric arrangements.

In spite of the uncertainty concerning the limit of validity of Darcy's Law, it is evident that for flows in coarse granular materials the inertial effects are likely

to cause considerable discrepancies from the linear relation, and a nonlinear regime of flow will occur.

2.1.2 The nonlinear laminar regime

In this regime Darcy's Law is no longer sufficiently accurate to describe the velocity-head loss relationship although the flow remains laminar. Schneebeli (1953) suggested that the breakdown of Darcy's Law was not necessarily associated with the onset of actual turbulence but was probably due to the emergence of the nonlinear inertia terms in a flow that remains laminar. Subsequent experimental work (Schneebeli, 1955) on flow through three dimensional packings showed visually that Darcy's Law did become inaccurate before the start of fluctuations in the lines of flow which would indicate the commencement of turbulence.

A number of authors have supported these conclusions. Computations by Tamada and Fujikawa (1957) of the drag on an array of cylinders in a two-dimensional flow indicate this effect and Philip (1958) suggested from theoretical considerations that similar results could be expected for flow through an actual porous solid. Ward (1964) introduced the idea of two effective transition regimes between fully laminar and fully turbulent flow. These were the laminar transition regime in which most of the flow

remained laminar but with some turbulent areas and the turbulent transition regime in which the majority of the flow was turbulent but where some pockets of laminar flow still existed. However, Ward obtained no direct experimental verification of the existence of these regimes either by visual observations or by measurement of the onset of turbulence in different areas of the flow.

Chauveteau and Thirriot (1967) reported experimental measurements and observations of flow through various geometrical arrangements in 2-dimensional models and indicated the existence of four regimes of flow. These were the linear laminar, the nonlinear laminar, the mixed laminar and turbulent, and the turbulent regimes. Wright (1968) used hot-wire anemometers to measure the onset of turbulence in the passage of air through a coarse grained gravel. By using gravel with a particle size of 1 inch, the pore space was large enough to allow the insertion of the anemometers within the porous medium itself. Although the measurements recorded from the hot-wire anemometers were not accurate at low air velocities, the results did indicate when the flow became unsteady as a result of the initiation of turbulence. By carrying out head loss measurements on coarse sands of similar shape and size distribution to the gravel, Wright showed that

deviations from the linear resistance law occurred at Reynolds numbers below that at which turbulence commenced in the gravel.

Stark and Volker (1967) reported the results of experimental work on the flow of water around arrays of idealised particles in a horizontal parallel plate model. By using a transparent upper sheet on the model, observations of flow lines were carried out with the aid of dye injected into the flow. Corresponding head loss and velocity measurements in the model showed that Darcy's Law was valid for only the lowest velocities measured, while the onset of turbulence occurred at substantially higher velocities.

Advances in numerical analysis techniques and in computer technology have enabled solutions of the Navier-Stokes equations to be obtained even when the nonlinear inertia terms are retained. Thom and Apelt (1961) solved some problems of 2-dimensional flow around circular cylinders. Watson (1963) applied the methods of Thom and Apelt to solve the Navier-Stokes equations for flow through an idealised arrangement of square cylinders. Stark (1968) revised and extended this approach to include variations in particle size and spacing and solved the equations for a comprehensive range of Reynolds numbers.

Pressure calculations from these results have shown conclusively that the linear Darcy Law is subject to error at any Reynolds number greater than zero although the error is small for small Reynolds numbers.

From the foregoing discussion, it is apparent that the increasing importance of the inertia effects will necessitate the use of a nonlinear relation even though the flow may not be turbulent in the commonly accepted fluid dynamic sense. It should be clearly understood that the turbulent regime referred to here implies the occurrence of actual turbulence.

2.1.3 The nonlinear turbulent regime

The problem of turbulence is by no means completely understood even for simple flow conditions such as flow through pipes and regular channels. In porous media there have been no reported attempts at a theoretical analysis of turbulence. It is logical, therefore, to refer again to the fundamental flow equations in the discussion of this regime.

The eddies or instantaneous fluctuations about the mean velocity which occur in turbulent flow give rise to additional terms in the Navier-Stokes equations. Thus, while these equations in their original form (equation 2.1-2) still hold for any particular element of fluid at

any instant of time, they do not hold for properties averaged over a finite period of time as they do in laminar flow. The various terms involved must be averaged with respect to time to obtain the equations for turbulent flow. Hinze (1959) gave these equations in tensor form as:

$$\left(\frac{\partial \bar{u}_i}{\partial t} + \bar{u}_j \frac{\partial \bar{u}_i}{\partial x_j}\right) + \overline{\rho u_j' \frac{\partial u_i'}{\partial x_j}}$$

$$= -\frac{\overline{\partial p}}{\partial x_i} + \overline{B_i} + \mu \overline{\frac{\partial^2 u_i}{\partial x_j \partial x_j}} \qquad \ldots\ 2.1\text{-}3$$

in which u_i is the instantaneous value of the velocity component in the direction i; $\bar{u}_i$ is the mean value of velocity in the i direction; u_i' is the instantaneous variation of the actual velocity from the mean velocity; and the bar over any term indicates averaging with respect to time.

Thus $$u_i = \bar{u}_i + u_i' \qquad \ldots\ 2.1\text{-}4$$

The extra term due to turbulence in equation 2.1-3, as compared to equation 2.1-2, is

$$\rho \overline{u_j' \frac{\partial u_i'}{\partial x_j}}$$

and is similar in form to the steady convective inertia terms except that its magnitude is governed by variations from the mean velocities instead of by the mean velocities themselves.

Equation 2.1-3 is sometimes written as

$$\rho \left(\frac{\partial \bar{u}_i}{\partial t} + \bar{u}_j \frac{\partial \bar{u}_i}{\partial x_j}\right) = - \frac{\partial \bar{p}}{\partial x_i} + \bar{B}_i + \frac{\partial}{\partial x_j} \left(\mu \frac{\partial \bar{u}_i}{\partial x_j} - \rho \overline{u_i' u_j'}\right) \quad \ldots. \text{ 2.1-5}$$

In this form the extra terms due to turbulence are $\frac{\partial}{\partial x_j} (\rho \overline{u_i' u_j'})$; and then the terms $\rho \overline{u_i' u_j'}$ can be interpreted as stresses on the fluid element due to turbulence. These are called Reynolds stresses. Equation 2.1-5 is even more difficult to solve than the corresponding steady flow equation and research is still being carried out on its application to flows with relatively simple boundary conditions such as flow in straight pipes and channels. However, the form of the Reynolds stress term indicates that the extra head loss it causes would, as a first approximation, be proportional to the square of velocity deviation from the mean; and if the deviation were linearly related to the mean velocity itself then the extra head loss due to turbulence would be a function of the square of the macroscopic velocity. Experimental work on flow through straight parallel pipes has shown that the head loss per unit length is proportional to the square of the velocity for turbulent flow. However, even experimental studies on porous media are much more difficult than with pipe flow and few conclusive results regarding truly

turbulent flow have been reported, although it is generally agreed that the head loss will approach a value proportional to the square of the macroscopic velocity for very high velocities.

Ananyan (1965) carried out a theoretical and an experimental study of turbulent flow through bends of conduits. A consideration of transverse circulation and of the turbulent viscosity coefficient was undertaken. Ananyan formulated the relevant equations governing the turbulent flow and introduced a variational method of solution for the equations. It appears that approaches of this type may eventually be extended to theoretical analyses of turbulent flow in porous media. Advances in the methods of numerical analysis may also allow the solution of the turbulent flow equations for idealised models of porous media. A corresponding increase in the understanding of the macroscopic flow conditions would follow as has been obtained from the solution of the steady form of the Navier-Stokes equations for laminar flow.

2.2 The Linear Darcy Law

Darcy (1856) first postulated the equation 1.1-1 as a result of experimental work on the downward flow of water through sands, but it has since been applied to the flow

of numerous fluids through all types of media. The constant of proportionality k as defined by equation 1.1-1 involves the properties of both the fluid and the porous medium and in order to separate the effects of the fluid properties, Muskat (1946) suggested the relation:

$$k = \frac{k_s \gamma}{\mu} \qquad \ldots\ldots 2.2\text{-}1$$

in which k_s is the specific permeability of the medium and has dimensions of length^2; γ is the specific weight of the fluid; μ is the coefficient of viscosity.

Since the experimental formulation of Darcy's Law there have been numerous attempts to justify it on theoretical grounds. Hazen (1893), Slichter (1897) and King (1899) were among the first to carry out analyses. Slichter, for example, derived an equation of the Darcy type from a study of the pore space existing within a mass of uniform spheres packed in a definite arrangement. Slichter's approach was probably the first of a series which have been based on a capillary bundle model for porous media. This approach considers the pore space of a porous medium to be represented by a series of capillary tubes, but although some quite complicated variations of the approach have been devised (Adzumi, 1939; Childs and Collis-George, 1950), the capillary bundle model does not

adequately explain the relationship between variables involved in flow through actual media. In the devious paths travelled by the fluid, it is obvious that fluid particles will suffer inertial accelerations due to curvature of the paths and these inertial effects are ignored by even the most complicated capillary models.

Another approach which has been used in the theoretical analysis of flows in the linear laminar regime is the hydraulic radius theory which is based on the representation of a porous medium by a series of channels through which the fluid flows. A representative dimension called the hydraulic radius is defined for each channel and this dimension is of direct significance in evaluating the permeability of the medium. One of the best known of the hydraulic radius theories is that due to Kozeny (1927) who considered the medium as an assemblage of channels of fixed length but of varying section. With simplifying assumptions, Kozeny solved the Navier-Stokes equations simultaneously for flow in these channels, and by averaging across a section normal to the flow, he obtained the following expression:

$$V = - \frac{CP^3 \ \text{grad}\ p}{\mu S^2} \qquad \ldots\ 2.2\text{-}2$$

in which C is a dimensionless constant; P is the porosity;

S is specific surface or the surface area per unit volume.

The hydraulic radius theories are usually more elegant than the capillary bundle models but they cannot fully explain all the characteristics of flow through porous media and they still contain some ill-defined factors so that, as Scheidegger (1960b) points out, little more than a qualitative description should be expected from them.

Hubbert (1956) derived the Darcy equation by a method somewhat analogous to that of Kozeny (1927) and showed that Darcy's Law is valid only for velocities such that inertial forces are negligible. Irmay (1958) derived a microscopic form of Laplace's equation by neglecting the inertia terms in the Navier-Stokes equations. The agreement between this microscopic form of the Laplace equation and the macroscopic form (equation 1.3-4) derived from Darcy's Law is superficial because the microscopic equation is in terms of the piezometric head at a particular point in the fluid at any time, whereas the macroscopic form contains the value of piezometric head averaged over a considerable volume of fluid and medium surrounding the point in question. Nevertheless, Irmay's analysis showed that the form of Darcy's Law is correct provided inertial effects are negligible, although a

complicated averaging process is necessary in order to obtain a value for the permeability coefficient from theoretical considerations.

The foregoing discussions indicate that a completely theoretical analysis of even linear laminar flow in porous media is not always possible and coefficients of permeability must often be obtained from experiment. However, it has been established that Darcy's Law is applicable for creeping flows such as would occur in the seepage of fluids through clays and fine silts and even through sands in underground aquifers at very low hydraulic gradients. These linear flow conditions have been extensively investigated both theoretically and experimentally and it is now proposed to consider the relevant flow equations which apply at Reynolds numbers above the limit of validity of Darcy's Law.

2.3 Nonlinear Head Loss Relations

A number of relations have been suggested to replace Darcy's Law at high velocities of flow. The relations suggested have been of a wide variety, both in the form of the expression, and in the values of the constants in any particular expression.

2.3.1 The Forchheimer relation

Forchheimer (1901) suggested the nonlinear equation given as equation 1.1-2 and repeated here for convenience:

$$i = aV + bV^2 \qquad \ldots. \ 2.3\text{-}1$$

Forchheimer postulated this equation as a result of semi-theoretical reasoning by an analogy with flow in tubes. It has been modified to:

$$i = aV + bV^2 + c_1 \frac{\partial V}{\partial t} \qquad \ldots. \ 2.3\text{-}2$$

(in which c_1 is a constant and t is time) by Irmay (1958) and Polubarinova-Kochina (1962), who stated, however, that the time dependent term was small and could be neglected for steady flow.

Muskat (1946) and Harr (1962) each suggested a relation:

$$i = aV + bV^m \qquad \ldots. \ 2.3\text{-}3$$

where m has values between 1 and 2 and approaches 2 as turbulence of flow increases. Aravin and Numerov (1965) observed that the soundest law both from theoretical and experimental viewpoints appeared to be of the form of equation 2.3-1.

Lindquist (1933) reported the results of a series of experiments on the flow of water through uniform lead shot contained in a vertical pipe of 4 inches diameter.

He computed two variables, a friction factor:

$$f = \frac{2gdh}{V^2 L} \qquad \ldots\ldots 2.3\text{-}4$$

in which d is the diameter of the lead shot; h is the head loss over length L; and a Reynolds number:

$$RN = \frac{Vd\rho}{\mu} \qquad \ldots\ldots 2.3\text{-}5$$

From the experimental results, Lindquist reported the following relation between f and RN:

$$f\,RN = 2500 + 40\,RN \qquad \ldots\ldots 2.3\text{-}6$$

On substituting for f and RN and rearranging, the result is:

$$i = \frac{h}{L} = \frac{1250\mu V}{\rho g d^2} + \frac{20V^2}{gd} \qquad \ldots\ldots 2.3\text{-}7$$

This is a Forchheimer relation with the coefficients a and b given by the equations:

$$a = \frac{1250\mu}{\rho g d^2} \qquad \ldots\ldots 2.3\text{-}8$$

$$b = \frac{20}{gd} \qquad \ldots\ldots 2.3\text{-}9$$

Engelund (1953) carried out experiments on flow through a uniform sand and found that his results plotted as a straight line on a graph of fRN against RN. This result again leads to a Forchheimer equation linking i and V. Engelund's expressions for the coefficients were slightly different to those obtained by Lindquist because

of the difference in the media used. For the sand he used, Engelund showed that:

$$a = \frac{2000\mu}{\rho g d^2} \qquad \text{.... 2.3-10}$$

$$b = \frac{35}{gd} \qquad \text{.... 2.3-11}$$

Morcom (1946) by semi-theoretical reasoning deduced an equation of the Forchheimer type and produced experimental results to justify it. He discussed work by Chilton and Colburn (1931) who had pointed out that the resistance to flow in a granular material is made up of two parts:

(a) frictional resistance at the surface of solids;

(b) loss of head due to successive expansions and contractions of channels through which fluid is passing.

Morcom concluded that the frictional resistance accounts for most of the head loss in the viscous range of flow while the expansion and contraction losses predominate in the higher flow range. As a result, Morcom obtained the relation:

$$\frac{\Delta p}{L} = \frac{\alpha \mu V}{\rho d^2} + \frac{\beta V^2}{\rho d} \qquad \text{.... 2.3-12}$$

in which Δp is the pressure drop over length L; d is the

effective mean particle diameter; α and β are experimental constants. This again is of the form $i = aV + bV^2$ provided μ, ρ and d are constants and provided horizontal flow is considered so that $i = \frac{h}{L} = \frac{\Delta p}{L}$.

Ergun and Orning (1949) extended the Kozeny theory to the nonlinear flow regimes. For fluid flow through fine powders at low velocities it was shown that viscous forces can account for the pressure drop, but that for higher velocities, kinetic effects become more important although they do not alone account for all the pressure drop. Ergun and Orning suggested that the transition from the dominance of viscous effects to kinetic effects was smooth for most packed systems and this indicated that a single continuous relation could be used for velocity head loss correlations. Their extension of the Kozeny approach led to the equation:

$$\frac{dp}{dL} = 2\alpha \frac{(1-P)^2}{P^3} \mu S^2 V + \frac{\beta}{8} \frac{(1-P)}{P^3} \rho S V^2 \qquad \text{.... 2.3-13}$$

in which α and β are coefficients depending on the properties of the system and which Ergun and Orning stated should be obtained from experiment. For any particular flow system, equation 2.3-13 reduces to a Forchheimer relation.

Tek (1957) derived "a generalised Darcy equation" in

which the coefficient of permeability is a function of the Reynolds number of the flow and is not a constant. Tek, although considering the porous medium as a succession of capillary passages, stated that an approximate relation between inertial and viscous losses could be obtained; however, a 'lithology factor' was then necessary to relate this expression to easily measured physical properties of the flow. From the relation between inertial and viscous losses, Tek derived a friction factor in terms of Reynolds number, the friction factor being that defined by the Fanning equation which may be simplified to:

$$f = \frac{C_i}{V^2} \qquad \text{.... 2.3-14}$$

in which f is the friction factor and C is a constant depending on the properties of the fluid and medium. The equation derived for the friction factor was:

$$f = \frac{C_1}{RN}\left(1 + \frac{\alpha}{P}\,RN\right) \qquad \text{.... 2.3-15}$$

in which C_1 is a constant depending on the properties of the fluid and medium; RN is Reynolds number; α is a dimensionless 'lithology factor'; and P is porosity.

A combination of equations 2.3-14 and 2.3-15 gives:

$$i = \frac{C_1}{C}\,\frac{V^2}{RN} + \frac{C_1}{C}\,\frac{\alpha}{P}\,V^2 \qquad \text{.... 2.3-16}$$

and since $RN = \frac{Vd\rho}{\mu}$ ... 2.3-17

in which d is the average grain diameter, then equation 2.3-16 may be written as:

$$i = aV + bV^2$$

in which a and b are properties of the fluid and medium. That is, equation 2.3-16 is a Forchheimer relation.

Tek's analysis is restrictive in application however, because it relies on an approximate expression for relating the viscous to the inertial losses and does not hold as Tek points out, for truly turbulent flow.

Chauveteau and Thirriot (1967) carried out an experimental study on 2-dimensional models in which the flow patterns could be observed visually. They postulated four regimes of flow and distinguished between the regimes on a plot of fRN against RN similar to that used by Lindquist (1933). Thus in the first or linear laminar regime fRN is a constant. In the following three regimes, the nonlinear laminar, the mixed laminar and turbulent, and the turbulent regimes the plot of fRN against RN was given as three slightly different straight lines. This is equivalent to an hypothesis of three Forchheimer equations with slightly different values of the coefficients a and b in each of the three nonlinear regimes. The experimental results, for flows above the linear regime, given by

Chauveteau and Thirriot plot as two straight lines with only a very slight change in slope between them. Although the values of the coefficients a and b will probably change in the nonlinear regime, with increasing Reynolds number, the results plotted by Chauveteau and Thirriot indicate that this change is very slight for the Reynolds number range they have used and one single straight line, and therefore one Forchheimer equation, would fit all their results, above a Reynolds number of 20, quite accurately.

Rumer and Drinker (1966) considered flow through a gravel bed from the viewpoint of the resisting forces of the individual particles. For creeping flow, corresponding to the linear laminar regime, the resistance of a single particle was assumed to be given by Stokes' law which expresses a linear relation between the resistance and the local average velocity of flow around the particle. After allowing for the presence of other particles in the region, by including effects due to the geometry of the pore system and due to the porosity, Rumer and Drinker obtained the macroscopic Darcy Law.

For higher velocities, corresponding to the nonlinear laminar regime, the resistance of a single particle was expressed in terms of a "drag coefficient":

$$F_p = C_D \alpha_1 d^2 \frac{\rho V^2}{2} \qquad \text{.... 2.3-18}$$

in which F_p is the resistance of a particle; α_1 is the area shape factor; and C_D is the coefficient of drag. Rumer and Drinker quoted a formula given by Goldstein (1938) for the coefficient C_D:

$$C_D = \frac{C_1}{RN}\left[1 + \sum_{j=1}^{j} (-1)^{j+1} C_j RN^j\right] \qquad \text{.... 2.3-19}$$

in which C_1 is a constant, C_j are coefficients that depend only on the geometry of the object, and the index j takes values 1, 2, 3, ... If the first term only of the series is retained, the analysis can be shown to yield a Forchheimer equation as an end result. If more terms of the series are included, a higher order equation is obtained. However, as Rumer and Drinker mention, equation 2.3-19 is only an approximate expression and is not applicable for Reynolds numbers greater than 2. The approach is therefore limited to only the lowest flows in the nonlinear regime.

Ward (1964) obtained a relation of the Forchheimer type from a dimensional analysis; this relation was:

$$\frac{dp}{dL} = \frac{\mu V}{k_s} + \frac{C\rho V^2}{k_s^{\frac{1}{2}}} \qquad \text{.... 2.3-20}$$

in which $\frac{dp}{dL}$ is the pressure drop per unit length; k_s is the specific permeability of the medium; and C is a

dimensionless constant which Ward stipulated should be constant for all porous media.

Experimental results for a substantial range of porous media indicated that a value of .550 for C would give good agreement with equation 2.3-20. However, there is some scatter of the experimental measurements about the theoretical curve. It should be noted also, that Ward plotted his results of friction factor against Reynolds number on logarithmic paper, and the use of such a logarithmic scale sometimes tends to indicate better agreement visually, than is actually obtained when percentage deviations from the theoretical curve are calculated.

Ward's analysis is probably more restricted than he indicated because it does not allow for all possible variables of the flow system. For example, individual changes in such properties as porosity and particle shape were ignored and, instead, it was assumed that these could all be taken into account in the one factor called permeability. This would suggest that the dimensionless constant C may vary for different media and should not be expected to have a unique value for all systems. Ward employed a Reynolds number based on a length dimension equal to the square root of the specific permeability.

Although the highest value of this Reynolds number was less than 20 for the experimental results, the Reynolds number defined in the usual way (in terms of the average particle diameter) would have an equivalent value of over 700. The agreement of the experimental results with the Forchheimer relation over this range of Reynolds numbers is therefore significant, especially as better agreement could probably be expected for one particular medium when errors due to particle shape etc. would be avoided.

Sunada (1965) also used a dimensional approach in approximating the terms of the Navier-Stokes equations. The analysis included both the steady laminar terms and the average temporal components of the Navier-Stokes equations. Using the approximations for the hydraulic gradient, as directly proportional to velocity for very small velocities, and proportional to the square of velocity for very high velocities, Sunada concluded from his dimensional analysis that an equation of the Forchheimer type would govern flow in porous media and that the form of the equation would hold for nonlinear laminar as well as nonlinear turbulent flow.

As with all dimensional analyses, experimental data were invoked to evaluate the coefficients in the head loss equation. Sunada's experimental work on flow through

glass spheres covered three orders of magnitude of velocity (0.01 cm/sec to 14 cm/sec) and a Forchheimer equation was fitted to all results by a proportional least-squares analysis. A standard error of estimate, defined as the root-mean-square of the average percentage deviation about the fitted curve, was evaluated in order to determine the accuracy of fit. For the complete range of velocities used the standard error of estimate was 4.4 percent, indicating that a Forchheimer curve can adequately describe the velocity head loss relation for a considerable range of Reynolds numbers.

Irmay (1958) derived a Forchheimer relation from the fundamental Navier-Stokes equations for the general case when inertia terms are included. The Navier-Stokes equations, for flow in the x-direction, were written in the form:

$$gH_x = \tfrac{1}{2}(v^2 + w^2 - u^2)_x - (uv)_y - (uw)_z - u_t + \frac{\mu}{\rho}(u_{xx} + u_{yy} + u_{zz}) \qquad \ldots\ 2.3\text{-}21$$

in which a subscript implies differentiation with respect to that subscript; double subscripts imply corresponding second derivatives; u, v and w are the components of velocity in the x, y and z directions respectively.

Irmay analysed equation 2.3-21 with respect to a volume which was sufficiently large to contain a great number of grains so that overall homogeneity and isotropy were satisfied, and yet was small enough so that the overall properties did not vary much within it. The spatial average of terms in the Navier-Stokes equations over this volume were then computed by an essentially dimensional approach. For example, the spatial average of the term $(v^2 + w^2)_x$ was obtained as:

$$\overline{(v^2 + w^2)}_x = - \frac{\alpha u^2}{L'} \qquad \ldots. \ 2.3\text{-}22$$

in which the bar denotes a spatial averaging; α is a numerical "shape factor"; L' is the distance between grains of the medium. By approximating the spatial average of all terms in this way, Irmay showed that the energy gradient could be represented by the sum of a viscous head loss term (proportional to velocity) and an inertial head loss term (proportional to velocity squared).

Stark and Volker (1967) have shown that Irmay's analysis basically assumes a constant velocity profile for all flows and so the values of a and b in his resulting Forchheimer equation will only be constant provided the velocity profile does not vary appreciably. In practical applications it is likely that a particular

velocity profile will apply over a substantial range of Reynolds numbers and so Irmay's result would give good correlation with experiment.

Stark (1968) solved the Navier-Stokes equations numerically for 2-dimensional flow through arrays of square cylinders. The numerical approach used was based on that outlined by Thom and Apelt (1961) in which the inertia terms are included in the analysis. The results apply only to the laminar regimes because no allowance was made for unsteady turbulent effects and, because of the complexity of the numerical analysis, only idealised particle arrays were investigated.

Stark's results showed that the coefficients in any head loss relation would not be strictly constant for different Reynolds numbers, as he had predicted from theory. However, he showed that macroscopic head loss equations could be applied over extended ranges of Reynolds number with small error. For example, the numerical solutions for the arrangement shown in Fig. 2-3-1 indicate that a Forchheimer relation, with constant values of the coefficients a and b, will depict the head loss within an accuracy of 2 percent for the Reynolds number range 0 to 50.

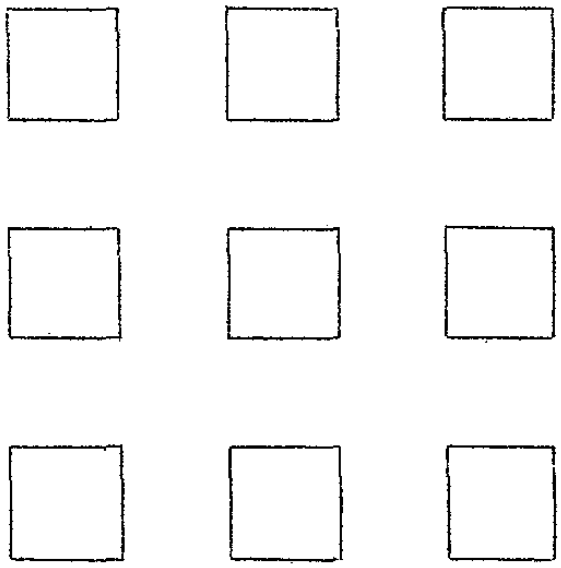

FIG. 2-3-1 SQUARE CYLINDER ARRANGEMENT
(After Stark, 1968)

Assuming the length of the side of a square cylinder is .01 ft and assuming a fluid with a kinetic viscosity coefficient $\nu = 1.0 \times 10^{-5}$ ft^2/sec, Stark's dimensionless results can be converted into actual velocities and hydraulic gradients. A macroscopic flow relation can then be fitted to these results by a proportional least-squares analysis. The proportional least-squares fit is necessary because an ordinary least-squares fit places too much emphasis on the higher Reynolds number values compared to the lower values.

A Forchheimer curve fitted by proportional least-squares, in the Reynolds number range 0 to 50, gave a value of a = .05853 sec/ft. and a value of b = .13636 sec^2/ft^2. The maximum discrepancy of any curve value of

hydraulic gradient from the corresponding numerical solution was 1.5 percent and this is in accordance with the value of 2% given by Stark. The standard error of estimate of the curve was .86 percent. An exponential relation was fitted in the same way and showed a maximum discrepancy of 3.3 percent and a standard error of estimate of 1.76 percent.

The minimum Reynolds number used (above zero) was .05 so that the range .05 to 50 represents three orders of magnitude. If curves are fitted to all results in the Reynolds number range 0 to 150, the Forchheimer curve shows a maximum discrepancy of 3.4 percent and a standard error of estimate of 1.82 percent while the exponential curve has a maximum discrepancy of 5.5 percent and a standard error of estimate of 2.25 percent.

It appears therefore that over the range of Reynolds numbers 0 to 150, macroscopic flow equations with constant coefficients will depict the velocity head loss relationship with sufficient accuracy for practical calculations under prototype conditions.

Above a Reynolds number of 150, it is doubtful if the numerical solutions are relevant for comparisons with flows in actual media. The numerical results are applicable only for laminar flow and assume that no

turbulence is initiated. Jolls and Hanratty (1966) showed experimentally that the transition from laminar to turbulent flow in a dumped bed of spheres occurred in the Reynolds number range 110 to 150, and it is therefore likely that turbulent inertia effects will be evident in actual media above a Reynolds number of 150.

The numerical results are particularly useful in an analysis of the accuracy of the macroscopic flow equations in the low Reynolds number range, however, because they are not affected by difficulties of accurate measurement of low velocities and low hydraulic gradients. The lowest hydraulic gradient in Stark's results (above zero) is 2.92×10^{-6} at a velocity of 5.0×10^{-5} ft/sec. With present day equipment, it would be extremely difficult, if not impossible, to measure accurately such low magnitudes of velocity and hydraulic gradient. The numerical solutions do contain errors resulting from the numerical analysis but Stark has shown these errors are small for low Reynolds numbers.

Experimental work by How Lum (1966) on flow of water through glass beads showed that a Forchheimer relation would depict the head loss over wide ranges of Reynolds numbers (50 to 30,000) with a standard error of estimate of less than 6 percent. His results however, showed that

better accuracy of fit could be obtained by allowing for 2 or 3 separate groups of Reynolds numbers and allowing a and b to vary between these groups. Each group incorporated a considerable range of velocities and, as an example, for flow through 15 mm beads in the Reynolds number range 5000 to 30,000 the standard error of estimate of the fitted Forchheimer curve was less than 2 percent.

Stark and Volker (1967) obtained results for flow through arrays of idealised particles in a parallel plate model. Velocity and hydraulic gradient measurements in this model showed that a Forchheimer relation fitted the experimental results accurately. For open arrays of squares, cylinders and hexagons in an arrangement similar to that shown for Stark's square cylinders in Fig.2-3-1, the results indicated that best accuracy of fit could be obtained by allowing for three groups of Reynolds numbers in the range 500 to 160,000. However, for a lower porosity arrangement using two sizes of square particles, as depicted in Fig.2-3-2, it was shown that a single Forchheimer relation with constant coefficients would adequately cover a similar range of Reynolds numbers.

2.3.2 The exponential relation

Missbach (1937) postulated the exponential head loss equation of the general form given as equation 1.1-3 and repeated here for convenience:

$$i = cV^m \qquad \ldots. \ 2.3\text{-}23$$

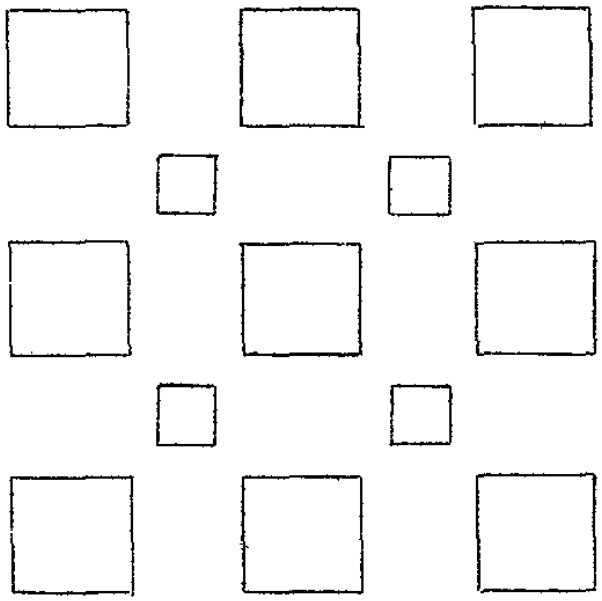

FIG.2-3-2 ARRANGEMENT OF SQUARES OF 2 SIZES
(After Stark and Volker, 1967)

White (1935) was chiefly concerned with the flow of gases through packed towers in which a countercurrent of liquid is circulated over the packings. However, for the case of flow of gases through dry packings, White showed that his own results, together with others obtained by previous researchers, satisfied an equation of the form of 2.3-23 with m approximately equal to 2. Better correlation for some results could have been obtained with a value of 1.88 for m, but White considered this refinement unnecessary in view of the changes caused by porosity variations on repacking a tower with the same material.

Bakhmeteff and Feodoroff (1937) suggested that for

high flow velocities the head loss relation could be either a Forchheimer relation or an exponential relation with m increasing from 1 for Darcy flow to "somewhere near 2". Experimental results obtained from flow through lead shot indicated a gradual increase in m from 1 to an apparently stable upper limit of 1.8. By plotting the results on a graph of fRN against RN, Bakhmeteff and Feodoroff also indicated that two Forchheimer relations would adequately depict the head loss in the Reynolds number range 0 to 2600.

Escande (1953) reported the results of experiments using crushed rock particles of approximately 2 inch mean size. He assumed that for particles of this size, the flow must be fully turbulent and suggested that the value of m must equal 2. However, Wilkins (1955) carried out tests on crushed rock of a number of sizes and obtained a value of m = 1.85 for all sizes. Wilkins used particles of up to 3 inch mean size in a tube of 9 inch diameter and with this arrangement there is likely to be a significant wall effect although he claimed that the use of a 22 inch diameter tube gave no significant difference for one or two measurements he checked. In another series of tests, Wilkins used larger particles which passed an eight-inch sieve and which were retained

on a 7 inch sieve. These tests were carried out in a 3 ft. diameter pipe and a significant wall effect could again result. Wilkins used a comparatively limited range of velocities in all experiments and included only about ten points on his graphs. However, his experiments represent one of the few attempts to obtain velocity head loss correlations for particles of diameters approaching the size which can be expected in prototype rockfill constructions. More work on these larger particle sizes will be required for applications of flow equations to actual rockfill although an alternative experimental approach may be necessary to eliminate wall effects.

Van der Tuin (1960) also used large particles (mean size 15 inches) but he conducted his experiments in an open channel. He suggested a value greater than 2 for the exponent m for one series of tests, although researchers have often postulated an upper limit of 2 for fully turbulent flow. The values of m given were 1.92 and 2.23.

Slepicka (1961) indicated that an exponential head loss relation would apply to flow in porous materials with different values of the exponent for the prelinear, linear and post linear regimes. Anandakrishnan and Varadarajulu (1963) reported the results of tests on a

number of sizes of sands and showed that a number of different values of m were required to cover the regimes of flow. For coarse sands three different values of m were necessary to depict the head loss relation even though all flows were above the linear laminar regime.

Parkin (1963a) obtained results for two aggregate sizes from tests in circular pipes and in a tilting flume and obtained a value of m = 1.85 for all results. Dudgeon (1966) used a special permeameter to eliminate wall effects in a study of flow through coarse granular materials for a wide range of hydraulic gradients. The results when plotted to a logarithmic scale indicated a number of flow regimes with different values of m and with reasonably abrupt changes between the regimes. No theoretical explanation of a number of abrupt changes in flow regimes has been formulated at this time.

2.3.3 Other head loss relations

A great variety of correlations between head loss and velocity have been given in the literature as a result of work in a wide range of disciplines. For example, Rose (1951) and Rose and Rizk (1949), by dimensional analysis, obtained an equation in terms of a resistance coefficient together with functions of other dimensionless groups. With all factors held constant

except the head loss and velocity of flow, the equation can be reduced to the form:

$$i = a_1 V + b_1 V^{1.5} + c_1 V^2 \qquad \ldots\ldots 2.3\text{-}24$$

in which a_1, b_1 and c_1 are constants determined by the fluid and the medium.

Martin (1948) gave a review of some of the friction factor versus Reynolds number correlations that have been reported for both laminar and turbulent flow conditions. Zabrodsky (1963) has outlined some of the relations most commonly used in chemical engineering applications.

These relations have not been used in the analyses undertaken in this thesis and will not, therefore, be considered further.

2.3.4 Summary

From the results reported in the literature and from theoretical considerations it has been shown that for a wide range of Reynolds numbers the coefficients in either the Forchheimer or the exponential head loss relation will not be strictly constant. However, both experimental and theoretical results have shown that a Forchheimer relation will be accurate for a considerable range of Reynolds numbers on either side of any particular Reynolds number under consideration. Similarly an exponential head loss

relation will be accurate over limited ranges of flow. Whether or not allowance must be made for a change in the coefficients of either equation, in the solution to a given flow problem, will depend on the range of Reynolds numbers encountered in the problem, and on the degree to which any change in coefficients affects the results. It may be, that although the coefficients actually change by a small amount, an accurate macroscopic solution for variables such as the discharge rate and the piezometric head can be obtained using "best fit" values of the coefficients over the range of Reynolds numbers involved.

The Forchheimer equation has been used, to a great extent, in the analyses undertaken in this thesis because most theoretical work reported, together with a substantial volume of experimental work, has tended to support this form of head loss relation. In addition, an analysis of some of the results reported (for example Parkin 1963a; Dudgeon 1964) has shown that a Forchheimer relation can be fitted to the results, at least as accurately as the exponential relations given. It is considered that a calculation of the percentage deviations of experimental results from fitted curves should be employed more widely as a check on the accuracy of postulated relations, rather than relying on a visual observation of fitted

curves and lines, especially where logarithmic scales are employed.

One further point may be noted in favour of the use of a Forchheimer relation. For the exponential relation the value of the exponent m must be 1 in the linear laminar regime to agree with Darcy's Law whereas at higher velocities it must approach 2 to agree with experimental observations. It is obvious therefore that any particular value of the exponent m can cover only a limited range of velocities. For the Forchheimer relation however, it is possible that the linear laminar regime may correspond to velocities such that the term bV^2 is negligible compared to the term aV, whereas in the turbulent flow regime the bV^2 term may become predominant so that the head loss approaches a value proportional to V^2. It is therefore possible that the coefficients a and b could remain constant for a larger velocity range than could be covered by constant coefficients c and m in the exponential relation.

There is, of course, a considerable advantage to be obtained in analytical work if the coefficients can be maintained constant without appreciable error. The experimental and numerical analyses discussed in later chapters were designed to investigate actual flow conditions

with a view to determining the accuracy of solutions based on constant coefficients.

2.4 Field Equations for Flow Analyses

Problems which require the solution of a differential equation throughout a physical region or "field" are often called field problems; in this context the differential equations which apply throughout the field may then be termed the field equations.

When dealing with flow through porous materials, the velocity head $\frac{v^2}{2g}$ can usually be neglected in comparison with the piezometric head h, even when velocities are large enough to cause a nonlinear head loss equation. This is borne out by calculations using measured velocities and heads in actual flows. Thus the complete solution to a problem can be obtained if the piezometric head distribution is known over the region of flow. Other quantities can be obtained from the values of piezometric head; for example, the discharge rate can be evaluated by calculating the hydraulic gradient and substituting in the head loss relation to obtain velocity and integrating over any particular area. Consequently, in the work which follows, the unknown will be considered as the piezometric head h whose value is required for all values of the co-ordinates x and y in the region of flow. The field equation then is

written in terms of piezometric head as the unknown function.

2.4.1 The Laplace equation for Darcy flow

Darcy's Law given as equation 1.1-1 may be rewritten in terms of piezometric head as:

$$V = - k \frac{\partial h}{\partial s} \qquad \ldots. \ 2.4\text{-}1$$

since the velocity head may be neglected. Assuming 2-dimensional flow, the vector velocity $\underline{V}$ in the s direction may be written in terms of its components in the x and y co-ordinate directions:

$$\underline{V} = u \, \underline{i} + v \, \underline{j} \qquad \ldots. \ 2.4\text{-}2$$

in which $\underline{i}$ and $\underline{j}$ are unit vectors in the x and y directions respectively. Similarly, the gradient of the scalar field h may be written in terms of its components:

$$\frac{\partial h}{\partial s} \, \underline{s} = \frac{\partial h}{\partial x} \, \underline{i} + \frac{\partial h}{\partial y} \, \underline{j} \qquad \ldots. \ 2.4\text{-}3$$

in which $\underline{s}$ is a unit vector in the s direction. Substituting equations 2.4-2 and 2.4-3 in 2.4-1:

$$u\underline{i} + v\underline{j} = - k \left(\frac{\partial h}{\partial x} \, \underline{i} + \frac{\partial h}{\partial y} \, \underline{j} \right) \qquad \ldots. \ 2.4\text{-}4$$

and equating components in equation 2.4-4:

$$\left.\begin{aligned} u &= - k \frac{\partial h}{\partial x} \\ v &= - k \frac{\partial h}{\partial y} \end{aligned}\right\} \qquad \ldots. \ 2.4\text{-}5$$

The continuity condition for 2-dimensional flow may be written:

$$\frac{\partial u}{\partial x} + \frac{\partial v}{\partial y} = 0 \qquad \text{.... 2.4-6}$$

Substituting equation 2.4-5 in 2.4-6 and assuming k is constant:

$$\frac{\partial^2 h}{\partial x^2} + \frac{\partial^2 h}{\partial y^2} = 0 \qquad \text{.... 2.4-7}$$

This is the Laplace equation for 2-dimensional flow in terms of the piezometric head.

Scheidegger (1960b) suggested that an alternative form of the differential equation might be acceptable in which the coefficient of permeability is included in the function under the derivative sign. However, Hubbert (1940) indicated, by a thermodynamic analogy, that equation 2.4-7 is valid and Jones (1962) has also supported equation 2.4-7 as being the correct differential form of Darcy's Law.

2.5 Field Equations for Nonlinear Flow

Kristianovich (1940) considered a general flow equation of the type:

$$i = \phi(V) \qquad \text{.... 2.5-1}$$

in which $\phi(V)$ is a function of velocity and may take different forms depending on the particular problem in

hand. Thus:

$$\left.\begin{aligned} \phi(V) &= \frac{V}{K} && \text{(Darcy's Law)} \\ \phi(V) &= aV + bV^2 && \text{(Forchheimer equation)} \\ \phi(V) &= cV^m && \text{(exponential equation)} \end{aligned}\right\} \quad \ldots 2.5\text{-}2$$

The continuity condition for 2-dimensional flow (equation 2.4-6) may then be combined with equation 2.5-1 to give the system of equations governing the flow.

Kristianovich introduced the velocity vector $\underline{V}$ and its angle θ to the x axis in lieu of the velocity components u and v in the x and y directions. With piezometric head h and a flow function ψ as independent variables the system becomes:

$$\left.\begin{aligned} \frac{\partial\theta}{\partial\psi} - \frac{\phi(V)}{V^2}\frac{\partial V}{\partial h} &= 0 \\ \frac{\partial\theta}{\partial h} + \frac{V\phi'(V)}{\phi(V)}\frac{\partial V}{\partial\psi} &= 0 \end{aligned}\right\} \quad \ldots\ldots 2.5\text{-}3$$

in which $\phi'(V)$ represents the derivative of $\phi(V)$ with respect to V. This system was then reduced to a system of four equations by the introduction of auxiliary independent variables ξ and η and Kristianovich outlined a method of solution in which the problem is first solved in the ξ, η plane and values of x and y are then obtained from integral relations.

The system of equations to be solved is complex and Kristianovich offered only an approximate method of solution. For complicated boundary conditions likely to be met in practical flow situations, the solution of the problem by this method would be very tedious, even if it is possible at all. Kristianovich therefore devoted a special section of his paper to the application of an electrical analogy method for the study of groundwater motion which does not obey Darcy's Law.

2.5.1 Field equation based on the Forchheimer relation

Engelund (1953) used a slightly different approach to the one outlined by Kristianovich to obtain the differential equation for seepage. The general flow equation was written in the form:

$$- \text{grad } h = F(|V|)\underline{V} \qquad \ldots\ldots \text{2.5-4}$$

in which $\underline{V}$ is the vector velocity; $|V|$ is the magnitude of $\underline{V}$; and $f(|V|)$ is a function of the magnitude of the velocity. Engelund assumed that grad h and $\underline{V}$ are oppositely directed vectors and for 2-dimensional flow the appropriate equations, in the x and y co-ordinate directions, then become:

$$\left.\begin{aligned} -\frac{\partial h}{\partial x} &= F(|V|)u \\ -\frac{\partial h}{\partial y} &= F(|V|)v \end{aligned}\right\} \qquad \ldots\ldots \text{2.5-5}$$

These equations may be combined with the continuity equation to give the complete system describing the flow. Engelund considered a Forchheimer relation to obtain $F(|V|)$ for the nonlinear flow range. Thus in this range:

$$F(|V|) = a + b|V| \qquad \ldots\ldots 2.5\text{-}6$$

However, with $F(|V|)$ defined as in equation 2.5-6 the equations 2.5-5 are nonlinear and are difficult to solve analytically so that Engelund introduced new variables in order to linearise the resultant differential equation. This final equation becomes:

$$\frac{\partial}{\partial V}\left(\frac{V}{F}\frac{\partial h}{\partial V}\right) + \frac{1}{F}\left(\frac{1}{V} + \frac{F'}{F}\right)\frac{\partial^2 h}{\partial \theta^2} = 0 \qquad \ldots\ldots 2.5\text{-}7$$

in which the independent variables are the velocity V and the angle θ between the vector velocity $\underline{V}$ and the x axis; and F' is the differential of the function F with respect to velocity. Although equation 2.5-7 is linear, it still remains intractable to direct solution for complex boundary conditions encountered in practice. Engelund gave a solution for one flow problem with simple boundary conditions and outlined a possible method of solution by series.

The derivations of Engelund and Kristianovich involve the introduction of new independent variables in place of

the cartesian co-ordinates x and y in order to simplify the analyses. This will usually involve more work in interpreting solutions once they are obtained. With progress in numerical analysis it is now possible to obtain solutions for differential equations as complex as those encountered in nonlinear seepage flow, and it is therefore unnecessary to introduce new independent variables.

Irmay (1958) gave a brief discussion of the use of the Forchheimer equation in deducing a differential field equation. This resultant field equation may be written:

$$\text{div}(i\underline{s}) + (i\underline{s}).\text{grad ln } f(|i|) = 0 \qquad \ldots\ldots 2.5\text{-}8$$

in which $\underline{s}$ is a unit vector in the direction of the hydraulic gradient i; ln denotes a natural logarithm; and

$$f(|i|) = \left\{ \left(\frac{a}{2}\right) + \sqrt{\left(\frac{a^2}{4}\right) + \frac{|i|}{b}} \right\}^{-1} \qquad \ldots\ldots 2.5\text{-}9$$

Irmay suggested that equation 2.5-8 be solved by the method of Kristianovich discussed previously.

The field equation for Forchheimer flow can be derived as follows. Assuming that grad h and $\underline{V}$ are oppositely directed vectors, as has been assumed by Kristianovich, Engelund and others, equation 2.3-1 in vector form becomes:

$$- \text{grad } h = (a + b|V|)\underline{V} \qquad \ldots\ldots 2.5\text{-}10$$

If the unit vector $\underline{s}$ is normal to the surface of constant h in the scalar field at any point, then:

$$- \text{grad } h = -\frac{\partial h}{\partial s}\,\underline{s} \qquad \ldots\ldots 2.5\text{-}11$$

Adopting the notation $h_s = \frac{\partial h}{\partial s}$; $h_x = \frac{\partial h}{\partial x}$ and $h_y = \frac{\partial h}{\partial y}$, and according to the usual vector notation in which $\underline{i}$ and $\underline{j}$ are unit vectors in the x and y directions respectively, it can be shown from vector theory that:

$$- h_s\underline{s} = - h_x\underline{i} - h_y\underline{j} \qquad \ldots\ldots 2.5\text{-}12$$

also
$$- h_s\underline{s} = (a + b|V|)\underline{V} \qquad \ldots\ldots 2.5\text{-}13$$

$$= (a + b|V|)\,(u\underline{i} + v\underline{j}) \qquad \ldots\ldots 2.5\text{-}14$$

Equating components of corresponding vectors in 2.5-12 and 2.5-14:

$$\left.\begin{aligned} - h_x &= (a + b|V|)u \\ \text{and } - h_y &= (a + b|V|)v \end{aligned}\right\} \qquad \ldots\ldots 2.5\text{-}15$$

From equation 2.5-12:

$$\underline{s} = \frac{h_x}{h_s}\,\underline{i} + \frac{h_y}{h_s}\,\underline{j} \qquad \ldots\ldots 2.5\text{-}16$$

and since $u\underline{i} + v\underline{j} = V\underline{s}$ $\qquad \ldots\ldots 2.5\text{-}17$

$$\therefore \quad u\underline{i} + v\underline{j} = V\,\frac{h_x}{h_s}\,\underline{i} + V\,\frac{h_y}{h_s}\,\underline{j} \qquad \ldots\ldots 2.5\text{-}18$$

so that components u and v may be written:

$$\left.\begin{aligned} u &= V\,\frac{h_x}{h_s} \\ v &= V\,\frac{h_y}{h_s} \end{aligned}\right\} \qquad \ldots\ldots \text{2.5-19}$$

But from equation 2.5-13 it is obvious that V and h_s are opposite in sign so that:

$$\frac{V}{h_s} = -\,\frac{|V|}{|h_s|} \qquad \ldots\ldots \text{2.5-20}$$

Thus

$$\left.\begin{aligned} u &= -\,h_x\,\frac{|V|}{|h_s|} \\ v &= -\,h_y\,\frac{|V|}{|h_s|} \end{aligned}\right\} \qquad \ldots\ldots \text{2.5-21}$$

Again from equation 2.5-13:

$$|h_s| = |(a + b|V|)V| \qquad \ldots\ldots \text{2.5-22}$$

and

$$|V| = -\,\frac{a}{2b} + \sqrt{\left(\frac{a}{2b}\right)^2 + \frac{|h_s|}{b}} \qquad \ldots\ldots \text{2.5-23}$$

Thus

$$\left.\begin{aligned} u\underline{i} &= \left\{-\,\frac{a}{2b} + \sqrt{\left(\frac{a}{2b}\right)^2 + \frac{|h_s|}{b}}\right\} - \frac{h_x}{|h_s|}\,\underline{i} \\ v\underline{i} &= \left\{-\,\frac{a}{2b} + \sqrt{\left(\frac{a}{2b}\right)^2 + \frac{|h_s|}{b}}\right\} - \frac{h_y}{|h_s|}\,\underline{i} \end{aligned}\right\} \qquad \ldots\ldots \text{2.5-24}$$

On application of the continuity condition, the result is:

$$\frac{\partial}{\partial x}\left[\left\{-\frac{a}{2b}+\sqrt{\left(\frac{a}{2b}\right)^2+\frac{|h_s|}{b}}\right\}\frac{(-h_x)}{|h_s|}\right]$$

$$+\frac{\partial}{\partial y}\left[\left\{-\frac{a}{2b}+\sqrt{\left(\frac{a}{2b}\right)^2+\frac{|h_s|}{b}}\right\}\frac{(-h_y)}{|h_s|}\right]=0 \quad \ldots\ldots \quad 2.5\text{-}25$$

Equation 2.5-25 is the field equation governing flow in a 2-dimensional flow field where equation 2.3-1 is the relation between head loss and velocity.

2.5.2 Field equation based on the exponential relation

Brooker (1961) derived a field equation for systems obeying the nonlinear exponential head loss relation. Parkin (1963a) used a vectorial approach for deriving Brooker's equation. After combining the exponential relation with the continuity condition, the resulting differential flow equation may be written:

$$(h_{xx}+h_{yy})(h_x^2+h_y^2)+\left(\frac{1}{m}-1\right)(h_x^2h_{xx}+2h_xh_yh_{xy}+h_y^2h_{yy})=0 \quad \ldots\ldots \quad 2.5\text{-}26$$

This equation reduces to the Laplace equation for the condition m = 1 as would be expected since the exponential head loss relation, with m = 1, is simply Darcy's Law. Parkin indicated that equation 2.5-26 would be applicable to flow through rockfill dams but suggested only a possible method of solution by sketching. Curtis (1965) employed a

finite difference form of equation 2.5-26 to analyse flow through rectangular shaped rockfill banks.

Mohar (1966) extended the differential field equation to allow for spatial variation of the coefficients c and m throughout the entire region of flow. Mohar applied this extended equation to investigate flow through a permeable wall with vertical upstream and downstream faces. The results of the analysis showed however, that the magnitudes of the terms resulting from the spatial variation of c and m were negligible compared to the terms with constant coefficients (which are the terms of equation 2.5-26) for the particular flow conditions investigated. Kirkham (1967) used a similar equation to that derived by Mohar to investigate confined nonlinear flow in a special model. The model was well suited for a finite difference numerical solution of the extended flow equation and good correlation between experimental and theoretical results was obtained.

The field equation based on the exponential relation can be derived as follows, by a procedure analogous to that used for the Forchheimer relation. Equation 2.3-23 in vector form becomes:

$$-h_s \underline{s} = (c|V|^{m-1})\underline{V} = (c|V|^{m-1})(u\underline{i} + v\underline{i}) \quad .... \quad 2.5\text{-}27$$

$$\left.\begin{aligned} \text{and} \qquad -h_x &= (c|V|^{m-1})u \\ -h_y &= (c|V|^{m-1})v \end{aligned}\right\} \quad \ldots\ldots 2.5\text{-}28$$

$$\left.\begin{aligned} \text{With} \qquad u\underline{i} &= -h_x \frac{|V|}{|h_s|}\underline{i} \\ v\underline{i} &= -h_y \frac{|V|}{|h_s|}\underline{j} \end{aligned}\right\} \quad \ldots\ldots 2.5\text{-}29$$

the continuity relation gives:

$$\frac{\partial}{\partial x}\left[\left\{\frac{|h_s|}{c}\right\}^{1/m}\frac{(-h_x)}{|h_s|}\right] + \frac{\partial}{\partial y}\left[\left\{\frac{|h_s|}{c}\right\}^{1/m}\frac{(-h_y)}{|h_s|}\right] = 0 \quad \ldots\ldots 2.5\text{-}30$$

Equation 2.5-30 is the field equation governing 2-dimensional flow when the head loss relation is of exponential form.

The field relations 2.4-7, 2.5-25 and 2.5-30 are the equations analysed by numerical methods in Chapter 4.

CHAPTER 3

APPLICATION OF THEORY TO SOME PRACTICAL FLOW SITUATIONS

3.1 Groundwater Flow to a Well in a Confined Aquifer

Analyses of flows in aquifers are usually based on a number of simplifying assumptions. The aquifer material is assumed to be saturated, homogeneous and isotropic and of uniform thickness, while the well is assumed to penetrate the entire aquifer. For horizontal confining layers, the flow conditions may be represented as in Fig. 3-1-1.

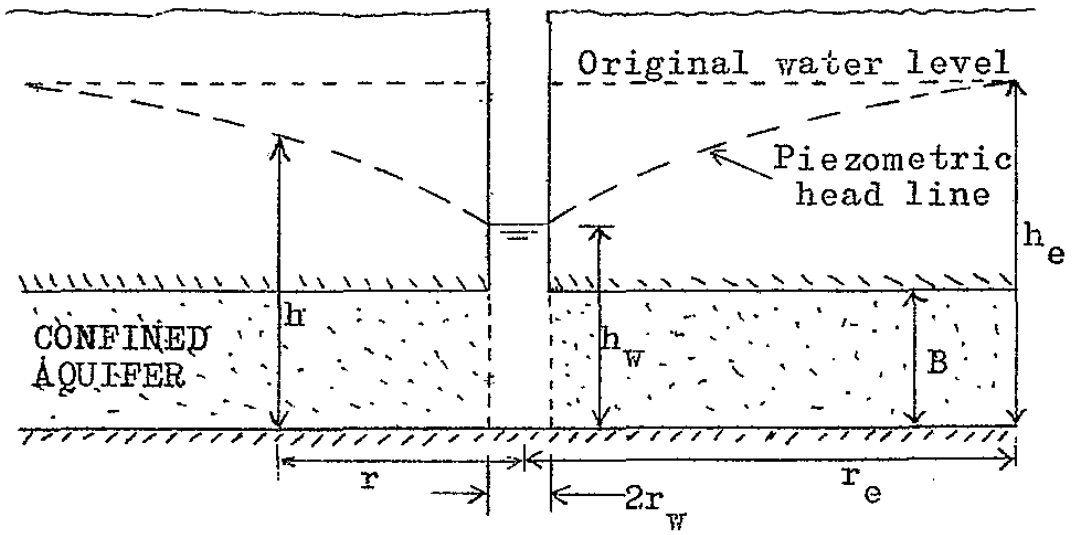

FIG. 3-1-1
RADIAL FLOW TO A WELL IN A CONFINED AQUIFER

If the flow obeys Darcy's Law with a constant permeability k, and if the head h_e at radius r_e is assumed to be unaffected by the well, then the relation

between the piezometric head h at radius r, and the discharge Q is given by:

$$h_e - h = \frac{Q}{2\pi kB} \ln \frac{r_e}{r} \qquad \text{.... 3.1-1}$$

in which B is the thickness of the aquifer. This equation is known as the equilibrium or Thiem equation (Thiem, 1906). For natural aquifers of large lateral dimensions the head h increases indefinitely with increasing radius so that steady flow is both theoretically and physically impossible (De Wiest, 1965). Under these conditions, equation 3.1-1 is applicable only within close proximity to the well.

Theis (1935) investigated the problem of unsteady flow in an extensive confined aquifer and showed that the piezometric head is a function of radius and time according to the equation:

$$\frac{\partial^2 h}{\partial r^2} + \frac{1}{r} \frac{\partial h}{\partial r} = \frac{S}{T} \frac{\partial h}{\partial t} \qquad \text{.... 3.1-2}$$

in which S is the storage coefficient of the aquifer and T (=kB) is the transmissivity. Solutions to equation 3.1-2 for specified boundary conditions have been widely used as the basis for field determinations of the aquifer properties S and T. However, for most aquifer materials, it is only in the area adjacent to the well that nonlinear

effects will be important so that no analysis, either experimental or theoretical, of unsteady flow conditions was carried out in this thesis.

One particular example of confined flow, for which equation 3.1-1 gives an exact solution, is that of a well discharging from a confined aquifer at the centre of an island. The flow situation is then as depicted in Fig. 3-1-2.

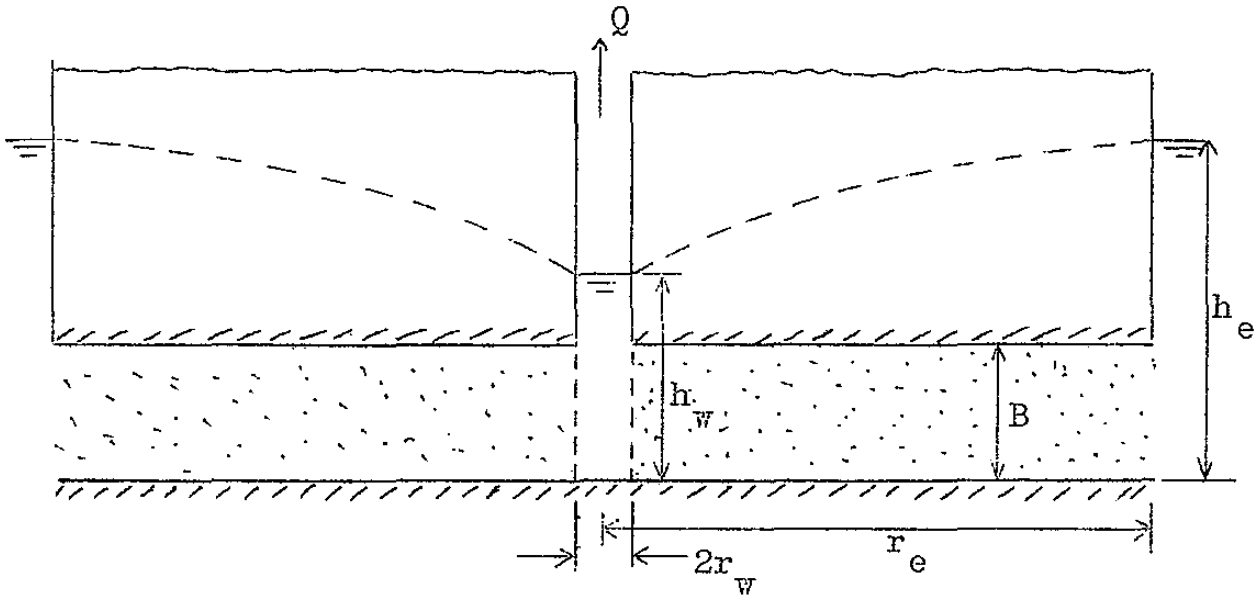

FIG. 3-1-2
WELL DISCHARGING FROM A CONFINED AQUIFER ON AN ISLAND

If the discharge Q is a constant and if the flow obeys Darcy's Law throughout, then the equilibrium equation will hold without error.

Engelund (1953) solved the problem of Fig. 3-1-2 allowing for a zone of nonlinear flow around the well.

Darcy's Law was assumed accurate for radii greater than r_t, the so-called radius of turbulence, but inside r_t a Forchheimer relation was employed to link head loss and velocity. In view of the considerations of Chapter 2 in which it was shown that a Forchheimer relation is accurate over a considerable range of flows, the flow situation depicted in Fig. 3-1-2 may be solved on the assumption that a Forchheimer relation governs the head loss throughout the entire aquifer. Thus if Q is the constant discharge, then the velocity at any radius r is $\frac{Q}{2\pi rB}$; and since $i = -\frac{\partial h}{\partial s} = \frac{\partial h}{\partial r}$, substitution in equation 1.1-2 yields:

$$\frac{\partial h}{\partial r} = a\left(\frac{Q}{2\pi rB}\right) + b\left(\frac{Q^2}{4\pi^2 r^2 B^2}\right) \qquad \ldots\ 3.1\text{-}3$$

After integration between the limits r_w, h_w and r_e, h_e the result is:

$$h_e - h_w = \frac{aQ}{2\pi B} \ln \frac{r_e}{r_w} + \frac{bQ^2}{4\pi^2 B^2}\left(\frac{1}{r_w} - \frac{1}{r_e}\right) \qquad \ldots\ 3.1\text{-}4$$

The derivation has assumed that velocity heads are negligible so that the piezometric head h can be used in lieu of the total head H and that there is no loss of piezometric head as the water enters the well. This latter condition would be fulfilled if the velocity head of the water passing through the well screening is equal

to the head lost on entering the well. This is similar to the assumption usually made where a closed conduit discharges into a reservoir: that the head loss at the exit is equal to the velocity head of the flow.

If the external head h_e and the height of water in the well h_w are known as well as the coefficients a and b for the aquifer material then equation 3.1-4 may be solved for the discharge Q.

Anandakrishnan and Varadarajulu (1963) have given a similar result for an exponential head loss relation. Thus the velocity at any radius r is $\frac{Q}{2\pi rB}$ and substitution in equation 1.1-3 yields:

$$\frac{\partial h}{\partial r} = c\left(\frac{Q}{2\pi rB}\right)^m \qquad \ldots. \text{ 3.1-5}$$

Integrating between r_w, h_w and r_e, h_e, the result is:

$$h_e - h_w = \frac{cQ^m}{(2\pi B)^m} \frac{r_e^{1-m} - r_w^{1-m}}{1 - m} \qquad \ldots. \text{ 3.1-6}$$

Equation 3.1-6 may then be solved for the discharge Q.

The flow situation shown in Fig. 3-1-2 can be simulated in the laboratory and, since it can be solved without recourse to numerical methods, provides a convenient initial problem for consideration of nonlinear effects in flow through coarse grained aquifers.

3.2 Groundwater Flow to a Well in an Unconfined Aquifer

The assumptions usually made in analysing unconfined aquifer flows are similar to those made for confined aquifers. Some solutions have been obtained for more general conditions such as flow to partially penetrating wells (Forchheimer, 1930; Boreli, 1955; Kirkham, 1959; Hantush, 1961); flow to wells in sloping sands (Forchheimer, 1886; Hantush, 1962a); and horizontal flow through aquifers where permeability varies with depth (Youngs, 1965). However the analysis of flow problems is considerably simplified when the assumptions of fully penetrating wells, horizontal layers, uniform permeability, etc. are made, and most investigations reported have been based on such assumptions.

The situation of unconfined flow to a well may be represented as shown in Fig. 3-2-1.

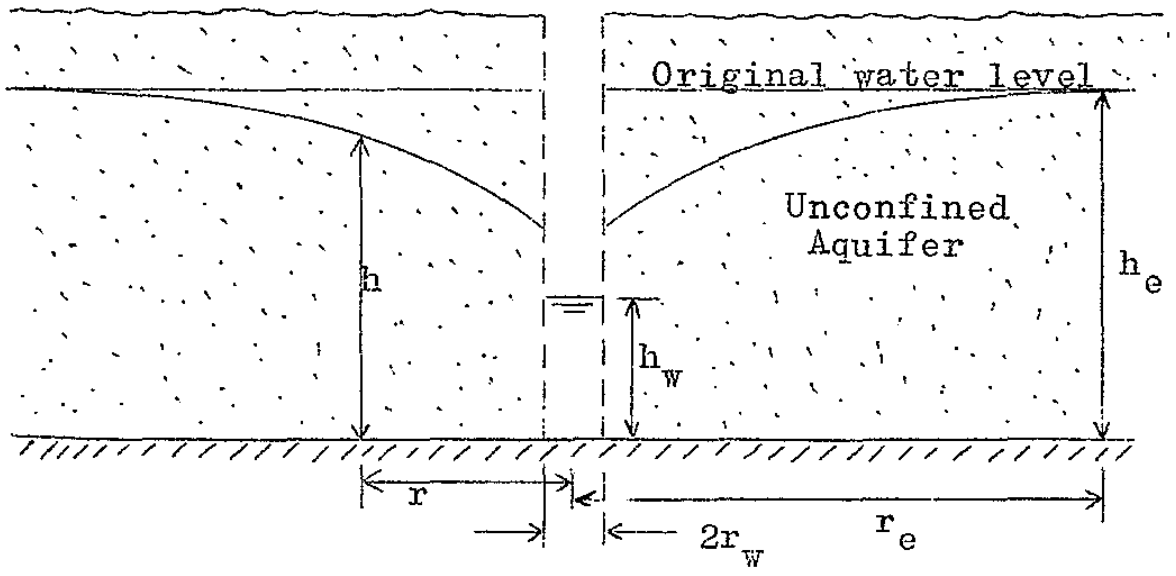

FIG. 3-2-1
RADIAL FLOW TO A WELL IN AN UNCONFINED AQUIFER

The aquifer is assumed to be homogeneous and isotropic; the saturated thickness before pumping starts is assumed uniform throughout and the well is assumed to penetrate to the horizontal impermeable base of the aquifer.

Dupuit (1863) solved the problem of Fig. 3-2-1 on the basis of further assumptions which have become known as Dupuit's conditions. These are:

(i) the velocity is horizontal across any vertical section;

(ii) the velocity is uniform over the depth of flow;

(iii) the velocity is proportional to the tangent of the slope of the free surface instead of to its sine.

For steady flow conditions and assuming Darcy's Law is valid throughout, Dupuit's solution may be stated as:

$$Q = \frac{\pi k \, (h_e^{\,2} - h_w^{\,2})}{\ln \, (r_e/r_w)} \qquad \ldots\ldots \; 3.2\text{-}1$$

This expression is often called the Dupuit-Forchheimer formula. At an intermediate radius r where the piezometric head is h, equation 3.2-1 may be rewritten as:

$$h^2 = \frac{Q}{\pi k} \ln \, (r/r_w) + h_w^{\,2} \qquad \ldots\ldots \; 3.2\text{-}2$$

Because there are actually large vertical components of flow neglected in Dupuit's assumptions, equation 3.2-2

fails to describe accurately the drawdown curve near the well. In practice there is found to be a seepage face at the well as shown in Fig. 3-2-2 and this is not accounted for in equation 3.2-2.

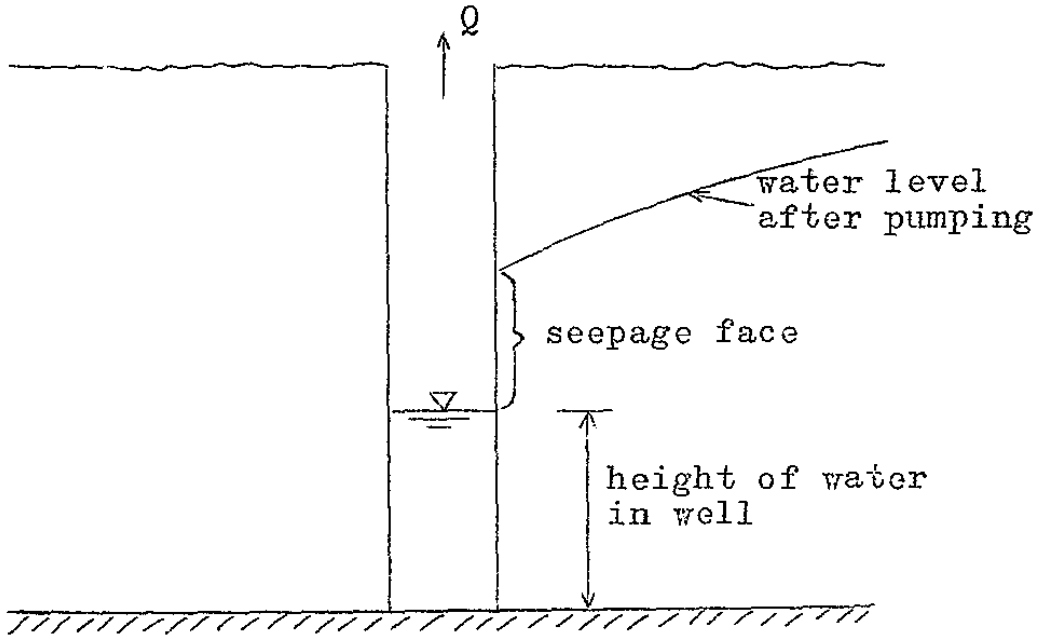

FIG. 3-2-2
SEEPAGE FACE AT WELL IN UNCONFINED FLOW

However, equation 3.2-1 has been shown to give accurate values of the discharge (Muskat, 1946), while Hantush (1962b) has shown that this equation can be rigorously derived between the limits h_w, r_w and h_e, r_e allowing for a seepage face at the well. A similar result for flow in dams with vertical sides was given by Huard de la Marre (1956). Thus while equation 3.2-1 gives accurate discharge values for Darcy flow conditions, equation 3.2-2 does not accurately predict the drawdown in the area adjacent to the well.

In view of its importance in groundwater applications, a number of theoretical and experimental investigations on the problem of unconfined flow to a well have been reported. Although most of these have dealt with Darcy flow, the methods involved can be applied, with suitable modifications, to nonlinear flow analyses.

3.2.1 Experimental investigations

Sand models, including sectors of a circle, have been used extensively in investigations of flow to wells. The results obtained by Wyckoff, Botset and Muskat (1932) using such a model indicated the importance of capillary effects in unconfined flow through sands. Their results also showed that Dupuit's curve gave good agreement with values of piezometric head measured along the impermeable base of the model. A comprehensive set of experiments was carried out by Babbitt and Caldwell (1948) using a sand model and also an electric carbon wedge analogy. From their results, Babbitt and Caldwell derived an empirical formula for the free surface, to replace Dupuit's curve which is inaccurate in the vicinity of the well.

An account of some of the experimental precautions which must be taken to prevent air entrainment was given by Hansen (1953) who used a 90 degree sector for

model tests on unconfined flow through sand. The effect of the capillary zone was shown to be important at least for the sand size used in the experiments. Hansen also discussed the occurrence of the seepage surface at the well face and showed that it was not due to well loss alone.

Flow into a tubular well was studied by Peter (1955) who compared his results with the theories of a number of previous workers. Mogg (1959) investigated the effect on well drawdown caused by nonlinear flow in the aquifer around the well. The results indicated that nonlinear effects would be significant only for gravels and coarse sands. Mogg suggested an empirical method, based on a varying exponent of velocity, for calculation of head losses and his work involved no fundamental analysis of nonlinear flow.

A 30 degree sector of sufficient size to limit errors to 3 percent was used by Grcic (1961) in his experiments to determine the height of the seepage surface for various conditions. Grcic showed that, for coarse sands, the height of the seepage face was affected by nonlinear flow near the well, although he recognised the difficulty of accounting for these effects analytically. Unconfined and confined aquifer flows were both summarised by Glover (1964) in a general report covering various types of

groundwater movement.

Various analogies have been applied to the solution of groundwater problems. For example, Lawson and Hendrick (1965) applied a membrane analogy to the solution of well flow problems including multiple wells with a number of boundary conditions. An electrical analogue was employed by Macawaris (1966) in studying flow to wells with wedge shaped boundary conditions formed by rivers and impervious foundations. Macawaris analysed the flow situations using complex variable theory and checked his results with the aid of the electrical analogue. Prickett (1967) also used electrical analogues in simulating pumped wells, to determine the effect of variables such as radius, length of screening and degree of penetration.

3.2.2 Numerical solutions

A number of numerical solutions to unconfined flow problems have been obtained in recent years, one of the first of these being obtained by Yang (1949) who analysed steady-state flow to a well in an unconfined aquifer by a modification of the relaxation method of Shaw and Southwell (1941). In his analysis, Yang assumed that the free surface could be approximated by the grid points which were closest to it throughout the flow field. Boulton

(1951) also used the relaxation process to solve four cases of unconfined well flow. A graded mesh was incorporated near the well and near the free surface and a modified form of the finite difference equations was employed, assuming logarithmic variation of piezometric head with radius in the area adjacent to the well. The value of the discharge calculated by Boulton from his numerical solutions agreed with the Dupuit discharge to within 0.3 percent.

Numerical solutions were also obtained by Luthin and Scott (1952) for unconfined flow to a well at the instant pumping starts; in this case the water table could be assumed horizontal so that treatment of the top boundary was considerably simplified. The results are therefore of little practical application, although consideration was given to nonhomogeneous formations separated by horizontal interfaces.

Some different forms of the relaxation equation for irregular grid lengths were discussed by Boreli (1953) who indicated their relevant merits with respect to the number of iterations required to obtain a given accuracy in a solution. Hall (1954) gave a comprehensive historical review of groundwater flow to wells, from the time of Darcy and Dupuit until 1954. Yang's method of step

representation of the free surface was used by Hall (1955) in a relaxation solution for unconfined well flow. Associated experimental work was carried out with a sand model using a 15 degree sector and the effect of capillary action was considered in some detail. Murray (1960) solved a number of free surface problems by the relaxation method including flow through a vertical sided permeable wall, flow through an earth dam with a central core, and unconfined flow to a well. A digital computer was employed by Hendrick (1965) in a relaxation analysis of unconfined well flow, to obtain a comparison with the results of his membrane analogy investigation.

3.3 Flow Through Rockfill

The application of rockfill to the construction of dams was considered by Wilkins (1956). Wilkins carried out permeameter tests on rockfill of large particle size, to determine the appropriate head loss equations and applied these equations to the design of dams. Sandie (1961) undertook a series of experiments on the self-spillway type of rockfill dam proposed by Wilkins and suggested that there were four main regions of flow as shown in Fig. 3-3-1.

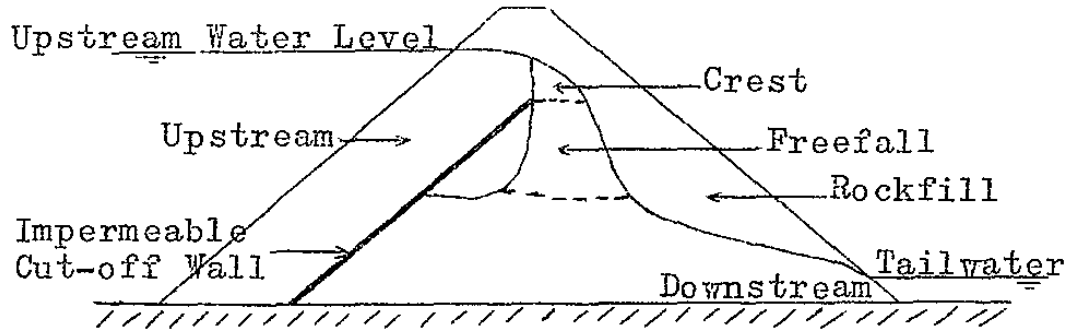

FIG. 3-3-1 FLOW REGIONS IN A SELF SPILLWAY DAM
(After Sandie, 1961)

These regions are:

(a) the upstream region, which is the part of the flow upstream of the impervious cut-off wall;

(b) the crest region, adjacent to the crest of the cut-off wall;

(c) the freefall region, where the water falls freely through the rockfill;

(d) the downstream region, where the water flows through the rockfill along the horizontal impervious base downstream of the cut-off wall.

Sandie also investigated the stability aspects of these dams and undertook theoretical considerations of the free surface profile in the downstream region. Sharp (1961) considered the height of the exit point at the downstream bank of self-spillway rockfill dams.

The results from further model studies on inbuilt spillway rockfill dams were discussed by Lawson, Trollope

and Parkin (1963) who suggested methods of analysis for some flow regions. Although the upstream region was considered intractable to direct analysis, approximate methods of solution were formulated for the other regions. Flow in the crest region was considered to be related to three representative lengths, the vertical depth of flow at the top of the spillway, the minimum width of flow in the crest region (at 45 degrees to the vertical), and the horizontal width of flow at the crest. Flow in the freefall region was shown to correspond to unit energy gradient while the downstream section was analysed by assuming uniform horizontal velocity at any section.

A comprehensive study of hydraulic characteristics of rockfill dams with inbuilt spillways was carried out by Parkin (1963a) who formulated methods for their design. Fenton (1968) obtained numerical solutions for flow through rockfill banks with no impervious membrane by a finite element analysis of the field equation based on the exponential law for head loss. Fenton investigated discharge variations as well as stability aspects for a number of values of the exponent m in the head loss relation.

The stability aspects of rockfill have been investigated by a number of authors including Lewis (1965), who

briefly discussed the shear strength of rockfill and the difficulties involved in measuring it. Wilkins (1963) drew flow nets from model tests on rockfill, but he indicated that there were considerable difficulties involved in measuring piezometric heads for turbulent flow through rockfill. Based on the flow nets and other considerations, Wilkins formulated a method of stability analysis and suggested most appropriate arrangements of steel bars to stabilise the downstream slope.

Deep seated slip failures of rockfill were investigated by Parkin (1963b) who applied the systematic arching theory developed by Trollope (1957) to the analysis of the stability of the downstream slope of rockfill dams. Discharge and stability aspects of flow through rockfill were considered by Parkin, Trollope and Lawson (1966). They indicated how non-Darcy flow could be analysed on the basis of an exponential head loss relation and discussed stability aspects in some detail. Design charts were produced for both stability and discharge calculations. Guidici (1967) commented on the mesh requirements for protection of the downstream face of a rockfill dam.

Sparks (1967) discussed the possibility of the two types of failure: erosion and sloughing, of the downstream

slope. He employed a tilting analogue model to simulate the activating forces on the slope. Sparks used the tilting analogue results and a nonlinear flow net obtained by the method of Wilkins (1963) to analyse the stability of the slope and to predict reinforcement requirements.

A comparatively recent development in dam construction methods is the practice of passing flood flows through and over rockfill coffer dams and partly completed earth and rockfill dams. Weiss (1951) discussed economic benefits of the use of the technique in the construction of a number of dams in Mexico. A comprehensive set of experiments on flow through and over rockfill was carried out by Olivier(1967). He considered the profiles established by rock when placed under various conditions in flowing water. Olivier developed a method for stability analysis based on the tractive force exerted on a rock by the flowing water and suggested a means of calculating the surface profile within rockfill from a modified open channel flow equation.

Model studies were reported by Speedie, Tadgell and Carr (1967) for two dams with upstream impermeable membranes. The model tests investigated the passing of flood flows through and over the rockfill during

construction and involved a consideration of the protection of the downstream face against erosion and slip failure. Lane (1967) discussed experience obtained in placing rockfill under flowing water, as a consequence of actual dam and coffer dam constructions chiefly in Africa. The results of model tests which were undertaken beforehand and observations of prototype flow conditions during construction showed that economical coffer dams may be achieved by designing rockfill to undergo several overtoppings.

Curtis and Lawson (1967), experimentally and theoretically, studied flow over and through rectangular shaped banks of rockfill. They considered overtopping flows by comparison with modified formulae for broad crested weirs. Flow within the rectangular shaped banks was analysed by a numerical solution of the field equation based on the exponential head loss relation.

Flow through jointed rock masses involves different principles from flow through rockfill because the particle size in the former case will usually be much larger than in the latter. Investigations such as that due to Barenblatt, Zheltov and Kochina (1960) have dealt with flow through rocks from the point of view of water movement in the fissures themselves rather than through

a homogeneous porous medium. Snow (1965) considered flow through joints in rock masses and suggested a parallel plate model to represent this flow condition. Wittke and Louis (1966) analysed laminar and turbulent flow within fissures and considered the effects of normal and shear stresses on the rocks.

Because of the larger particle size encountered in jointed rock masses, the analysis of flow conditions will usually need to be based on flow within the fissures. The assumptions made in the derivation of the partial differential field equations will often not be applicable so that analyses based on these equations will become inadequate. The solutions obtained in this thesis will therefore only be applicable to flow in rock masses, if the rock mass can be considered as a homogeneous porous medium; and, even in this case, a linear flow solution would usually be adequate.

CHAPTER 4

METHODS OF NUMERICAL ANALYSIS

4.1 Finite Difference and Finite Element Approaches

The field equations for steady saturated flow in undeformable porous media, derived in Sections 2.4 and 2.5, are partial differential equations of elliptic type and as such are amenable to solution by a numerical field approach. To obtain solutions to these equations it is necessary to delineate a region of flow and to specify relevant boundary conditions over a closed curve surrounding the region. The approach in obtaining a numerical solution to such problems is to solve for piezometric head values at a finite number of points throughout the field. Equations are written which involve the function value at discrete points throughout the field so that the solution of the problem reduces to the solution of a finite number of algebraic equations. This process is often referred to as discretization. The discretization procedures utilised in this thesis are the direct finite difference method and the finite element method.

The finite difference method is based on an approximation to the differential terms in the field equations by finite difference formulae involving the

function values at a node and its surrounding nodes. The differential equation at each interior nodal point is therefore replaced by an algebraic equation; the resultant set of equations, together with relevant conditions on the closed boundary, specify a unique set of values which may be obtained by solving the equations. The set of simultaneous equations may be solved by direct or iterative methods but because of the large number of unknowns, iterative methods are usually employed.

In an iterative solution, initial values of the function are assumed at all points and then better values are calculated from the surrounding nodal values by application of finite difference formulae. Southwell (1940; 1946) pioneered the relaxation process which involves calculation of the residual difference between the value at any point and the improved value obtained from the finite difference equation. The relaxation process allows a systematic reduction of the residuals at all points until the solution is obtained to a required degree of accuracy.

A slightly different iterative approach, called the method of squaring, had previously been developed by Thom (1928a, 1928b) and is described in detail by Thom and Apelt (1961). This approach has an advantage over

the relaxation process when computers are employed because it does not require the storage of residuals at all points in the field. The iterative finite difference formula is applied at all points until the change between successive values is smaller than some specified amount. The method of squaring has been employed in the finite difference solutions obtained in this thesis.

The finite element approach relies on the variational method of setting up the difference equations for the field. The region is divided into a finite number of elements in each of which the variation in properties is assumed to be linear. The problem of solving the differential equation is converted into a corresponding extremum problem involving the minimisation of an integral throughout the field. Minimisation with respect to each nodal value again yields an equal number of algebraic equations which are usually solved by iterative procedures.

In both the finite difference and finite element methods, the continuous field is assumed to be well represented by the solutions obtained for the nodal points, with a linear variation between the nodes.

4.2 Finite Difference Form of Field Equations

4.2.1 The Laplace equation

The Laplace differential equation, which was given

as equation 2.4-7 is of fundamental importance to a wide range of problems including steady heat flow, ideal fluid flow and linear laminar flow through porous media. For this reason, the numerical solution of the equation has been well treated in the literature (Shaw and Southwell, 1941; Thom and Apelt, 1961; Jeppson, 1968a). However a brief outline of the procedures involved will be given here as an introduction to the numerical approach which is similar to that used for the nonlinear flow field equations.

Consider a point 0, in a flow field, surrounded by other points in a regular array as shown in Fig. 4-2-1.

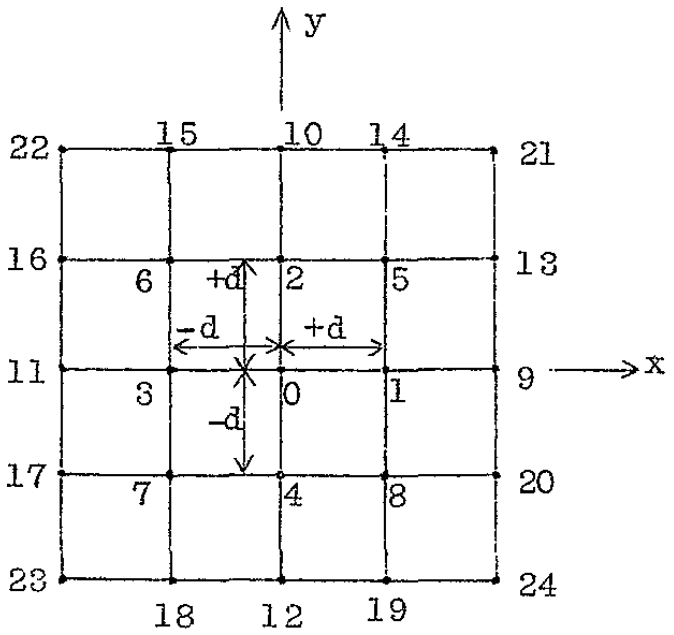

FIG. 4-2-1 FINITE DIFFERENCE NETWORK

The following commonly used shorthand representation of differentials will be used frequently throughout the remainder of this thesis:

$$\left.\begin{aligned} h_x &= \frac{\partial h}{\partial x} \quad ; \quad h_{xx} = \frac{\partial^2 h}{\partial x^2} \\ h_y &= \frac{\partial h}{\partial y} \quad ; \quad h_{yy} = \frac{\partial^2 h}{\partial y^2} \\ h_{xy} &= \frac{\partial^2 h}{\partial x \partial y} \; ; \quad h_{yx} = \frac{\partial^2 h}{\partial y \partial x} \end{aligned}\right\} \qquad \ldots\ldots 4.2\text{-}1$$

A Taylor series expansion about 0 in the positive and negative x directions then yields:

$$h_1 = h_o + d\, h_{ox} + \frac{d^2}{2!} h_{oxx} + \ldots\ldots \qquad \ldots\ldots 4.2\text{-}2$$

$$h_3 = h_o - d\, h_{ox} + \frac{d^2}{2!} h_{oxx} - \ldots\ldots \qquad \ldots\ldots 4.2\text{-}3$$

in which d, as used in this Chapter, represents the grid length of the finite difference mesh.

Combining equations 4.2-2 and 4.2-3 an expression for the derivative $\frac{\partial^2 h}{\partial x^2}$ at the point 0 is obtained as:

$$h_{oxx} = \frac{h_1 + h_3 - 2h_o}{d^2} \qquad \ldots\ldots 4.2\text{-}4$$

provided that terms of magnitude d^4 and above may be neglected. A similar analysis in the y direction yields:

$$h_{oyy} = \frac{h_2 + h_4 - 2h_o}{d^2} \qquad \ldots\ldots 4.2\text{-}5$$

Substitution in equation 2.4-7 results in a finite difference form of Laplace's equation:

$$h_1 + h_2 + h_3 + h_4 - 4h_o = 0 \qquad \ldots\ldots 4.2\text{-}6$$

provided again that terms of the order d^4 and above are negligible. Thus the finite difference equation to be applied at all points throughout the field is:

$$h_o = \frac{h_1 + h_2 + h_3 + h_4}{4} \qquad \ldots\ldots 4.2\text{-}7$$

This is the so-called "unit square" formula. In view of the assumption that terms of the order d^4 and higher are negligible, an obvious means of increasing the accuracy of a numerical solution is to decrease the grid size. However a decrease in grid size effectively increases the number of nodal points so that more equations have to be solved and, in computer applications, more variables stored in the memory. Thus the number of grid points should be chosen to give the required degree of accuracy with a minimum amount of computer storage and time.

An alternative method of increasing the accuracy of solution for a given number of iterations is to use finite difference formulae which include more points in

the field and so reduce the truncation error. Thom and Apelt (1961) gave an account of some higher-molecule formulae and their possible applications. Examples include the '20 formula', the '100 formula' and the '476 formula' which, for the points shown in Fig. 4-2-1, may be written as:

$$20h_o = 4S_1 + S_2 - 6d^2\nabla^2 h_o - \tfrac{1}{2}d^4\nabla^4 h_o + O(d^6)$$

$$100h_o = 10S_3 + 7S_4 + S_5 - 118d^2\nabla^2 h_o - \frac{215}{6}\, d^4\nabla^4 h_o$$
$$-\tfrac{1}{3}d^4 D^4 h_o + O(d^6)$$

$$476h_o = 46S_3 + 32S_4 + 9S_5 - 576d^2\nabla^2 h_o - 176d^4\nabla^4 h_o$$
$$- 48d^4 D^4 h_o + O(d^6)$$

.... 4.2-8

in which $\nabla^2 \equiv \dfrac{\partial^2}{\partial x^2} + \dfrac{\partial^2}{\partial y^2}$; $\nabla^4 \equiv \dfrac{\partial^4}{\partial x^4} + \dfrac{\partial^4}{\partial y^4}$

$$D^2 \equiv \frac{\partial^2}{\partial x \partial y} \qquad ; \quad D^4 \equiv \frac{\partial^4}{\partial x^2 \partial y^2}$$

and O means a term of the order of the function in the brackets; and:

$$S_1 = h_1 + h_2 + h_3 + h_4$$

$$S_2 = h_5 + h_6 + h_7 + h_8$$

$$S_3 = h_9 + h_{10} + h_{11} + h_{12}$$

$$S_4 = h_{13} + h_{14} + h_{15} + h_{16} + h_{17} + h_{18} + h_{19} + h_{20}$$

$$S_5 = h_{21} + h_{22} + h_{23} + h_{24}$$

.... 4.2-9

For Laplace's equation, Thom and Apelt indicate that the '100 formula' allows a solution to be obtained most quickly at least when using a desk calculator. However, it cannot be applied at points adjacent to the boundaries and the '20 formula' is therefore applied at these points when the boundaries are regular. At nodes adjoining the free surface, the situation is more complex because irregular grid lengths are involved. At these points a modification of the unit square formula for unequal arms is therefore employed. Fig. 4-2-2 shows a possible configuration where short arm lengths occur on both the vertical and horizontal grids.

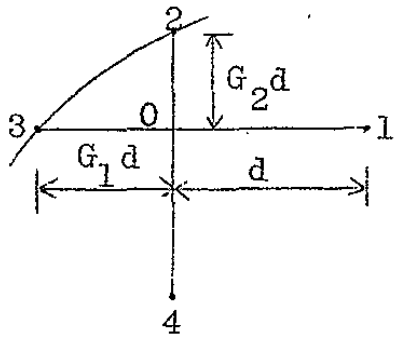

FIG. 4-2-2 IRREGULAR GRID LENGTHS AT FREE SURFACE

The shorter horizontal arm is of length $G_1 d$ while the vertical one is of length $G_2 d$, where d is the normal grid length. Taylor series expansions about the point 0 again enable a finite difference expression to be derived. For two-dimensional flow and for the configuration of Fig. 4-2-2, this expression is:

$$h_o = \frac{G_1(h_2+G_2h_4)}{(1+G_2)(G_1+G_2)} + \frac{G_2(h_3+G_1h_1)}{(1+G_1)(G_1+G_2)} \quad \ldots\ldots 4.2\text{-}10$$

If only one short arm occurs, equation 4.2-10 still applies with the value of the other ratio, G_1 or G_2 set to unity. Equation 4.2-10 reduces to the unit square formula when both ratios G_1 and G_2 are unity. However if either G_1 or G_2 differ from unity, the truncation error for the irregular star equation is of the order d^3 which is an order of magnitude larger than that for the unit square formula.

The preceding finite difference formulations of Laplace's equation apply to two-dimensional linear laminar flow through porous media, such as would be encountered in flow through a vertical sided permeable wall. For axisymmetric flow to a well, with co-ordinates as shown in Fig. 4-2-3, the corresponding form of Laplace's equation may be written:

$$\frac{\partial^2 h}{\partial r^2} + \frac{1}{r}\frac{\partial h}{\partial r} + \frac{\partial^2 h}{\partial z^2} = 0 \quad \ldots\ldots 4.2\text{-}11$$

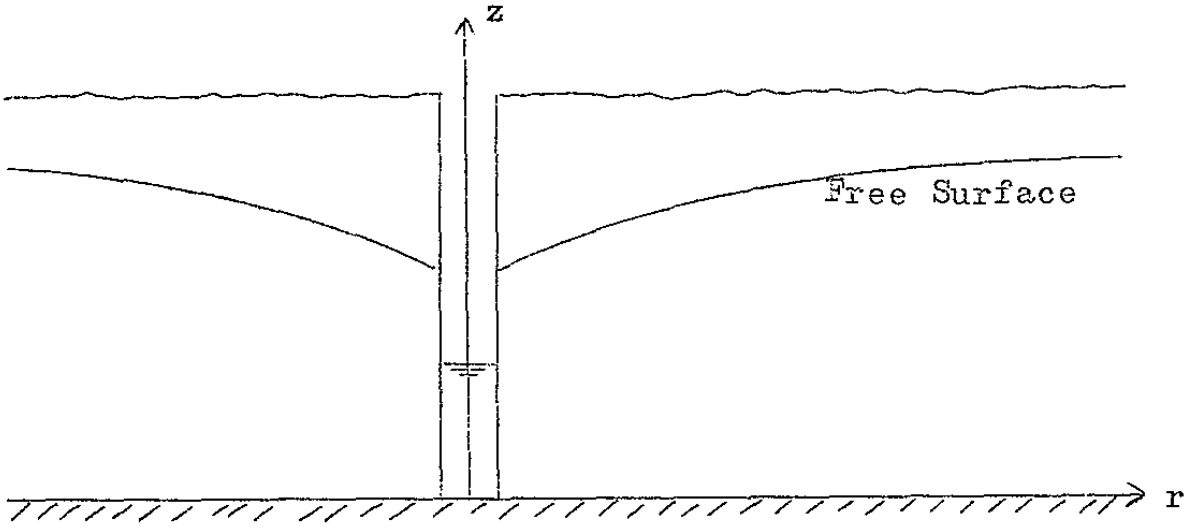

FIG. 4-2-3 CO-ORDINATES FOR AXISYMMETRIC FLOW

Substituting r for x in Fig. 4-2-1 the finite difference approximation to the term $\frac{\partial h}{\partial r}$ may be obtained by subtracting equation 4.2-3 from 4.2-2:

$$h_1 - h_3 = 2dh_{or}$$

or
$$h_{or} = \frac{h_1 - h_3}{2d} \qquad \ldots\ldots 4.2\text{-}12$$

where the truncation error is of the order d^3. The complete finite difference formulation for the axisymmetric Laplace equation may then be written as:

$$h_o = \frac{h_1 + h_2 + h_3 + h_4}{4} + \frac{h_1 - h_3}{r\ 8d} \qquad \ldots\ldots 4.2\text{-}13$$

where the unit square approximation to the term $\frac{\partial^2 h_o}{\partial r^2} + \frac{\partial^2 h_o}{\partial z^2}$ has been used. Observation of the higher molecule formulae, equation 4.2-8, indicates that in each

of the '20, 100 and 476 formulae' the term $\nabla^4 h_o$ must be zero before the truncation error is reduced to the order of d^6 and in the '100 and 476 formulae' the term $D^4 h_o$ would also have to be zero. For two-dimensional flow the condition of $\nabla^4 h_o$ being zero is satisfied from the fact that $\nabla^2 h_o$ is zero. However, for axisymmetric flow, equation 4.2-11 indicates that $\nabla^2 h_o$ is not zero and for small values of r the term $\frac{1}{r}\frac{\partial h}{\partial r}$ will be quite significant.

In representing the term $\nabla^2 h_o$ then for axisymmetric flow the truncation error in the higher molecule formulae, equation 4.2-28, is effectively increased to the order of d^4. As a result there appears to be little advantage in using these formulae instead of the unit square formula especially when the increased time per iteration is considered for the higher molecule approximations. For example Fromm (1963) and Stark (1968) in computerised solutions of the Navier-Stokes equations showed that there was no advantage in the use of the '20 or 100 formulae' because, while the number of iterations to achieve a required accuracy was reduced, the total computer time was longer because of the increased time per iteration with the more complex formulae. Also, the '100 formula' for example, cannot be used at nodes immediately adjacent to the boundary and the 20 or unit formula must then be

applied; and as error terms differ from equation to equation, combining these formulae in effect introduces new error terms which may be of increased magnitude. For axisymmetric flow, equation 4.2-13 has therefore been applied throughout the finite difference network to yield successively better approximations to the true value of piezometric head at each point.

For points adjacent to the free surface, equation 4.2-13 must be revised for short arm lengths. The derivative $\frac{\partial h}{\partial r}$ becomes:

$$\frac{\partial h}{\partial r} = h_{or} = \frac{G_1^2 h_1 - h_3 + (1-G_1^2)h_o}{G_1 d(1+G_1)} \qquad \ldots\ 4.2\text{-}14$$

Dividing equation 4.2-14 by r and adding to the finite difference expression for $\frac{\partial^2 h}{\partial r^2} + \frac{\partial^2 h}{\partial z^2}$ yields the appropriate axisymmetric finite difference equation for short arm lengths:

$$h_o\left\{(G_1+G_2) - \frac{dG_2(1-G_1)}{2r}\right\} = \frac{G_1(h_2+G_2h_4)}{(1+G_2)} +$$

$$\frac{G_2(G_1h_1+h_3)}{(1+G_1)} + \frac{dG_2(G_1^2h_1-h_3)}{2r(1+G_1)} \qquad \ldots\ 4.2\text{-}15$$

Equation 4.2-15 then is the iterative formula for a node with unequal surrounding grid lengths.

Because the free surface necessitates the use of cumbersome finite difference equations to allow for irregular grid lengths, Thom and Apelt (1961) suggested an alternative method of solution for free-streamline problems. This method is based on the property that if ϕ and ψ are conjugate functions which satisfy Laplace's equation in the x-y plane then x and y will be conjugate functions satisfying Laplace's equation in the ϕ, ψ plane.

Thus if $$\frac{\partial^2\phi}{\partial x^2} + \frac{\partial^2\phi}{\partial y^2} = 0$$

and $$\frac{\partial^2\psi}{\partial x^2} + \frac{\partial^2\psi}{\partial y^2} = 0 \qquad \text{.... 4.2-16}$$

then $$\frac{\partial^2 x}{\partial\phi^2} + \frac{\partial^2 x}{\partial\psi^2} = 0$$

and $$\frac{\partial^2 y}{\partial\phi^2} + \frac{\partial^2 y}{\partial\psi^2} = 0 \qquad \text{.... 4.2-17}$$

For porous media flow obeying Darcy's Law a potential function ϕ can be defined as:

$$\phi = - kh \qquad \text{.... 4.2-18}$$

and a streamline function ψ can be defined as:

$$\frac{\partial\psi}{\partial x} = v \quad \text{and} \quad \frac{\partial\psi}{\partial y} = -u \qquad \text{.... 4.2-19}$$

The functions ϕ and ψ can then be shown to satisfy equation 4.2-16 so that equation 4.2-17 also applies in the inverse plane. The solution in the inverse plane has the advantage

that it is often possible to obtain a field of rectangular shape so that the finite difference grid can be fitted exactly without recourse to short arm lengths. Jeppson (1966) used this method to solve a number of problems including seepage from ditches, axisymmetric jet flows and seepage through a dam with a horizontal downstream under-drain. Cassidy (1965) obtained solutions for flow over spillways by the inverse function approach while Markland (1966) solved the problem of a free overfall at the end of an open channel.

However the method has two major disadvantages in the problems analysed in this thesis. The main object of obtaining Laplace solutions was to give reasonable initial values for the nonlinear solutions. For the nonlinear flow equations no corresponding simple relationships between conjugate functions can be obtained so that the method of inverse functions cannot readily be applied. Since the nonlinear solutions are carried out in the physical plane, it is logical to obtain initial values from Darcy flow solutions in this plane also.

In addition, the problems discussed herein have usually involved a seepage surface, either at the downstream bank of a dam or permeable wall, or at the well face in unconfined flow to a well. This seepage surface

is neither an equipotential line nor a streamline so that the boundaries on the inverse plane do not form a rectangular pattern. The situation is illustrated for seepage through a two-dimensional vertical sided permeable wall as shown in Fig. 4-2-4.

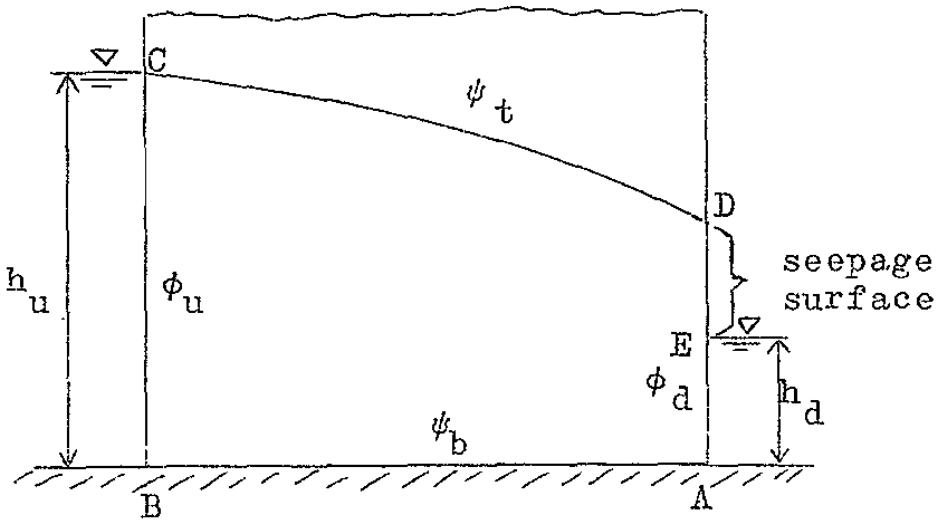

FIG. 4-2-4 FLOW THROUGH PERMEABLE WALL - PHYSICAL PLANE

The impervious base AB and the free surface CD are streamlines while the upstream and downstream boundaries below water level, BC and AE are equipotential lines, but the seepage surface DE does not belong to either category. Thus in representing the flow field on the inverse plane as shown in Fig. 4-2-5, DE forms an initially unknown section of the boundary. The boundary configuration is therefore not rectangular so that short grid lengths and associated cumbersome finite difference formulae will still be necessary. It is, however,

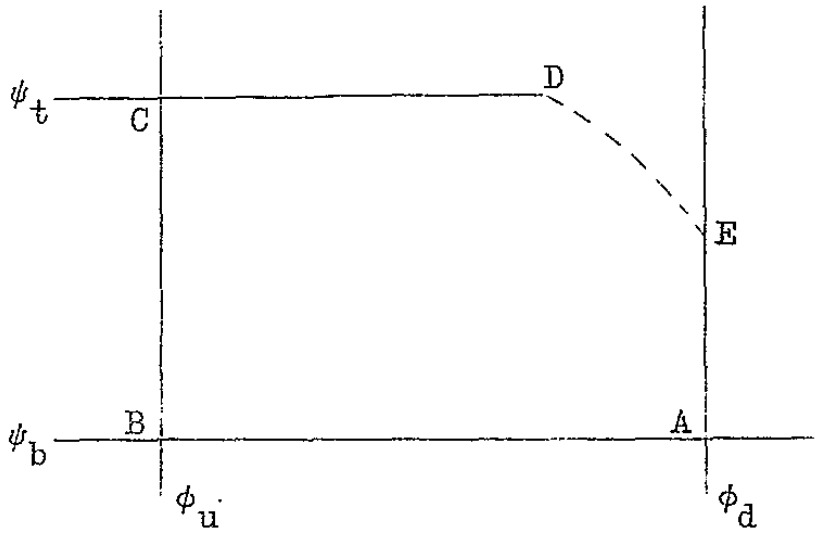

FIG. 4-2-5 FLOW THROUGH PERMEABLE WALL - INVERSE PLANE

possible that the free surface adjustment procedure may be simplified in the inverse plane but two fields of values, x and y, have to be solved whereas only one field of h values need be considered in the physical plane. The numerical solutions outlined in this thesis have therefore been obtained by solving for piezometric head values in the physical plane.

4.2.2 Forchheimer field equation

In section 2.5.1 the Forchheimer field equation for two-dimensional flow was derived as equation 2.5-25. For finite difference applications, equation 2.5-25 can be more suitably restated as:

$$\frac{\partial}{\partial x}\left[\frac{h_x}{\frac{a}{2}+\sqrt{\frac{a^2}{4}+b|h_s|}}\right]+\frac{\partial}{\partial y}\left[\frac{h_y}{\frac{a}{2}+\sqrt{\frac{a^2}{4}+b|h_s|}}\right]=0 \quad \ldots 4.2\text{-}20$$

To simplify the derivation, the term h_s will now be taken to mean the magnitude of the head gradient. That is h_s will be written instead of $|h_s|$.

$$\text{If} \quad f = f(h_s) = \left\{ \frac{a}{2} + \sqrt{\frac{a^2}{4} + bh_s} \right\}^{-1} \qquad \ldots\ldots 4.2\text{-}21$$

$$\text{then} \quad \frac{\partial f}{\partial x} = (-1)\left\{ \frac{a}{2} + \sqrt{\frac{a^2}{4} + bh_s} \right\}^{-2} \frac{1}{2}\left(\frac{a^2}{4} + bh_s\right)^{-\frac{1}{2}} b.\frac{\partial h_s}{\partial x} \qquad \ldots\ldots 4.2\text{-}22$$

$$\text{and} \quad \frac{\partial f}{\partial y} = (-1)\left\{ \frac{a}{2} + \sqrt{\frac{a^2}{4} + bh_s} \right\}^{-2} \frac{1}{2}\left(\frac{a^2}{4} + bh_s\right)^{-\frac{1}{2}} b.\frac{\partial h_s}{\partial y} \qquad \ldots\ldots 4.2\text{-}23$$

Now at any point, the hydraulic gradient in the direction of flow is given by:

$$\left.\begin{aligned} h_s \, \underline{s} &= h_x \, \underline{i} + h_y \, \underline{j} \\ h_s^{\,2} &= h_x^{\,2} + h_y^{\,2} \end{aligned}\right\} \qquad \ldots\ldots 4.2\text{-}24$$

$$\left.\begin{aligned} \text{Thus} \quad 2h_s \frac{\partial h_s}{\partial h_x} &= 2h_x \\ \text{or} \quad \frac{\partial h_s}{\partial h_x} &= \frac{h_x}{h_s} \end{aligned}\right\} \qquad \ldots\ldots 4.2\text{-}25$$

$$\text{Similarly} \quad \frac{\partial h_s}{\partial h_y} = \frac{h_y}{h_s} \qquad \ldots\ldots 4.2\text{-}26$$

$$\text{Then} \quad \frac{\partial h_s}{\partial x} = \frac{\partial h_s}{\partial h_x} \cdot \frac{\partial h_x}{\partial x} + \frac{\partial h_s}{\partial h_y} \cdot \frac{\partial h_y}{\partial x}$$

$$= \frac{h_x}{h_s} h_{xx} + \frac{h_y}{h_s} h_{yx} \qquad \ldots\ldots 4.2\text{-}27$$

Similarly $\frac{\partial h_s}{\partial y} = \frac{h_y}{h_s} \cdot h_{yy} + \frac{h_x}{h_s} \cdot h_{xy}$ 4.2-28

Substituting equations 4.2-21 and 4.2-27 in equation 4.2-22 yields:

$$\frac{\partial f}{\partial x} = - \frac{f^2 b}{2}\left(\frac{a^2}{4} + bh_s\right)^{-\frac{1}{2}} \left(\frac{h_x}{h_s} h_{xx} + \frac{h_y}{h_s} h_{yx}\right) \quad .... \ 4.2\text{-}29$$

Similarly equation 4.2-23 becomes:

$$\frac{\partial f}{\partial y} = - \frac{f^2 b}{2}\left(\frac{a^2}{4} + bh_s\right)^{-\frac{1}{2}} \left(\frac{h_y}{h_s} h_{yy} + \frac{h_x}{h_s} h_{xy}\right) \quad .... \ 4.2\text{-}30$$

The field equation 4.2-20 may now be rewritten:

$$\frac{\partial}{\partial x}(h_x f) + \frac{\partial}{\partial y}(h_y f) = 0$$

or $$h_x \frac{\partial f}{\partial x} + f h_{xx} + h_y \frac{\partial f}{\partial y} + f h_{yy} = 0 \quad .... \ 4.2\text{-}31$$

Substitution of equations 4.2-29 and 4.2-30 in equation 4.2-31 gives the field equation for Forchheimer flow in a form suitable for direct application of finite difference approximations:

$$h_{xx} - \frac{h_x}{h_s} \frac{f}{2} b\left(\frac{a^2}{4} + bh_s\right)^{-\frac{1}{2}} (h_x h_{xx} + h_y h_{yx})$$

$$+ h_{yy} - \frac{h_y}{h_s} \frac{f}{2} b\left(\frac{a^2}{4} + bh_s\right)^{-\frac{1}{2}} (h_y h_{yy} + h_x h_{xy}) = 0$$

.... 4.2-32

The finite difference formulation for equation 4.2-32 is best carried out in a number of steps. For the arrange-

ment of nodes shown in Fig. 4-2-1 the derivatives h_{ox} and h_{oy} become:

$$\left.\begin{aligned} h_{ox} &= \frac{h_1 - h_3}{2d} \\ h_{oy} &= \frac{h_2 - h_4}{2d} \end{aligned}\right\} \quad \ldots\ldots 4.2\text{-}33$$

The gradient h_{os} can then be calculated from equation 4.2-24 and substituted in equation 4.2-21 to obtain the function f. Having calculated h_{os} and f, a number of terms in equation 4.2-32 can now be grouped into one factor denoted as FACT:

$$\text{FACT} = \frac{f}{h_{os}} \frac{b}{2} \left(\frac{a^2}{4} + bh_s\right)^{-\frac{1}{2}} \quad \ldots\ldots 4.2\text{-}34$$

The second derivative h_{oyx} can be obtained by evaluating h_y at points 1 and 3 and considering expansions about point 0 in the x direction. Thus:

$$h_{oyx} = \frac{h_5 - h_8 - h_6 + h_7}{4d^2} = h_{oxy} \quad \ldots\ldots 4.2\text{-}35$$

since h_{oxy} and h_{oyx} are equal.

Using equation 4.2-35 and equations 4.2-4 and 4.2-5, equation 4.2-32 in finite difference form becomes:

$$h_1 + h_2 + h_3 + h_4 - 4h_o - \text{FACT}\, h_{ox}^2(h_1+h_3-2h_o) - \text{FACT}\, h_{oy}^2(h_2+h_4-2h_o) - 0.5\ \text{FACT}\, h_{ox}\, h_{oy} (h_5-h_8-h_6+h_7) = 0 \quad \ldots 4.2\text{-}36$$

or on rearranging:

$$h_o = \Big[h_1+h_2+h_3+h_4-\text{FACT}\Big\{h_{ox}^{\,2}(h_1+h_3)+h_{oy}^{\,2}(h_2+h_4) + 0.5\, h_{ox}h_{oy}(h_5-h_8-h_6+h_7)\Big\}\Big]\Big/(4-2\text{FACT}\, h_{os}^{\,2}) \quad \ldots\ldots 4.2\text{-}37$$

in which h_{ox} and h_{oy} are given by equation 4.2-33.

Higher molecule formulae for the $\nabla^2 h_o$ terms are not considered since $\nabla^2 h_o$ is not zero for nonlinear flow, while higher molecule approximations to equation 4.2-37 as a whole, with significantly lower truncation errors would result in very complex iterative formulae with substantially increased iteration time. Equation 4.2-37 has therefore been employed as the iterative finite difference formula for successive application at regular interior nodal points when the flow is governed by a Forchheimer head loss relation.

At points adjacent to the free surface, equation 4.2-37 has to be modified to allow for either one or two grid lengths to be shorter than the standard length. The procedure follows the same steps as outlined for regular grid lengths. For the configuration of nodes shown in Fig. 4-2-2, the derivatives h_{ox} and h_{oy} may be evaluated as:

$$h_{ox} = \frac{G_1^2 h_1 - h_3 + (1 - G_1^2)h_o}{G_1 d(1 + G_1)}$$

$$h_{oy} = \frac{h_2 - G_2^2 h_4 - (1 - G_2^2)h_o}{G_2 d(1 + G_2)} \qquad \text{.... 4.2-38}$$

The gradient h_{os} is again obtained from equation 4.2-24 and the function f from equation 4.2-21. The combined term FACT is then calculated according to equation 4.2-34.

The second derivatives h_{oxx} and h_{oyy} in this case are given by:

$$h_{oxx} = \frac{2\{G_1 h_1 + h_3 - h_o(1+G_1)\}}{G_1(1+G_1)d^2}$$

$$h_{oyy} = \frac{2\{G_2 h_4 + h_2 - h_o(1+G_2)\}}{G_2(1+G_2)d^2} \qquad \text{..... 4.2-39}$$

The second derivative h_{oyx} is more difficult to calculate especially if a short arm occurs in the horizontal direction. For this case, h_{oyx} is calculated from the values of h_y at points 0 and 1 because it is impossible to obtain an accurate value of h_y at point 3. When only one short arm, in the vertical direction, occurs h_{oyx} is obtained from values of h_y at points 1 and 3. Substitution of all terms in equation 4.2-32 allows the final finite difference formula for h_o to be obtained.

For axisymmetric flow to a well, the field equation 4.2-20 must be modified to allow for the radial convergence

of the flow. For axisymmetric flow, the continuity equation is:

$$\frac{\partial V_r}{\partial r} + \frac{V_r}{r} + \frac{\partial V_z}{\partial z} = 0 \qquad \ldots\ 4.2\text{-}40$$

in which V_r and V_z are the velocities in the r and z co-ordinate directions of Fig. 4-2-3. Substituting for V_r and V_z, equation 4.2-40 becomes:

$$\frac{\partial}{\partial r}\left[\frac{h_r}{\frac{a}{2}+\sqrt{\frac{a^2}{4}+bh_s}}\right] + \frac{h_r}{h_s}\frac{V}{r} + \frac{\partial}{\partial z}\left[\frac{h_z}{\frac{a}{2}+\sqrt{\frac{a^2}{4}+bh_s}}\right] = 0 \qquad \ldots\ 4.2\text{-}41$$

in which V is the velocity in the s direction and is given by

$$V = -\frac{a}{2b} + \sqrt{\left(\frac{a}{2b}\right)^2 + \frac{h_s}{b}} \qquad \ldots\ 4.2\text{-}42$$

It is apparent that equation 4.2-41 is equivalent to equation 4.2-20 with the extra term $\frac{h_r}{h_s}\frac{V}{r}$ added to the left hand side. The finite difference approximation is therefore obtained by an analogous procedure to that used for equation 4.2-20. The derivatives h_{or} and h_{oz} are first obtained and then h_{os} is calculated from them. Substitution of h_{os} in equation 4.2-21 gives the function f. The term FACT is again calculated from equation 4.2-34 and all the subsidiary variables can be substituted into equation 4.2-41 to give the final finite difference equation for axisymmetric Forchheimer flow:

$$h_o = \Big[h_1+h_2+h_3+h_4-\text{FACT}\Big\{h_{or}^{\,2}(h_1+h_3)+h_{oz}^{\,2}(h_2+h_4) + 0.5\, h_{or}h_{oz}(h_5-h_8-h_6+h_7)\Big\}\Big]/(4-2\ \text{FACT}\ h_{os}^{\,2}) + \big[h_{or}d^2\ l\big]/\big[r\ (4-2\ \text{FACT}\ h_{os}^{\,2})\big] \qquad \ldots. \ 4.2\text{-}43$$

since V and f h_{os} are equal. A similar analysis, to that for the two-dimensional flow case, can again be undertaken when one or two grid lengths are shorter than normal.

4.2.3 Exponential field equation

The field equation for flow obeying an exponential head loss relation was given in section 2.5.2 as equation 2.5-30. After multiplying by the constant -c in this equation and writing h_s instead of $|h_s|$ as before, equation 2.5-30 may be rewritten:

$$\frac{\partial}{\partial x}\left(h_s^{\,1-m/m}\,h_x\right)+\frac{\partial}{\partial y}\left(h_s^{\,1-m/m}\,h_y\right)=0 \qquad \ldots. \ 4.2\text{-}44$$

If $M = \frac{1-m}{m}$

then equation 4.2-44 becomes:

$$h_{xx}\,h_s^{M}+h_x\,Mh_s^{M-1}\frac{\partial h_s}{\partial x}+h_{yy}\,h_s^{M}+h_y\,Mh_s^{M-1}\frac{\partial h_s}{\partial y}=0 \qquad \ldots. \ 4.2\text{-}45$$

Using equations 4.2-27 and 4.2-28, equation 4.2-45 becomes:

$$h_{xx}+h_{yy}+\frac{M}{h_s^{\,2}}\left(h_x^{\,2}h_{xx}+2h_xh_yh_{xy}+h_y^{\,2}h_{yy}\right)=0 \qquad \ldots. \ 4.2\text{-}46$$

This is the equation which has been obtained by Brooker (1961), Parkin (1963a) and others. Using equations 4.2-4, 4.2-5 and 4.2-35, equation 4.2-46 may be written in finite difference form. For the configuration of points shown in Fig. 4-2-1 this becomes:

$$h_o = \Big[h_{os}^2 (h_1+h_2+h_3+h_4)+M\Big\{h_{ox}^2(h_1+h_3)+0.5\, h_{ox}h_{oy} (h_5-h_8-h_6+h_7)+ h_y^2 (h_2+h_4)\Big\}\Big]/2(2+M)h_{os}^2 \quad .... \quad 4.2\text{-}47$$

where h_{ox} and h_{oy} are given by equation 4.2-33 and h_{os} is given by equation 4.2-24. This is the iterative formula to be applied at interior nodes when the flow is governed by an exponential head loss relation. For points adjacent to the free surface, equation 4.2-47 must be modified to allow for short arm lengths. The modification is made in a manner similar to that employed for the Forchheimer field equation.

For axisymmetric flow the field equation 4.2-44 must be modified also and, in cylindrical co-ordinates, becomes:

$$\frac{\partial}{\partial r}(h_r\, h_s^M) + \frac{h_r h_s^M}{r} + \frac{\partial}{\partial z}(h_z\, h_s^M) = 0 \quad .... \quad 4.2\text{-}48$$

Using the configuration of points of Fig. 4-2-1 this equation may be written in finite difference form as:

$$h_o = \Big[h_{os}^2(h_1+h_2+h_3+h_4)+ \frac{h_{os}^2 h_{or}}{r} + M\Big\{h_{or}^2(h_1+h_3) + 0.5\, h_{or}h_{oz}(h_5-h_8-h_6+h_7)+h_{oz}^2(h_2+h_4)\Big\}\Big]/2(2+M)h_{os}^2$$

.... 4.2-49

For points adjacent to the free surface, the corresponding form of equation 4.2-49 for irregular arm lengths may be derived as before.

4.3 Boundary Conditions and Adjustment of the Free Surface in the Finite Difference Approach

The boundary conditions and surface adjustment techniques are similar for two-dimensional flow through a vertical sided permeable wall and axisymmetric flow to a well. Only flow through the permeable wall will therefore be considered in the following discussion, the axisymmetric flow situation being treated by the same procedures. Consider flow through a vertical sided bank as shown in Fig. 4-3-1.

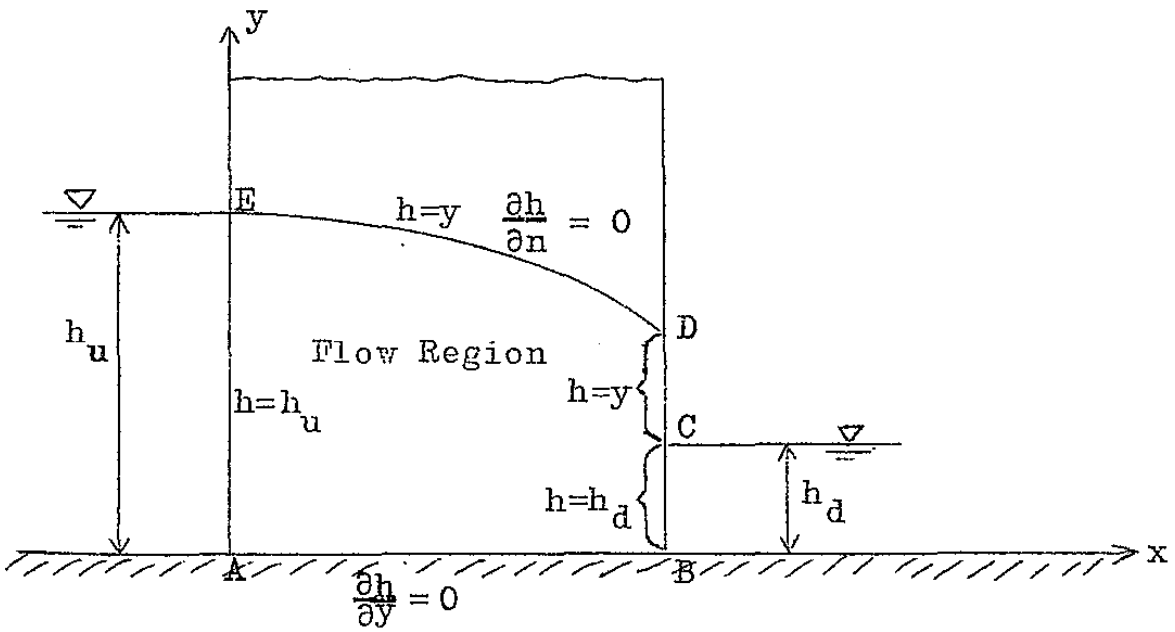

FIG. 4-3-1 BOUNDARY CONDITIONS

The boundary conditions include a number of types. The upstream wall AE and the submerged downstream section BC are lines of constant piezometric head with resultant Dirichlet boundary conditions:

$$\left.\begin{array}{ll} \text{On AE} & h = h_u \\ \text{on BC} & h = h_d \end{array}\right\} \quad \ldots\ldots 4.3\text{-}1$$

Along the seepage surface CD, the piezometric head is equal to the height above the impermeable stratum:

$$\text{On CD} \quad h = y \qquad \ldots\ldots 4.3\text{-}2$$

The impervious base AB is a streamline so that the head gradient normal to this line must be zero, resulting in a Neumann type boundary condition:

$$\text{On AB} \quad \frac{\partial h}{\partial y} = 0 \qquad \ldots\ldots 4.3\text{-}3$$

The free surface ED involves a mixed type of boundary condition. Since it is a streamline the head gradient normal to it must be zero and since the pressure is atmospheric along ED the piezometric head must equal the elevation above the impermeable base:

$$\text{On CD} \quad \frac{\partial h}{\partial n} = 0 \qquad \ldots\ldots 4.3\text{-}4$$

$$\text{and} \quad h = y \qquad \ldots\ldots 4.3\text{-}5$$

in which n represents the direction of the normal to the free surface at any point.

The imposition of the Dirichlet boundary conditions in the numerical solutions is relatively simple. The piezometric heads at all nodes on AE and BC are set equal to h_u and h_d respectively, while at each node on CD the piezometric head is set equal to the elevation of the node above the base.

The Neumann boundary condition on AB could be imposed by first calculating the normal derivative, in terms of h values at nodes on AB and at the nodes directly above them; and when this normal derivative is set to zero new values of h on AB could be obtained. For nodes as depicted in Fig. 4-3-2, the following relation can be obtained by Taylor series expansions from h_o:

$$18h_1 - 9h_2 + 2h_3 = 11h_o + 6d\, h_{oy} \qquad \ldots. \ 4.3\text{-}6$$

where the truncation error is of the order d^4.

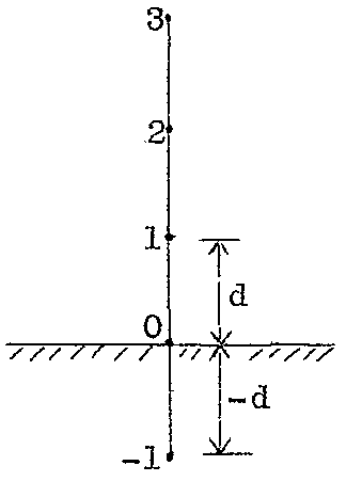

FIG. 4-3-2 NODE ARRANGEMENT AT BOTTOM BOUNDARY

Since h_{oy} is zero according to equation 4.3-3, equation 4.3-6 may be rewritten to evaluate a new value of h_o for the boundary node:

$$h_o = \frac{18h_1 - 9h_2 + 2h_3}{11} \qquad \ldots\ 4.3\text{-}7$$

However, equation 4.3-7 is derived from one-sided difference formulae about h_o, so that Forsythe and Wasow (1960) suggested an alternative method using more suitable central differences. Shaw and Southwell (1941) had also used this method which is based on the inclusion of a fictitious row of nodes at distance d below the line AB, one node of this row being shown as the point -1 in Fig. 4-3-2. The requirement of zero normal derivative at 0 is then met by putting:

$$h_{-1} = h_1 \qquad \ldots\ 4.3\text{-}8$$

Although the truncation error in equation 4.3-8 is theoretically of the order d^3, this equation is more suitable than equation 4.3-7 because it is based on central differences, and Giese (1958) has shown that smaller discretization errors occur with centred differences than with one-sided differences. The row of nodes AB is therefore treated as an interior row for application of the finite difference form of Laplace's equation and the bottom boundary condition is imposed by application of equation 4.3-8 to obtain new h values for the

fictitious row below AB.

Flow problems involving a free surface usually cause considerable difficulty in imposing the required boundary conditions. One treatment of free surface flow has been incorporated in the "marker and cell" method developed by the Los Alamos Scientific Laboratory team, and reported by Harlow and Welch (1965), in which the full Navier-Stokes equations are analysed for fluid flow problems. However this method, which incorporates a polynomial representation of the free surface for imposing the boundary conditions, has been employed in the analysis of time-dependent problems where the initial position of the free surface is known.

In the present analysis, where steady flow is assumed, the initial position of the free surface is not known and an adjustment technique has to be incorporated to allow for errors in the assumption of the initial free surface position. The technique described below is similar to that used by Boulton (1951) (and discussed in more detail by Mohar, 1966 and Hendrick, 1965) but with some modifications.

Consider a portion of the free surface at an angle α to the horizontal as shown in Fig. 4-3-3.

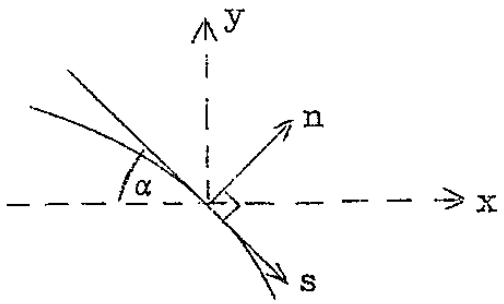

FIG. 4-3-3 NOMENCLATURE AT THE FREE SURFACE

Boulton (1951) has shown that the condition expressed by equation 4.3-4 can be rewritten in terms of the derivatives with respect to x and y. Thus:

$$\frac{\partial h}{\partial y} = \sin^2 \alpha \qquad \text{.... 4.3-9}$$

and $$\frac{\partial h}{\partial x} = -\sin \alpha \cos \alpha \qquad \text{.... 4.3-10}$$

in which α is the angle of the free surface to the horizontal at any point. Because of the curved nature of the free surface it is inappropriate to employ fictitious nodes above it, and a similar approach to that used for the bottom boundary is therefore not possible. As a result, one-sided difference formulae are necessary and these also must account for a shortened grid length between the surface node and the adjacent interior node in each direction. Consider first a vertical grid line intersecting the free surface as shown in Fig. 4-3-4. Since h = z at the free surface then

$$z_{oy} = h_{oy} \qquad \text{.... 4.3-11}$$

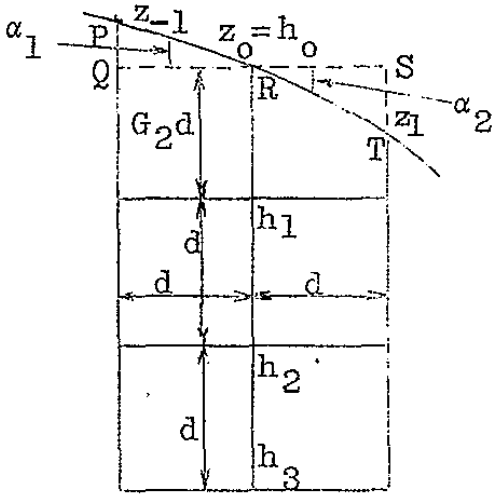

FIG. 4-3-4
INTERSECTION OF VERTICAL
GRID LINE WITH FREE SURFACE

and Taylor series expansions about z_o to h_1 and h_2 allow z_{oy} to be calculated as:

$$z_{oy} = \frac{z_o(1+2G_2) + G_2^2 h_2 - (1+G_2)^2 h_1}{G_2 d(1+G_2)} \qquad \ldots\ 4.3\text{-}12$$

in which the truncation error is of the order d^3. More points below z_o could be employed to reduce the order of the truncation error. However, since one-sided differences are used it is considered better to restrict the Taylor series expansion to points in the immediate vicinity of z_o; otherwise the points used for calculating the derivative extend too far away from the point at which the derivative is to be determined. For this reason only the two closest points have normally been incorporated in the finite difference formula.

Now from equations 4.3-9 and 4.3-11:

$$z_{oy} = \sin^2 \alpha \qquad \ldots\ 4.3\text{-}13$$

A value of $\sin\alpha$ is therefore required at the point R. Since the finite difference network can only approximate the free surface by a number of discrete points along it, the calculation of $\sin\alpha$ must be based on the assumption of short straight line segments joining these points. The value of $\sin\alpha$ at point R is assumed to be the average of $\sin\alpha_1$ and $\sin\alpha_2$ where α_1 and α_2 are as shown in Fig. 4-3-4. $\sin\alpha_1$ is calculated from the triangle PQR and $\sin\alpha_2$ from triangle RST. Once $\sin^2\alpha$ has been determined, a new value for z_o can be obtained by combining equations 4.3-12 and 4.3-13 to give:

$$z_o = \frac{G_2 d(1+G_2)\sin^2\alpha + (1+G_2)^2 h_1 - G_2^2 h_2}{1+2G_2} \qquad \ldots. \text{ 4.3-14}$$

The height of the free surface above the base at the vertical grid line is then set equal to this value of z_o and the shortened grid length, $G_2 d$ from the nearest node, is recalculated. When the surface is being adjusted downwards, equation 4.3-14 does not allow z_o to decrease below the value of h_1 so that once the intercept $G_2 d$ becomes smaller than some preset value, the adjustment is carried out from the second closest node. Equation 4.3-14 can still be applied but with G_2 replaced by $1 + G_2$, h_1 replaced by h_2 and h_2 by h_3. This allows the surface adjustment to proceed downwards across

horizontal grid lines. No similar problem is encountered in adjusting the surface upwards.

Equation 4.3-14 is not applied at the upstream and downstream banks; that is to say it is not applied at the vertical grid lines AE and BD in Fig. 4-3-1. The height h_u to E is fixed so that the position of E remains constant, while at D, the junction of the free surface with the downstream face, equation 4.3-14 alone does not adequately represent the boundary requirement. From theoretical considerations, Dachler (1934) suggested that ED should meet CD tangentially at D; but an extremely fine net would be required to represent this condition satisfactorily in a finite difference solution. A solution was therefore attempted on the basis of equating the flow across the vertical line DB to the flow across the third vertical grid line from the upstream boundary. The third line was chosen for calculating the reference flow because it is close to the upstream boundary where the surface position should be most stable and because, at this line, central differences can be incorporated for accurate calculations of gradients in the flow determination. The position of D was adjusted by calculating the magnitude of the grid intercept to the nearest regular node required to produce a flow across

BD equal to the reference flow. The change in height of D for each adjustment was, however, restricted to less than twice the normal grid spacing d. An added precaution was also necessary to prevent the position of D rising above the height of the free surface at the closest vertical line, less the increment between this line and the next closest line upstream.

In coarse grid solutions for axisymmetric flows it was usually found that the latter requirement was the limiting one. The flow calculation across BD is based on one-sided finite difference formulae for determining the piezometric head gradients and, especially with axisymmetric flow, this results in an inaccurate value of discharge. It is to be expected then that there may be some degree of error in the determination of the height of the seepage surface DC. For this reason a fine grid was incorporated near the well for some axisymmetric flow solutions. The fine grid was included after the solution had been obtained on the coarser grid throughout the field. The number of coarse grid lengths away from the well, which were to be included in the fine grid section, was read in as data as was the number of fine grid mesh lengths per coarse grid length. The initial values of piezometric head at the intermediate

points on the fine grid were obtained by interpolation from the closest coarse grid values.

Consider now the intersection of a horizontal grid line with the free surface as shown in Fig. 4-3-5.

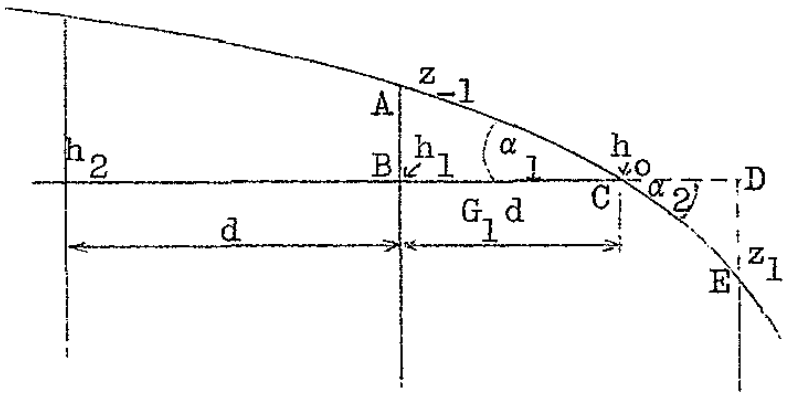

FIG. 4-3-5
INTERSECTION OF HORIZONTAL GRID LINE WITH FREE SURFACE

Application of Taylor series expansions about h_o allows a finite difference approximation to h_{ox}:

$$h_{ox} = \frac{G_1^2 h_2 + (1+2G_1)h_o - h_1(1+G_1)^2}{G_1 d(1+G_1)} \qquad \ldots. \ 4.3\text{-}15$$

In this case $\sin\alpha\cos\alpha$ is substituted for h_{ox} according to equation 4.3-10; $\sin\alpha$ and $\cos\alpha$ are calculated as the average of the respective functions for α_1 and α_2 in Fig. 4-3-5. However the value of h_o cannot change since it must equal the height of the particular horizontal grid line above the base. Equation 4.3-15 can therefore be used to calculate a new value of the shortened grid

length $G_1 d$ at which the grid line intersects the free surface. This extra adjustment however, is only necessary for a coarse mesh with a high vertical component of flow. Provided the mesh is reasonably fine, the free surface can be well represented by straight line segments between the vertical grid lines. The mesh size has therefore been kept small enough in all analyses so that this requirement is satisfied to a sufficient degree of accuracy. After the vertical grid adjustments have been completed, the horizontal intercepts are adjusted on the assumption of a straight line intercept between the two neighbouring vertical lines.

4.4 Selection of Initial Values for Finite Difference Solutions

4.4.1 Initial values for Darcy solutions

Numerical solutions to elliptic partial differential equations, in which a whole or part of the closed boundary is subject to a Dirichlet boundary condition, may be obtained by initially assuming all interior nodal values to be zero. However a solution can often be obtained much more quickly by judicious selection of initial values, both for the interior nodes and also for those parts of the boundary, if any, which are subject to other types of boundary conditions. In free streamline problems, the accuracy of the assumed initial

position of the free surface also affects the time required for a complete solution.

For two-dimensional flow through a permeable wall as shown in Fig. 4-4-1, the length of the seepage surface CD was assumed to be one-third of the difference between upstream and downstream water levels, so that hs in Fig. 4-4-1 is given by:

$$hs = h_d + \frac{1}{3}(h_u - h_d) \qquad \ldots\ 4.4\text{-}1$$

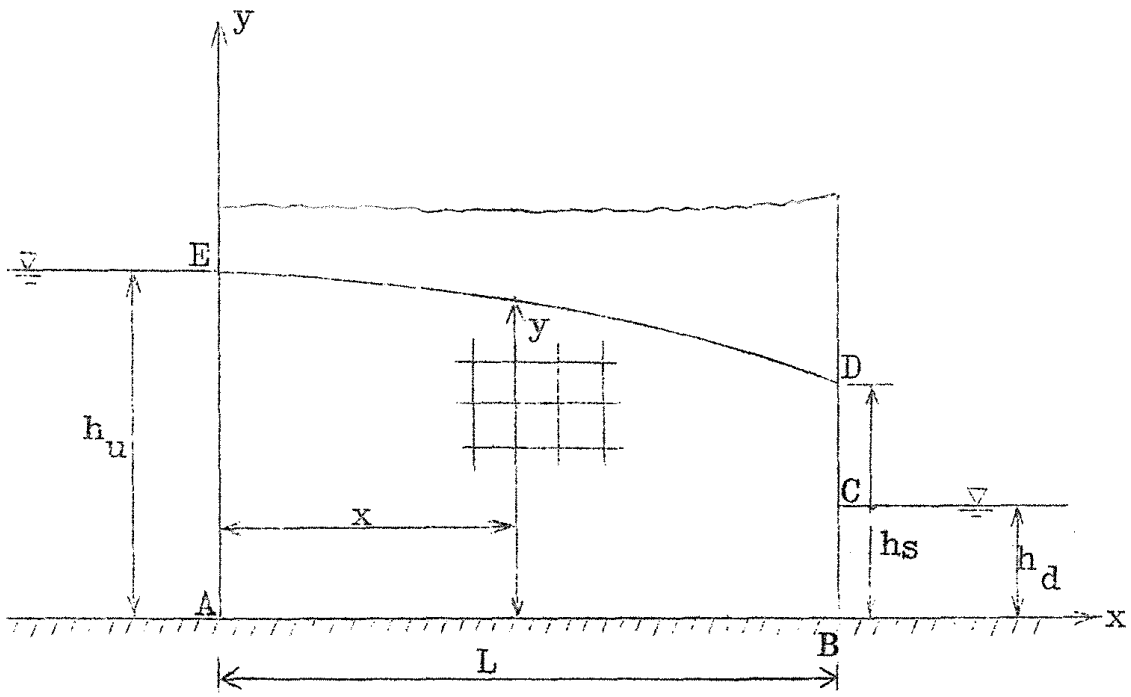

FIG. 4-4-1 PERMEABLE WALL INITIAL VALUES

The free surface curve ED is assumed to follow a power law between h_u and h_s; thus if y is the initially assumed height of the free surface at distance x from the upstream face then:

$$y^n = h_u{}^n - \frac{x}{L}(h_u{}^n - hs^n) \qquad \ldots\ 4.4\text{-}2$$

in which L is the length of the wall and n is an exponent between 1 and 2. Similarly the piezometric head, h(x), on the bottom boundary at distance x is assumed to follow a power law between h_u and h_d:

$$h(x)^n = h_u^n - \frac{x}{L}(h_u^n - h_d^n) \qquad \ldots\ldots 4.4\text{-}3$$

For larger flow values, that is where the difference in water levels is large compared to the length of the wall, the value of n was taken as 2 in both equations 4.4-2 and 4.4-3. Although this assumption could also have been made for smaller water level differences, better initial values were obtained by taking n as 1.5 in both equations. The values of piezometric head at nodes between the bottom boundary and the free surface were obtained by linear interpolation over each vertical grid line.

In obtaining initial values for the axisymmetric flow situation, advantage was taken of some empirical relations suggested by previous researchers. For unconfined flow to a well as shown in Fig. 4-4-2, Hall (1955) obtained empirical equations for the height of the seepage surface hs and for the free surface curve ED. For the nomenclature of Fig. 4-4-2, the seepage surface height hs is given by:

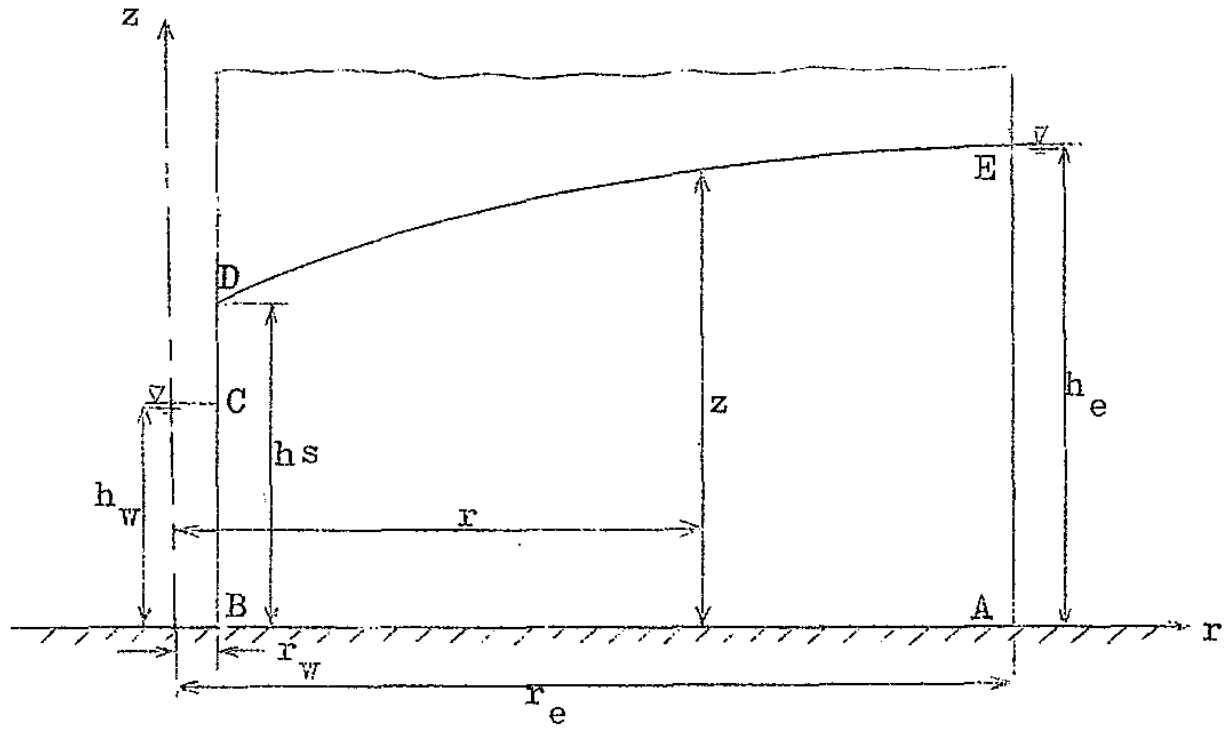

FIG. 4-4-2 UNCONFINED WELL FLOW INITIAL VALUES

$$hs = h_w + \frac{(h_e - h_w)\left\{1 - \left(\frac{h_w}{h_e}\right)^{2.4}\right\}}{\left\{1 + \frac{1}{50}\ln\left(\frac{r_e}{r_w}\right)\right\}\left\{1 + \frac{5}{(h_e/r_w)}\right\}} \quad \ldots\ldots 4.4\text{-}4$$

while the height z of the free surface at radius r is given by:

$$z = hs + (h_e - hs)\left\{\frac{2.5(r-r_w)}{(r_e-r_w)} - 1.5\left(\frac{r-r_w}{r_e-r_w}\right)^{1.5}\right\} \ldots 4.4\text{-}5$$

Since the flow along the impermeable base must be horizontal, it would seem reasonable to assume that the initial values of piezometric head could be taken from the Dupuit curve between h_e and h_w. Wyckoff, Botset and Muskat (1932) have shown experimentally that

Dupuit's relation is approximately true for head measurements along the impermeable base and this was supported by Hall (1955). If h(r) is the base piezometric head at radius r, then the initial value for h(r) can be assumed to be given by:

$$h(r)^2 = h_w^2 + \frac{\ln(r/r_w)}{\ln(r_e/r_w)} (h_e^2 - h_w^2) \qquad \ldots\ldots 4.4\text{-}6$$

For flow conditions corresponding to larger differences in water levels h_e and h_w, the initial values were calculated using equations 4.4-4, 4.4-5 and 4.4-6 and interpolating along vertical grid lines, between the base piezometric head and free surface height, to obtain internal nodal values. For medium water level differences the seepage surface height hs was calculated from the assumption:

$$hs = h_w + \frac{1}{3} (h_e - h_w) \qquad \ldots\ldots 4.4\text{-}7$$

and equations 4.4-5 and 4.4-6 were again employed to obtain free surface heights and base piezometric heads respectively. For small differences in water levels, hs was set by equation 4.4-7 and h(r) by equation 4.4-6 but the free surface height was set by a Dupuit curve between hs and h_e.

No attempt was made to investigate the best initial

value assumptions in terms of representative aquifer parameters as the choice of initial values usually only affects computer time requirements and is therefore not of fundamental importance to the problem being analysed. However at low differences in water levels it was observed that initial values calculated from equations 4.4-4, 4.4-5 and 4.4-6 gave a free surface that was too low near the well. After a number of iterations the piezometric heads in the field near the well increased to values greater than the height of the free surface vertically above. The free surface adjustment could not cater for this situation, so that a solution could not be obtained by the usual method. For this reason the Dupuit curve between hs and h_e was employed to calculate an initial free surface position and a solution was then obtained without further difficulty. In all cases, by calculating discharge values at each vertical grid line, an indication could be obtained, within a few iterations, of whether or not the initial assumptions were suitable so that the selection of appropriate initial values presents no real problem.

4.4.2 Initial values for Forchheimer solutions

The computer time per iteration is considerably longer for nonlinear flow than for linear Darcy flow

analyses because of the greater complexity of the finite difference formulae for the former. A saving in computer time can therefore be effected by solving a given flow situation on the basis of Darcy's Law and then using the results as initial values for the nonlinear solutions.

For two-dimensional flow problems, the results from the Darcy solution were used directly as initial values for the nonlinear analyses. For axisymmetric problems, however, the Darcy solutions were modified to obtain initial values which further reduced the computation time. This modification was based on a corresponding confined flow problem for which exact solutions can be obtained for both Darcy and Forchheimer flow. Observation of the Darcy and Forchheimer confined flow solutions at corresponding radii showed that the difference between the Forchheimer head value and the Darcy head value, bore an approximately constant ratio to the difference between the Darcy head value and the external head h_e. This observation led to a method of obtaining better initial values for the axisymmetric nonlinear analyses.

The value of the discharge QF for confined Forchheimer flow is obtained from equation 3.1-4 using the same water levels h_w and h_e at r_w and r_e respectively, and assuming any convenient aquifer thickness B as this does not

affect the distribution of piezometric heads. The piezometric head for confined Forchheimer flow, FHC(r), at any radius r can then be obtained as:

$$FHC(r) = h_w + \frac{aQF}{2\pi B} \ln\left(\frac{r}{r_w}\right) + \frac{bQF^2}{4\pi^2 B^2}\left(\frac{1}{r_w} - \frac{1}{r_e}\right) \quad \ldots 4.4\text{-}8$$

The corresponding piezometric head for confined Darcy flow DHC(r) is given by:

$$DHC(r) = h_w + \frac{\ln(r/r_w)}{\ln(r_e/r_w)}\,(h_e - h_w) \quad \ldots 4.4\text{-}9$$

If FH(r,z) is the required initial value for the Forchheimer analysis at any point r,z and if DH(r,z) is the solution at the corresponding point from the numerical analysis of Darcy flow, then FH(r,z) can be obtained from:

$$\frac{FH(r,z) - DH(r,z)}{h_e - DH(r,z)} = \frac{FHC(r) - DHC(r)}{h_e - DHC(r)} \quad \ldots 4.4\text{-}10$$

The improvement of initial values so obtained enhanced the speed of solution by up to 50 percent in some cases. For low head gradients the relation:

$$\frac{FH(r,z)}{DH(r,z)} = \frac{FHC(r)}{DHC(r)} \quad \ldots 4.4\text{-}11$$

was also found to give satisfactory initial values for the nonlinear Forchheimer analysis.

4.4.3 Initial values for exponential solutions

For two-dimensional flow, the Darcy results were used directly as initial values for the analysis of flows obeying an exponential head loss relation. For axisymmetric flow, initial values were obtained in a manner analogous to that for Forchheimer flow. The discharge QE for a corresponding exponential confined flow problem can be obtained from equation 3.1-6, so that the piezometric head for confined exponential flow, EHC(r), at any radius r can be obtained as:

$$EHC(r) = h_w + \frac{c\ QE^m}{(2\pi B)^m}\ \frac{r^{1-m} - r_w^{1-m}}{1-m} \qquad \ldots\ 4.4\text{-}12$$

If EH(r,z) is the required initial value for the exponential flow analysis at any point r,z, and DH(r,z) is the numerical solution at the corresponding point for Darcy flow then EH(r,z) is obtained from:

$$\frac{EH(r,z) - DH(r,z)}{h_e - DH(r,z)} = \frac{EHC(r) - DHC(r)}{h_e - DHC(r)} \qquad \ldots\ 4.4\text{-}13$$

where DHC(r) is again obtained from equation 4.4-9. Alternatively the relation:

$$\frac{EH(r,z)}{DH(r,z)} = \frac{EHC(r)}{DHC(r)} \qquad \ldots\ 4.4\text{-}14$$

is employed for low hydraulic gradients.

4.5 Convergence of Finite Difference Numerical Solutions

The iterative method used in the solution of the finite difference equations is the Gauss-Seidel procedure of successive displacements with an over relaxation factor. The method, which appears to have been first introduced for elliptic differential equations by Liebmann (1918), uses the latest values of the function at all points when calculating the improved value and also incorporates an over correction for the new value. The method has been discussed at some length by Forsythe and Wasow (1960), who pointed out that convergence is not guaranteed for all systems of equations.

The over relaxation process may be represented as follows:- if $h^{(n)}$ represents the value of h, at a particular node, obtained from the n^{th} iteration and if $h'^{(n+1)}$ is the value at that node which would be calculated by direct application of the finite difference equation for the $n+1^{th}$ iteration, then the over corrected value actually taken, $h^{(n+1)}$, is given by:

$$h^{(n+1)} = h^{(n)} + W\left\{h'^{(n+1)} - h^{(n)}\right\} \quad \ldots\ 4.5\text{-}1$$

in which W is the over relaxation factor. The selection of the optimum over relaxation factor to give quickest convergence to a solution is a problem which has only been solved for isolated cases. Young (1954) formulated

rules for deriving the optimum factor under certain conditions. Russell (1963) suggested equations for determining optimum under relaxation factors ($W < 1$) for numerical solution of the Navier-Stokes equations. However for most elliptic differential equations the selection of an optimum value of W cannot yet be carried out on completely theoretical grounds and must be obtained from a trial and error approach. The factor will usually depend on the finite difference operator itself and also on the shape of the field in which an equation is to be solved.

Because of the importance of the Laplace equation in many fields, the convergence of finite difference solutions to this equation has been reasonably well studied. Thom and Apelt (1961) evaluated the relative merit of the unit square and higher molecule formulae for solutions to the two-dimensional Laplace equation using a desk calculator. They showed that, without using an over relaxation process, the '100 formula' (equation 4.2-8) could be up to five times as fast as the unit square formula for a square shaped field of values. However Jeppson (1966), in Laplace solutions to free streamline problems on the inverse plane, showed that by using optimum over relaxation factors with each formula,

the computer time saved by using the '100' formula was only 25 percent of that required to obtain a solution with the unit square formula. This does not give an exact indication of the relative merits of the formulae because, in free streamline problems, not all of the time is involved in applying the finite difference operators; but it does indicate that, with computer applications and with appropriate over relaxation factors, the discrepancy in relative merits of the formulae is considerably reduced.

Jeppson (1966) obtained optimum over relaxation factors for the two finite difference operators by plotting the results of trials with a number of values of W. His results are reproduced in Fig. 4-5-1. This shows that for the rectangular field considered the optimum over relaxation factor for the unit square operator was approximately 1.5 while that for the higher molecule formula was approximately 1.3.

The optimum value of the over relaxation factor varies with the shape of the finite difference grid even for one particular operator but, for the unit square Laplace operator, it usually has been found to be in the range 1.5 to 1.8 and, for the axisymmetric flows analysed in this thesis, a value of about 1.6 to 1.7 was found to

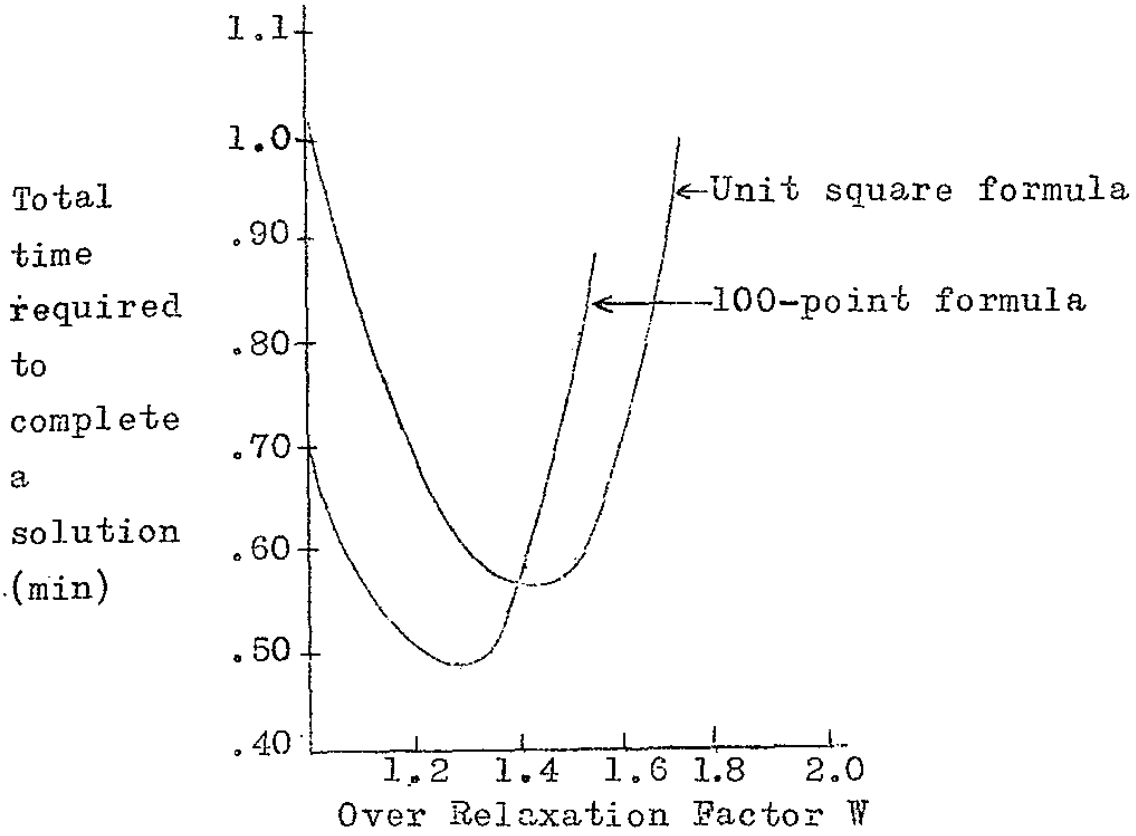

FIG. 4-5-1 CONVERGENCE OF FINITE DIFFERENCE SOLUTIONS OF THE LAPLACE EQUATION (After Jeppson, 1966)

yield best results. For the higher molecule formula used in two-dimensional flow solutions a lower value was used in accordance with the results of Jeppson (1966).

The general theory of convergence of finite difference solutions for nonlinear elliptic partial differential equations has not been developed in any detail and the selection of appropriate iterative methods is still largely a matter of trial and error. For some nonlinear equations, such as the Navier-Stokes equations for steady incompressible fluid flow, an under relaxation process

must be used to obtain convergence of numerical solutions; that is, W in equation 4.5-1 must be less than unity. For this reason a number of trial runs were carried out with the nonlinear finite difference operators using an over relaxation factor of unity, or in effect no over relaxation at all. As no difficulty was experienced in obtaining convergence, a series of over relaxation factors between 1 and 2 were employed to determine the optimum over relaxation factor for a typical problem.

The surface adjustment affects the solution at interior nodes although surface adjustments are best carried out with a reasonably settled field of values so that, in determining the optimum over relaxation factor, the free surface was assumed constant and the solution obtained for the field of values under this surface. For a range of values of W, the number of iterations required to obtain a given accuracy of solution was determined. The accuracy was stipulated as a maximum change between successive iterations of 1×10^{-6} in the value at all points in the field. Fig. 4-5-2 shows a plot of the number of iterations required to obtain this accuracy, against the corresponding over relaxation factor for the particular problem investigated (in the case of Forchheimer flow).

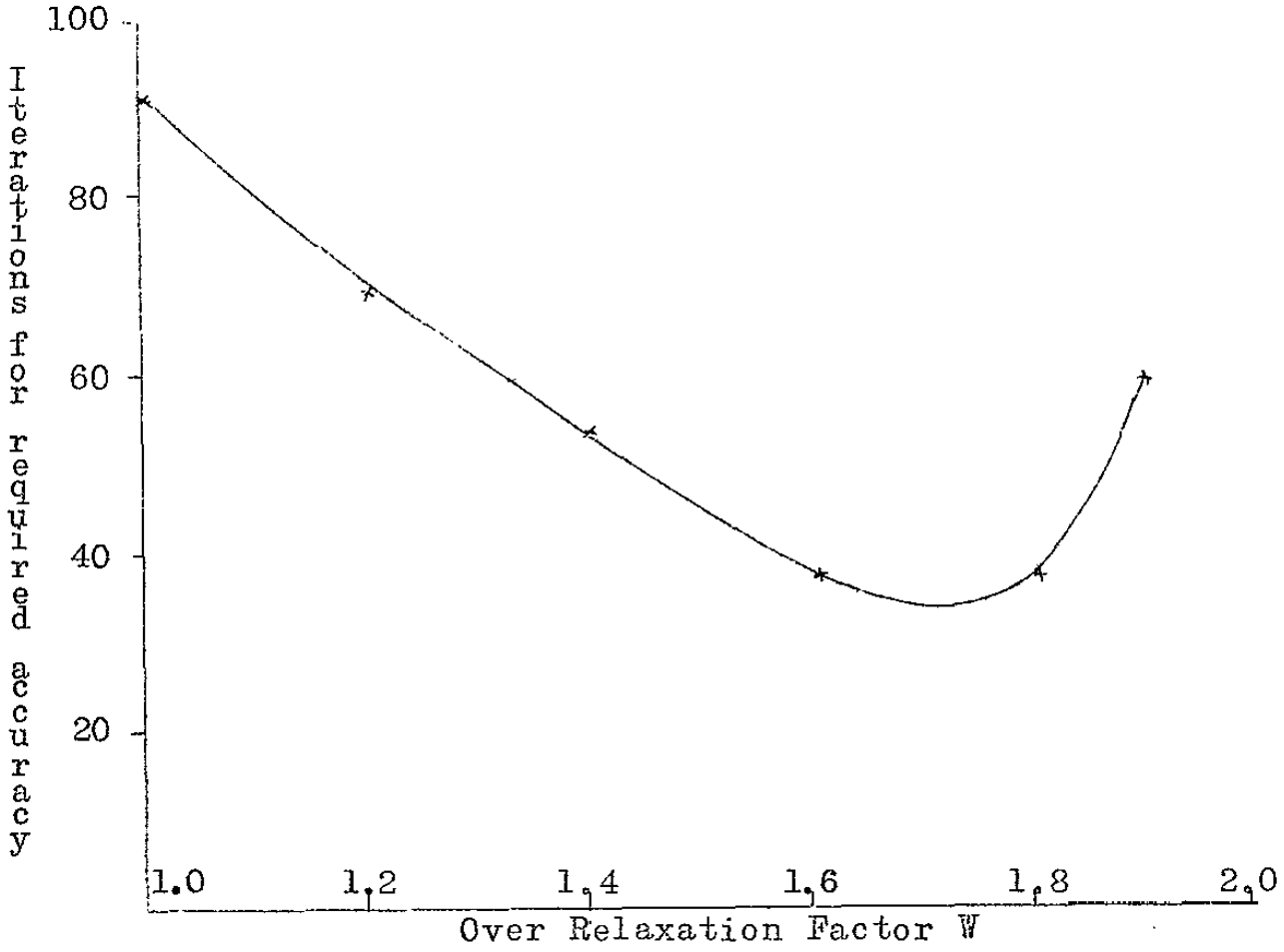

FIG. 4-5-2 OPTIMUM OVER RELAXATION FACTOR FOR FORCHHEIMER FINITE DIFFERENCE SOLUTIONS

The optimum over relaxation factor from Fig. 4-5-2 is approximately 1.7. The curve depicted in Fig. 4-5-2 shows the results obtained from a particular two-dimensional flow problem but the value of 1.7 was found to give a comparatively fast rate of convergence for all the Forchheimer finite difference analyses including those for axisymmetric flow.

The results of a similar investigation into the convergence of the exponential finite difference solution

for the same problem are shown in Fig. 4-5-3.

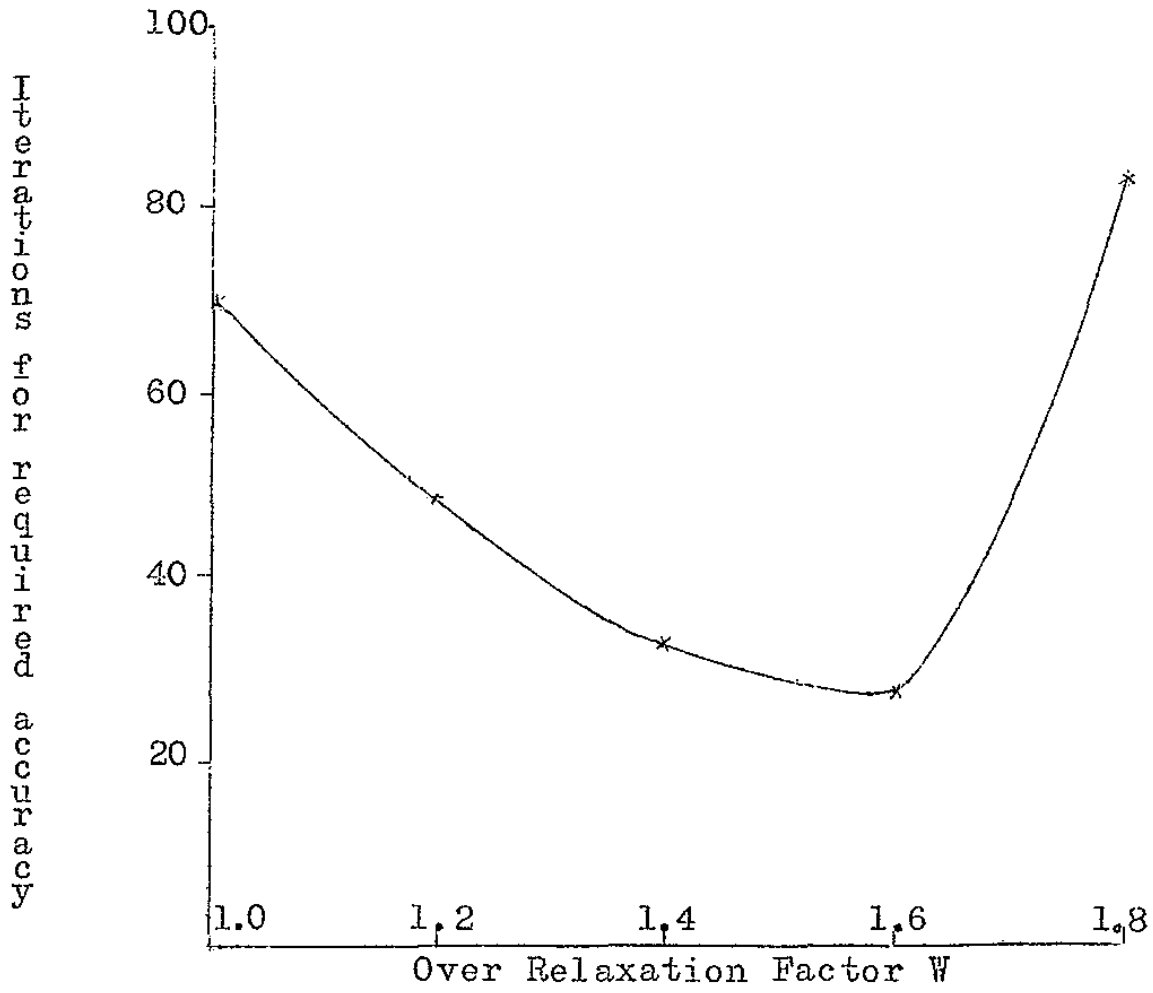

FIG. 4-5-3 OPTIMUM OVER RELAXATION FACTOR FOR EXPONENTIAL FINITE DIFFERENCE SOLUTIONS

From Fig. 4-5-3 the optimum over relaxation factor for the exponential flow solutions is approximately 1.6.

In obtaining the numerical finite difference solutions allowance has to be made for adjustment of the boundary values both at the free surface and at the bottom boundary. The position of the lower impermeable base is fixed and the finite difference form of the boundary condition at this boundary is applied each

iteration to obtain improved values. However the free surface adjustment involves a change in the boundaries of the actual field being solved and, for a stable adjustment technique, the free surface boundary condition is applied only after the field of values is reasonably well 'settled down'. Thus for the first three or four surface adjustments, twenty or more iterations were carried out per surface adjustment until the field of values was fairly stable, after which only three or four iterations per adjustment were needed. The exact numbers of iterations varied for different problems and the most appropriate values were determined at the time of solution.

4.6 General Program Arrangement and Output of Finite Difference Solutions

The finite difference numerical solutions were carried out using the University College of Townsville's IBM 1620 computer with extended memory capacity. Most of the programs were written in PDQ Fortran, which is a modification of Fortran II and which operates approximately three times as fast as Fortran II, although it has limited error detection facilities. The programs were arranged in sets of link programs using a 'common' data storage area so that the maximum number of nodal points could be included for each problem analysed. Because of the

amount of computer time required on the IBM 1620, the programs were written so that the iterative process could be interrupted at any stage and then continued on from this stage at a later time.

The interrelation between computer programs is shown in Fig. 4-6-1. The initial position of the free surface is calculated in the initial input program for Darcy flow; the finite difference grid is set to a predetermined scale throughout the field and the short arm lengths, where the grid lines intersect the free surface, are calculated. Initial values for piezometric head are then set at all points in the field. The Main Program for Darcy flow is called into the working section and the iterative solution of the finite difference equations is carried out including automatic adjustments of the free surface. The flow calculation program can be called at any stage to print out the flow across each vertical grid line. A comparison of these flows serves as a continuity check and gives some indication of the accuracy of the solution. This feature was incorporated because it is sometimes difficult to ascertain the accuracy obtained simply from the change in value at a point between successive iterations. After completion of the flow calculation, the program can either return

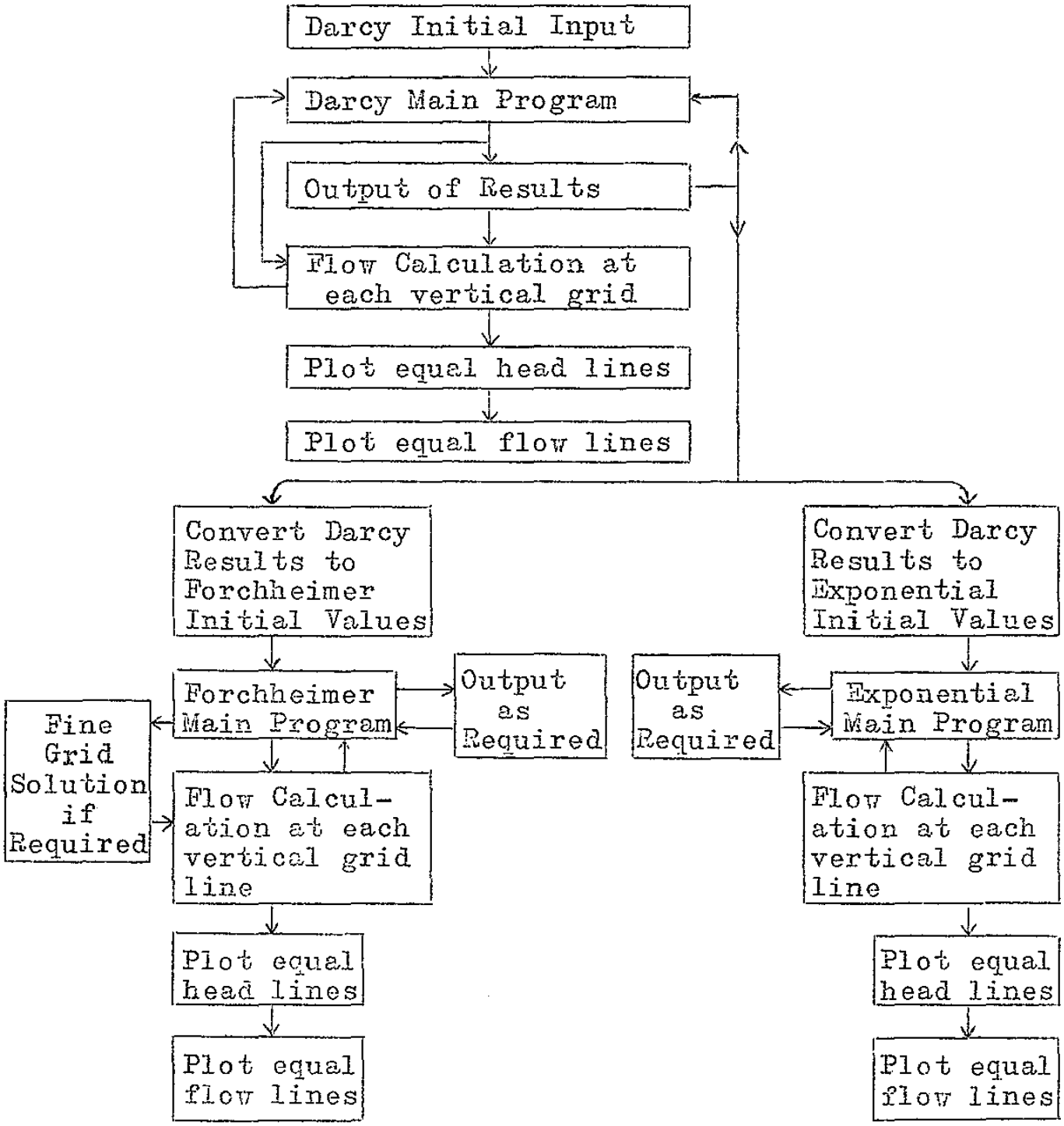

FIG. 4-6-1 INTERRELATION OF COMPUTER PROGRAMS

to the Main Program for more iterations or proceed to plot equal head lines and lines of equal flow.

The Darcy solutions for piezometric head were then converted to initial values for either Forchheimer or exponential flow analyses; for two-dimensional flow, the solutions were input directly as discussed in section 4.4. The procedure for solution of either the Forchheimer or exponential flow problems was similar to that described for the Darcy solutions. In the case of the Forchheimer solutions for axisymmetric flow, provision was made for the inclusion of a fine grid area near the well to increase the accuracy in determining the height of the seepage surface.

The average value of discharge calculated from the finite difference solutions was printed out while a flow net for the problem was produced by the on-line plotter. The flow net showed equal head lines and lines of equal flow throughout the field including the fine grid area when this was incorporated in a solution.

4.7 Finite Element Methods of Analysis

Many problems involving elliptic partial differential equations can be related to the minimisation or maximisation of an integral. This property, which is discussed more fully by Courant and Hilbert (1953), leads to an

alternative variational formulation of the problem. Instead of attempting to solve the partial differential equation in its original form, the problem is converted to one of maximising or minimising an integral throughout the field.

Although originally developed as a direct application of the principles of structural analysis, the method of finite elements has since been shown to have wider applications. De Veubeke (1965) showed that it could be interpreted on the basis of minimisation of the total potential energy of a physical system, and in effect becomes a numerical method for the solution of problems analysed by the variational principles of mechanics, which were discussed by Lanczos (1962). Zienkiewicz and Cheung (1965) demonstrated the logical extension of the method of finite elements to solve the alternative variational formulation of field problems involving elliptic partial differential equations. The specific equations they solved were those of Laplace and Poisson. The method is ideally suited to the analysis of problems involving nonhomogeneity and anisotropy for linear flow through porous media, as shown by Zienkiewicz, Mayer and Cheung (1966), while Finn (1967) and Taylor and Brown (1967) have demonstrated its versatility in handling free streamline problems with the Laplace equation.

4.8 Mathematical Considerations and Boundary Conditions with the Finite Element Method

Equations 2.4-7, 2.5-25 and 2.5-30 are the differential equations for which solutions are required in the flow domain. For purposes of discussion, consider flow through the dam with a lower impermeable boundary as depicted in Fig. 4-8-1.

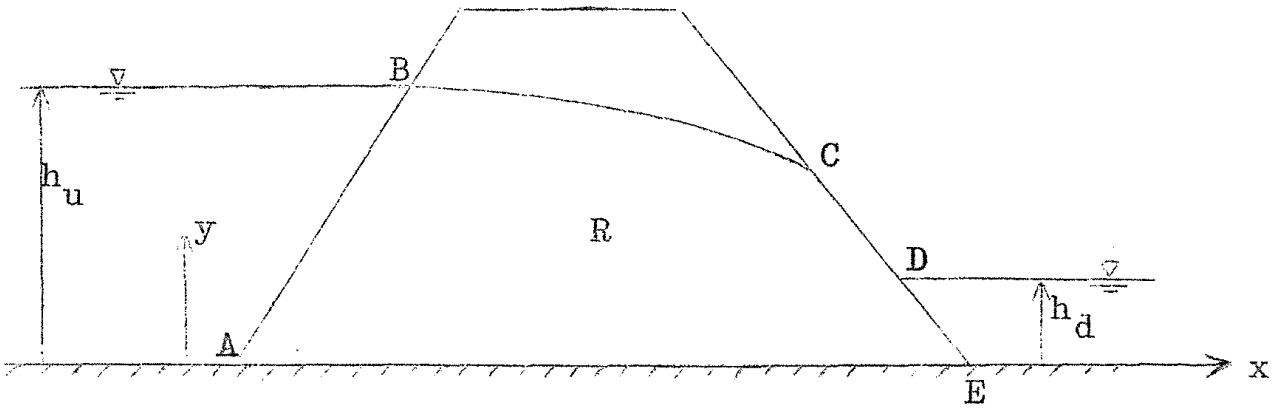

FIG. 4-8-1 FLOW THROUGH A DAM

A function h is required which satisfies equation 2.4-7, 2.5-25 or 2.5-30 inside the domain ABCDEA. The boundary conditions are similar to those outlined for flow through a permeable wall, in section 4.3 and can be stated briefly as follows:

$h = h_u$ on AB

$h = h_d$ on DE

$h = y$ on CD

$h = y$ and $\frac{\partial h}{\partial n} = 0$ on BC in which n is the direction of the normal to the boundary at any point.

$$\frac{\partial h}{\partial n} = 0 \qquad \text{on EA}$$

The mathematical theory behind the variational method has been developed in some detail for linear partial differential equations. It has been shown (Forsythe and Wasow, 1960) that only self-adjoint problems can be solved by minimising an equivalent integral expression. For a given differential equation:

$$L(h) = 0 \qquad \ldots\ldots 4.8\text{-}1$$

the requirement for a self-adjoint problem is that the operator L itself be self-adjoint and that the boundary conditions take a special form:

$$\alpha h + \lambda + \beta \frac{\partial h}{\partial n} + \delta \frac{\partial h}{\partial s} = 0 \qquad \ldots\ldots 4.8\text{-}2$$

in which α , λ , β , δ are continuously differentiable functions of s on the boundary; $\frac{\partial h}{\partial n}$ is the inner normal derivative and $\frac{\partial h}{\partial s}$ the positive tangential derivative on the boundary. Conversely if the boundary conditions take the special form (4.8-2) and if the operator L is self-adjoint, the problem is also self-adjoint and may be solved by the variational method.

For the general variational problem:

$$E(h) = \iint_R G\,(h,\ h_x,\ h_y,\ x,\ y)\,dxdy \qquad \ldots\ldots 4.8\text{-}3$$

the Euler equation, from the Calculus of Variations

(Pars, 1962) for the minimisation of E in the region R is

$$\frac{\partial G}{\partial h} - \frac{\partial}{\partial x}\left(\frac{\partial G}{\partial h_x}\right) - \frac{\partial}{\partial y}\left(\frac{\partial G}{\partial h_y}\right) = 0 \qquad \ldots\ 4.8\text{-}4$$

and if the boundary condition is of the special form (4.8-2) it is called the natural boundary condition because it is automatically satisfied by the function h minimising E(h), without being imposed (Forsythe & Wasow, 1960). For the expression given in equation 4.8-3 the values of α, λ, β, δ can be shown to give the natural boundary condition:

$$-\frac{\partial G}{\partial h_x}\frac{dy}{ds} + \frac{\partial G}{\partial h_y}\frac{dx}{ds} = 0 \qquad \ldots\ 4.8\text{-}5$$

Thus if the actual boundary conditions in a given problem are of this "natural" type, the variational method is a powerful analytical technique because it requires only the minimisation of the integral E(h) without any special allowance for boundary conditions.

The mathematical background for the application of the variational method to nonlinear partial differential equations appears to be relatively undeveloped and, at this stage, guidance can only be obtained from the conclusions reached for the linear case. Thus, for a given nonlinear equation, if it is possible to derive an integral expression E(h) such that minimisation of E(h) according to the Euler equation yields the original

differential equation and if the boundary condition is of the special form of equation 4.8-5, then such a nonlinear equation should be tractable by a variational formulation.

It should be noted that the boundary condition may differ from the natural one for some sub-section of the boundary, provided this new condition is then imposed on the solution; such a condition is the requirement that h have prescribed values on AB and CDE in Fig. 4-8-1.

4.8.1 Darcy flow

According to equations 4.8-3, 4.8-4 and 4.8-5, the Laplace equation is mathematically equivalent to minimising the integral:

$$E(h) = \iint \{(h_x)^2 + (h_y)^2\}\, dxdy \qquad \ldots. \text{ 4.8-6}$$

with the natural boundary condition:

$$-2h_x \frac{dy}{ds} + 2h_y \frac{dx}{ds} = 0 \qquad \ldots. \text{ 4.8-7}$$

$$\text{or} \quad \frac{\partial h}{\partial n} = 0 \qquad \ldots. \text{ 4.8-8}$$

The natural boundary condition 4.8-5 agrees with the actual one along the free surface and along the impermeable base since zero head gradient perpendicular to the boundary fulfils the requirement of no flow across it.

4.8.2 Nonlinear flow

In order to express equation 2.5-25 as equivalent to

minimising an integral, according to the general expressions 4.8-3 and 4.8-4, the following requirements must be met:

$$\frac{\partial G}{\partial h} = 0$$

$$\left.\begin{aligned} \frac{\partial G}{\partial h_x} = u = C_1 \left\{ -\frac{a}{2b} + \sqrt{\left(\frac{a}{2b}\right)^2 + \frac{|h_s|}{b}} \right\} \frac{(-h_x)}{|h_s|} \\ \frac{\partial G}{\partial h_y} = v = C_1 \left\{ -\frac{a}{2b} + \sqrt{\left(\frac{a}{2b}\right)^2 + \frac{|h_s|}{b}} \right\} \frac{(-h_y)}{|h_s|} \end{aligned}\right\} \quad \ldots 4.8\text{-}9$$

in which C_1 is any constant value. If C_1 is put equal to -1, these requirements are fulfilled by the function

$$G = -\frac{a}{2b}|h_s| + \frac{2}{3}b\left\{\left(\frac{a}{2b}\right)^2 + \frac{|h_s|}{b}\right\}^{3/2} \quad \ldots. 4.8\text{-}10$$

and the integral to be minimised is

$$E(h) = \iint\left[-\frac{a}{2b}|h_s| + \frac{2}{3}b\left\{\left(\frac{a}{2b}\right)^2 + \frac{|h_s|}{b}\right\}^{3/2}\right] dxdy \quad \ldots. 4.8\text{-}11$$

The natural boundary condition is

$$-\frac{\partial G}{\partial h_x}\frac{dy}{ds} + \frac{\partial G}{\partial h_y}\frac{dx}{ds} = 0 \quad \ldots. 4.8\text{-}12$$

or $$u\frac{dy}{ds} - v\frac{dx}{ds} = 0 \quad \ldots. 4.8\text{-}13$$

or $$\frac{-h_x}{(a+b|v|)}\frac{dy}{ds} + \frac{h_y}{(a+b|v|)}\frac{dx}{ds} = 0 \quad \ldots. 4.8\text{-}14$$

This reduces to

$$- h_x \frac{dy}{ds} + h_y \frac{dx}{ds} = \frac{\partial h}{\partial n} = 0 \qquad \text{.... 4.8-15}$$

which again agrees with the actual boundary condition on the free surface and along the impermeable base.

A similar analysis for the differential equation 2.5-30 shows that the integral to be minimised is

$$E(h) = \iint \left[\frac{1}{c^{1/m}} \frac{m}{m+1} |h_s|^{\frac{m+1}{m}} \right] dxdy \qquad \text{.... 4.8-16}$$

with the natural boundary condition:

$$\frac{\partial h}{\partial n} = 0 \qquad \text{.... 4.8-17}$$

For c and m constants the integral to be minimised reduces to

$$E(h) = \iint h_s^{\frac{m+1}{m}} dxdy \qquad \text{.... 4.8-18}$$

4.8.3 Concepts of energy minimisation

In treating problems of flow through porous media, velocity is usually considered as the superficial velocity or flow per unit total area, ignoring the presence of the solid particles; the piezometric head value at a point is considered to be the average of values over a region of fluid and medium centred on the point in question. For analytical purposes therefore, the fluid-medium system is replaced by an imaginary fluid occupying the total volume and which behaves in a manner governed by the velocity

head loss relation for the flow.

When Darcy's Law is valid the imaginary fluid behaves analogous to an ideal fluid in irrotational flow; because, although all the energy is assumed to be dissipated in friction, the head loss relation is of such a form that the imaginary fluid occupying the total volume can be considered as a frictionless fluid within the same boundaries.

From hydrodynamic theory (Lamb, 1932), it can be shown that the integral:

$$\iint \left(u \frac{\partial p}{\partial x} + v \frac{\partial p}{\partial y}\right) dxdy \qquad \ldots\ldots 4.8\text{-}19$$

(for two-dimensional flow) represents the rate at which the pressure forces do work on the boundaries of all elements of a fluid in a given region. When the work done by gravity is included, the integral becomes:

$$\iint \left(u \frac{\partial h}{\partial x} + v \frac{\partial h}{\partial y}\right) dxdy \qquad \ldots\ldots 4.8\text{-}20$$

This work done on any portion of the fluid has two possible effects. It may either increase the kinetic energy of the fluid or it may be dissipated as some other type of energy, for example heat energy, due to the action of viscous stresses in the element.

The rate of increase of kinetic energy is given by $\frac{d}{dt}\left\{\frac{1}{2}(u^2 + v^2)\right\}$ at any point. That is:

$$u \frac{du}{dt} + v \frac{dv}{dt}$$

or $$u\left(\frac{\partial u}{\partial t} + u \frac{\partial u}{\partial x} + v \frac{\partial u}{\partial y}\right) + v\left(\frac{\partial v}{\partial t} + u \frac{\partial v}{\partial x} + v \frac{\partial v}{\partial y}\right) \quad \ldots\ldots \text{4.8-21}$$

In deriving Darcy's Law on a theoretical basis from the Navier-Stokes equations, it is assumed that all terms of the type included in brackets in the expression 4.8-21 are negligible. This, in effect, means that the rate of increase in kinetic energy at any point in the flow is considered negligible, so that, if Darcy's Law applies then all the work done by the pressure and gravity forces must be dissipated as friction.

In actual practice the expression 4.8-20 will only exactly give the rate of energy dissipation when there is no change in the velocity components throughout the flow. This is also the only situation in which Darcy's Law will hold exactly because, if there is a change in velocity then there will be a change in kinetic energy, and some of the work done by the pressure and gravity forces must be responsible for this change. As a result the integral 4.8-20 would not then precisely express the rate of energy dissipation.

However when Darcy's Law applies, the integral 4.8-20 does represent the rate of energy dissipation as shown by Muskat (1946). Thus in applying the method of finite

elements to Darcy flow, the minimisation of the integral 4.8-6 has physical significance in that it is the requirement for the rate of energy dissipation in the flow to be a minimum, as discussed by Zienkiewicz, Mayer and Cheung (1966).

Engelund (1953) briefly considered the Calculus of Variations as applied to groundwater flow. He considered a nonlinear relation in the form:

$$i = F(|V|)V \qquad \ldots. \ 4.8\text{-}22$$

in which $F(|V|) = a + b|V|$ 4.8-23

After obtaining expressions for u and v from equation 4.8-22 and substituting in the continuity equation, the system describing the flow becomes:

$$\frac{\partial}{\partial x}\left(\frac{h_x}{F}\right) + \frac{\partial}{\partial y}\left(\frac{h_y}{F}\right) = 0 \qquad \ldots. \ 4.8\text{-}24$$

Engelund suggested that equation 4.8-24 was, by virtue of Euler's theorem, equivalent to minimising the expression:

$$\iint \left[\frac{1}{F}(h_x)^2 + \frac{1}{F}(h_y)^2\right] dxdy \qquad \ldots. \ 4.8\text{-}25$$

However when F is defined as in equation 4.8-23, it is a function of V and therefore of h_x and h_y so that application of the Euler theorem to the expression 4.8-25 does not yield equation 4.8-24 in this case.

In addition, the expression 4.8-20 has not been shown to represent the rate of energy dissipation when Darcy's

Law does not apply. The reason for the application of a nonlinear equation, rather than Darcy's Law, is to account for the contribution of terms such as those included in brackets in 4.8-21. Thus for nonlinear flow the rate of change of kinetic energy can no longer be considered negligible. This means, in effect, that the integral 4.8-20 now represents the sum of the rates at which kinetic energy is being increased and at which energy is being dissipated in friction. Hence for the case of nonlinear flow in porous media, although the integral 4.8-20 can still be evaluated, any physical significance in terms of minimising the rate of energy dissipation, is lost.

4.9 Details of the Method for Triangular Elements

The numerical technique of finite elements has been applied to linear seepage problems as noted earlier (Zienkiewicz, Mayer and Cheung, 1966; Finn, 1967; Taylor and Brown, 1967), while Fenton (1968) adopted the technique for the analysis of flow governed by the exponential relation and compared solutions for different values of the exponent m.

Consider a general region divided into triangular elements with one particular element denoted by nodes I, J, M as shown in Fig. 4-9-1.

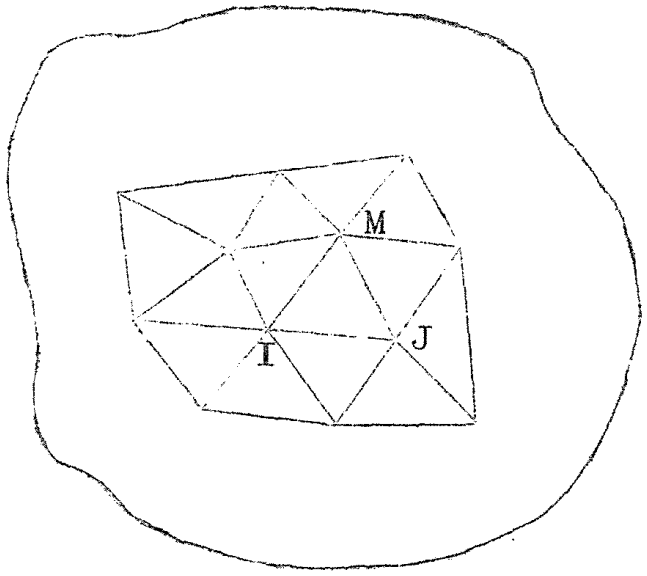

FIG. 4-9-1 THE FINITE ELEMENT FORMULATION

The elements are assumed to be small enough so that the nodal values of h accurately define the piezometric head function within each element. Then by representing the function as a linear polynomial in each element and minimising the integral E(h) in equation 4.8-6 with respect to each nodal value, Zienkiewicz (1967) has shown that, for Darcy flow, a solution is obtained from a set of simultaneous equations in h_I where h_I is the piezometric head value at node I; I has values 1 to N for N nodes. These equations may be solved by an iterative method for the unknown values of h_I.

For the particular element IJM, h may be expressed as:

$$h = (a_I + b_I x + c_I y)h_I + (a_J + b_J x + c_J y)h_J + (a_M + b_M x + c_M y)h_M \quad \ldots\ldots 4.9\text{-}1$$

in which $$a_I = \frac{x_J y_M - x_M y_J}{2\Delta}$$

$$b_I = \frac{y_J - y_M}{2\Delta}$$

$$c_I = \frac{x_M - x_J}{2\Delta}$$

.... 4.9-2

and the remaining coefficients are obtained by cyclic permutation of subscripts; and 2Δ = 2 x area of triangle IJM.

The process of minimisation of the integral E is best accomplished by evaluating the contribution to each differential, such as $\frac{\partial E}{\partial h_I}$, from a typical element, then adding all such contributions and equating to zero.

A similar approach based on triangular elements will be used in the present analysis for the nonlinear flow problem.

For flow governed by the Forchheimer equation the integral E(h) to be minimised is given by equation 4.8-11. If E^e is the value of E associated with an element (implying an integration limited to the area of the element) then differentiating equation 4.8-11 yields:

$$\frac{\partial E^e}{\partial h_I} = \iint \left[-\frac{a}{2b} + \left\{ \left(\frac{a}{2b}\right)^2 + \frac{|h_s|}{b} \right\}^{\frac{1}{2}} \right] \frac{\partial |h_s|}{\partial h_I} \, dxdy$$

.... 4.9-3

but $$|h_s| = (h_x^2 + h_y^2)^{\frac{1}{2}} \qquad \ldots\ldots 4.9\text{-}4$$

so that $$\frac{\partial |h_s|}{\partial h_I} = \frac{1}{|h_s|}(h_x b_I + h_y c_I) \qquad \ldots\ldots 4.9\text{-}5$$

and since h_s, h_x and h_y are assumed constant over the area of the element then:

$$\frac{\partial E^e}{\partial h_I} = \left[-\frac{a}{2b} + \left\{ \left(\frac{a}{2b}\right)^2 + \frac{|h_s|}{b} \right\}^{\frac{1}{2}} \right] \frac{1}{h_s} (h_x b_I + h_y c_I) \iint dxdy \qquad \ldots\ldots 4.9\text{-}6$$

From equation 4.9-1 it may be shown that:

$$\left.\begin{aligned} h_x &= \frac{\partial h}{\partial x} = b_I h_I + b_J h_J + b_M h_M \\ h_y &= \frac{\partial h}{\partial y} = c_I h_I + c_J h_J + c_M h_M \end{aligned}\right\} \qquad \ldots\ldots 4.9\text{-}7$$

and since $\iint dxdy = \Delta$ $\qquad \ldots\ldots 4.9\text{-}8$

then $$\frac{\partial E^e}{\partial h_I} = \frac{\Delta}{|h_s|} \left[-\frac{a}{2b} + \left\{ \left(\frac{a}{2b}\right)^2 + \frac{|h_s|}{b} \right\}^{\frac{1}{2}} \right] \cdot \left[b_I(b_I h_I + b_J h_J + b_M h_M) + c_I(c_I h_I + c_J h_J + c_M h_M) \right] \qquad \ldots\ldots 4.9\text{-}9$$

or $$\frac{\partial E^e}{\partial h_I} = A b_I(b_I h_I + b_J h_J + b_M h_M) + A c_I(c_I h_I + c_J h_J + c_M h_M) \qquad \ldots\ldots 4.9\text{-}10$$

in which $$A = \frac{\Delta}{|h_s|} \left[-\frac{a}{2b} + \left\{ \left(\frac{a}{2b}\right)^2 + \frac{|h_s|}{b} \right\}^{\frac{1}{2}} \right] \qquad \ldots\ldots 4.9\text{-}11$$

Since any element contributes to only three of the differentials associated with its nodes:

$$\left\{\frac{\partial E^e}{\partial h}\right\} = \left\{\begin{array}{c} \frac{\partial E^e}{\partial h_I} \\ \\ \frac{\partial E^e}{\partial h_J} \\ \\ \frac{\partial E^e}{\partial h_M} \end{array}\right\} \qquad \ldots\ 4.9\text{-}12$$

then $$\left\{\frac{\partial E^e}{\partial h}\right\} = [S]\{h^e\} \qquad \ldots\ 4.9\text{-}13$$

in which an example of one element of the S matrix S_{IJ} is:

$$S_{IJ} = Ab_I b_J + Ac_I c_J \qquad \ldots\ 4.9\text{-}14$$

The final equations are obtained by adding all parts of a differential such as $\frac{\partial E}{\partial h_I}$ for all elements connected to Node I and equating to zero.

$$\frac{\partial E}{\partial h_I} = \sum \frac{\partial E^e}{\partial h_I} = 0 \qquad \ldots\ 4.9\text{-}15$$

$$\sum [S]\{h^e\} = 0 \qquad \ldots\ 4.9\text{-}16$$

For flow governed by the exponential relation the integral to be minimised is given by equation 4.8-18. The process of minimising the integral associated with an element again leads to equation 4.9-13 in which one term of the S matrix is given by equation 4.9-14 except that in this case the factor A is:

$$A = \frac{\Delta}{|h_s|^{\frac{m-1}{m}}} \qquad \ldots\ldots 4.9\text{-}17$$

Assembly of the total derivative for any node again yields equation 4.9-16.

For all nodes the result is a narrow band width set of simultaneous equations in h_I, h_J, h_M, ... etc which may be solved by an iterative method. The iterative procedure used was the accelerated Gauss-Seidel method with an over-relaxation factor of approximately 1.7; this has been shown to give rapid convergence of the finite difference solutions and was found to be satisfactory for the finite element solutions also. It should be noted that the expressions for A as given by equations 4.9-11 and 4.9-17 contain the derivative h_s which must be evaluated in terms of the nodal values h_I, h_J and h_M. Thus, in order to solve for values of h at the nodal points some initial value at each of these points must be known. The solutions to the Darcy flow situation provide convenient starting values for h at the nodes. The procedure is to calculate the [S] matrix in terms of these initial values and then solve for more accurate values of h_I, h_J, h_M etc; then use these more accurate values to re-form the [S] matrix and calculate more accurate values still. The process is repeated until the change in successive values of h_I, h_J, h_M, ... etc is

negligible. To determine the optimum number of iterations performed between successive formations of the [S] matrix, a compromise has to be reached between: (a) the time taken by more iterations producing only small changes in the values, and (b) the extra time involved in setting up the matrix more times at an earlier stage with less accurate values of h at the nodes. This optimum number will depend on the problem in hand but for the problems solved in this thesis, from 10 to 15 iterations between successive formations of the [S] matrix were found to give shortest overall computer time requirements.

The method used for handling the free surface was similar to that outlined by Finn (1967). If y and h are both measured from the impermeable base as datum then one boundary requirement on the free surface is that h = y. The initial position of the free surface was taken as the result obtained for Darcy flow. Surface adjustments to make y = h on the top boundary were carried out after the values of h had 'settled down' under the assumed boundary at any time. Usually only 1 or 2 adjustments were needed to obtain an agreement between y and h to within 1 percent for the flows with no cut-off wall; however, for the flows with cut-off walls the increased complexity in the bottom boundary shape necessitated more adjustments to the free surface.

The initial position of the free surface for the analysis of flow through a dam was obtained by sketching while the initial values of piezometric head at the nodes were guessed from the adjacent free surface height and were incorporated with the input data for the nodes.

The finite element solutions were output by plotting the elements with the on-line plotter, and printing out values of piezometric head at each node and velocity components for each element. The position of the free streamline was therefore obtained automatically from the plotter output while equal head lines could be sketched by hand from the nodal head values. The discharges across a number of vertical grid lines throughout the field were calculated and the average of these gave the finite element solution for discharge. Because of the difficulty of writing a general computer program to plot equal flow lines from a random arrangement of elements, these flow lines were not usually included in the finite element outputs. However, there is no disadvantage in this because all the desired information about any particular flow problem can be obtained from the plot of piezometric head values.

CHAPTER 5

EXPERIMENTAL APPARATUS AND PROCEDURES

5.1 Permeameter Tests

To determine appropriate values of the coefficients in the head loss relations, permeameter tests were carried out on the aggregates used in the experiments. The constant head permeameter was an upward flow vertical type of length 3 ft. 6 in., with piezometric head measurements being taken over a 1 ft. 6 in. central section. The permeameter was constructed from 1/8 in. perspex tubing of 6 in. outside diameter. Four brass taps, spaced 6 in. apart vertically, and at each corner of the four quadrants of a circle, served as outlets to manometers for pressure measurement.

Water was inlet to the permeameter via a steel basin, 1 ft. 0 in. deep and 1 ft. 9 in. in diameter, which was partly filled with coarse gravel to dampen any fluctuations in the flow. The sample of aggregate was supported on a gauze covered ring at the bottom, and held in place with another gauze covered ring at the top. An overall view of the permeameter is shown in Fig.5-1-1.

A thermometer was inserted in the flow to record temperatures; and the flow rates were measured gravimetrically. Petrol ether was used in the manometers, at

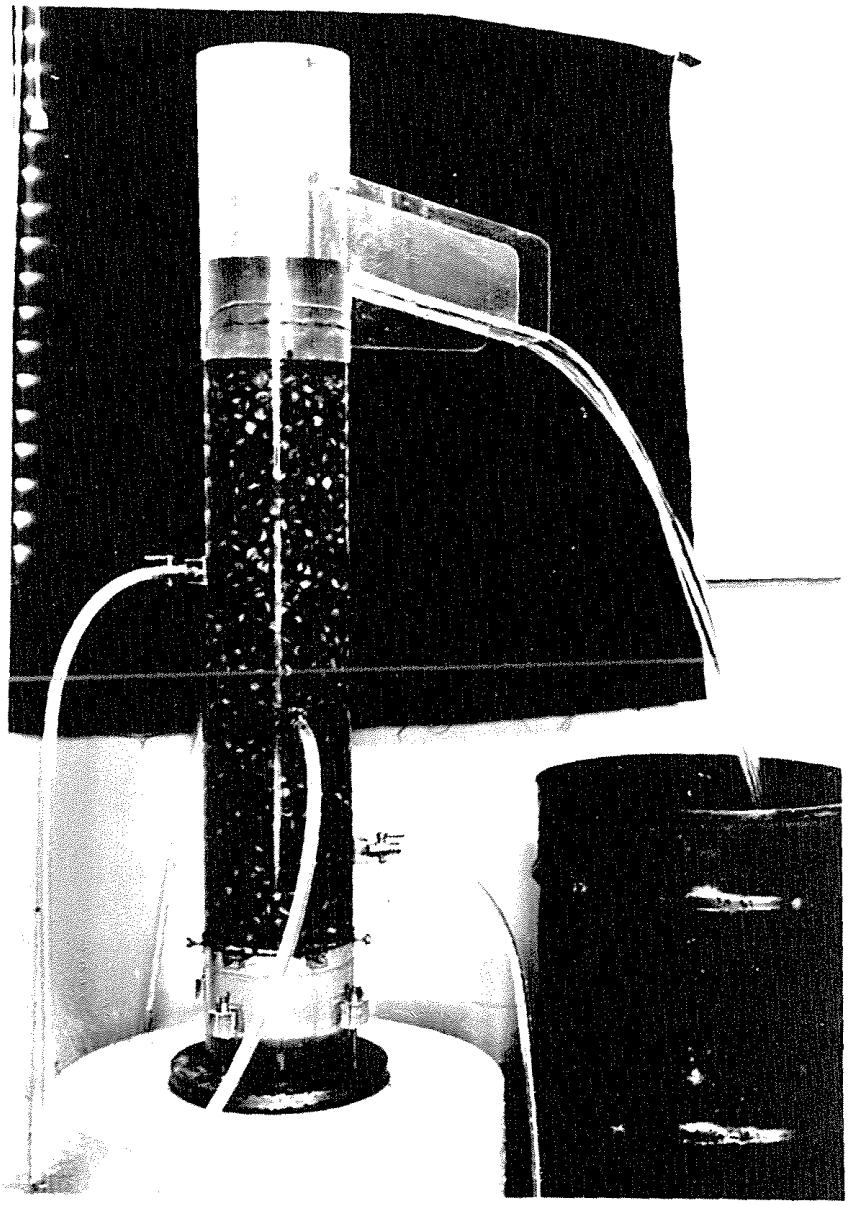

FIG. 5-1-1 VIEW OF PERMEAMETER

low flow rates, to increase the accuracy of measurement, while for larger flows water manometers were used. For porosity determinations, the permeameter was weighed empty, and again when filled to a measured depth with dry aggregate. After obtaining the specific gravity of the aggregate material, the porosity of the sample in the permeameter could be calculated.

5.2 Circular Tank Apparatus for Well Flow Experiments

5.2.1 Construction details

The circular tank of 20 ft. diameter was constructed with 6 ft. high walls and with a base formed by a reinforced concrete slab 25 ft. square. The walls were attached to the slab via a circular metal band which was rolled from 4 in. by 3/8 in. flat steel and which was set 2 in. into the slab. The band and slab reinforcing were spot welded, and the band was levelled with a dumpy level before the concrete was poured, to ensure that it was horizontal. Special precautions were taken when pouring the concrete, to produce a slab surface which was as uniformly horizontal as possible. A check on levels taken over the 25 ft. square, after the concrete had set, showed that the maximum deviation of the slab from the horizontal was less than 1/4 in.

The walls of the tank were constructed from flexiform which consists of 2 ft. by 6 ft., 14 gauge metal sheets,

braced in the longitudinal direction by light angles at 8 in. centres. This allowed the sheets, when bolted together, to flex and take up the required circular shape. The joint between the sheets was sealed with secostrip (a sealing compound in long thin strips), as was the joint between the walls and the metal band in the slab. The tank was braced in the circumferential direction by $1\frac{1}{4}$ in. diameter pipes, rolled to the diameter of the tank. Fig. 5-2-1 shows details of the flexiform construction, with circumferential pipe bracing, and longitudinal angle bracing on individual sheets.

Two larger removable panels were constructed from 3/16 in. rolled steel plate to allow access of trucks and end loaders for filling and emptying the tank. These panels were also braced with angles in the longitudinal direction and circumferentially with pipes. Fig. 5-2-2 shows the tank with these panels removed.

5.2.2 Inlet arrangement

The constant head required at the external radius of the simulated aquifer was produced by a porous wall of hollow concrete building blocks. The blocks, with openings in the vertical direction, were stacked in a single layer around the circumference as shown in Fig. 5-2-3. The water could then seep through into the aquifer

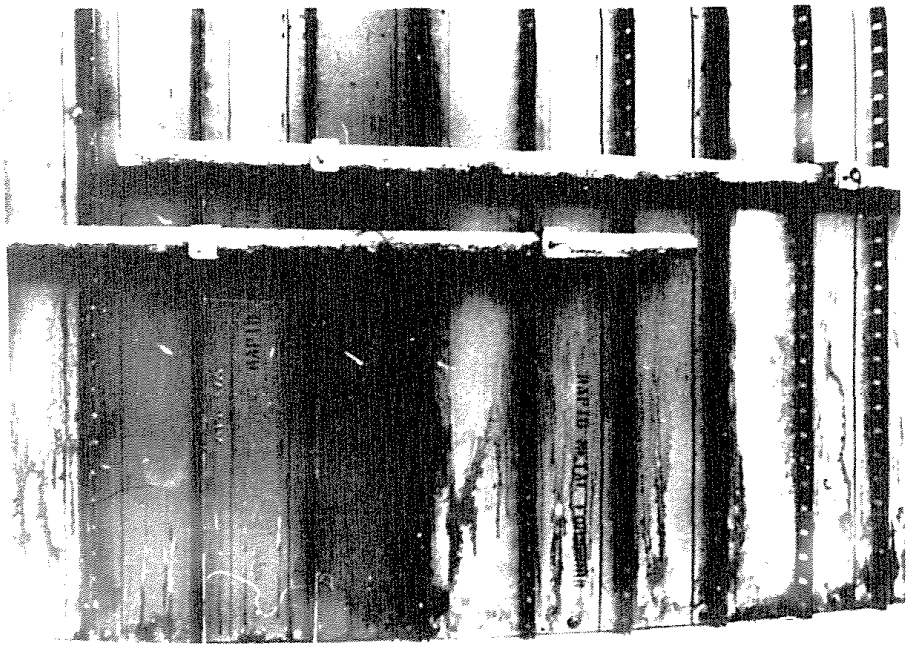

FIG. 5-2-1 DETAILS OF FLEXIFORM CONSTRUCTION

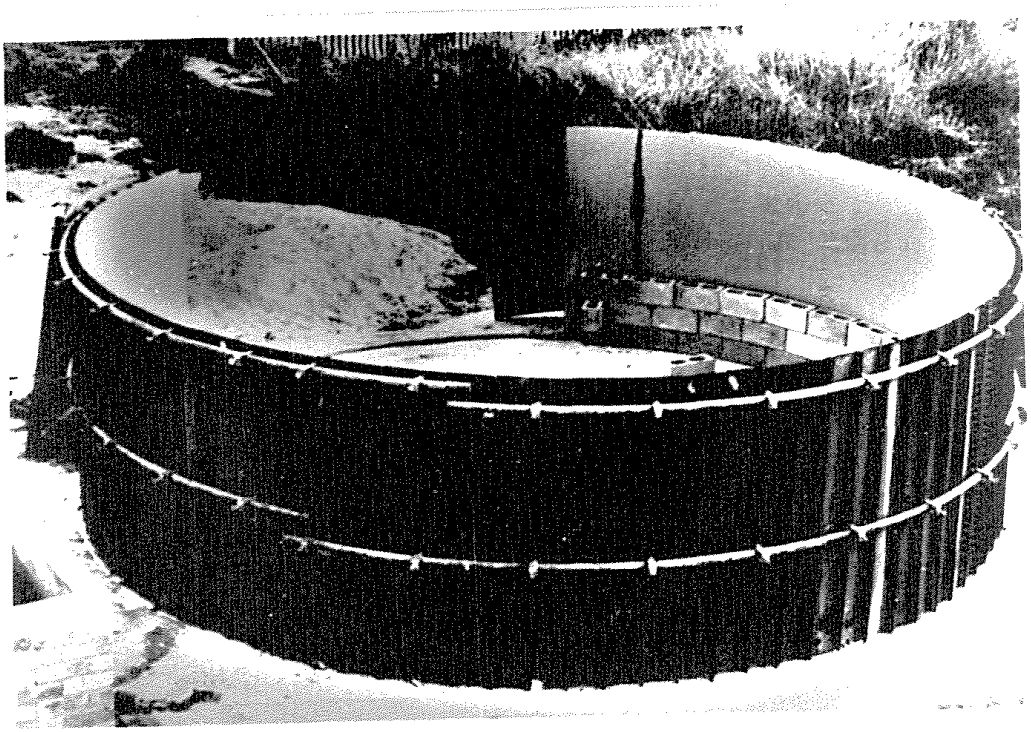

FIG. 5-2-2 CIRCULAR TANK WITH ACCESS PANELS REMOVED

material horizontally at the outer boundary. The water for the experiments was supplied from a constant head reservoir via a 5 in. aluminium pipe and hexagonal ring main. The ring main was supported on brackets attached to the circumference of the model and water was conducted into the layer of blocks by a number of 1½ in. diameter tubes spaced around the ring main. The flow to the tank was controlled by a gate valve in the line from the constant head reservoir. The inlet arrangement including the ring main is shown in Fig. 5-2-4.

5.2.3 Outlet arrangement and flow measurement

The well at the centre of the aquifer was constructed from pipe which was drilled over the section subjected to flow. A 4½ in. outside diameter pipe was used for the confined flow experiments, while one of 8½ in. external diameter was used for the unconfined tests. The holes were drilled at close intervals so that only a skeleton of metal remained to support a fine gauze, which covered the holes in an attempt to prevent movement of fines from the aquifer material. For example, with the 8½ in. diameter pipe, holes of 13/16 in. diameter were drilled at 1 in. centres. In this way, negligible additional head loss would be incurred as there is little increase in curvature of the flow lines at the slots. Although

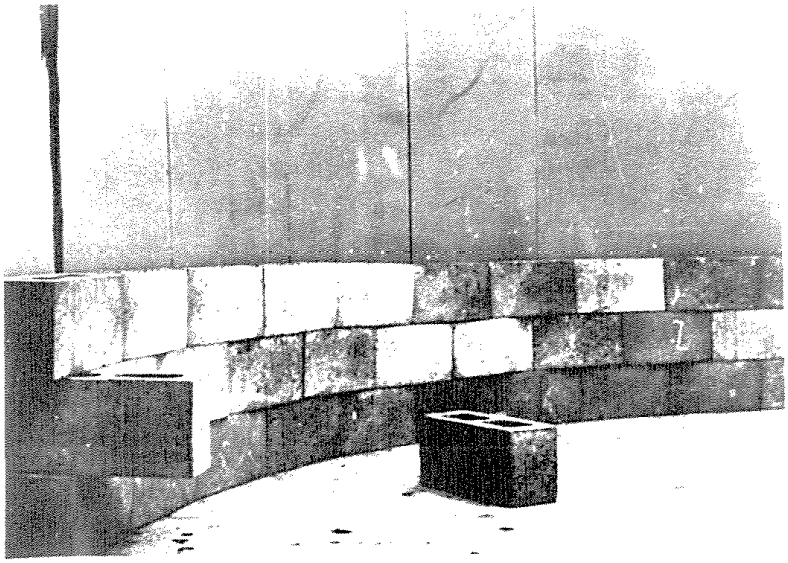

FIG. 5-2-3
VIEW SHOWING PART OF HOLLOW CONCRETE BRICK WALL

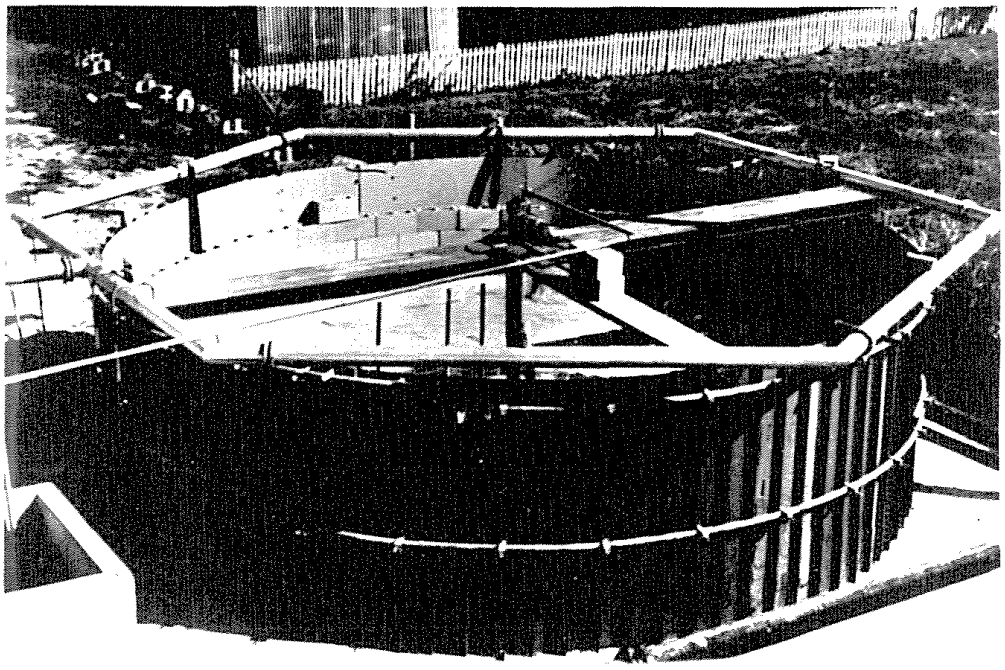

FIG. 5-2-4 VIEW OF TANK SHOWING INLET ARRANGEMENT

some slight head loss may result at the highest velocities, due to the small amount of metal remaining between the holes, the well can be assumed to be uncased for the purposes of the investigation. In each case the well was placed at the centre of the tank and rested on the concrete slab.

The drawdown to the well was maintained by pumping the water back through flow measuring devices to a storage reservoir. Two electric pumps were used to produce constant flows over extended periods of time. For low discharges, a small self-priming unit capable of pumping 30 gallons per minute was used while for larger flows, a unit capable of up to 1.25 cusecs was employed. The flow from each pump was regulated by means of valves on their delivery lines. The flow into the tank from the main, and the outflow from the pumps were varied to produce constant head conditions at the external radius and in the well itself. Measurements of discharge showed that the output from the electric pumps was constant, to a high degree of accuracy, over long intervals.

Two methods of flow measurement were used. Most discharges were measured gravimetrically using a drum on a set of scales which could be inserted under the

outflow for a measured period of time. This method is depicted in Fig. 5-2-5 in which only the outlet for the small pump is shown, although flows from the larger pump were measured similarly in some cases.

The other method of measurement involved a 90 degree vee-notch weir with its associated inlet channel, in which a gravel wall was included to act as a baffle for stabilising the flow on the upstream side of the weir. The weir had been previously calibrated and the height of the water above the vee-notch was measured using a hook-gauge. The arrangement is shown in Fig. 5-2-6.

5.3 Confined Axisymmetric Flow Tests

5.3.1 Technique for confining the flow

A confined aquifer was obtained by using visqueen as the confining medium. This is a soft, yet durable plastic-like material which is used extensively in constructing ground-level concrete slabs, to prevent seepage of groundwater upwards through the slab. A sheet of visqueen 30 ft. square was laid over the aquifer medium and was drawn up at the sides to cover the layers of bricks above the level of the aquifer. Fig. 5-3-1 shows the visqueen covering the aquifer medium, and ready to be drawn up to cover the upper layers of concrete bricks at the outer wall. Sand ballast was then placed

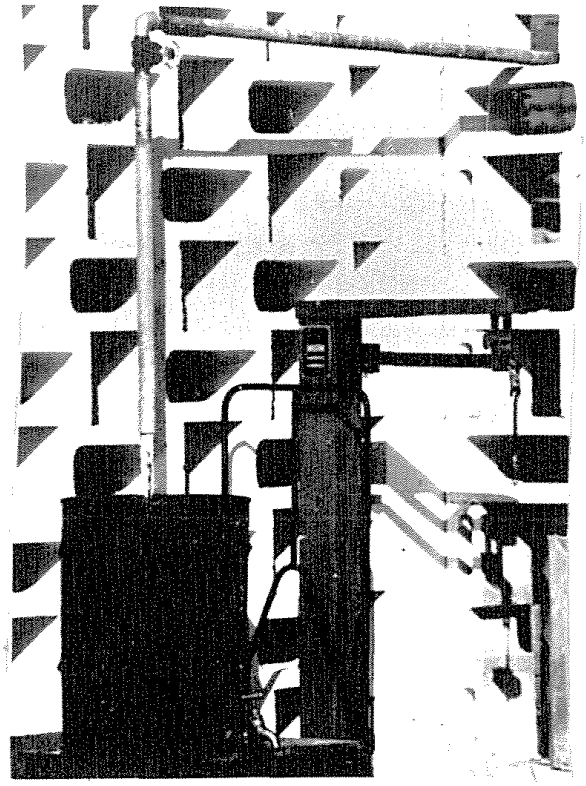

FIG. 5-2-5
FLOW MEASUREMENT USING SCALES
AND WEIGHING DRUM

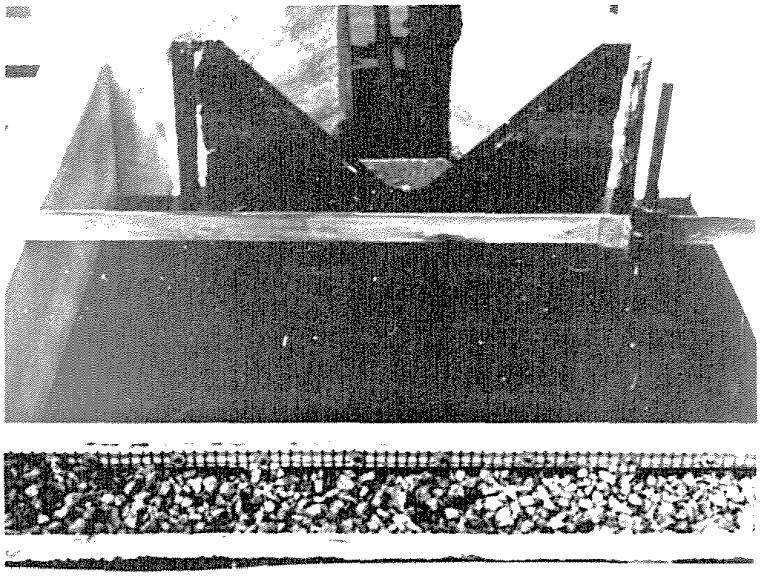

FIG. 5-2-6 90 DEGREE VEE-NOTCH WEIR

on top of the visqueen to seal it against the aggregate in the aquifer and against the outer brick wall. This method of sealing the flow proved to be quite satisfactory and heads of water at the outer boundary could be obtained up to any desired level, by introducing sand ballast up to that level. The sand ballast is shown in position in Fig. 5-3-2. A section through the model showing the flow path for the confined aquifer is given in Fig. 5-3-3.

5.3.2 Piezometric head measurements

The depth of water in the hollow concrete brick wall at the outer boundary, was measured by means of a standpipe attached to a scale, and connected to a tapping point at the base of the tank via a piece of flexible hose. A number of these standpipes were placed around a quadrant of the circle and the average of their readings was taken as the external head h_e. A comparison of the readings showed that differences between the heads measured were small. Fig. 5-3-4 shows the arrangement for one of the standpipes.

The depth of water in the well was measured by means of an electrical resistance device. This consisted of a volt-ohmmeter with its own power source, and a pair of wires which produced a change in resistance when a probe

FIG. 5-3-1
CONFINING VISQUEEN
LAYER

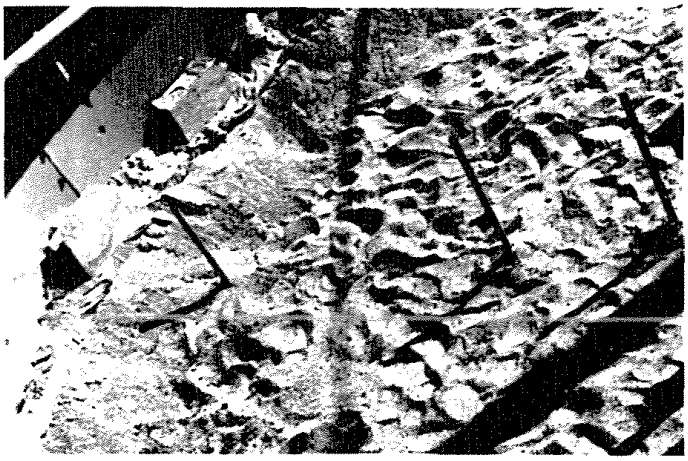

FIG. 5-3-2
SAND BALLAST COVERING
VISQUEEN

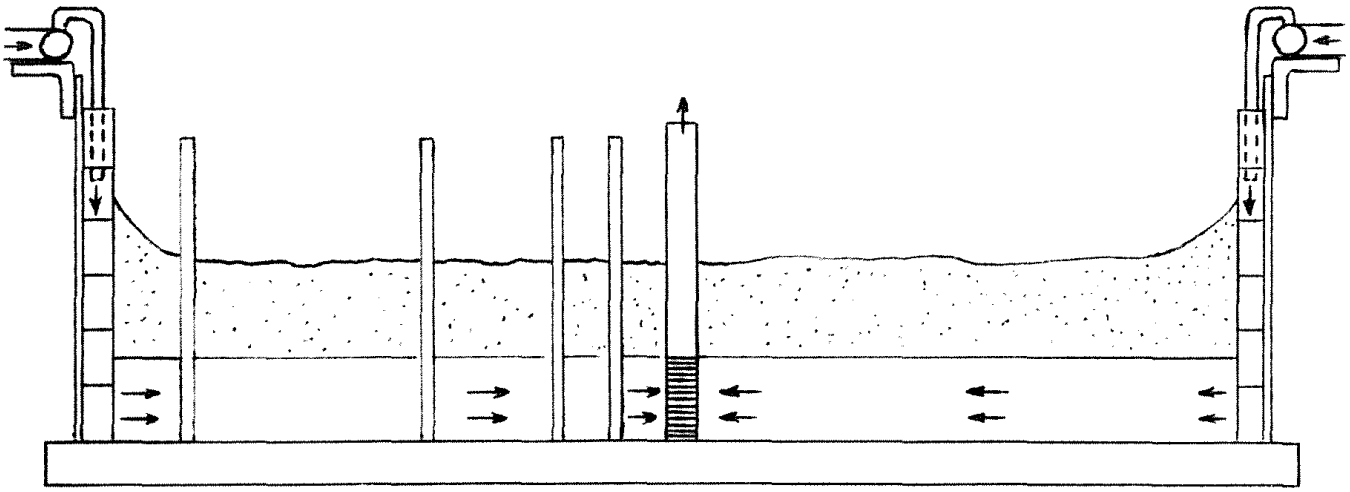

FIG. 5-3-3 SECTION SHOWING PATH OF WATER THROUGH MODEL

(to which they were attached) passed from air into water. The wires were bared at the end for $\frac{1}{4}$ in. and were separated by $\frac{1}{4}$ in. They were wound on a 3/16 in. graduated brass rod which could be lowered into the well. The change in resistance when the probe intered the water was registered as a sharp deflection on the volt-ohmmeter. Fig. 5-3-5 shows the probe with bared wire tips, while Fig. 5-3-6 shows the volt-ohmmeter used.

Since the theoretical calculation of discharge for a confined aquifer depends on the difference in level, between the water heights in the well and at the external radius, as well as on the magnitudes of the heights themselves, the maximum possible accuracy must be ensured in measuring the difference in levels. A horizontal datum line was therefore set with a dumpy level and the depths to the two water levels below this line were measured, allowing an accurate calculation of the difference between them.

It was originally intended to use porous plug type piezometers, developed by Casagrande (1949), in determining the shape of the piezometric head line through the model. However, as these could not be obtained in time, some alternative piezometers were fabricated from $\frac{3}{4}$ in. diameter pipe, which was drilled with 3/8 in. diameter holes and

FIG. 5-3-4
STANDPIPE FOR MEASURING
EXTERNAL HEAD

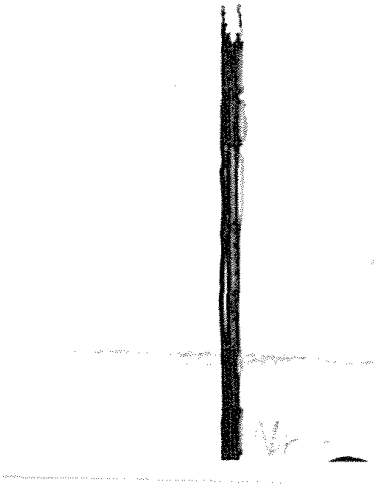

FIG. 5-3-5
ELECTRICAL RESISTANCE
PROBE

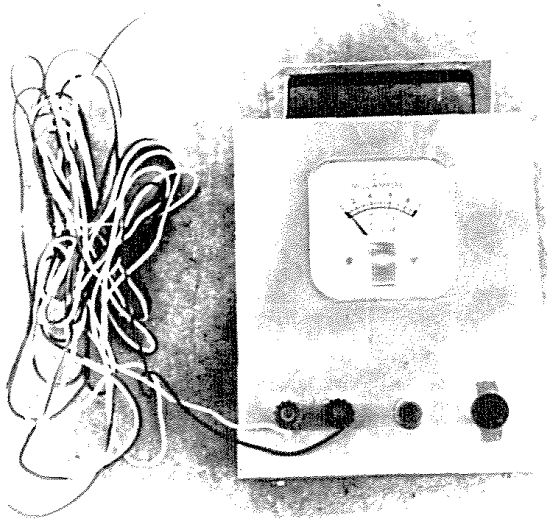

FIG. 5-3-6 VOLT-OHMMETER

covered with gauze for a length of 4 in. at one end. The end was shaped to a point for ease of insertion in the aquifer and to ensure that the piezometer rested on the base slab. Fig. 5-3-7 shows the end section of the piezometer, drilled and gauzed and shaped to a point, while Fig. 5-3-8 shows the whole piezometer.

When the piezometers are inserted into the aquifer, the water rises to the level of the piezometric head at the point. The piezometric heads at a number of radii can therefore be obtained by measuring the depth to the water levels in the piezometers, using the electrical resistance gauge.

5.3.3 Experimental procedure

The model was filled to the required depth with aquifer material by removing the gate panels and allowing trucks to enter the model and discharge their loads. The well was then set into position, the panels replaced and the aquifer material spread and levelled by hand. The thickness of the aquifer was checked with a dumpy level to ensure uniform thickness. The gravel material used in the experiments was placed to a depth of 1.33 ft. and a check on the levels showed that the maximum deviation from the horizontal was less than 3 percent.

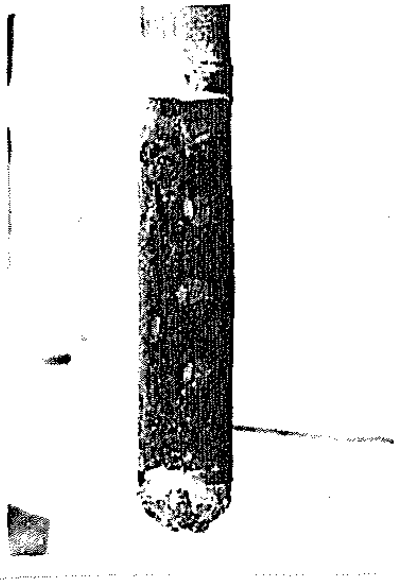

FIG. 5-3-7
END SECTION OF
PIEZOMETER

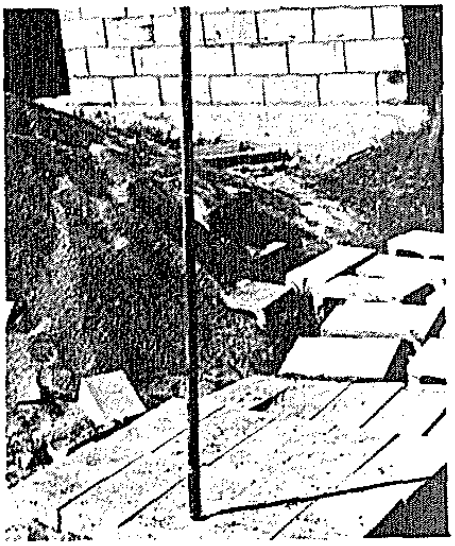

FIG. 5-3-8
PIEZOMETER

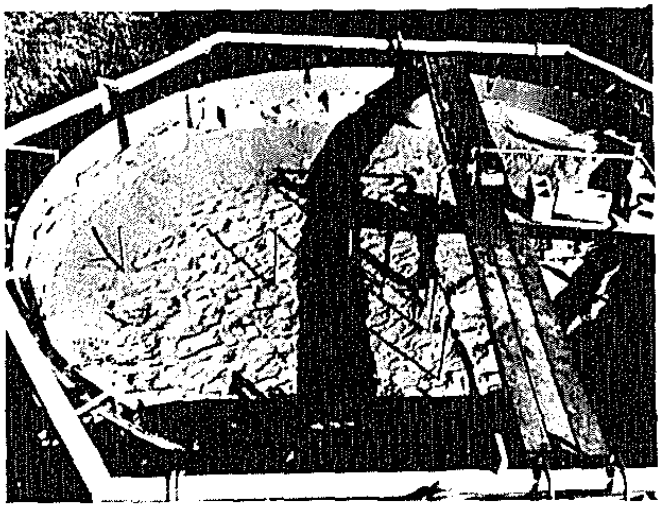

FIG. 5-3-9 PIEZOMETER LAYOUT

When the aquifer had been levelled, the visqueen sheet was laid and the piezometers were inserted and sealed in the visqueen. These were placed in two lines at right angles to enable an average value of piezometric head to be determined at each radius chosen. Four piezometers were included in each line at radii of 1 ft., 2 ft., 4 ft., and 8 ft. The sand used to hold the visqueen in position was then placed in the model by a front loader. Fig. 5-3-9 shows the tank prepared for testing, with the two lines of piezometers and the ballast sand in position.

Water was allowed to enter at the outer boundary and when the level in the well had risen above the aquifer depth, pumping was commenced. As a gravel was used for the aquifer material, no problem was envisaged with air entrainment, after a large flow had been drawn through the aquifer initially, to wash out any entrapped air. However, some small amount may have remained in the aquifer but it is not considered that this would have significantly affected the results.

The pump output was set to the required flow value and the inflow-rate was then adjusted until the desired head at the external boundary had achieved a steady value. By checking water levels and discharge rates before and

after each test, it was found that an essentially steady state could be maintained over long intervals of time.

5.4 Unconfined Axisymmetric Flow Tests

5.4.1 Experiments with complete circle of material

The confined flow experiments, described in section 5.3 were carried out using a complete circle of material so that no wall effects from side walls were introduced. However, the agreement of results from the two lines of piezometers at right angles indicated that the flow was accurately axisymmetric as assumed. This demonstrated that for small gravel sizes, a sector of material could be used to represent the complete circle of flow as had been used by a number of previous researchers, and discussed in section 3.2.1. However, one set of results was obtained for unconfined flow to a central well in a complete circle of material. This set of experiments was carried out because a sufficient supply of gravel material was readily available and because, in this case, wall effects were completely eliminated, and the flow situation was similar to that likely to occur in practical applications.

The experimental procedure was similar to that outlined for the confined flow experiments except that the porous plug piezometers had been obtained and were

used, in conjunction with the electrical resistance meter, to determine the height of the free surface. These piezometers, which were discussed by Casagrande (1949) were 2 ft. long hollow tubes, porous throughout their entire length. They were placed so as to intersect the free surface at a number of points between the well and the external boundary of the aquifer material. However, the water level in these piezometers does not exactly represent the height of the phreatic line. Hantush (1962b) indicated that, in an unconfined aquifer, an unlined well will register the average of the piezometric heads taken over that part of its length below water level. The error, thus incurred in determining the height of the free surface, can be minimised by having only a small length of tube below water level; nevertheless, only an approximate measurement of the free surface position was obtained.

Measurements of the water levels at the outer boundary and in the well, together with discharge measurements, were obtained as in the confined flow experiments discussed in section 5.3.

5.4.2 Experiments using a sector of material

A fifty-one degree sector was constructed as a part of the large circular tank described in section 5.2, using

the access panel section of the larger tank for the outside boundary of the sector, to facilitate removal and replenishment of aquifer materials. One radial wall of the sector was constructed from sheet steel while the other was fabricated from perspex. Both sheets were reinforced and braced to withstand the pressure from the aquifer material and from the water. The sheets were sealed against the concrete base by bolting to steel angles which were in turn bolted to the concrete. The well casing was also bolted down and sealed against the concrete slab, while the radial walls were attached to the well via vertical angles welded to the casing. The well, of $8\frac{1}{2}$ in. outside diameter, was drilled and gauzed only over the section enclosed between the sector walls. A view of the empty sector, with the outside wall removed, is shown in Fig. 5-4-1 looking towards the well.

A row of hollow concrete blocks was again used at the outer boundary to allow water to percolate into the aquifer from a constant level. However, in this case, an overflow was arranged at the outside wall to enable a constant level to be maintained with a minimum adjustment of the quantity of incoming flow. Water was conducted to the sector via a 5 in. aluminium pipe terminating in a tee-section, from which six $1\frac{1}{2}$ in.

diameter inlet tubes were fed into the hollow concrete brick wall. Five standpipes were spaced around the outer boundary to check the water level and, by adjusting the flow in each inlet tube, the external head h_e could be maintained constant to within 1/10 in. over the complete sector boundary. The inlet arrangement to the sector is shown in Fig. 5-4-2.

The water level h_w, in the well, was also measured with a standpipe attached to a tapping point in the sealed section of the well casing. Both levels were measured from the same horizontal datum, to eliminate any small errors due to variation in the concrete base level.

Piezometric head measurements throughout the flow were obtained from brass taps inserted into the radial steel wall at various points. Fig. 5-4-3 shows the arrangement of tapping points which were used for measuring piezometric heads.

The position of the phreatic surface was obtained by plotting along the transparent perspex sheet. Although surface tension effects were small for the gravel materials used, they did slightly affect the free surface height along the perspex sheet. To minimise these effects as far as possible, the material was excavated next to the perspex sheet, almost to the free surface level. The

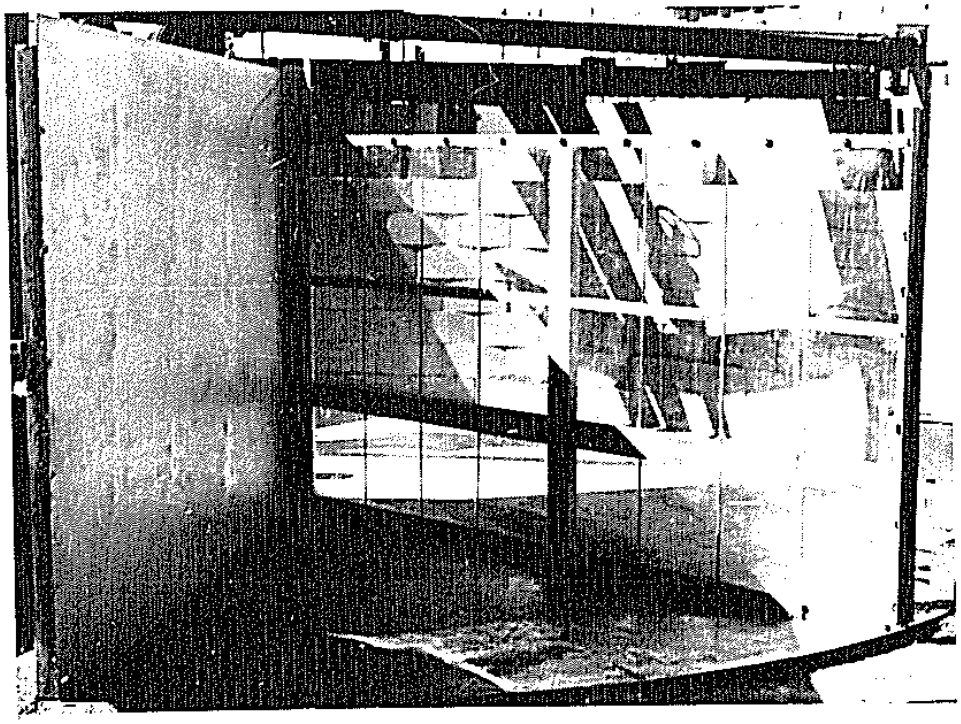

FIG. 5-4-1 VIEW SHOWING SECTOR CONSTRUCTION

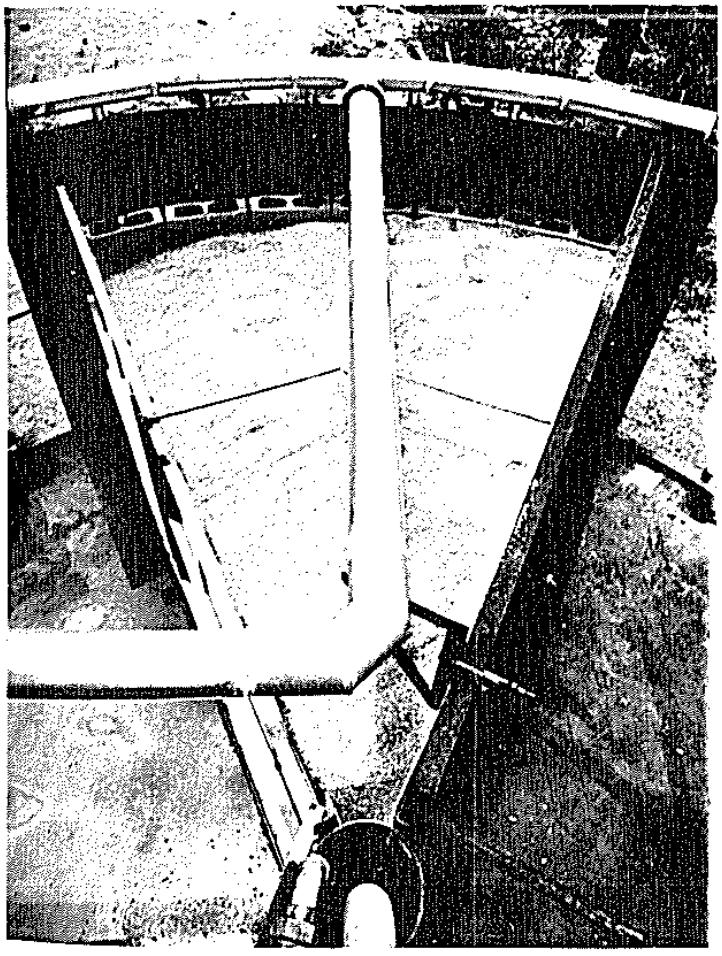

FIG. 5-4-2
INLET ARRANGEMENT FOR
SECTOR

phreatic line was then drawn on a square grid which had been marked on the perspex sheet. This facilitated the recording of the free surface position for each test.

The measurements obtained by this method were shown to be satisfactory, by checking the levels in a glass tube, of sufficient diameter to nullify surface tension effects, which was inserted next to the perspex wall. This procedure was described by Boulton (1951) who used it to check his free surface heights.

One free surface line is shown as drawn on the perspex sheet in Fig. 5-4-4.

5.5 Two-Dimensional Flow Experiments

5.5.1 Gravel bank tests

The two-dimensional flow tests were carried out in an open flume 2 ft. wide, 2 ft. deep and with one clear perspex side for viewing purposes. Water was supplied to the flume from the constant head reservoir via a 6 in. diameter pipe discharging into a stilling basin on the upstream side of the flume. The inlet arrangement and an overall view of the flume are shown in Fig. 5-5-1.

At the outlet end, the flume discharged into a calibrated measuring tank. A set of scales and a weighing drum could also be set under the outlet, so that flow rates could either be measured gravimetrically with the

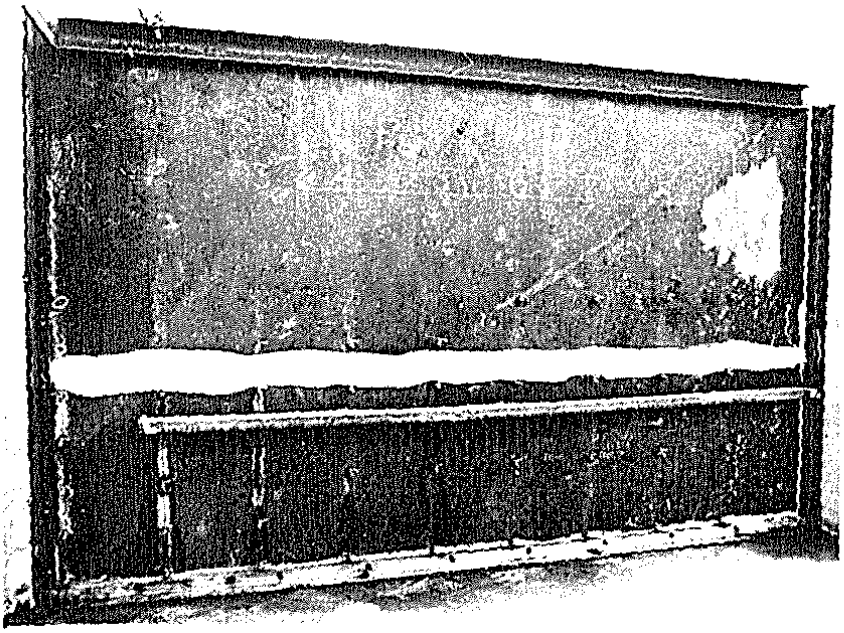

FIG. 5-4-3 PIEZOMETRIC HEAD TAPPING POINTS

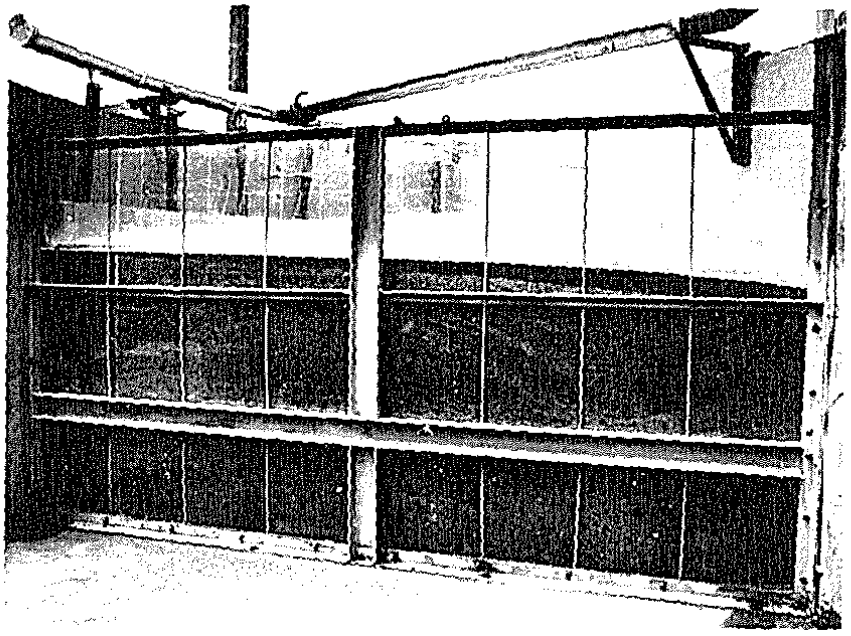

FIG. 5-4-4 FREE SURFACE DETERMINATION

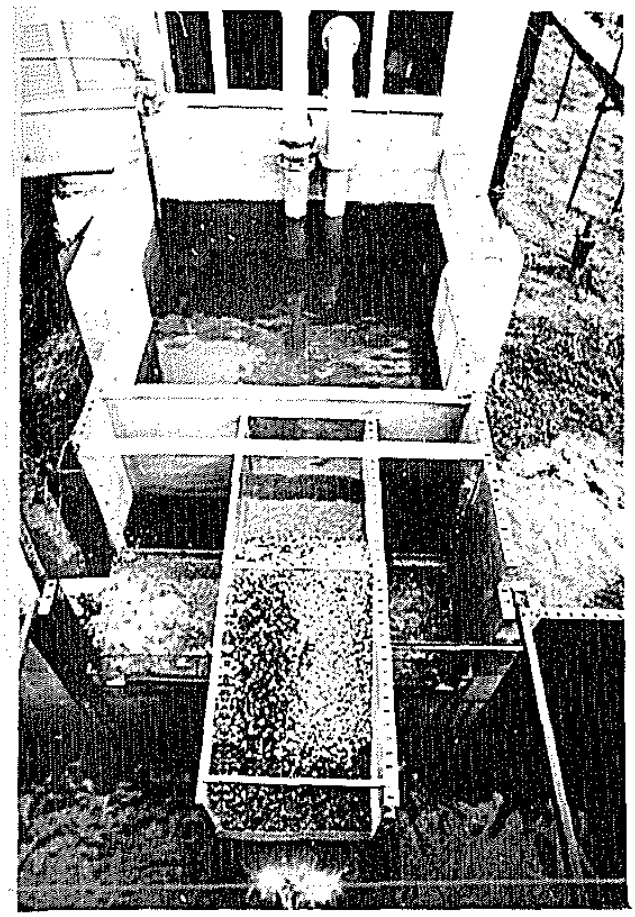

FIG. 5-5-1
ARRANGEMENT FOR OPEN
FLUME EXPERIMENTS

FIG. 5-5-2
DISCHARGE MEASUREMENTS FOR
OPEN FLUME EXPERIMENTS

scales or with the calibrated tank. The scales are shown inside the calibrated tank in Fig. 5-5-2.

In the experiments on flow through gravel dams and banks no attempt was made to model actual dam conditions, as the purpose of the investigation was simply to determine whether the numerical solution of the differential equations for nonlinear flow, could predict accurately the position of the phreatic surface and the quantity of discharge, for known boundary conditions and material properties. For larger flows therefore, a wire screen was positioned at the tow of the gravel dam to prevent scour of material on the downstream end; the flow then ended in a vertical drop off at the screen resulting in zero tailwater depth. For smaller flows however, the gravel material was stable without the use of the screen and a finite value of tailwater depth occurred at the downstream end of the flume. No experimental or theoretical analysis of stability aspects was contemplated in this project.

The gravel used in the dam flow experiments was $\frac{3}{4}$ in. nominal size and no difficulty was encountered with surface tension effects. The free surface position was drawn on the perspex side of the flume and was recorded from the grid of lines marked on the perspex. Fig. 5-5-3

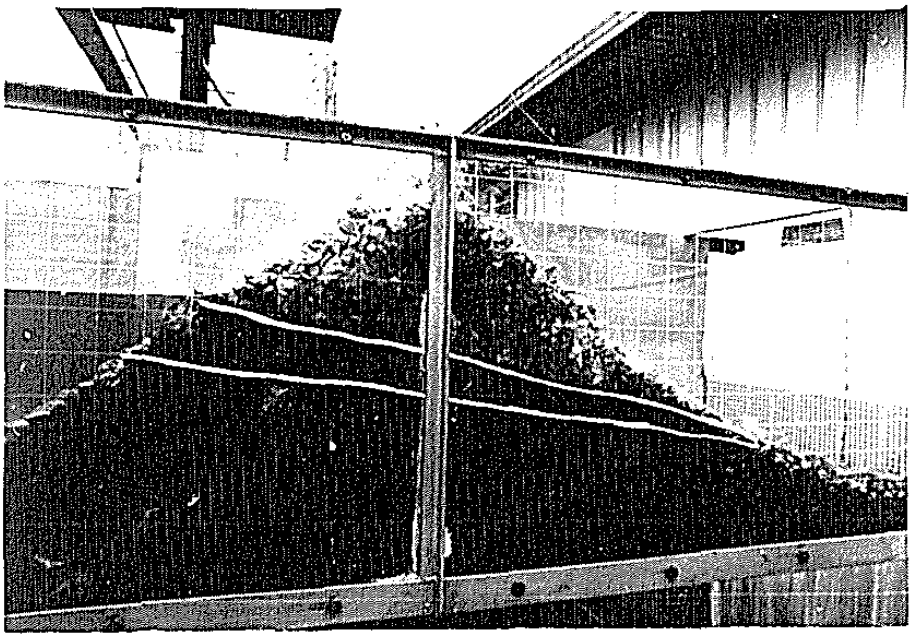

FIG. 5-5-3 PHREATIC LINE DETERMINATION IN DAM FLOW EXPERIMENTS

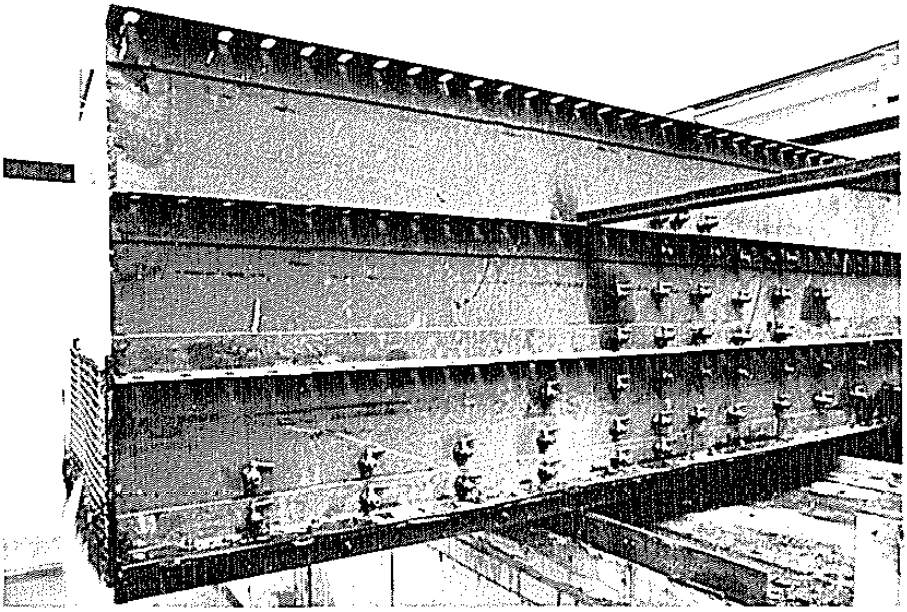

FIG. 5-5-4 PIEZOMETRIC HEAD TAPPING POINTS FOR FLUME EXPERIMENTS

shows two phreatic lines drawn on the transparent side of the flume.

Measurements of piezometric head in the experiments were obtained from tapping points on the steel side of the flume. The arrangement of these tapping points is shown in Fig. 5-5-4.

Some of the dam flow experiments involved an impervious cut-off wall which was sealed at the bottom and sides of the open flume. A cut-off wall is shown in position in Fig. 5-5-5.

5.5.2 Tests on permeable walls with vertical sides

These experiments were also conducted in the open flume. The gravel, in this case, was retained between two vertical sheets of gauze placed perpendicular to the direction of flow. The experimental procedures for measuring discharge, piezometric head, free surface position etc, were similar to those discussed in section 5.5.3. A view of the flume showing a bank of gravel between the gauze retainers is given in Fig. 5-5-6.

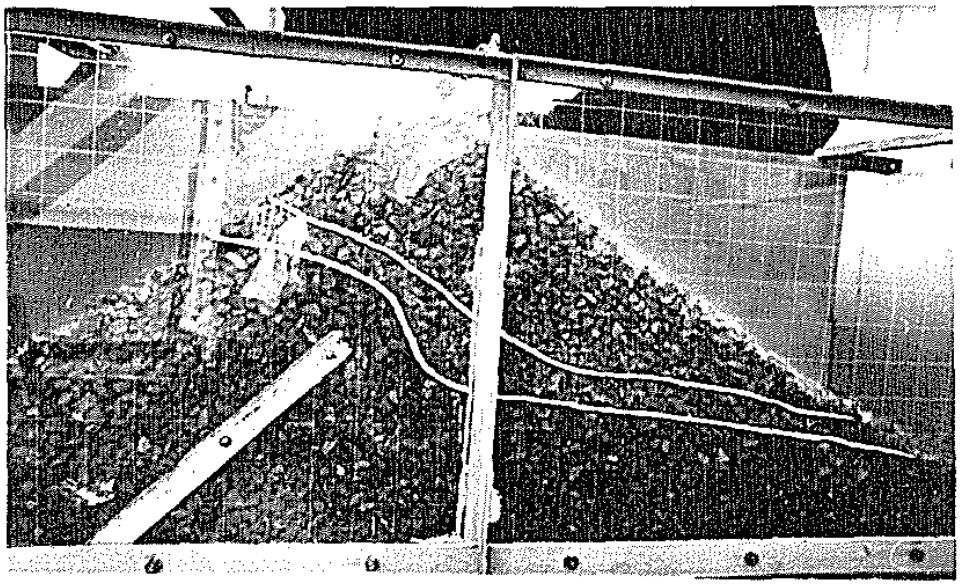

FIG. 5-5-5 IMPERVIOUS CUT-OFF WALL

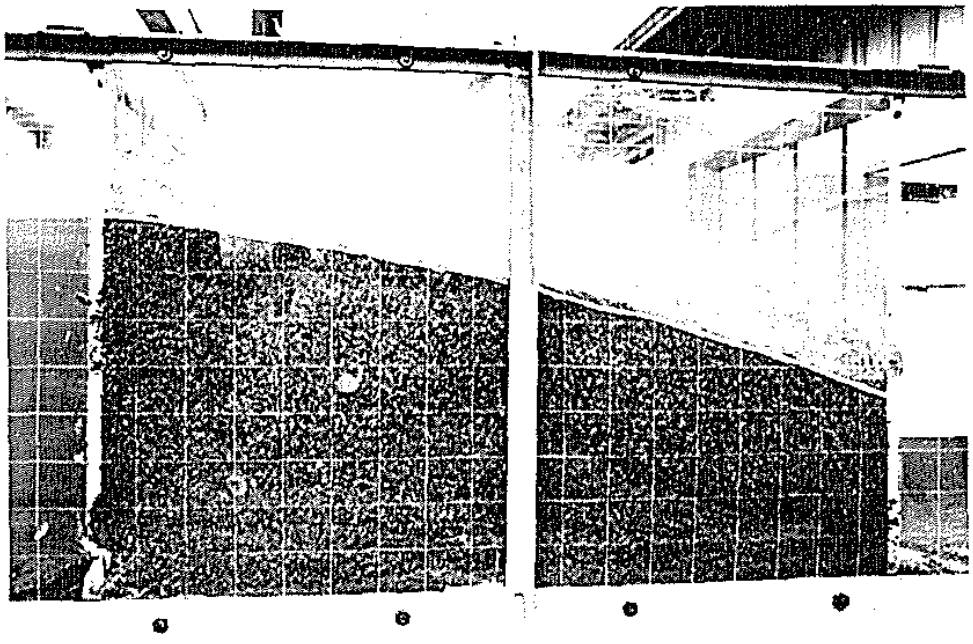

FIG. 5-5-6 ARRANGEMENT FOR VERTICAL SIDED PERMEABLE WALL EXPERIMENTS

CHAPTER 6

DISCUSSION AND COMPARISON OF RESULTS - PART I

6.1 Confined Axisymmetric Flow Experiments

6.1.1 Coefficients in head loss equations

The material used in the confined flow experiments was a gravel of nominal size 3/16 inch. To obtain the appropriate coefficients to be inserted in the head loss relations, permeameter tests were carried out on the material being used. If the coefficients are to correspond exactly with those which apply to the material in the actual well flow experiments, the sample taken from the circular tank should be packed in the permeameter in the same way as the parent material is packed in the tank, with porosities, arrangement of solid particles, etc being identical. However this requirement of identical packing can only ever be approximately met and the coefficients obtained from the results of the permeameter tests were therefore checked by comparing one calculated flow with the experimental result from the tank experiments. This is somewhat analogous to obtaining the Darcy coefficient of permeability from a well pump test, except that no associated permeameter results are required for the Darcy coefficient.

For correspondence of the coefficients, the Reynolds number range in the permeameter should also coincide with

that in the circular tank. Since the material is assumed uniform, the particle diameters will be equal and the Reynolds number criterion reduces to a requirement that the velocity to viscosity ratios be equal. Since the coefficients in the head loss equations are affected by the viscosity of the water, the axisymmetric well flow experiments were carried out at temperatures which were sufficiently uniform to render variations in viscosity negligible. By carrying out the experiments at similar times on successive days, no difficulty was experienced in maintaining the temperature constant to within 1 or 2 degrees Fahrenheit.

During the permeameter tests, however, the temperature range was greater and the temperatures at which the tests were carried out differed from that of the well flow experiments. In order to eliminate differences due to viscosity the permeameter results were reduced to equivalent readings at the temperature of the well flow experiments. Because the arrangement of the material in the permeameter is constant, the Reynolds number criterion of similarity can be applied to reduce the actual results to corresponding results at the reference temperature. For similarity of flow conditions the Euler numbers are also equated since the flow in the permeameter is confined and

gravity effects do not influence the flow pattern. Thus if the subscript o is used to denote the reference state and if the subscript 1 is used to denote properties actually measured in the permeameter then the following relationships apply. For the two states of flow to be dynamically similar the Reynolds numbers must be equal:

$$\frac{V_o d_o}{\nu_o} = \frac{V_1 d_1}{\nu_1} \qquad \text{.... 6.1-1}$$

and since $d_o = d_1$ then

$$V_o = V_1 \frac{\nu_o}{\nu_1} \qquad \text{.... 6.1-2}$$

Also since pressure forces predominate in the permeameter, the Euler numbers must be equal:

$$\frac{V_o}{\sqrt{2\Delta p_o/\rho_o}} = \frac{V_1}{\sqrt{2\Delta p_1/\rho_1}} \qquad \text{.... 6.1-3}$$

and because the pressure drops are measured over the same length in the permeameter then:

$$\frac{\Delta p_o}{\Delta p_1} = \frac{i_o}{i_1} \qquad \text{.... 6.1-4}$$

whence equation 6.1-3 may be written:

$$i_o = \frac{\rho_o}{\rho_1} \frac{V_o^2}{V_1^2} i_1 \qquad \text{.... 6.1-5}$$

Thus equations 6.1-2 and 6.1-5 can be used, if necessary, to reduce the permeameter measurements V_1, i_1, to V_o, i_o at the standard temperature at which the well flow experiments were performed. With the elimination of effects due to viscosity differences, the requirement of a similar range of Reynolds numbers in the permeameter will be satisfied by including a range of velocities similar to those occuring in the tank.

The nominal size of the aggregate was given as 3/16 inch but calculations from sieve analysis results showed that the arithmetic mean particle diameter (after Dalla Valle, 1948) was .110 inches. The ratio of diameter of particle to diameter of the permeameter is therefore less than 1:50. There still appears to be some contention as to the required ratio of these dimensions to eliminate wall effects. Mott (1951) showed that for spherical particles the wall effect was negligible for ratios of less than 1:10; but that for irregular shaped particles the wall effect was present at smaller values than 1:10. Recent work by Dudgeon (1967) indicates that some wall effect may be present at very small values of the ratio of mean particle diameter to permeameter tube diameter. However, both Mott and Dudgeon used particles of essentially uniform size and the wall effect is then likely to be more pronounced than

with a graded material as used in the experimental work discussed here. Franzini (1968) suggested that for field work a ratio of 1:10 should be sufficient, while for research type work a ratio of 1:40 should be attempted, to eliminate wall effects. The ratio of 1:50 involved with the 3/16 inch nominal size material is less than both the suggested figures, and no further consideration was given to the wall effect.

The coefficients in the head loss equations were obtained by fitting the appropriate curves to the experimental data by a least squares analysis. Because of the wide range of readings taken, a direct least squares curve fit was unsuitable as it placed too much emphasis on the higher readings and tended to ignore the lower order results. A proportional least squares analysis was therefore employed to yield values of the coefficients which would enable accurate prediction of the head loss for the full range of velocities encountered. Sunada (1965) introduced a proportional least squares procedure to fit a Forchheimer relation to a wide range of experimental results. This procedure involved minimisation of the square of the ratio of the difference between the observed and calculated gradients to the corresponding velocity. A slightly different approach used by How Lum

(1966) minimised the square of the ratio obtained by dividing the deviation of the calculated hydraulic gradient from the measured gradient by the measured gradient itself. The latter approach was utilised in this thesis and was extended to a proportional least squares fit of the exponential relation.

Thus if T_k represents the theoretical hydraulic gradient calculated from the fitted curve and if O_k is the observed or experimental value of the gradient, both corresponding to the k^{th} velocity reading V_k, then the function to be minimised is:

$$S = \sum_{k=1}^{n} \left(\frac{T_k - O_k}{O_k} \right)^2 \qquad \text{.... 6.1-6}$$

in which n is the total number of experimental readings taken.

For the Forchheimer curve, equation 6.1-6 becomes:

$$S = \sum_{k} \left(\frac{aV_k + bV_k^2 - O_k}{O_k} \right)^2 \qquad \text{.... 6.1-7}$$

Since S is to be minimised with respect to a and b then:

$$\frac{\partial S}{\partial a} = 2 \sum_{k} \left(\frac{aV_k + bV_k^2 - O_k}{O_k} \right) \frac{V_k}{O_k} = 0 \qquad \text{.... 6.1-8}$$

or

$$a \sum_{k} \left(\frac{V_k}{O_k} \right)^2 + b \sum_{k} \left(\frac{V_k}{O_k} \right)^2 V_k = \sum_{k} \left(\frac{V_k}{O_k} \right) \qquad \text{.... 6.1-9}$$

Similarly on minimising S with respect to b, the result is:

$$a\sum_k\left(\frac{V_k}{O_k}\right)^2 V_k + b\sum_k\left(\frac{V_k}{O_k}\right)^2 V_k^2 = \sum_k\left(\frac{V_k}{O_k}\right)^2 O_k \quad \ldots\ldots 6.1\text{-}10$$

Equations 6.1-9 and 6.1-10 may then be solved simultaneously to yield the coefficients a and b.

An estimate of the accuracy of fit of the Forchheimer curve was obtained by calculating a standard percent error of estimate defined as:

$$SE = \sqrt{\frac{1}{n}\sum_{k=1}^{n}\left\{\left(\frac{aV_k+bV_k^2-O_k}{O_k}\right) \times 100\right\}^2} \quad \ldots\ldots 6.1\text{-}11$$

For the exponential relation, the curve fitting process is not as straightforward since logarithms have to be taken before the least squares analysis is performed; thus

$$\ln i = \ln c + m\ln V \quad \ldots\ldots 6.1\text{-}12$$

Equation 6.1-6 might then be written in terms of the appropriate logarithms:

$$S = \sum_{k=1}^{n}\left(\frac{\ln T_k - \ln O_k}{\ln O_k}\right)^2 \quad \ldots\ldots 6.1\text{-}13$$

By minimising S with respect to c and m the coefficients may be calculated. A standard error of estimate for the exponential relation may then be obtained as:

$$SE = \sqrt{\frac{1}{n}\sum_{k=1}^{n}\left\{\left(\frac{cV_k^m - O_k}{O_k}\right) \times 100\right\}^2} \quad \ldots\ldots 6.1\text{-}14$$

However, by virtue of taking logarithms, the effective range of values is decreased; as a result, a least squares curve fit was obtained by minimising the following quantity:

$$S = \sum_{k=1}^{n} \frac{(\ln T_k - \ln 0_k)^2}{\ln 0_k} \qquad \ldots\ldots 6.1\text{-}15$$

After trials it was found that this process resulted in a curve with a smaller standard error of estimate (defined as in equation 6.1-14) than the curve obtained by minimising S in equation 6.1-13. The coefficients c and m were therefore obtained by this method. Minimising S with respect to c in equation 6.1-15 gives:

$$\frac{\partial S}{\partial c} = 0 = 2 \sum_{k} \frac{(\ln c + m \ln V_k - \ln 0_k)}{\ln 0_k} = 0$$

or

$$\sum_{k} \frac{\ln c}{\ln 0_k} + m \sum_{k} \frac{\ln V_k}{\ln 0_k} - \sum_{k} 1 = 0 \qquad \ldots\ldots 6.1\text{-}16$$

Similarly minimising S with respect to V_k results in the equation:

$$\sum_{k} \frac{\ln c \ln V_k}{\ln 0_k} + m \sum_{k} \frac{(\ln V_k)^2}{\ln 0_k} - \sum_{k} \ln V_k = 0 \qquad \ldots\ldots 6.1\text{-}17$$

Thus the coefficients c and m can be obtained by simultaneous solution of equations 6.1-16 and 6.1-17

The experimental results and fitted curves for the material used in the confined flow experiments are plotted in Fig. 6-1-1.

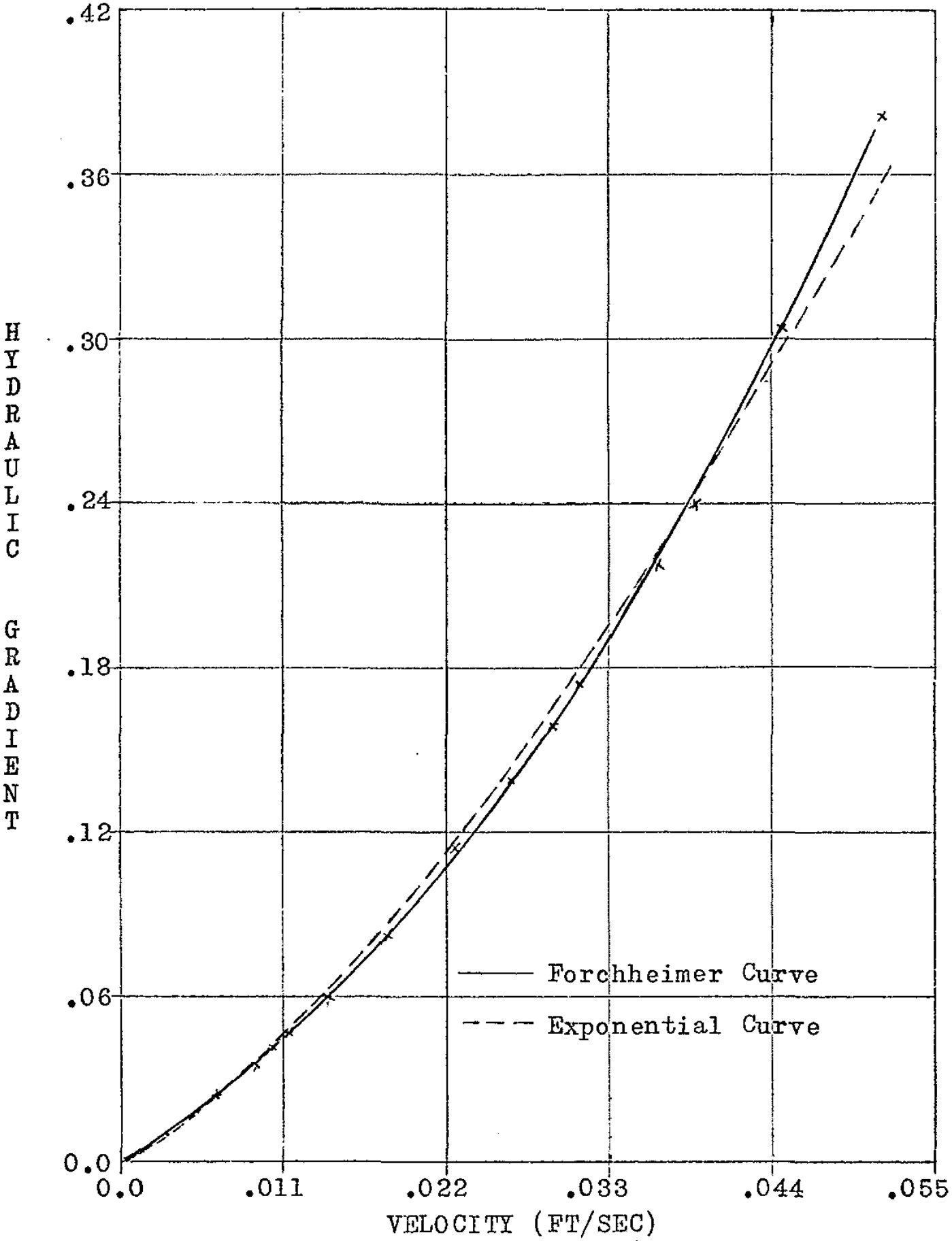

FIG. 6-1-1 PERMEAMETER RESULTS FOR MATERIAL IN CONFINED FLOW EXPERIMENTS

The coefficients in the head loss relations and the standard error of estimate SE for each relation are given in Table 6-1-1.

Forchheimer Relation	a(sec/ft)	b(sec^2/ft^2)	SE
	3.054	83.613	4.5%
Exponential Relation	c	m	SE
	15.355	1.283	11.4%

TABLE 6-1-1 COEFFICIENTS FOR CONFINED FLOW EXPERIMENTS

As there was no guarantee that the porosity of the material in the permeameter would be the same as that of the material in the tank, a check was made on the coefficients by comparing one of the experimental flows with the corresponding calculated flow. Thus for the external head h_e = 3.156 ft. and the internal head h_w = 2.696 ft., the experimental discharge was .177 cusecs. The theoretical value obtained from the Forchheimer relation was .179 cusecs but that from the exponential relation was .191 cusecs. However, in view of the close agreement of the Forchheimer result with the experimental one, the coefficients obtained from the permeameter tests, and given in Table 6-1-1, were accepted.

6.1.2 Experimental and analytical results

For the confined flow problem, analytical solutions are available for each of the Darcy, Forchheimer and

exponential relations. In the analytical solutions it was assumed that no additional loss of head occurred at the well screen. As was noted in section 5.2.3, the well was perforated at close intervals and covered with gauze so that little distance between openings occurred. For this reason, the assumption of an uncased well should be valid within the limits of experimental error. The assumption is made that the exit head loss at the well surface is equal to the velocity head of the water entering the well. Also, as the velocity is very small at the external boundary, no inlet loss of head is considered. Thus the boundary conditions for piezometric head in the analytical solutions are that $h = h_w$ at the well and $h = h_e$ at the external boundary.

To obtain a discharge value from the Darcy solution, the permeability must be known. However, it is obvious from the permeameter results that the permeability varies continuously with velocity and, for this reason, a reference value of the coefficient of permeability was obtained in a manner similar to that which would be employed in practical situations. The coefficient was calculated from one of the well flow tests, this test being the one which was used to check the coefficients in the nonlinear equations. The value thus obtained for the permeability coefficient was

.181 ft/sec. A comparison of the accuracy of the solutions obtained from the linear and nonlinear head loss relations could then be made directly. Four flows were carried out and are designated as flow Nos. 1 to 4 in order of increasing magnitude of discharge. Flow No.1 was taken as the reference flow. Some of these results have been reported by Tapiolas (1967).

The experimental results obtained for flow No.3 are compared with the Darcy, Forchheimer and exponential solutions in Figs. 6-1-2, 6-1-3 and 6-1-4 respectively. The piezometric head curves are plotted in each diagram and the radii r_w, r_e, internal and external heads h_w, h_e and the experimental and theoretical discharge values in cusecs are also given in each figure. The corresponding results for flow Nos. 1, 2 and 4 are given in Figs. A-I-1 to A-I-9 inclusive, in Appendix I.

A comparison of the discharges for flow No.3 shows that the Forchheimer relation gives by far the most accurate value when compared to the experimental one. However inspection of the piezometric head lines shows that the Darcy result compares most favourably with the experimental result, while the Forchheimer and exponential lines show a substantial deviation from it. This is surprising in view of the fact that the permeameter results

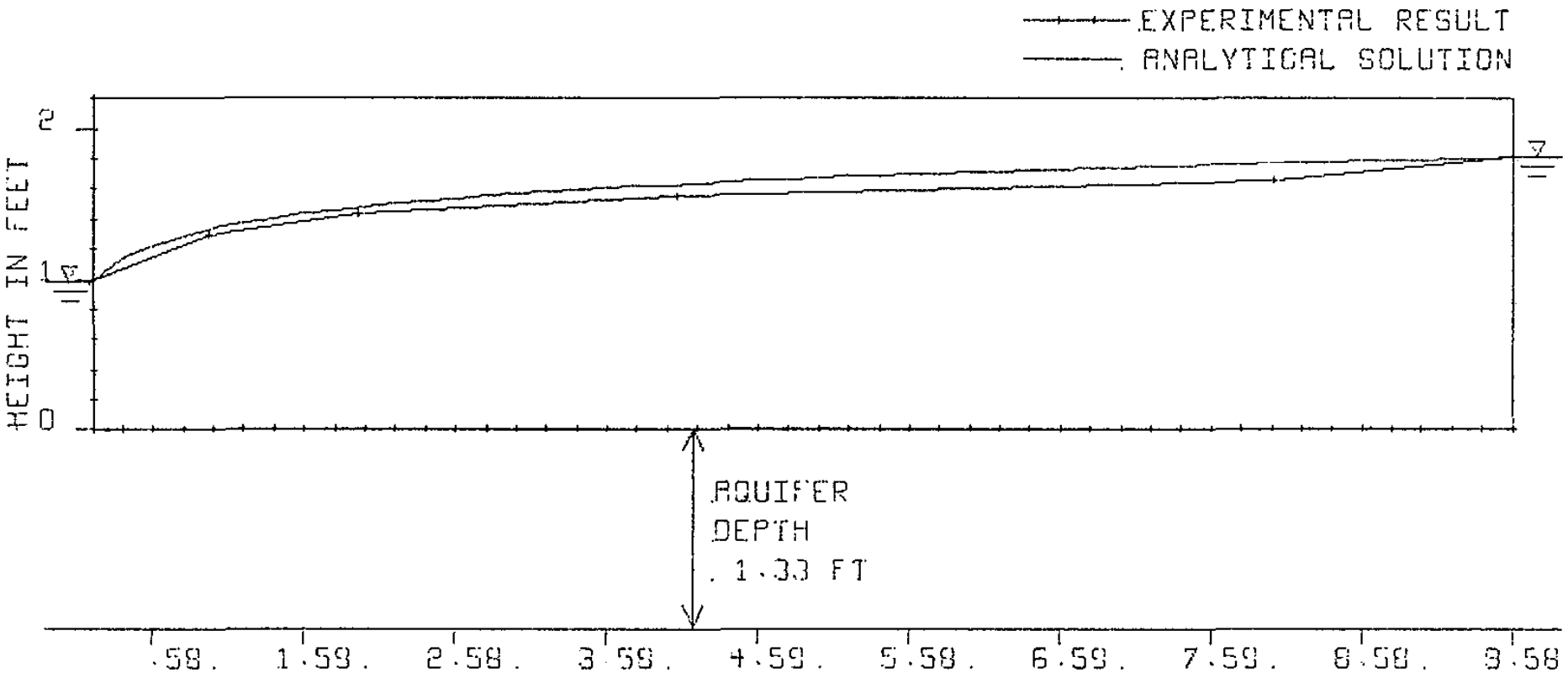

CONFINED FLOW EXPERIMENT
FLOW NO 3
RESULTS FOR DARCY FLOW

RW= .187 RE= 9.597
HW= 2.312 HE= 3.137
Q(CALC) = .317 Q(EXPER) = .264 CUSEC

FIG. 6-1-2

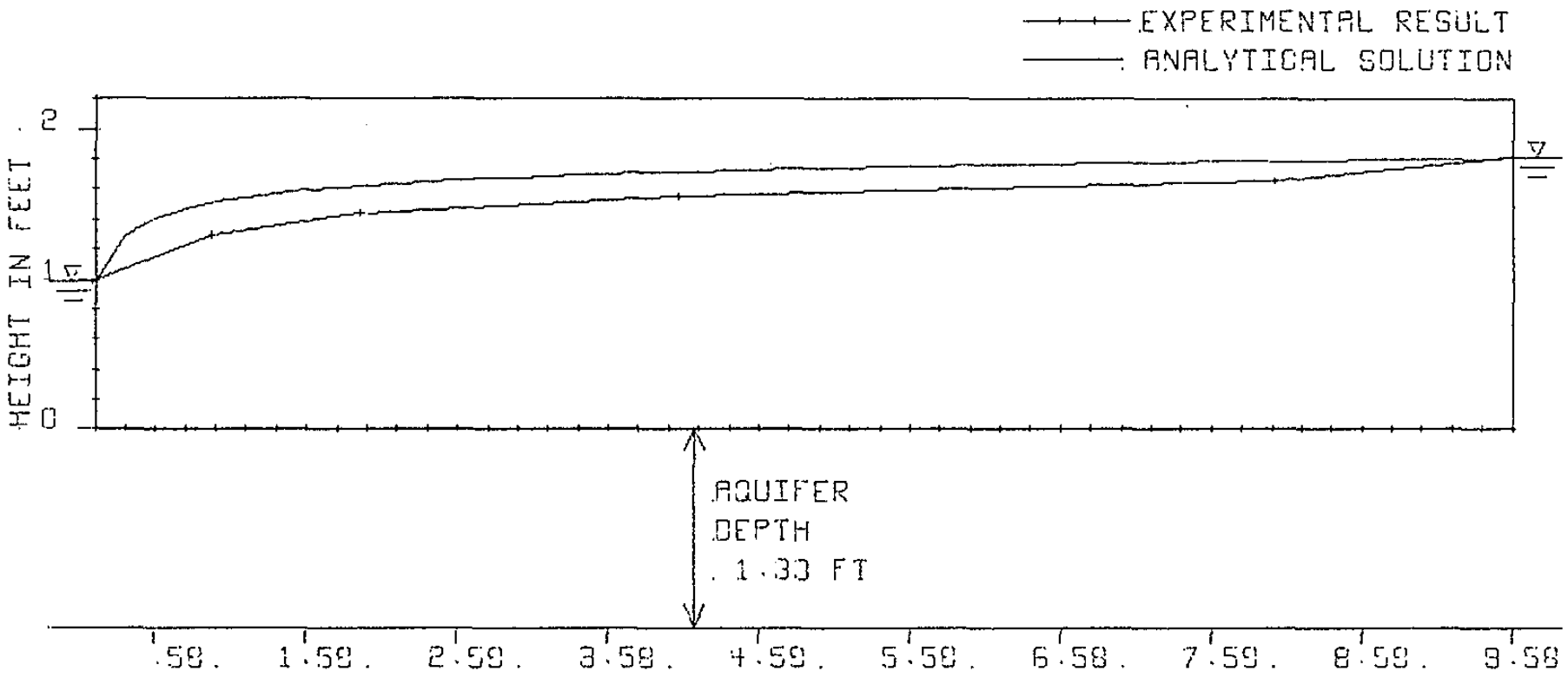

CONFINED FLOW EXPERIMENT
FLOW NO 3
RESULTS FOR FORCHHEIMER FLOW

RW= .187 RE= 9.587
HW= 2.312 HE= 3.137
Q(CALC) = .265 Q(EXPER) = .264 CUSEC

FIG. 6-1-3

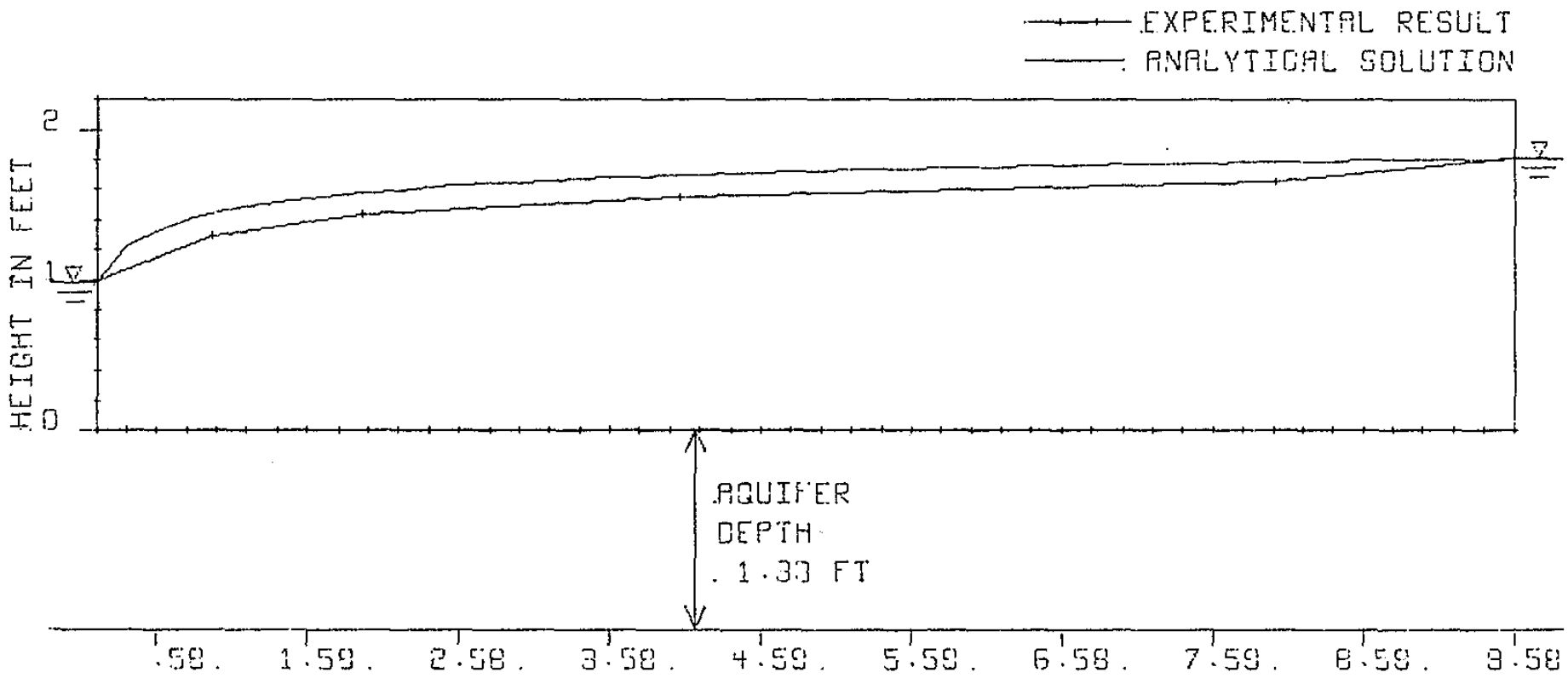
EXPERIMENTAL RESULT
ANALYTICAL SOLUTION
HEIGHT IN FEET
2
1
0
AQUIFER
DEPTH
1.33 FT
.58
1.59
2.58
3.58
4.59
5.59
6.58
7.59
8.59
9.58
RADIUS IN FEET
CONFINED FLOW EXPERIMENT
FLOW NO 3
RESULTS FOR EXPONENTIAL FLOW
RW= .187
HW= 2.312
RE= 9.587
HE= 3.137
Q(CALC) = .301
Q(EXPER) = .264
CUSEC

FIG. 6-1-4

show that Darcy's Law is decidedly inaccurate over the range of velocities which occur between the external radius and the well for any particular flow. A study of the results for flow Nos. 2 and 4 shows similar trends, although for flow No.4, the discharge obtained from the exponential relation agrees slightly more closely with the experimental result than does that from the Forchheimer relation. Considering the close agreement of the Forchheimer calculated discharges with the corresponding experimental ones over the range of flows investigated, it would be expected that the Forchheimer piezometric head lines should agree accurately with the experimental results.

It is considered that some of the discrepancy between the experimental piezometric head line and the corresponding analytical result from the nonlinear relations may be due to experimental error. Some difficulty was experienced in forming a watertight seal around the piezometer tapping points which penetrated the visqueen impervious layer, and consequently the piezometric head measured may have been less than that which actually occurred. This hypothesis is reinforced by the fact that even the Darcy calculated head lines are higher than the recorded results. However in spite of the discrepancies between calculated and measured piezometric head lines, the flow results showed that

solutions based on the nonlinear relations could accurately predict discharge values over a range of head differences.

In Fig. 6-1-5, the experimental and various calculated discharge values are plotted against the corresponding head difference between the external and internal radii. As the depth of aquifer is constant the discharges are plotted directly against the head differences causing flow.

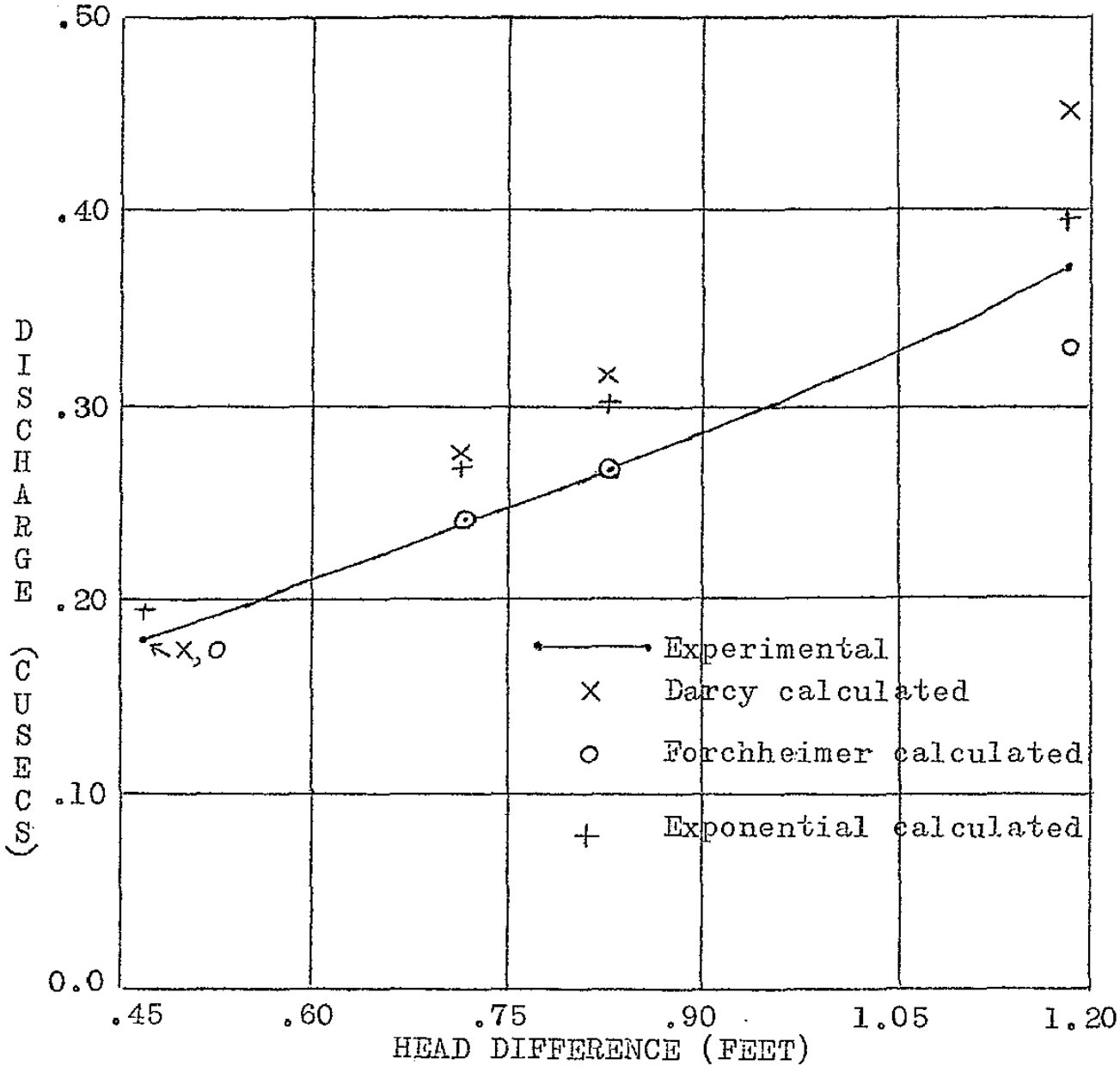

FIG. 6-1-5
DISCHARGE RESULTS FOR CONFINED FLOW EXPERIMENTS

Fig. 6-1-5 shows that, while the discharge calculated from the Forchheimer relation agrees accurately with the experimental value for flow Nos. 1, 2 and 3, it exhibits a larger discrepancy for flow No.4 although it is still more accurate than the Darcy calculated value. The velocity at the well radius for flow No.3 is about .15 ft/sec whereas the largest values involved in the permeameter experiments are of the order of .06 ft/sec. The radius at which the velocity decreases to .06 ft/sec is approximately 6 inches so that this represents the extent of the area in which the Reynolds numbers in the tank exceed those in the permeameter. For flow No.4 the velocity at the well is about .25 ft/sec while the radius at which the velocity decreases to .06 ft/sec is $8\frac{1}{2}$ inches. There is thus a larger area in which the Reynolds number range of the permeameter tests is exceeded and, in addition, the discrepancy is greater than for flow No.3. It appears that some of the difference between the observed discharge and that calculated from the Forchheimer relation for flow No.4 is due to the fact that the coefficients are applied too far outside the Reynolds number range for which they were ascertained. It is clear therefore that, as far as possible, the coefficients in the nonlinear head loss equations should be obtained over the Reynolds number range for which they are to be applied.

The situation of steady confined flow to a well at the centre of an island, as examined in the confined flow experiments, occurs rarely in practice, where confined flow situations usually involve unsteady flow over a large area. The confined flow experiments were undertaken as a prelude to steady unconfined flow.

6.2 Unconfined Axisymmetric Flow with Complete Circle

6.2.1 Permeameter tests

The material used in this set of experiments was similar to that used in the confined flow tests, being gravel of 3/16 inch nominal size. However it was supplied at a different time and contained a higher percentage of fines which caused a marked difference in the flow properties from those of the material of the confined flow experiments. One of the problems involved in determining the flow properties of an insitu material from permeameter tests is the necessity to duplicate the porosity of the insitu material in the permeameter, and this problem was found to be accentuated by the higher percentage of fines. Engelund (1953) noted that, for sands, a small change in the porosity could have a marked effect on the value of the Forchheimer coefficients. With a cohesionless substance such as sand or gravel, it is difficult to obtain an undisturbed sample and for this reason a method was devised

to obtain the coefficients in the head loss equations from actual flow tests in the tank, in conjunction with permeameter tests on samples of the material at two different porosities. The theory of obtaining the coefficients from an unconfined flow test is outlined in section 6.2.2.

In an attempt to cover a wide range of porosities of the material, one sample was placed loosely in the permeameter with only light tamping to maintain uniformity of packing, while another was placed as tightly as possible. The loosely placed material resulted in a higher porosity sample on which permeameter tests were carried out for a range of Reynolds numbers. Average seepage velocities and corresponding hydraulic gradients were calculated. A study of these results showed a continuous variation in the permeability coefficient indicating that Darcy's Law is again invalid for this material. The coefficients a and b in the Forchheimer equation and c and m in the exponential relation were obtained by least squares curve fitting to the results. A proportional least squares fit was again employed in order to obtain representative coefficients to cover a wide range of Reynolds numbers. Precautions were taken to reduce the permeameter results to equivalent readings at the temperature of the well flow experiments. The results for the higher porosity sample together with

best fit Forchheimer and exponential curves are plotted in Fig. 6-2-1.

The other test was carried out on a sample which was compacted as much as possible by ramming and tamping in the permeameter. This resulted in a low porosity sample and the experimental results together with the fitted curves are plotted in Fig. 6-2-2.

The standard errors of estimate of the curves were obtained as described in section 6.2.1. The coefficients in the head loss equations for the two samples and the standard errors of estimate of each fitted curve are set out in Table 6-2-1.

High Porosity Sample			
Forchheimer Relation	a	b	SE
	2.499	67.617	3.06%
Exponential Relation	c	m	SE
	23.834	1.499	13.33%
Low Porosity Sample			
Forchheimer Relation	a	b	SE
	4.850	133.224	5.51%
Exponential Relation	c	m	SE
	39.363	1.394	16.22%

TABLE 6-2-1
COEFFICIENTS FOR UNCONFINED FLOW WITH COMPLETE CIRCLE

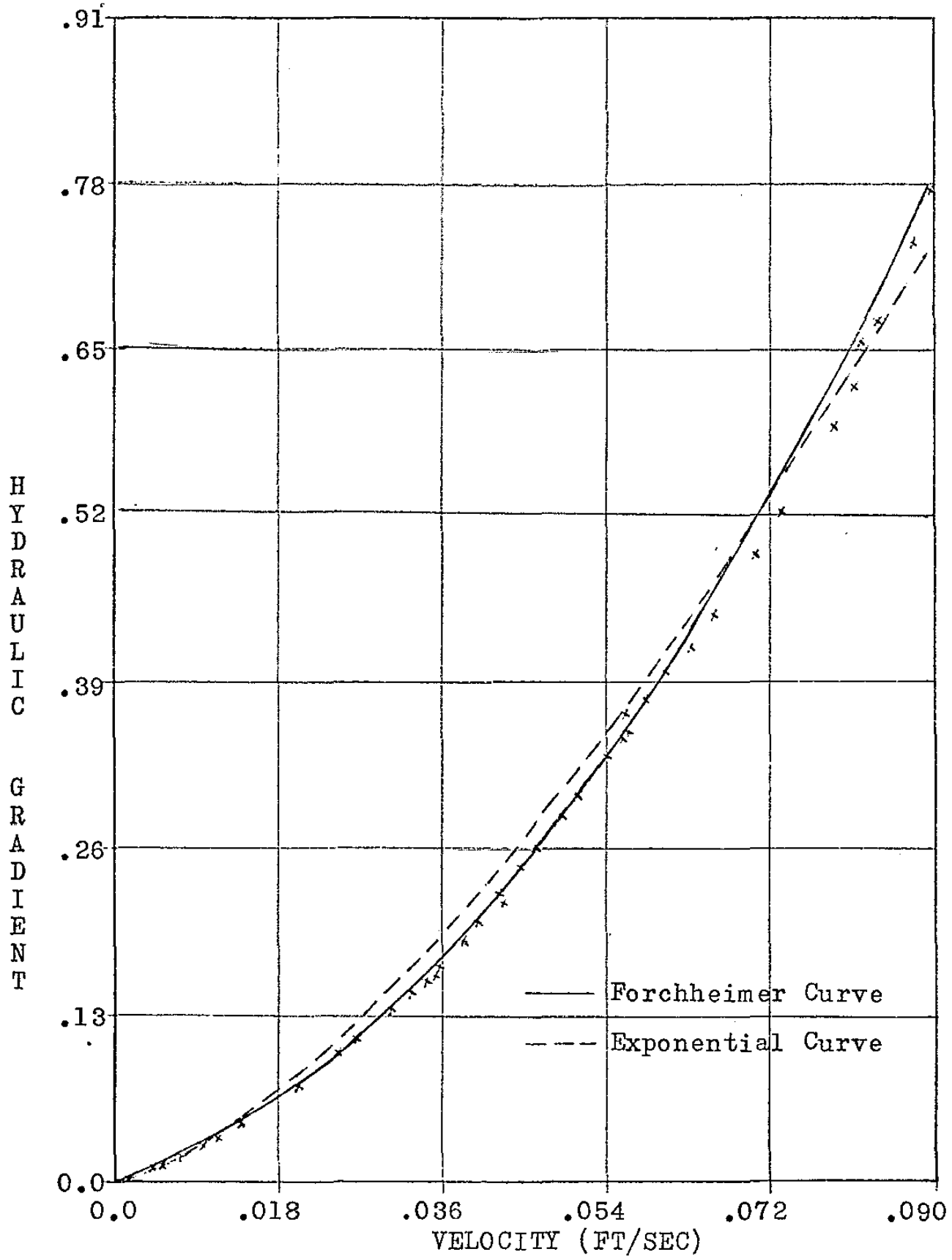

FIG. 6-2-1 HIGH POROSITY PERMEAMETER RESULTS

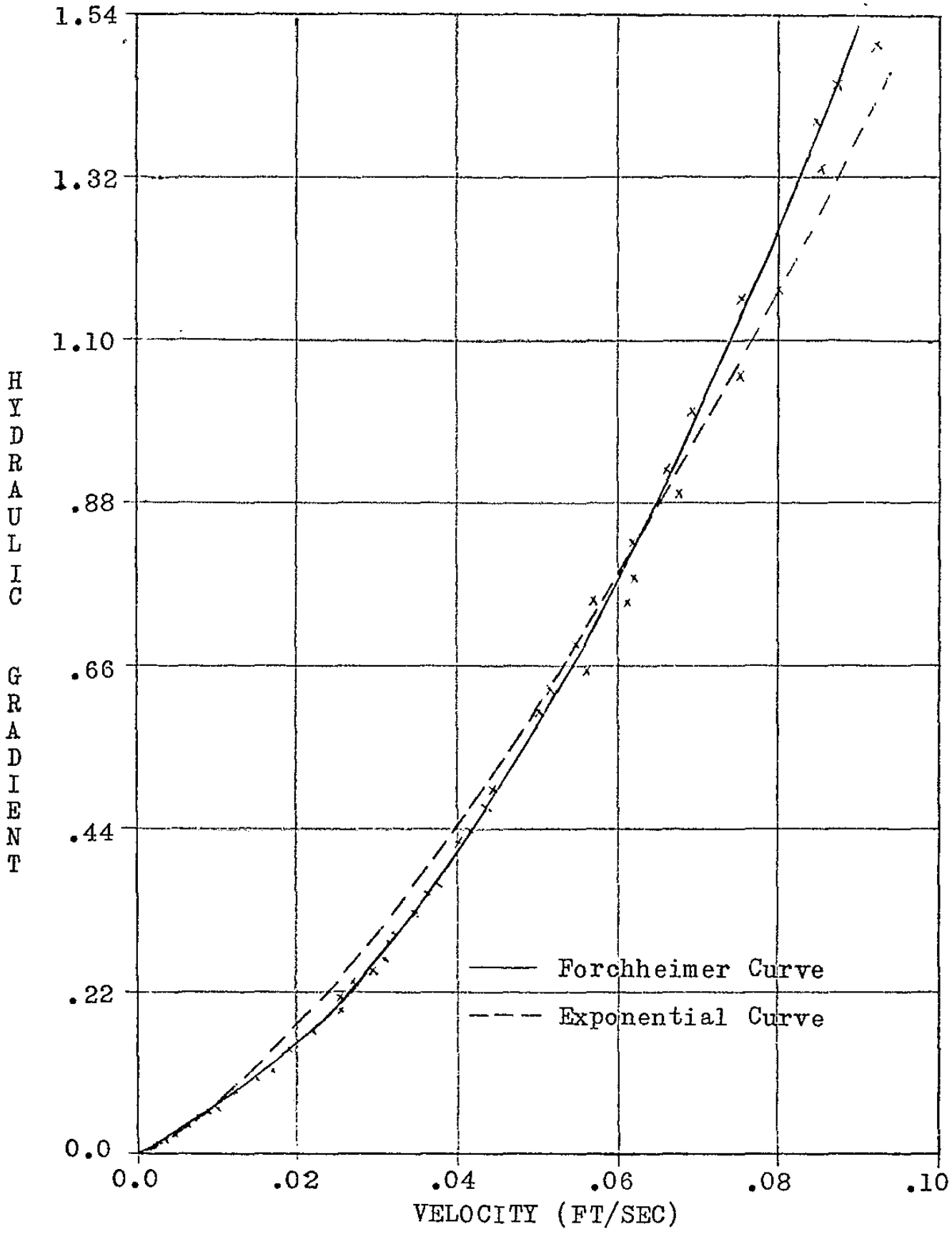

FIG. 6-2-2 LOW POROSITY PERMEAMETER RESULTS

The permeability k varied continuously with Reynolds number, there being a range of +67 to -43 percent of the mean value in the high porosity sample, and +62 to -49 percent of the mean value in the low porosity sample.

6.2.2 Determination of appropriate coefficients from an actual flow

The problem of determining appropriate coefficients for the nonlinear head loss equations, which will apply to materials under practical flow conditions, has already been mentioned. This problem appears to be of greater importance with finer grained gravels and coarse sands than with coarse grained gravels (of say 3/8 inch nominal size and above), where packings at similar porosities are more easily obtained. Fox and Ali (1968) studied unsteady unconfined flow through a porous medium consisting of 5/8 inch stone chippings and employed a Forchheimer relation to deduce the head loss gradient. To determine the correct coefficients a and b, they obtained a steady state draw-down curve to the well, and the corresponding discharge value. From these results a plot was drawn of surface gradient $\frac{dh}{dr}$ at any radius r, against the mean radial velocity at that radius. The value of the coefficient a was obtained from the tangent to this curve at the origin. The coefficient b was determined by plotting the surface gradient against the mean velocity on logarithmic paper and by taking the extreme case where head

loss was assumed proportional to the square of the velocity. An alternative method also based on the latter assumption was used to check the value of b.

These methods used by Fox and Ali thus depend on a number of approximations. The assumption is made that the value of a, which is determined at the lowest Reynolds number will be valid for the entire range of Reynolds numbers encountered, whereas a does in fact vary with Reynolds number (Stark and Volker, 1967). Likewise the term aV will usually have a finite value compared to bV^2 even at the largest velocities involved and this will result in some error in determining the coefficient b. The method also assumes that the mean velocity at any section corresponds to the surface gradient and this will be true only for nearly horizontal flow. The approach used by Fox and Ali has the advantage that it requires no permeameter results for the material at equivalent porosities but it depends on the availability of an accurate drawdown curve for the well. This would not usually be available under prototype conditions where a large number of observation wells would be required and where precise depth measurements would be necessary to produce sufficiently accurate values of the gradient $\frac{dh}{dr}$ for plotting the curve against the mean velocity.

In the present analysis therefore, a method was devised by which the appropriate coefficients were obtained from permeameter tests, in conjunction with the results from one actual well flow, for discharge and depths of water at the well and at an external radius. Field permeability tests in unconfined aquifers have long been based on the Dupuit-Forchheimer expression (equation 3.2-1) for well discharge. This expression depends on Darcy's Law and when Darcy's Law is invalid it is obvious that the permeability obtained at one particular discharge will not hold at any other discharge. Although the derivation of the Dupuit-Forchheimer equation was originally based on the Dupuit assumptions, it has since been shown (Hantush 1962b) to yield an exact value of the discharge for unconfined flow to a well on a horizontal impervious base. An analogous set of assumptions for flows with low hydraulic gradients were made to obtain an approximate analysis of nonlinear unconfined flow.

Consider the unconfined flow situation depicted in Fig. 6-2-3. It is assumed that velocities are horizontal and uniform over any vertical section. The velocity at radius r is therefore given by:

$$V = \frac{Q}{2\pi rh} \qquad \ldots. \ 6.2\text{-}1$$

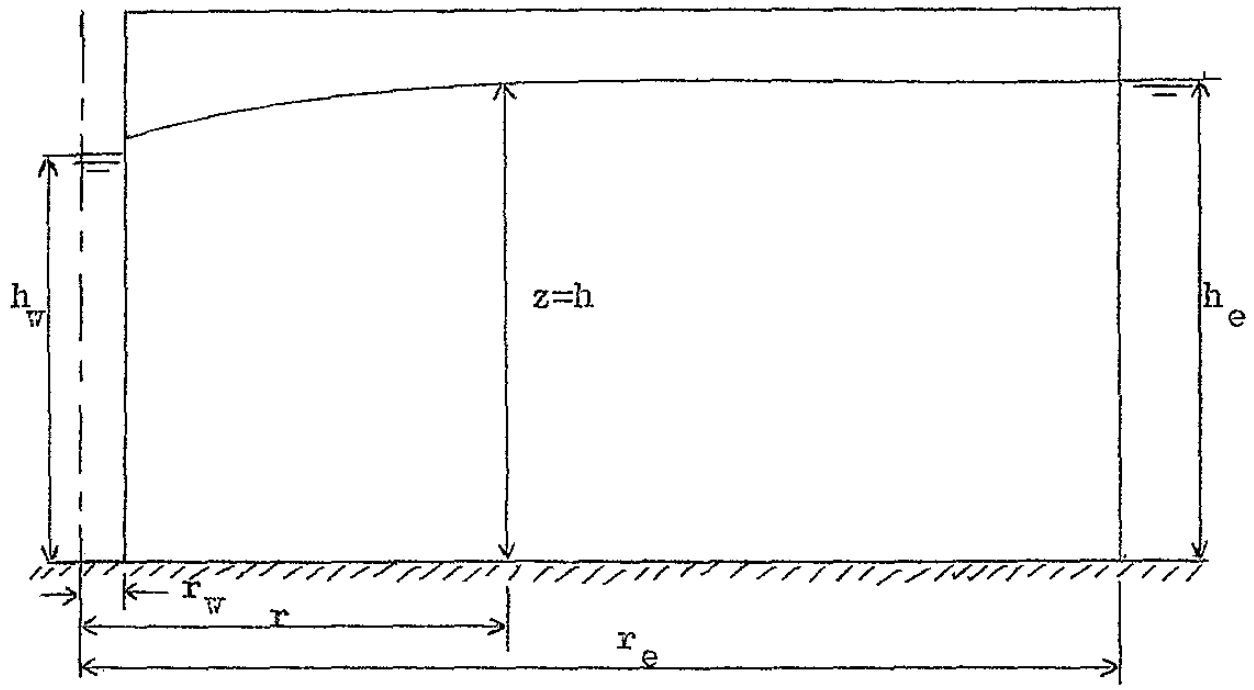

FIG. 6-2-3
FLOW FIELD FOR APPROXIMATE HORIZONTAL FLOW SOLUTION

in which Q is the discharge to the well and h is the height of the free surface at radius r. If the hydraulic gradient at radius r is assumed to be $\frac{dh}{dr}$, then since h is considered to be independent of z, substitution in the Forchheimer relation yields:

$$\frac{dh}{dr} = aV + bV^2$$

$$= a\frac{Q}{2\pi rh} + b\frac{Q^2}{4\pi^2 r^2 h^2} \qquad \ldots\ 6.2\text{-}2$$

This is an ordinary differential equation which cannot be readily integrated between the limits r_w, h_w and r_e, h_e to give an expression for the discharge Q in terms of known variables. However the equation can be solved by a

numerical method. A Runge-Kutta solution was therefore carried out to obtain the discharge Q from the known boundary conditions after having substituted the appropriate coefficients in the head loss equation. The steps involved in the Runge-Kutta solution are outlined as follows:

An initial value of the discharge is calculated from the Dupuit-Forchheimer expression based on an average permeability from the permeameter tests. This allows a value of $\frac{dh}{dr}$ to be calculated at the well radius r_w, by substitution in equation 6.2-2. The field is divided into an equal number of increments of radius and the value of $\frac{dh}{dr}$ at each successive radius is then calculated. The Runge-Kutta method used was Merson's fourth order process for which the basic equation may be stated as:

$$h^{r+\delta r} = h^{r} + \frac{1}{2}(K_1+K_4+K_5) \qquad \ldots\ldots 6.2\text{-}3$$

in which $h^{r+\delta r}$ is the free surface height at radius $r+\delta r$ and h^{r} is the height at radius r. If f(r,h) is written for the right hand side of equation 6.2-2 so that:

$$f(r,h) = a\frac{Q}{2\pi rh} + b\frac{Q^2}{4\pi^2 r^2 h^2} \qquad \ldots\ldots 6.2\text{-}4$$

then the terms K_1 to K_5 in equation 6.2-3 are given by:

$$
\left.
\begin{aligned}
K_1 &= \tfrac{1}{3}\delta r f(r,h) \\
K_2 &= \tfrac{1}{3}\delta r f(r+\tfrac{1}{3}\delta r,\ h+K_1) \\
K_3 &= \tfrac{1}{3}\delta r f(r+\tfrac{1}{3}\delta r,\ h+\tfrac{1}{2}K_1+\tfrac{1}{2}K_2) \\
K_4 &= \tfrac{1}{3}\delta r f(r+\tfrac{1}{2}\delta r,\ h+\tfrac{3}{8}K_1+\tfrac{9}{8}K_3) \\
K_5 &= \tfrac{1}{3}\delta r f(r+\delta r,\ h+\tfrac{3}{2}K_1-\tfrac{9}{2}K_3+6K_4)
\end{aligned}
\right\} \quad \ldots\ 6.2\text{-}5
$$

Starting from the known head h_w at the well, the piezometric head at each successive radius can be obtained (from equation 6.2-3) out to the piezometric head at the external radius r_e. If the discharge value is correct and the assumptions are sufficiently accurate, then the head obtained at r_e should coincide with the known value h_e. Initially there will be a discrepancy between the calculated value h_1 at r_e and the true value h_e, due to the error in the assumed value of the discharge. This discrepancy can then be used to calculate an improved approximation to the discharge. In integrating from the well to the external boundary, the particular value of $\frac{dh}{dr}$ assumed at the well has most influence on the result for piezometric head at the external boundary. Thus to calculate an improved value for discharge, the assumption is made that the ratio of the new gradient $(dh/dr)_{new}$ to the old gradient $(dh/dr)_{old}$ is given by:

$$
\frac{(\frac{dh}{dr})_{new}}{(\frac{dh}{dr})_{old}} = \frac{h_e - h_w}{h_1 - h_w} \qquad \ldots\ 6.2\text{-}6
$$

in which h_1 is the calculated value of head at r_e and h_e is the actual value. Or if the improved discharge result is designated by Q_I, then:

$$\frac{aQ_I}{2\pi r_w h_w} + \frac{bQ_I^2}{4\pi^2 r_w^2 h_w^2} = \left(\frac{h_e - h_w}{h_1 - h_w}\right)\left(\frac{aQ}{2\pi r_w h_w} + \frac{bQ^2}{4\pi^2 h_w^2 r_w^2}\right)$$

.... 6.2-7

in which Q is the initially assumed discharge. The improved value of discharge Q_I can then be obtained from equation 6.2-7.

The process is an iterative one with the calculated value of h_1 converging to the correct value h_e as the discharge Q_c converges to the required final result. The iterative procedure is repeated until the correct piezometric head h_e is obtained at the external radius, at which stage there is negligible change in successive calculated values of Q_c, which then gives the required value of discharge for Forchheimer flow under the assumed conditions.

The numerical process is subject to discretization errors but these can be minimised by using a small grid length; and since the solution of the ordinary differential equation does not involve a field solution, a small increment in radius can be used without difficulty. The solution is, however, subject to error caused by the assumptions of completely radial flow and of no variation

in h with the height z. This error will be small provided only those flows are analysed which involve low hydraulic gradients and therefore closely approximate horizontal flow.

A similar solution for horizontal flow according to the exponential relation was carried out but the resultant differential equation in this case could be integrated directly to yield an expression for the discharge Q, without the need for a numerical solution. Thus for horizontal flow where the piezometric head h is assumed a function only of radius r and is independent of the height z, then the exponential relation at any radius may be written:

$$\frac{dh}{dr} = c\left(\frac{Q}{2\pi rh}\right)^m \qquad \ldots. 6.2\text{-}8$$

or $$h^m dh = \frac{cQ^m}{(2\pi)^m}\frac{dr}{r^m} \qquad \ldots. 6.2\text{-}9$$

Integrating between r_w, h_w and r_e, h_e gives:

$$\frac{h_e^{m+1} - h_w^{m+1}}{1+m} = \frac{cQ^m}{(2\pi)^m}\frac{(r_e^{1-m} - r_w^{1-m})}{1-m} \qquad \ldots. 6.2\text{-}10$$

Thus Q may be obtained directly from equation 6.2-10 after substituting for the known variables.

The solutions for discharge from both head loss relations can therefore be employed in successive inter-

polations to obtain the appropriate values of the coefficients in the two relations. A value of the discharge can be calculated using the coefficients obtained from each of the low porosity and high porosity samples. The experimental discharge should then lie between these two extremes, since the material in the tank will usually be at some porosity between the minimum and maximum porosities obtained in the permeameter.

The coefficients in the head loss equations depend on some function of the porosity but the form this function should take has been stated differently by various authors. Engelund (1953) gave a review of some of the suggested functions for the coefficients a and b in the Forchheimer relation. Dudgeon (1968) also discussed some of the porosity functions recorded in the literature and showed that none of them should be expected to have general applicability. In view of the uncertainty associated with the dependence on porosity, the simplest approach was used, whereby the coefficients a and b (or c and m) which would produce the experimentally measured well discharge were calculated by direct interpolation between the extreme values fitted to the two sets of permeameter results.

Some improvement on this approach may have been possible by using a range of porosities in the permeameter

between the two extremes. However, in field applications, the interpolation process to produce an actual well discharge will usually have to account for some non-uniformity of the medium in which the well is situated, so that as a first trial, only the two sets of results were used and the interpolation carried out directly between them. The results were found to be satisfactory so that no further sets of permeameter tests were undertaken.

The two extreme values of Q are calculated and more accurate values of the coefficients are determined by interpolation, to give a closer approximation to the discharge value obtained experimentally for one particular well test at a low hydraulic gradient. The process again is a repetitive one. After new coefficients are obtained by interpolation, a new discharge is calculated with these coefficients; this value will usually not exactly equal the experimental value and a second interpolation is carried out to obtain more accurate coefficients. The process is repeated until the difference between the calculated and experimental discharges is negligible. The coefficients so obtained are accepted as the values to be employed in the analyses.

Seven flows in all were studied for the unconfined axisymmetric experiments with the complete circle, with

discharges ranging from .341 cusecs to .87 cusecs. There are conflicting limitations on the flow conditions to produce greatest accuracy of fit of the coefficients. Small head differences should be used so that the curvature of the free surface is small and the flow is approximately horizontal. However at low differences in head, the relative accuracy of measuring the drawdown is reduced. While the relative error in measuring each water level, at the well and at some external radius, may be small, the accuracy of discharge calculations depends on the accuracy of measuring the difference in water levels. Thus a small error in measuring each of the water levels separately may produce a substantial error in the value obtained for the difference in levels. The well test with the second smallest discharge was therefore employed in interpolating for the nonlinear head loss relation coefficients and in determining the permeability coefficient k; for, while the drawdown is small and the flow is nearly horizontal, the difference in water levels is sufficient to give a reasonable accuracy of measurement of this difference.

For the experimental well discharge of .414 cusecs, the water levels measured were:

$$h_w = 2.59 \text{ ft. at } r_w = .35 \text{ ft.}$$

and

$$h_e = 3.08 \text{ ft. at } r_e = 9.6 \text{ ft.}$$

For a = 2.499 sec/ft and b = 67.617 sec^2/ft^2, then Q = .602 cusecs and for a = 4.850 sec/ft and b = 133.224 sec^2/ft^2, then Q = .372 cusecs. Direct interpolation between the two sets of coefficients gives a = 4.42 and b = 121.22 at which a discharge of .414 cusecs would be expected. However calculation with these coefficients shows that the discharge would be .395 cusecs. Further interpolations show that coefficients a = 4.21 sec/ft. and b = 116.93 sec^2/ft^2 produce a discharge of .412 cusecs which is within $\frac{1}{2}$ percent of the experimental value of .414 cusecs and these coefficients were accepted for subsequent analysis of the unconfined flow conditions for the experiments with the full circle.

For the exponential relation, similar calculations are carried out for the same flow:
Thus for c = 39.36 and m = 1.39, then Q = .367 cusecs, and for c = 23.83 and m = 1.45, then Q = .609 cusecs. Interpolation yields coefficients c = 36.043 and m = 1.405 at which a discharge of .414 cusecs would be expected. However recalculation shows that, for these coefficients, the discharge is actually .405 cusecs. Subsequent trials and interpolations yield coefficients c = 35.45 and m = 1.41 at which the calculated discharge is .413 cusecs. These coefficients were then employed in the analysis of the

well flows when the exponential relation was considered. It may be noted that for these results, even though the exponential curve fits the permeameter results less accurately than the Forchheimer curve, the well discharges calculated from the two relations differ by only about 1% at each of the two porosities involved. The Darcy coefficient of permeability k, calculated from this flow, is .156 ft/sec.

6.2.3 Experimental results and finite difference solutions

Seven flows were investigated in this set of experiments and are designated as flow Nos. 1 to 7 in order of increasing magnitude of discharge. The experimental free surface was obtained approximately by measuring the depth to the water surface in piezometers located near the surface as discussed in section 5.4.1. The theoretical analysis of the unconfined flow conditions involves a finite difference numerical solution as discussed in Chapter 4. The boundary conditions assumed for the piezometric head function at the well and at the outer boundary were the same as those used in the confined flow experiments. Thus an uncased well was assumed and the piezometric head at the well was taken as the height of water in the well and the loss of head as the water enters the stationary pool in the well was equated to the velocity head of the water entering the well.

In accordance with discussions in Chapter 1, exponential solutions were not obtained for all flows. However solutions for the exponential relation were carried out for flow Nos. 5, 6 and 7 for comparison purposes, as these were the highest flows in the range considered. The finite difference solutions for flow No.6 for Darcy, Forchheimer and exponential flow are plotted in Figs. 6-2-4, 6-2-5 and 6-2-6 respectively. The plots include lines of equal piezometric head as well as equal flow lines. The flow lines were not plotted from stream-line function values even for the case of linear Darcy flow. For nonlinear flow, the flow lines are most conveniently plotted by joining points below which the quantity of flow is constant, and this procedure was adopted for Darcy flow also. The experimental free surface position is plotted in each of Figs. 6-2-4, 6-2-5 and 6-2-6. The water levels h_w and h_e, the radii r_w and r_e, the experimental discharge Q(EXP), and the calculated discharge Q(CALC), are also given in each figure.

The results obtained for Darcy and Forchheimer solutions for flow Nos. 1 to 4 inclusive are plotted, together with the experimental free surface, in a similar manner in Figs. A-II-1 to A-II-8 in Appendix II. The finite difference results for Darcy, Forchheimer and exponential

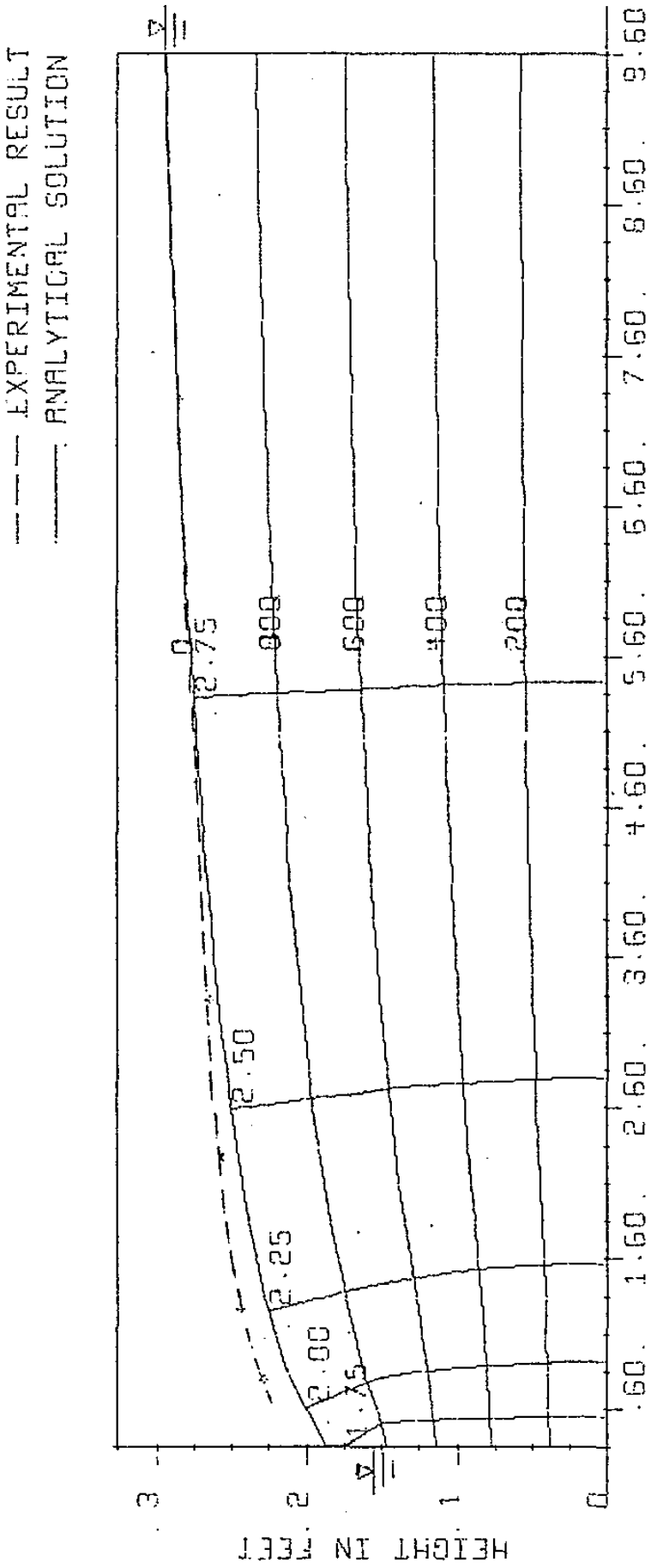

EXPERIMENT WITH COMPLETE CIRCLE. RW= .354 RE= 9.604
. FLOW NO 6 . HW= 1.549 HE= 2.942
RESULTS FOR DARCY FLOW Q(CALC) = .933 Q(EXP) = .710 CUSEC

FIG. 6-2-4

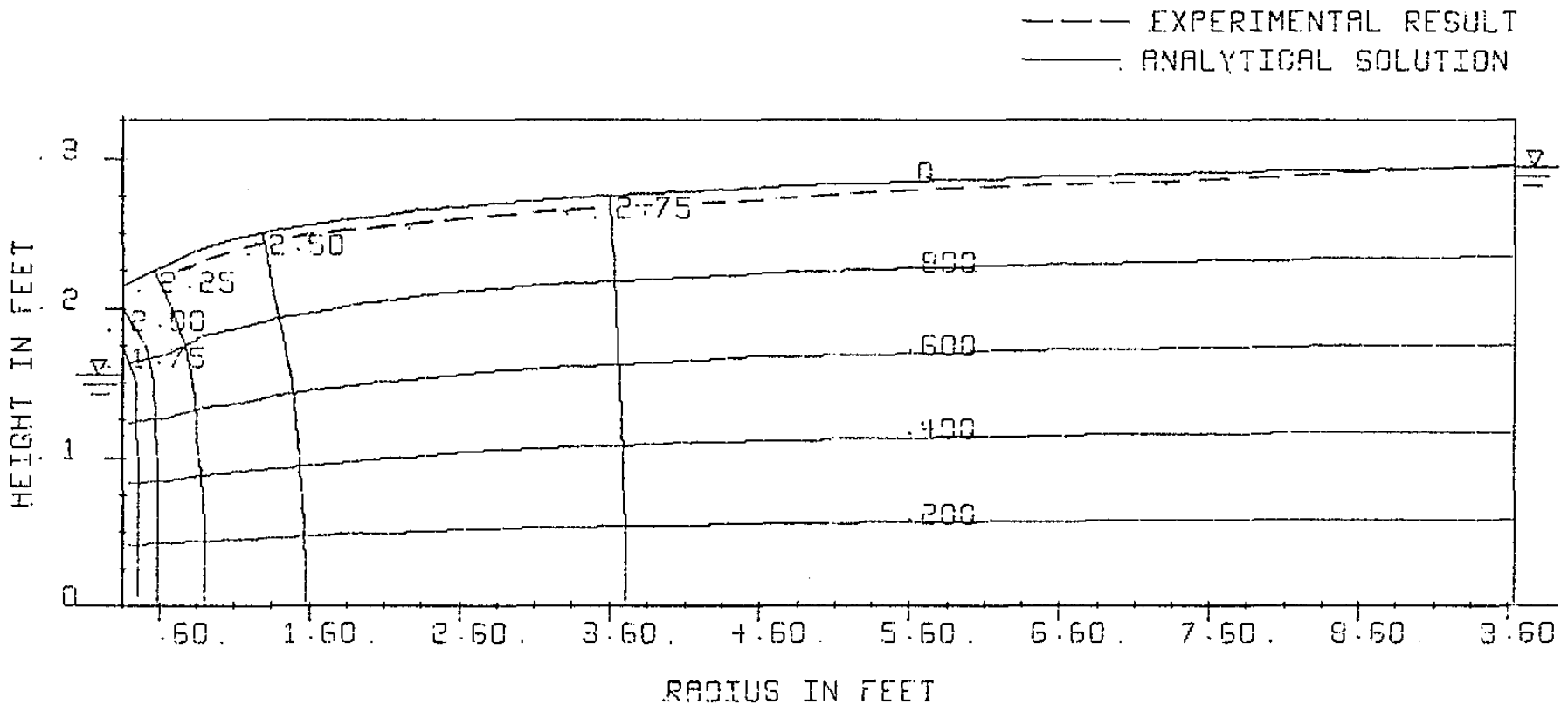

EXPERIMENT WITH COMPLETE CIRCLE . RW= .354 RE= 9.604
. FLOW NO 6 . HW= 1.543 HE= 2.342
RESULTS FOR FORCHHEIMER FLOW Q(CALC) = .705 Q(EXP) = .710 CUSEC

FIG. 6-2-5

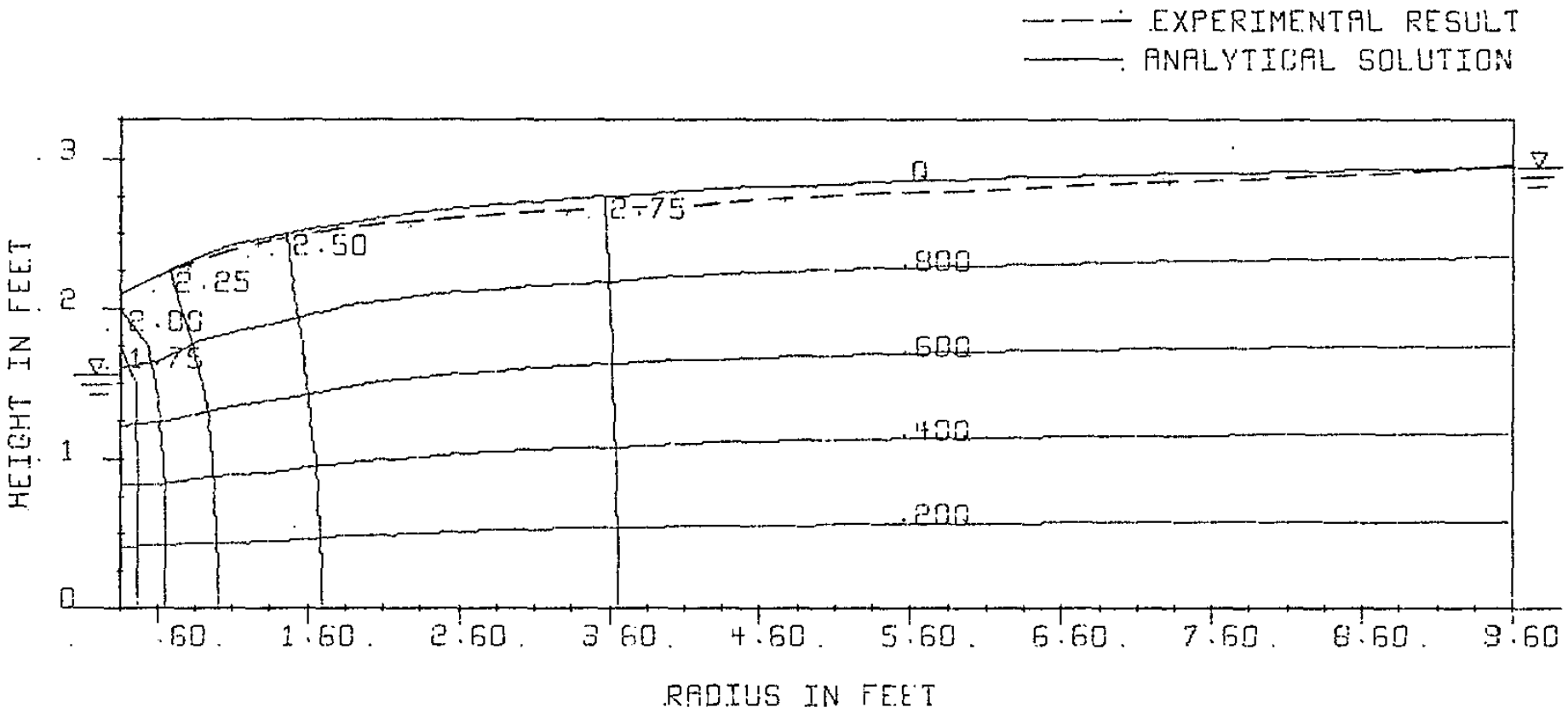

EXPERIMENT WITH COMPLETE CIRCLE . RW= .354 RE= 9.604
. FLOW NO 6 . HW= 1.549 HE= 2.342
RESULTS FOR EXPONENTIAL FLOW Q(CALC) = .731 Q(EXP) = .710 CUSEC

FIG. 6-2-6

solutions and the experimental free surfaces for flow Nos. 5 and 7 are plotted in Figs. A-II-9 to A-II-14, also in Appendix II. The discharge obtained from the Forchheimer finite difference solution for flow No.2 agrees with that obtained from the Runge-Kutta solution to within 1 percent, thus justifying the assumption of completely radial flow in the process for obtaining appropriate coefficients in the head loss relation.

A comparison of the results for flow No.6 shows that the Forchheimer solution gives the most accurate discharge when compared with the experimental result. The Darcy solution for discharge is considerably in error, as would be expected from the change in permeability encountered in the permeameter tests. The exponential relation however, gives a more accurate result. The free surfaces obtained from the Forchheimer and exponential solutions also agree much more accurately with the experimental free surface than does the Darcy solution. A study of Figs. A-II-1 to A-II-14 shows that similar conclusions can be drawn for the other flows.

The comparison of the experimental and numerical results raises the question of accuracy of the finite difference solutions. The solutions were carried out using a grid length of 3 inches over the flow field. The

grid network together with the calculated free surface, is shown in Fig. 6-2-7. The finite difference solutions were carried out until the difference between head values, obtained from successive iterations, was less than .00010 ft.

A further indication of the accuracy of the numerical results was obtained by comparing discharge values calculated at each vertical grid line for any particular solution. For example in the Darcy, Forchheimer and exponential solutions for flow No.6, the total discharge calculated at the grid lines designated A-A to D-D in Fig. 6-2-7 are tabulated in Table 6-2-2.

Grid line as marked in Fig. 6-2-7	Total Calculated Discharge (cusecs)		
	Darcy	Forchheimer	Exponential
A-A	.916	.708	.738
B-B	.942	.712	.747
C-C	.944	.714	.740
D-D	.944	.691	.722

TABLE 6-2-2 DISCHARGE CALCULATIONS AT VERTICAL GRID LINES

The maximum discrepancy between the values at the different grid lines quoted for flow No.6 for any of the solutions is therefore about 3 percent. The agreement between values at different radii could be enhanced by extending the number of iterations, to obtain a still

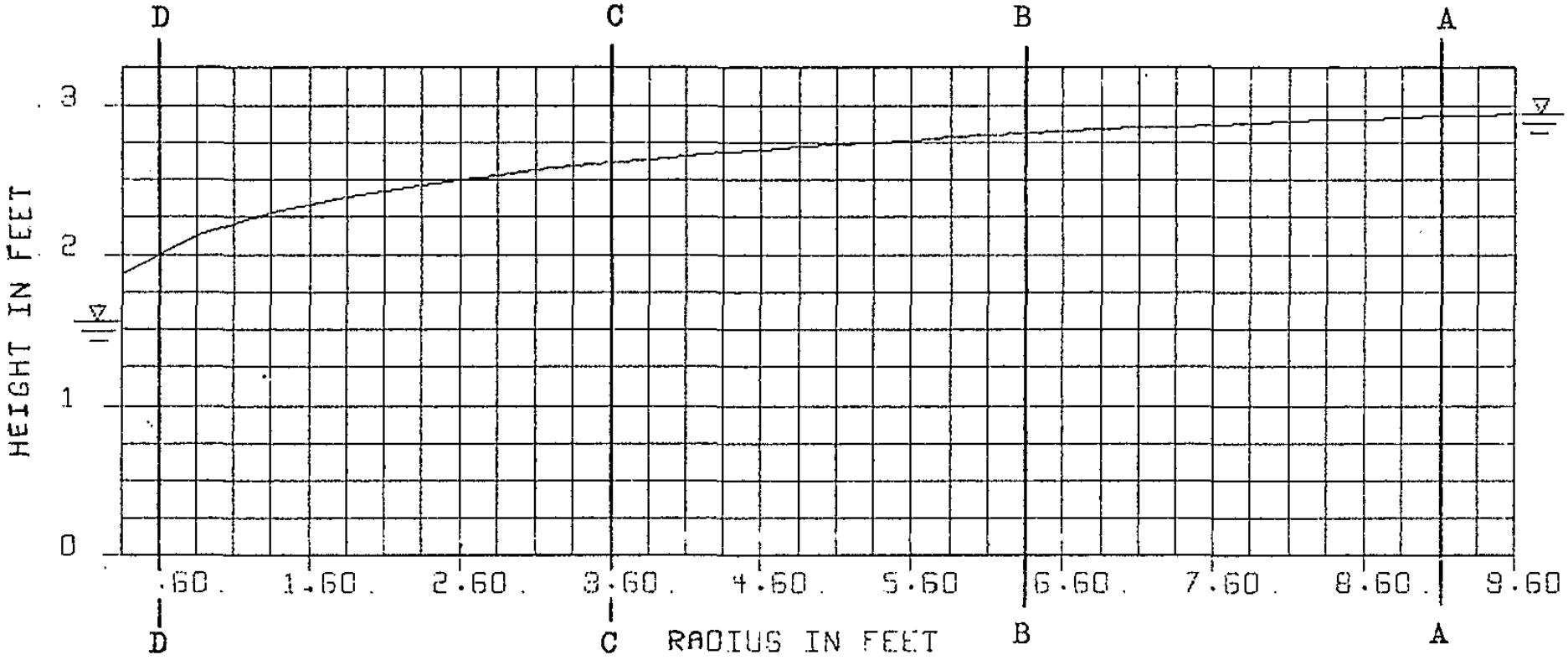

FIG. 6-2-7

FINITE DIFFERENCE GRID FOR EXPERIMENTS WITH COMPLETE CIRCLE

smaller change in piezometric head value with successive iterations. However, investigations with a number of flows showed that, once the agreement between discharge values at different radii was within about ± 3 percent of the average, then further iterations caused a very small change in the average calculated discharge from the finite difference solutions. The change in the free surface position and in the flow net diagram was also slight. As a result, solutions were not generally extended to obtain better agreement than a maximum difference in discharge of ± 2 percent over all vertical grid lines, from the well to the outer boundary.

The discharge obtained in the Darcy flow solution agrees with that from the Dupuit-Forchheimer expression usually to within 0.5 percent. This result also indicates that the finite difference solutions, at least for linear flow, are accurate since it has been shown that the Dupuit-Forchheimer formula gives an exact solution for discharge for this flow situation when Darcy's Law applies.

A comparison of the results obtained for the seven flows investigated, shows that the discharge obtained from the linear Darcy solution is considerably in error, as compared to the experimental result, when the calculations are based on the permeability at one particular flow.

The free surface position from the Darcy solution is also in error for the higher flows. For flow Nos. 4, 5, 6 and 7 the Darcy solution for the free surface shows a substabtial discrepancy from the experimental one especially in the vicinity of the well, reaching an error of approximately 10 percent for flow No.7. The mean velocity increases rapidly as the well is approached, and therefore the inaccuracy of the Darcy solution is more marked in this region. The free surface positions obtained from the nonlinear solutions are accurate, however, to within a few percent. For example the maximum error in the Forchheimer free surface position for all flows is about 4 percent, while that of the exponential solutions, for the three flows analysed, is about 6 percent.

For comparison purposes, the discharge values obtained experimentally and from each of the theoretical solutions are plotted against $(h_e^2-h_w^2)$ in Fig. 6-2-8. The quantity $h_e^2-h_w^2$ plotted as the abscissa in Fig. 6-2-8 is not necessarily a completely representative parameter for discharge calculations when the flow is nonlinear. For linear Darcy flow, provided h_w and h_e are measured at fixed radii as in the results plotted here, then the discharge is directly proportional to $h_e^2-h_w^2$. However when the head loss obeys a nonlinear relation there may be an increase

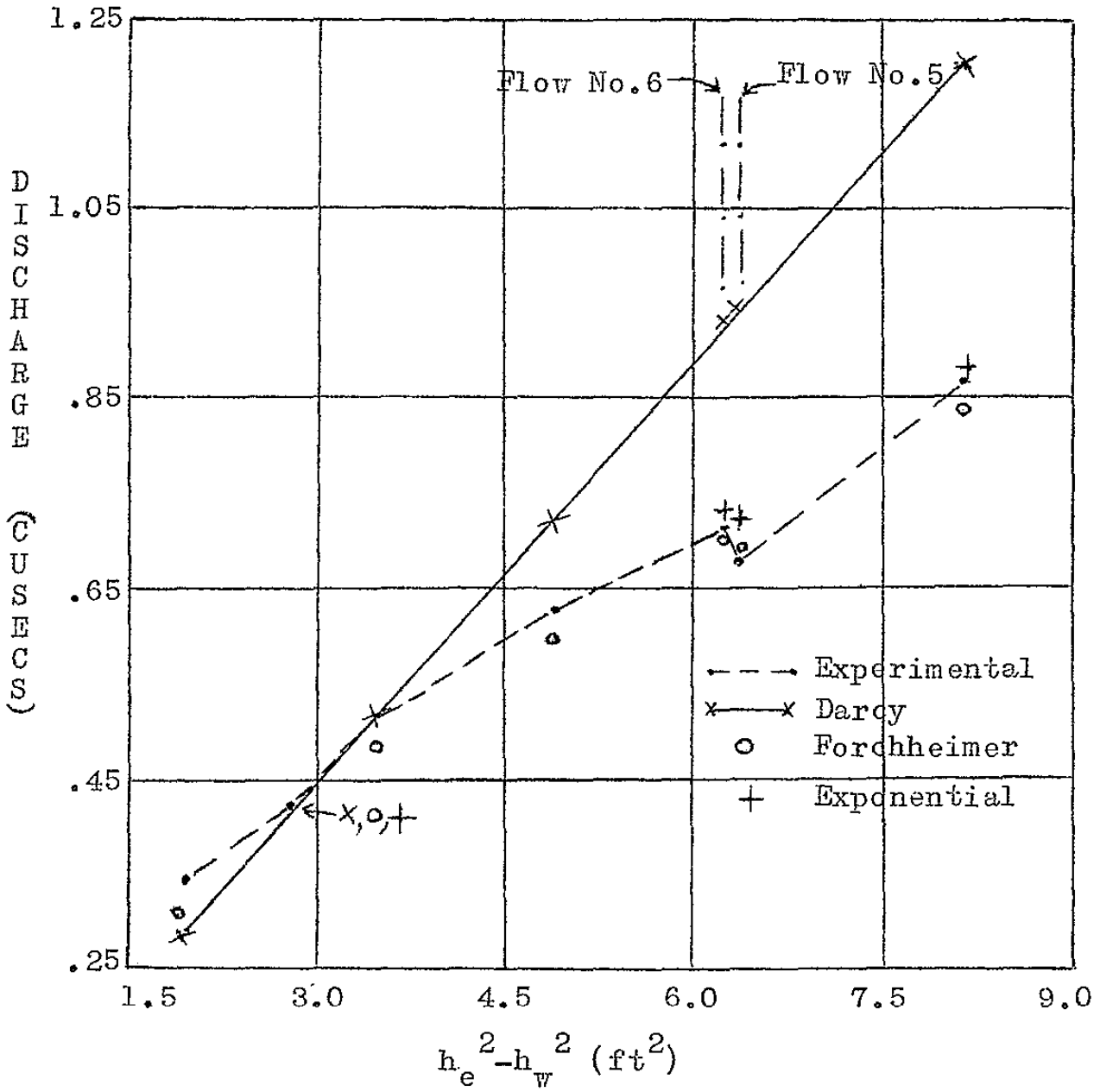

FIG. 6-2-8
DISCHARGE COMPARISONS FOR UNCONFINED AXISYMMETRIC FLOW WITH COMPLETE CIRCLE

in discharge for a decrease in $h_e^2-h_w^2$ under certain conditions. This is exemplified by a study of the points plotted for flow Nos.5 and 6 in Fig. 6-2-8. Thus while the magnitude of $h_e^2-h_w^2$ for flow No.5 is greater than for flow No.6, the discharge is smaller. The Darcy solutions of course show an opposite trend indicating a higher discharge for flow No.5. However both the Forchheimer and exponential finite difference solutions follow the trend of the experimental results, showing a lower discharge for flow No.5 than for flow No.6. A study of the magnitude of the internal and external water levels for the two flows shows that while the difference in levels is greater for flow No.5, the absolute magnitudes of both levels are greater for flow No.6. Thus when a nonlinear relation connects head loss and velocity, even though the gradients, and therefore the velocities, are smaller for flow No.6, this is more than compensated for by the increase in area of flow over that available in flow No.5. However for the linear head loss relation the reverse is true and the increase in area of flow is not sufficient to compensate for the smaller velocities in flow No.6.

Nevertheless, while the quantity $h_e^2-h_w^2$ does not give a completely representative parameter for discharge comparisons under these conditions, no dimensionless or

other quantity is readily available for comparing all discharge solutions and the plot has therefore been made against the quantity $h_e^2 - h_w^2$ in Fig. 6-2-8.

Fig. 6-2-8 shows that the nonlinear relations give solutions for discharge which are accurate to within a few percent for all flows. Apart from flow No.2 which was used as the reference flow for equating experimental and all theoretical results, the only accurate discharge calculated from a Darcy solution is that for flow No.3 which is closest to No.2; the errors for the remaining flows are considerable, rising as high as 38 percent for flow No.7. For a material as coarse as that used in these experiments therefore, it is obvious that only by carrying out a comprehensive set of field permeability tests over a wide range of flows could any accuracy be obtained in discharge calculations based on the Dupuit-Forchheimer formula. But even then the Darcy finite difference solution for the free surface would be in error as it is unaffected by the permeability coefficient.

The preceding analysis of results, however, shows that the nonlinear head loss relations do give solutions, both for discharge and free surface position which are accurate over a wide range of Reynolds numbers. This accuracy is obtained by determining two sets of head loss coefficients

from permeameter tests over a range of Reynolds numbers, at two different porosities, and by using the results of one prototype flow as a basis for interpolation to give the relevant coefficients applicable for the prototype medium.

6.3 Unconfined Axisymmetric Flow with Sector

6.3.1 Determination of coefficients

The material used in the unconfined flow experiments with the sector was similar to that used in the unconfined experiments with the full circle, but again with slightly different properties. Permeameter tests were therefore carried out on a sample of the material packed at two different porosities. The experimental results for the high porosity sample together with the fitted Forchheimer and exponential curves are plotted in Fig. 6-3-1.

The permeameter results and fitted curves for the low porosity sample are plotted in Fig. 6-3-2.

The results obtained for the coefficients are given in Table 6-3-1, together with the corresponding standard errors of estimate (SE).

The process of interpolating to obtain the appropriate coefficients for the well flow experiments was carried out in a manner similar to that described in section 6.2.2.

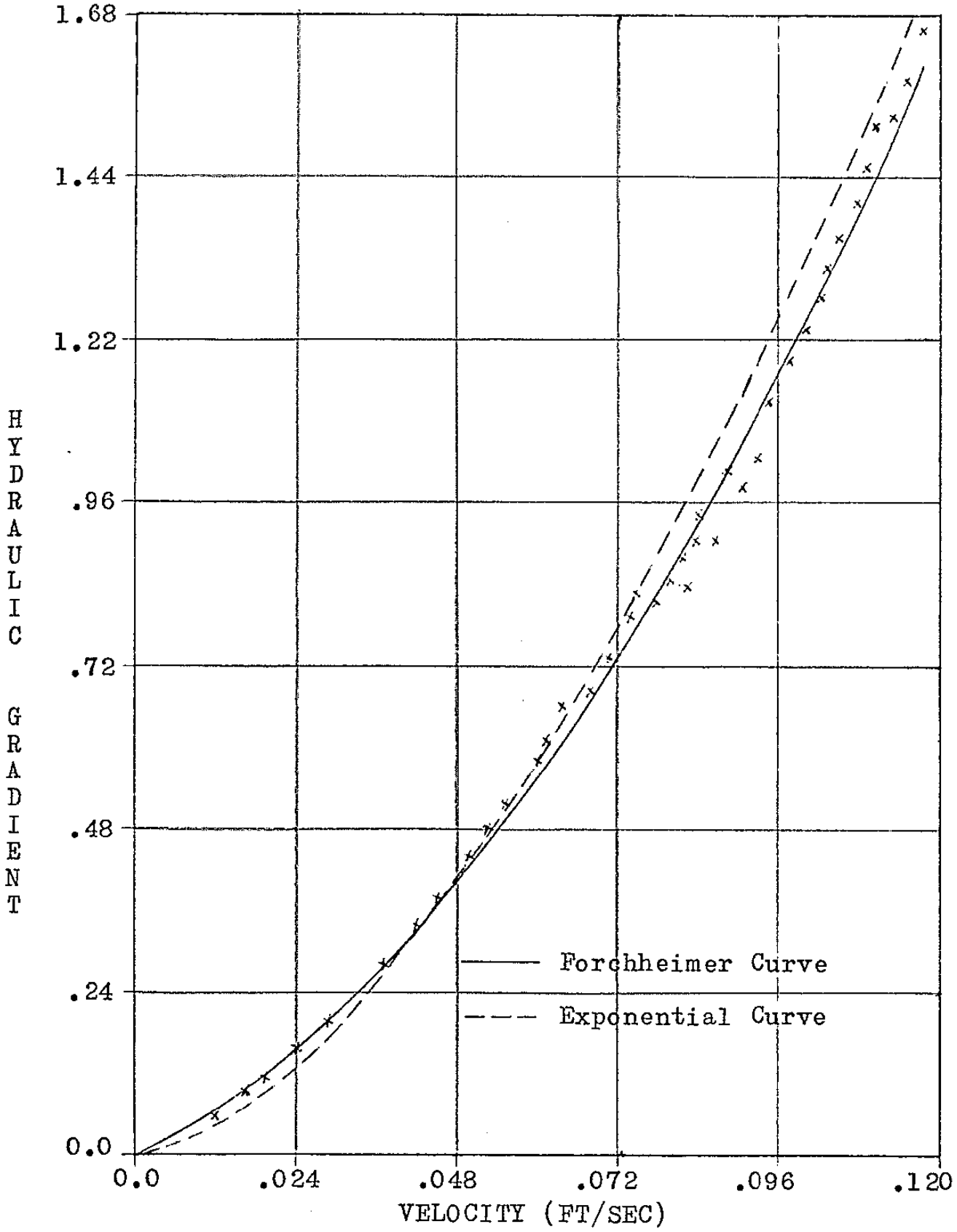

FIG. 6-3-1 HIGH POROSITY PERMEAMETER RESULTS FOR THE MATERIAL FOR SECTOR EXPERIMENTS

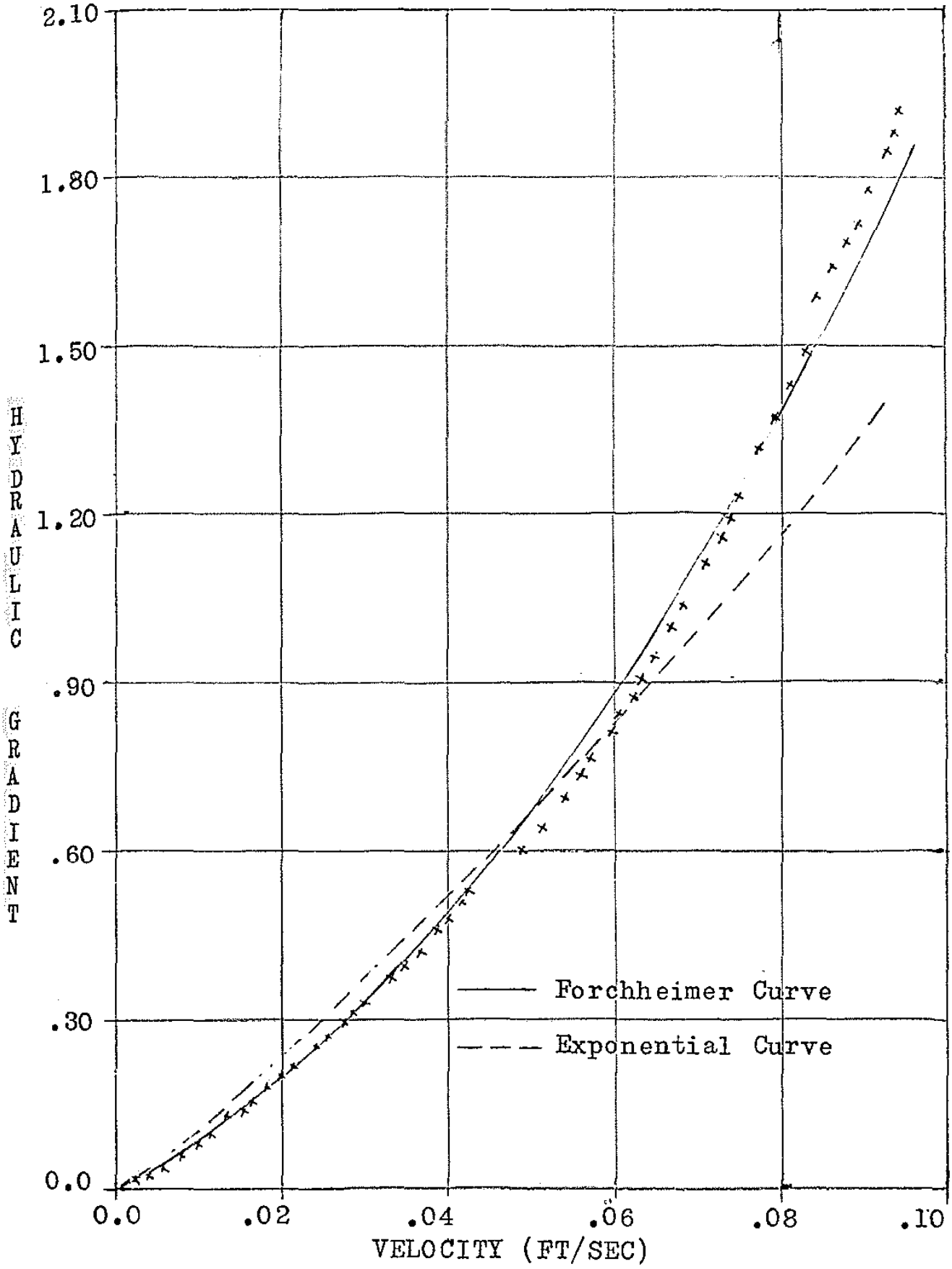

FIG. 6-3-2 LOW POROSITY PERMEAMETER RESULTS FOR THE MATERIAL FOR SECTOR EXPERIMENTS

High Porosity Sample			
Forchheimer Relation	a(sec/ft)	b(sec^2/ft^2)	SE
	4.62	76.58	4.6%
Exponential Relation	c	m	SE
	54.51	1.62	11.6%
Low Porosity Sample			
Forchheimer Relation	a(sec/ft)	b(sec^2/ft^2)	SE
	7.22	128.37	5.4%
Exponential Relation	c	m	SE
	19.72	1.13	20.8%

TABLE 6-3-1 COEFFICIENTS FOR UNCONFINED FLOWS WITH SECTOR

Seven well flows were again investigated in this set of experiments and the flow with the third smallest discharge was selected as the reference flow for obtaining the permeability and for interpolating the nonlinear head loss coefficients. The drawdown for this flow was sufficient to allow accurate measurement of the difference in water levels but was small enough to give a close approximation to horizontal, completely radial flow. The relevant variables for the flow are:

r_w = .35 ft. r_e = 9.60 ft.

h_w = 3.31 ft. h_e = 3.77 ft.

Experimental discharge = .395 cusecs.

The results from the Forchheimer discharge calculations, assuming horizontal flow, were:

for $a = 4.62$ sec/ft. and $b = 76.58$ sec^2/ft^2, $Q = .508$ cusecs;

for $a = 7.22$ sec/ft. and $b = 128.37$ sec^2/ft^2, $Q = .348$ cusecs.

Repeated interpolation between the coefficients showed that for $a = 6.31$ sec/ft and $b = 110.13$ sec^2/ft^2, then $Q = .391$ cusecs, which is within about 1% of the experimental result, so that these coefficients were accepted for the unconfined Forchheimer flow analyses.

Similar calculations for the exponential relation yield:

for $c = 54.51$ and $m = 1.62$, $Q = .631$ cusecs

and for $c = 19.72$ and $m = 1.13$, $Q = .295$ cusecs.

After successive interpolations, the final coefficients accepted are $c = 33.28$ and $m = 1.32$ which give a discharge of .393 cusecs, which closely approximates the experimental result.

It may be noted that the Forchheimer calculation for discharge, using the high porosity coefficients, differs from that of the exponential relation at the same porosity. A similar remark applies to the low porosity results. The exponential solution for discharge is higher than the corresponding Forchheimer result for the high porosity and lower for the low porosity sample. Thus the exponential discharge varies more rapidly with porosity than the

Forchheimer discharge. In addition, it is probable that the process of obtaining relevant coefficients does not only account for a porosity change but also overcomes some error due to the inaccuracy of fit of the curves, especially the exponential, to the permeameter results.

The nonlinear finite difference solutions for the reference flow, which are reported in section 6.3.2, show that for Forchheimer flow with the coefficients derived above, the discharge is .394 cusecs, while the corresponding exponential solution for discharge is .397 cusecs. These values are sufficiently close to the experimental result of .395 cusecs and indicate the validity of assuming horizontal flow in the procedure for obtaining optimum values of the coefficients. The Darcy permeability coefficient from the Dupuit-Forchheimer formula for the above flow was .127 ft/sec.

6.3.2. Finite difference solutions for Darcy, Forchheimer and exponential flow

The seven flows investigated were designated as flow Nos. 1 to 7 in order of increasing magnitude of discharge. Similar boundary conditions were assumed in the analytical solutions to those assumed for the solutions discussed in section 6.2.3. Solutions were obtained for all flows for each of the Darcy, Forchheimer and exponential head loss

relations. The basic grid size employed in the solutions was 3 inches. However for Forchheimer flow, after the solution had been obtained to the required accuracy on the 3 inch grid, a fine grid was incorporated near the well to obtain a more accurate representation of the free surface. Nevertheless, this produced only a slight change in the free surface position from that given by the coarser grid solution.

The iterative procedure in each case was extended until the change in values of piezometric head at any point was less than .0001 ft. and until the variation in discharge at different grid lines was less than about $\pm$ 2 percent of the mean. The basic grid over which solutions were obtained for flow No.5 is shown in Fig. 6-3-3, with the fine grid used near the well for the Forchheimer solution superimposed on it. The grid actually used is bounded at the top by the calculated free surface position for Forchheimer flow which is shown in Fig. 6-3-3.

A comparison of the calculated discharges for each solution of the flow No.5, at the grid lines designated in Fig. 6-3-3, is given in Table 6-3-2. The discharges quoted for the Forchheimer equation are those obtained from the initial basic grid solutions.

Grid Line	Total Calculated Discharge (cusecs)		
	Darcy	Forchheimer	Exponential
A-A	1.215	.922	.931
B-B	1.209	.924	.927
C-C	1.212	.921	.919
D-D	1.196	.901	.903

TABLE 6-3-2
DISCHARGE AT VERTICAL GRID LINES FOR SECTOR FLOW No.5

The maximum overall variation in discharge for these grid lines is therefore about 3 percent. For the majority of solutions the maximum variation was kept smaller than 4 percent. The results obtained for Darcy flow agree with those from the Dupuit-Forchheimer expression at the same permeability, usually to within 0.5 percent.

6.3.3. Comparison with experimental results

Flow net diagrams obtained from the finite difference solutions for each of the three head loss relations are plotted separately for each of the seven flows. The experimental free surface position, together with equal head lines obtained from the experimental results, are drawn on each of these plots. The analytical solutions for the Darcy, Forchheimer and exponential relations for flow No.5 are plotted in Figs. 6-3-4, 6-3-5 and 6-3-6 respectively, and the experimental results are plotted on

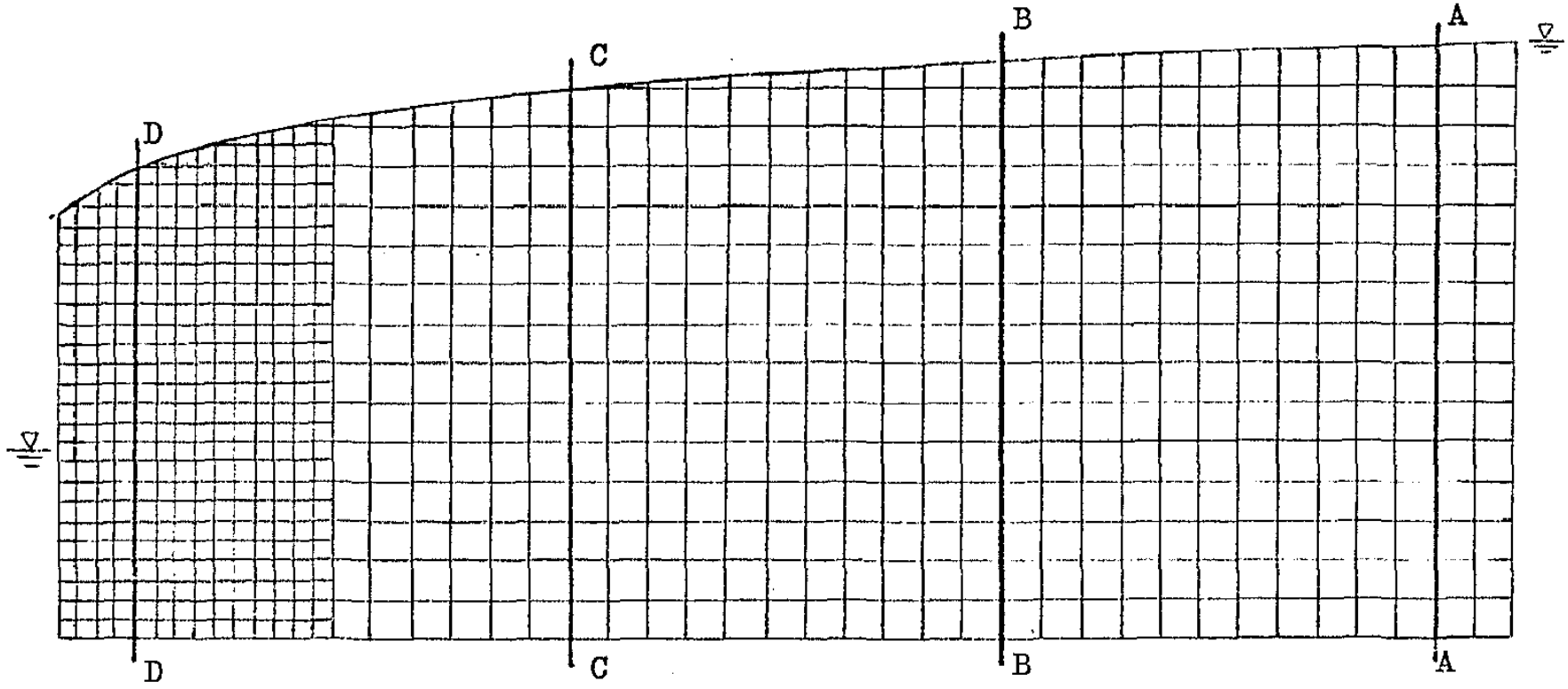

FIG. 6-3-3
FINITE DIFFERENCE GRID FOR ANALYSIS OF SECTOR FLOWS
(Fine Grid incorporated in Forchheimer Flow Analyses)

each of these diagrams. The boundary conditions r_w, h_w and r_e, h_e and the experimental and appropriate analytical discharge values are given in each diagram. The discharge given for Forchheimer flow is that obtained from the numerical solution with the original grid size so that it can be directly compared with the results from the other equations. Corresponding plots for each of flow Nos. 1, 2, 3, 4, 6 and 7 are given in Figs. A-III-1 to A-III-18 in Appendix III.

A study of the discharge values obtained for flow No.5 shows that the Darcy solution differs from the experimental result by 30 percent, while both the Forchheimer and exponential solutions are accurate to within 0.5 percent. The Darcy free surface solution is also considerably in error especially in the vicinity of the well, the error being as high as 18 percent at the well face. The equal head lines for the Darcy solution exhibit discrepancies from the experimental results as shown in Fig. 6-3-4. Observation of Figs. 6-3-5 and 6-3-6 indicates that the nonlinear relations give much more accurate equal head lines and free surface positions. The Forchheimer solution gives the most accurate result but even then, there is a difference of 8 percent right at the well face. Part of this discrepancy may be due to well casing loss incurred

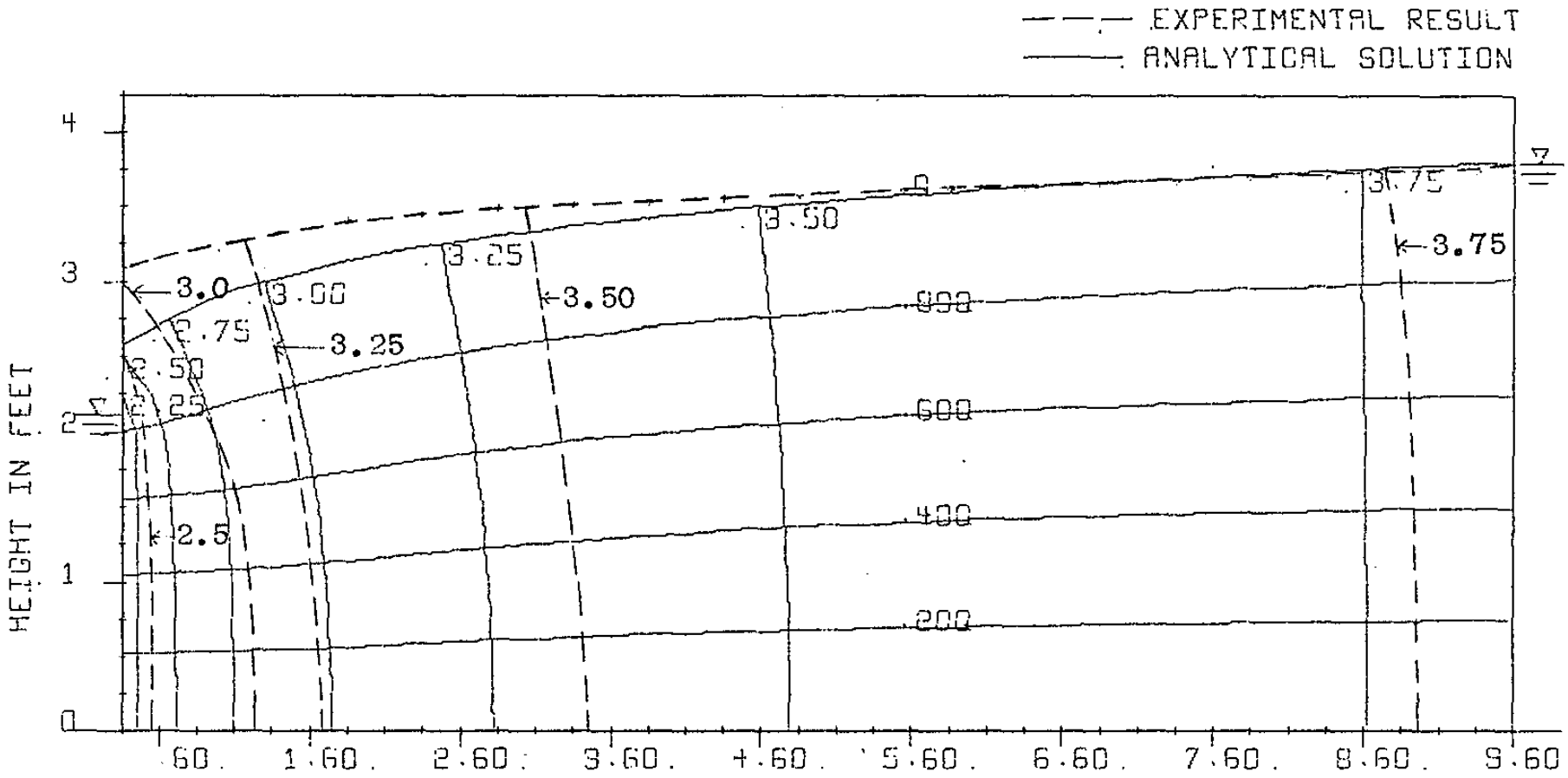

EXPERIMENT WITH SECTOR
FLOW NO 5
RESULTS FOR DARCY FLOW

RW= .354 RE= 9.604
HW= 2.114 HE= 3.794
Q(CALC)= 1.207 Q(EXP)= .910 CUSEC

FIG. 6-3-4

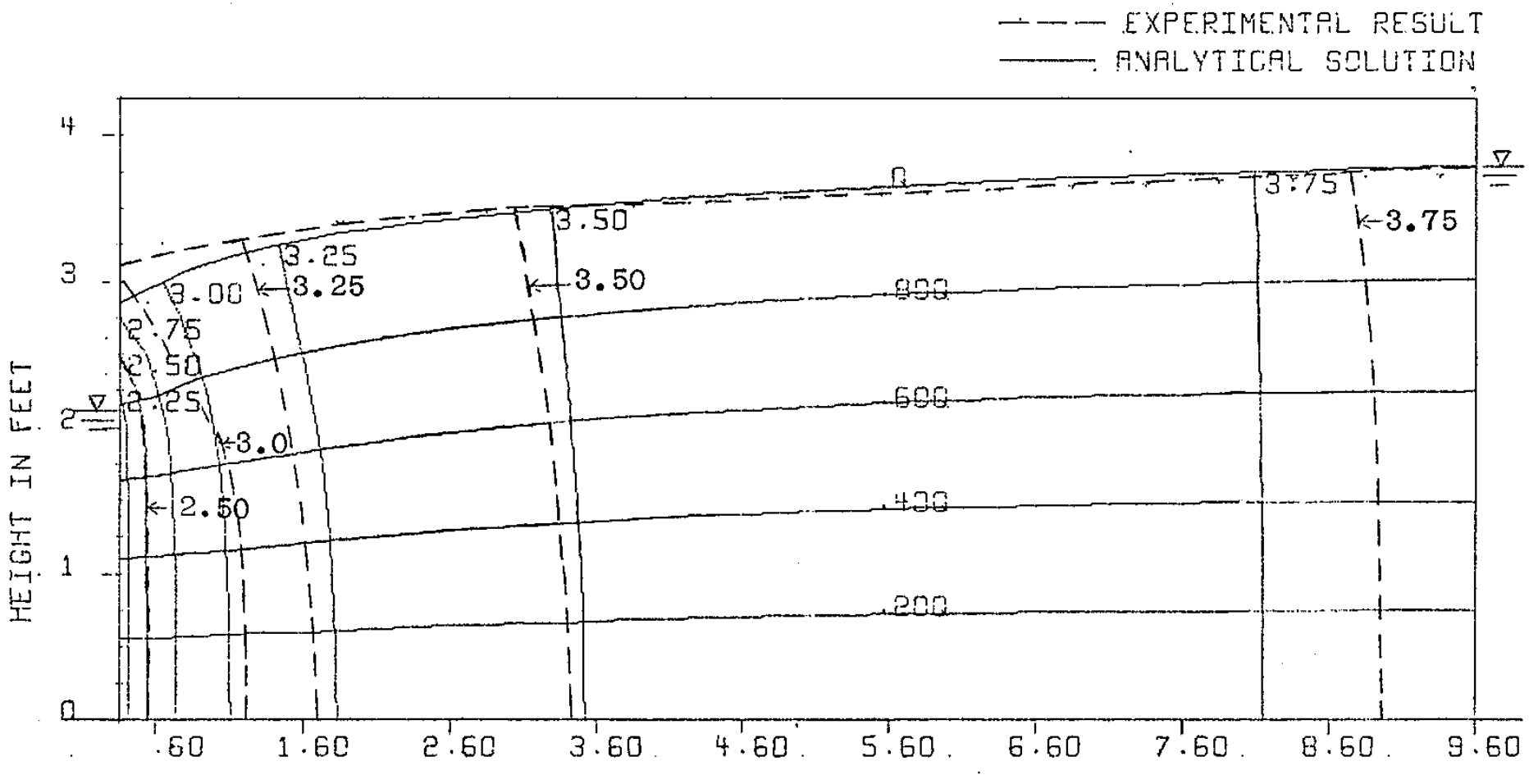

EXPERIMENT WITH SECTOR . RW= .354 RE= 9.604

. FLOW NO 5 . HW= 2.114 HE= 3.734

RESULTS FOR FORCHHEIMER FLOW Q(CALC) = .913 Q(EXP) = .910 CUSEC

FIG. 6-3-5

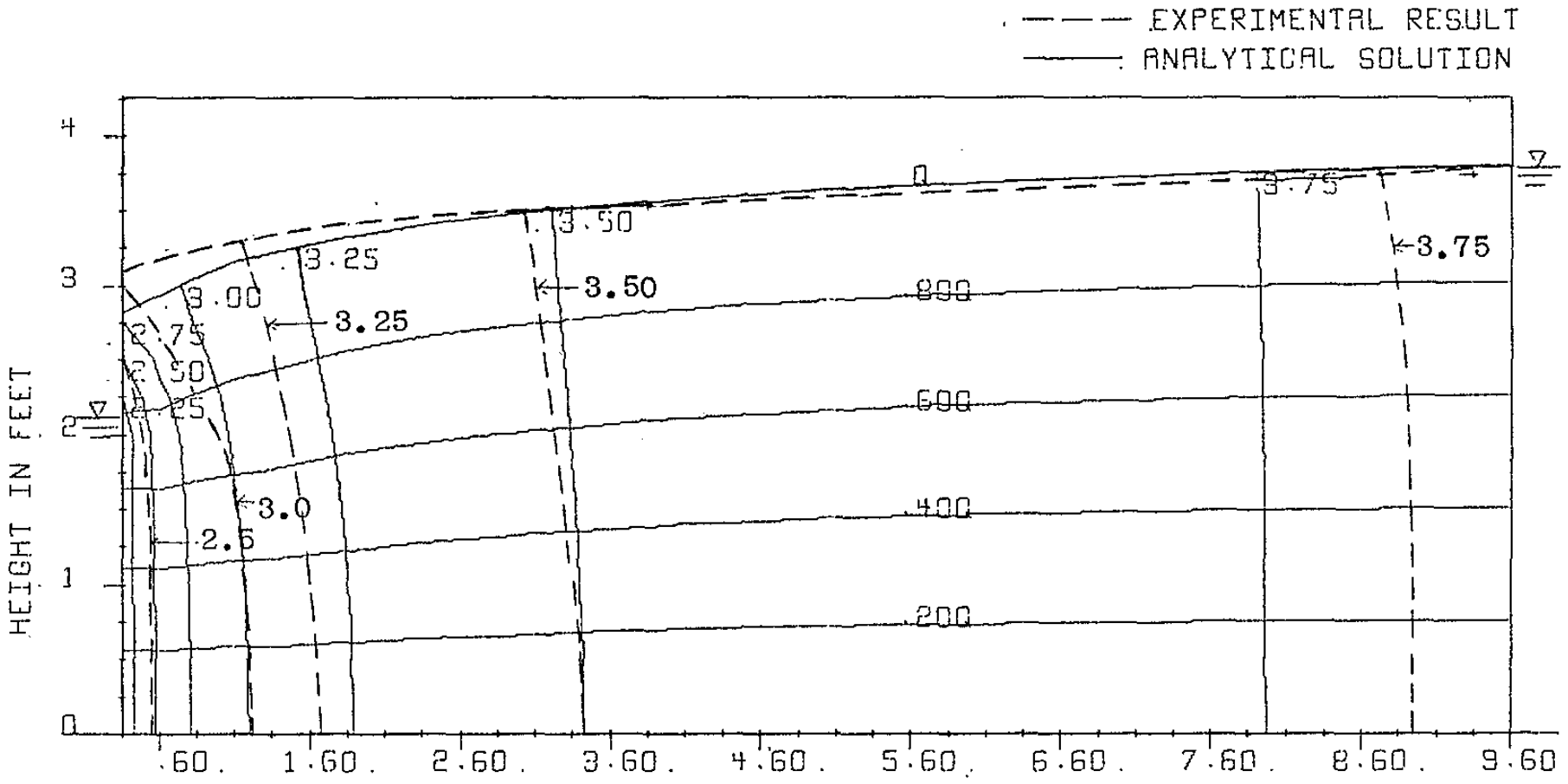

EXPERIMENT WITH SECTOR . RW= .354 RE= 9.604
. FLOW NO 5 . HW= 2.114 HE= 3.794
RESULTS FOR EXPONENTIAL FLOW Q(CALC) = .914 Q(EXP) = .910 CUSEC

FIG. 6-3-6

because of the skeleton of metal remaining to support the gauze. Part may also be due to variation in porosity of the aggregate in the sector, although the accurate result for discharge would suggest that the coefficients employed in the head loss relation are correct. Some improvement may be obtained by using a smaller mesh size in the numerical solutions, although the small change resulting from the finer grid Forchheimer solution near the well suggests that a finer grid size still, would produce only a marginal change in the free surface position.

The experimental position of the equal head line for 3.75 ft. appears to be separated from the nonlinear solutions for this value by some distance. However, near the external boundary, where the piezometric head changes slowly with radius, a small difference in head values shows as a wide separation of equal head lines. Thus a small experimental error would result in a substantial separation of the equal head line from the true location. Although the nonlinear solutions for the 3.75 ft. equal head line are located at some distance from the experimental line in Figs. 6-3-5 and 6-3-6, the agreement between the observed and calculated piezometric heads at any particular point in this area is within 2 percent.

A study of the results for the other six flows shows that similar conclusions can be drawn with regard to the free surface and equal head lines for these flows. The error near the well increases with increasing discharge for all three relations but it is much greater for linear Darcy flow than for the nonlinear solutions. Thus for flow No.7, the error in the free surface position right at the well face is 25 percent for Darcy flow, 15 percent for exponential flow and 10 percent for Forchheimer flow.

A comparison of the discharge results shows that the nonlinear solutions accurately predict the discharge throughout the range of flows. The experimental and theoretical results are plotted against $h_e^2-h_w^2$ in Fig. 6-3-7. A study of Fig. 6-3-7 shows that the nonlinear relations give more accurate discharge results for every flow apart from the reference flow No.3. The error in the Darcy calculated discharges is highest for the flows with greatest drawdown reaching a maximum of 52 percent of the experimental result for flow No.7. The corresponding error of the Forchheimer solution for flow No.7 is 4.6 percent while that of the exponential relation is 7.2 percent. The results again show that the nonlinear relations can adequately cover a large range of Reynolds numbers under practical flow conditions. Although the curve fitting

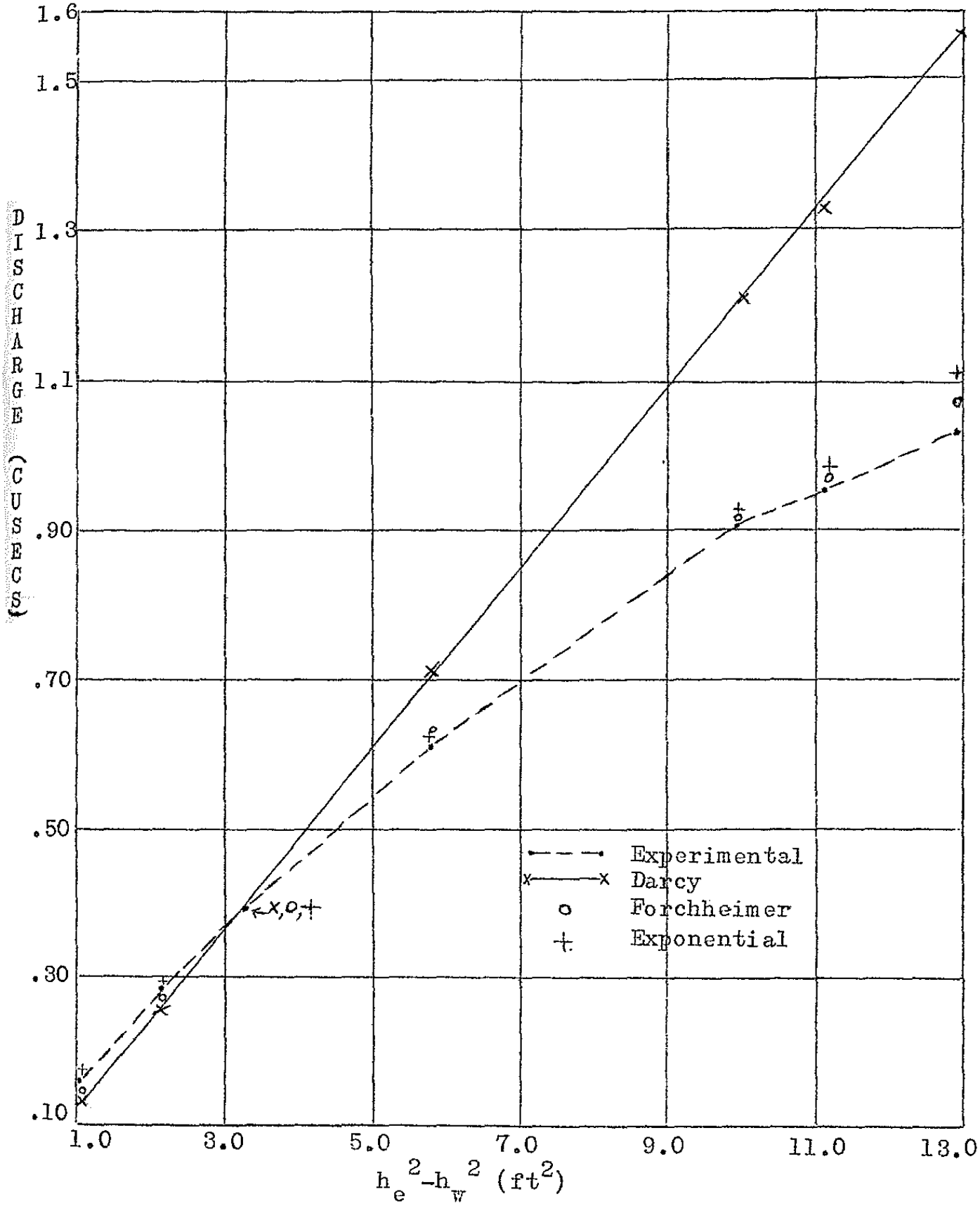

FIG. 6-3-7
DISCHARGE COMPARISONS FOR UNCONFINED AXISYMMETRIC FLOW WITH SECTOR

results indicated that the Forchheimer relation holds more accurately than the exponential relation over a wide Reynolds number range, the actual well tests show that the exponential relation gives satisfactory discharge results over the full range of drawdowns, and it is only at the highest drawdown incorporated, that the Forchheimer relation shows any appreciable superiority.

6.4 Unconfined Two-Dimensional Flow through a Permeable Wall

6.4.1 Determination of coefficients for head loss relations

The gravel used in these experiments was the same as was used in the axisymmetric experiments with a sector. Hence the coefficients for high and low porosity samples are those listed in Table 6-3-1, and the curve-fitting results are depicted in Figs. 6-3-1 and 6-3-2 respectively.

An approximate solution for discharge through a vertical sided wall was obtained from the two nonlinear relations by assuming horizontal flow. The analysis was similar to that used for the unconfined axisymmetric flows, involving a Runge-Kutta numerical solution for the Forchheimer relation. The results for one particular flow in the open flume were used to determine the values for permeability k, the Forchheimer coefficients a and b, and the exponential coefficients c and m.

Three flows were analysed in the experiments and the determination of coefficients was based on the results of the first of these (with the lowest discharge). The measured upstream and downstream heads were .790 ft. and .443 ft. respectively while the length of the wall was 3.00 ft. and the experimental discharge was .012 cusecs. Analysis showed that for Forchheimer coefficients corresponding to the higher porosity sample in the permeameter, a = 4.62 sec/ft and b = 76.58 sec^2/ft^2, the theoretically expected discharge for the above water levels is also .012 cusecs, thus indicating that these coefficients would be accurate for the permeable wall analyses. However as already discussed in section 6.3.1, the Forchheimer and exponential coefficients obtained from the same porosity sample in the permeameter yield different calculated flows through the permeable wall. Although no interpolation for coefficients is required with the Forchheimer relation, it is required with the exponential relation.

For c = 54.51 and m = 1.62, the expected discharge is .014 cusecs,

while for c = 19.72 and m = 1.13, the expected discharge is .006 cusecs.

Successive interpolation indicates that with c = 48.71 and m = 1.53 the exponential relation would give a

discharge of .012 cusecs for the reference flow. These coefficients were therefore employed in the finite difference solutions.

6.4.2 Experimental results and finite difference solutions

Flow net diagrams from the Darcy, Forchheimer and exponential finite difference solutions for flow No.3 are plotted in Figs. 6-4-1, 6-4-2 and 6-4-3 respectively. The experimental flow net is drawn, and the relevant variables including length of wall, upstream (HU) and downstream (HD) waterlevels, and calculated (Q(CALC)) and experimental (Q(EXP)) discharges are given in each diagram. The corresponding results for flow No.2 are given in Figs. A-IV-1 to A-IV-3 in Appendix IV. The flow nets are not shown for flow No.1 but the discharges obtained from the finite difference solutions agreed with the experimental measurement for this flow, thus confirming the validity of the assumption of horizontal flow employed in determining coefficients.

A study of the results shows that the nonlinear relations give more accurate solutions than Darcy's Law both for piezometric head distributions and discharge values. The Forchheimer relation again gives a small but significant increase in accuracy over the exponential relation especially in discharge calculations. There is

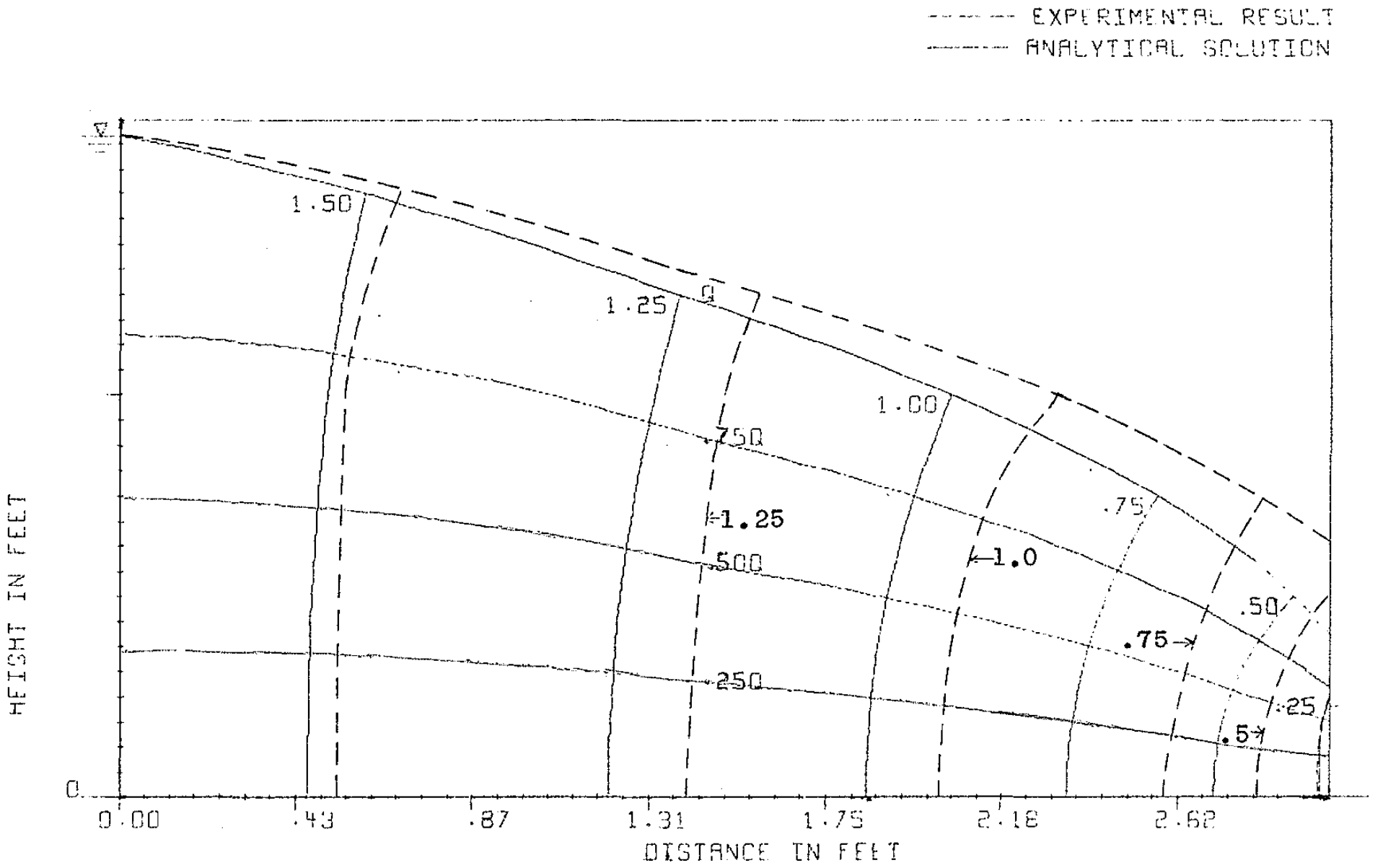

PERMEABLE WALL PROBLEM
FLOW NO 3
RESULTS FOR DARCY FLOW

LENGTH OF WALL = 3.000
HD = .225 HU = 1.646
Q(CALC) = .076 Q(EXP) = .052 CUSEC

FIG. 6-4-1

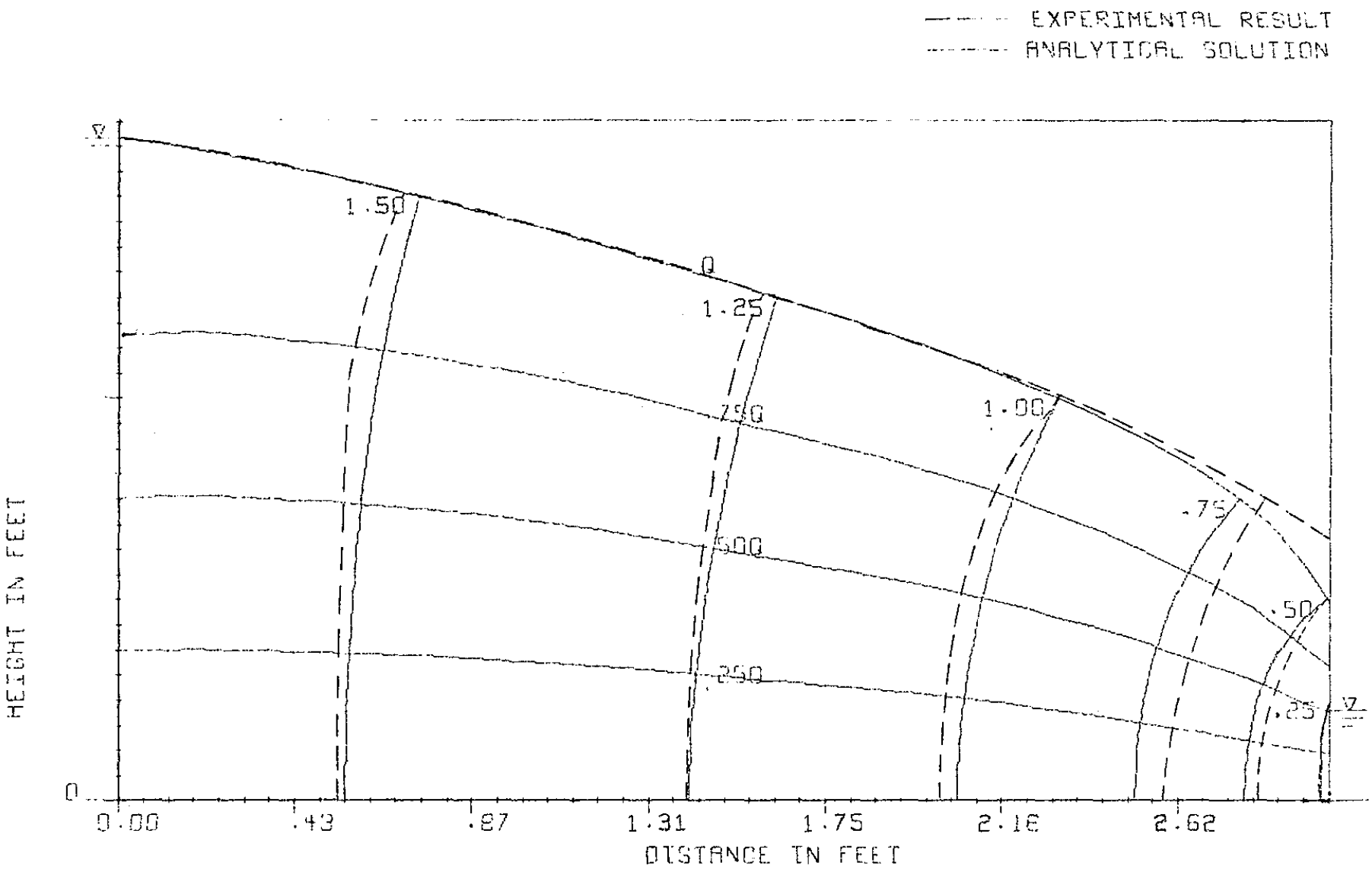

PERMEABLE WALL PROBLEM — LENGTH OF WALL = 3.000
FLOW NO 3 — HD = .225 HU = 1.646
RESULTS FOR FORCHHEIMER FLOW — Q(CALC) = .052 Q(EXP) = .052 CUSEC

FIG. 6-4-2

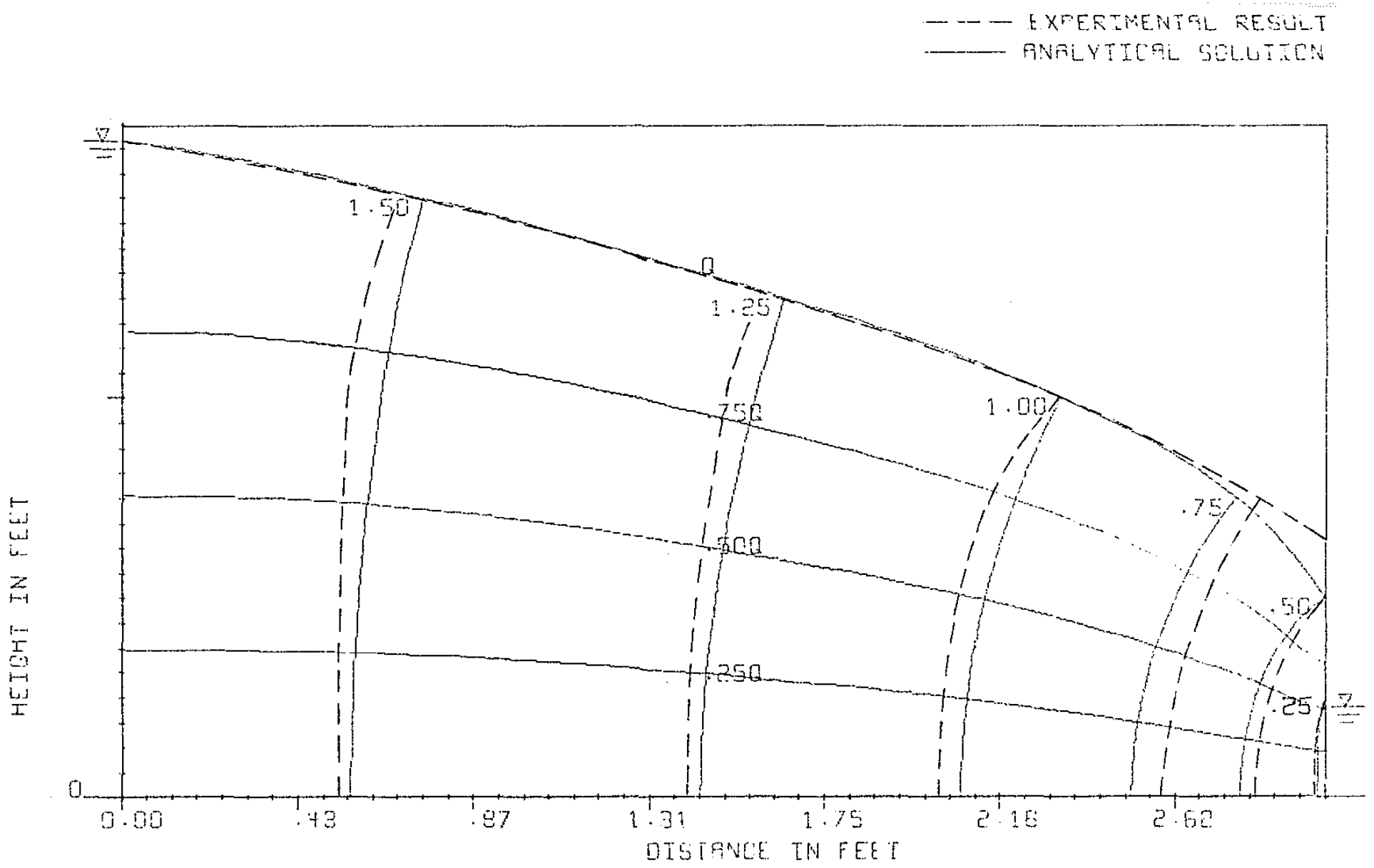

PERMEABLE WALL PROBLEM — LENGTH OF WALL= 3.000

FLOW NO 3 — HD= .225 HU= 1.646

RESULTS FOR EXPONENTIAL FLOW — Q(CALC) = .048 Q(EXP) = .052 CUSEC

FIG. 6-4-3

only a very slight difference in piezometric head distributions obtained from the two nonlinear relations but the discharge difference is appreciable.

The discharges obtained from each of the head loss relations and also the experimental results are plotted against the quantity $(h_u^2-h_d^2)$ for each flow in Fig. 6-4-4 for comparison purposes. The increased accuracy of the nonlinear solutions for discharge as compared to that from Darcy's Law is clearly illustrated in Fig. 6-4-4.

The finite difference grid size used for analysing flow No.2 was 1 inch while that for flow No.3 was $\frac{3}{4}$ inch. Similar accuracies of the finite difference solutions were obtained as for the axisymmetric flows and trials showed that the accuracy could be further improved with increases in the number of iterations for any particular flow, if desired.

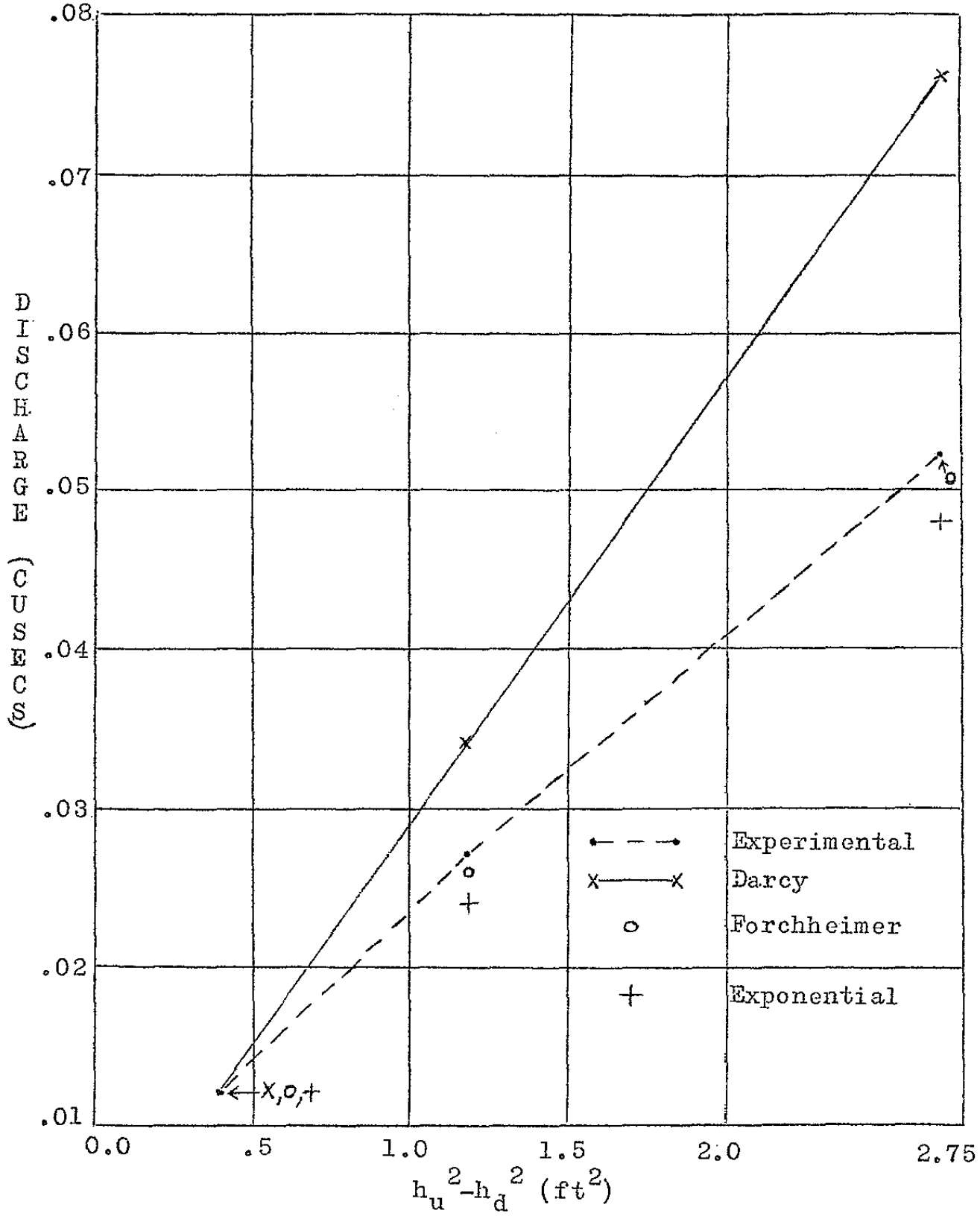

FIG. 6-4-4 DISCHARGE COMPARISONS FOR PERMEABLE WALL FLOWS

CHAPTER 7

DISCUSSION AND COMPARISON OF RESULTS - PART II

7.1 Material Properties for Finite Element Analyses

A crushed aggregate of $\frac{3}{4}$ inch nominal size, and arithmetic mean diameter .55 inch, was used to build up the gravel banks for the flow tests in the open flume. To determine the values of the coefficients to be employed in the head loss relations, permeameter tests were carried out on the aggregate. The ratio of diameter of particle to diameter of permeameter was approximately 1:11 for the aggregate in this case. The aggregate was graded to some extent and this would tend to reduce the wall effect as compared to a uniform coarse material; and in view of the difficulties in eliminating the wall effect completely, as discussed in section 6.1.1, it was decided to base the determination of the coefficients on actual average values of velocity calculated in the permeameter tests. It is noted that there may also be some wall effect, though probably not appreciable, in the flume tests, due to the plane surfaces occurring on the sides and bottom of the gravel banks.

The analyses of flow through gravel banks were carried out because of the need for accurate knowledge of flow conditions through banks of rockfill in connection with dam and coffer-dam constructions in practice. In such

cases, analyses will usually need to be based on material properties which are obtained prior to any prototype flows. The coefficients used in the analyses were therefore determined from permeameter tests on material packed in a similar way to the prototype material. With coarser grained aggregates which contain only a small percentage of fines, it appears that similar porosities can be reproduced more easily than with finer grained, graded materials. The aggregate in the flume tests was placed loosely without any compacting or tamping, and for the permeameter tests it was placed similarly. The Reynolds number range for the permeameter flows should again correspond approximately with that in the flume tests. Thus with the same material packed in approximately the same way, the temperatures at which both sets of tests were carried out were sufficiently close to render differences due to viscosity negligible, and the range of velocities in the permeameter varied from the smallest at which an accurate measurement could be made to values larger than any expected in flow through the banks. This latter requirement can be checked after an analytical solution is obtained.

The values of coefficients a and b in the Forchheimer relation and c and m in the exponential relation were

again obtained from the permeameter results by least squares curve fitting methods. Values of the coefficients for the material together with the corresponding standard errors of estimate (SE) are given in Table 7-1-1.

Forchheimer Coefficients		SE	Exponential Coefficients		SE
a(sec/ft)	b(sec^2/ft^2)	%	c	m	%
.319	11.821	1.57	8.893	1.745	3.02

TABLE 7-1-1 COEFFICIENTS IN VELOCITY HEAD LOSS EQUATIONS

The accuracy of fit of the Forchheimer equation is seen to be better than that of the exponential relation but the difference in accuracy is not great. The accuracy of fit is shown visually in Fig. 7-1-1 where the permeameter results together with the fitted curves, are plotted to scale.

A calculation of the permeability ratio k at each experimental flow shows that permeability varies continuously, decreasing with increasing velocity as would be expected. The mean value of k for all the permeameter flows was .486 ~~.529~~ ft/sec, while the range of permeabilities is such that the deviation from the mean value varies from approximately +230 percent of the mean to -40 percent. Thus while the Laplace equation can be solved for piezometric head values in the region of flow, any meaningful interpretation of

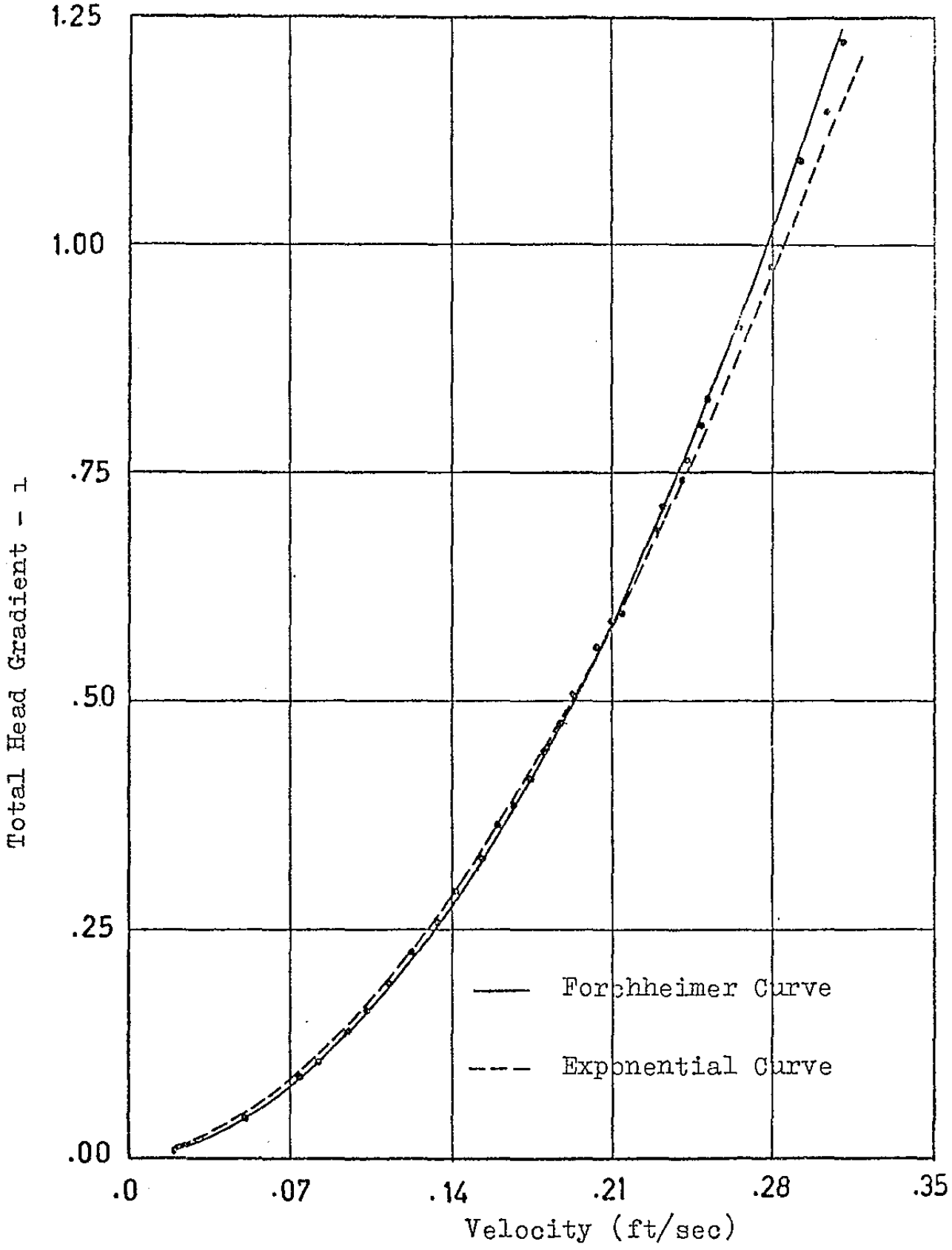

FIG. 7-1-1 PERMEAMETER RESULTS AND FITTED CURVES

discharges calculated from these head values would be difficult.

7.2 Finite Element Solutions and Experimental Results for Actual Flow Tests

7.2.1 Flow through an aggregate bank with no cut-off wall

Results were obtained for two different flows through a bank of the $\frac{3}{4}$ inch nominal size gravel with no cut-off wall. The finite element analysis of both these flows showed only a very slight difference in piezometric head values for solutions based on the Forchheimer equation and the exponential relation; the difference at corresponding points was usually less than 1 percent. In addition, the piezometric head values for the Darcy flow solution did not deviate much from those of the nonlinear solutions.

Flow 1 Upstream Water Level = 0.996 ft.

The experimental free surface for this flow is shown in Fig. 7-2-1, together with the theoretical free surface for both Darcy and nonlinear flow. The equal head lines shown in Fig. 7-2-1 are obtained from the finite element solution for Forchheimer flow, but those obtained for the exponential relation are virtually coincident with these lines.

The experimental free surface agrees well with the calculated position especially as there is a degree of

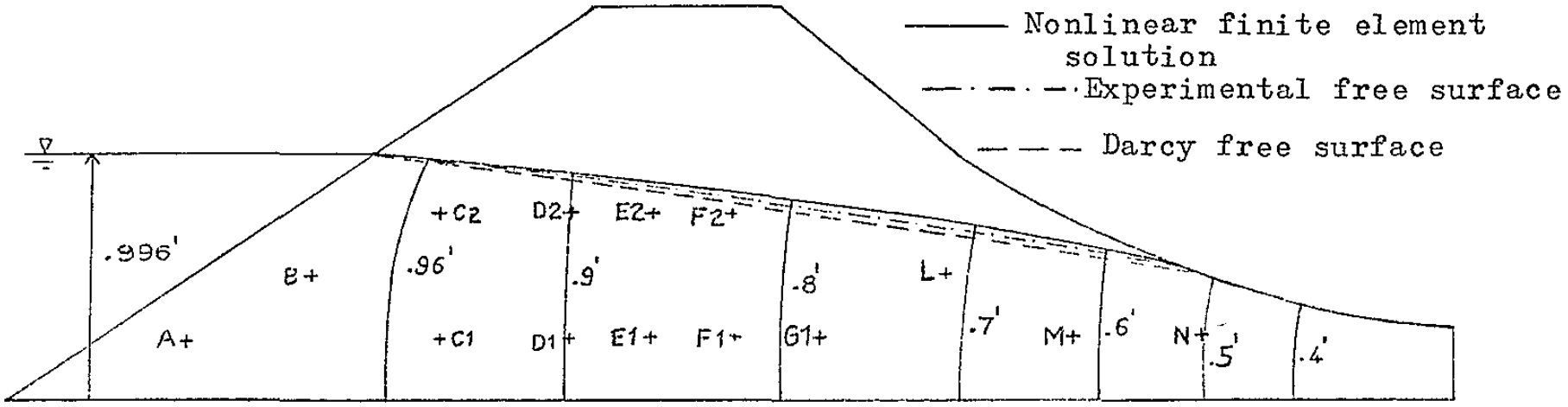

FIG. 7-2-1 FLOW NO.1 THROUGH DAM WITH NO CUT-OFF WALL

uncertainty associated with drawing the experimental line due to minor variations from individual particles. A comparison of experimental and calculated values of piezometric head was made at a number of points throughout the flow marked as A to N in Fig. 7-2-1. Table 7-2-1 shows the experimental values as well as values obtained from the Darcy, Forchheimer and exponential relation solutions. The experimental measurements were obtained from the tapping points on the steel side of the flume.

Point	Piezometric Head (ft)			
	Experimental	Forchheimer	Exponential	Darcy
A	.99	.99	.99	.99
B	.98	.98	.98	.98
C1	.95	.95	.95	.93
C2	.96	.95	.95	.94
D1	.89	.90	.90	.88
D2	.90	.90	.90	.88
E1	.83	.86	.86	.84
E2	.86	.86	.86	.84
F1	.79	.82	.82	.79
F2	.80	.83	.83	.80
G1	.75	.78	.78	.75
L	.69	.71	.71	.68
M	.58	.62	.62	.59
N	.46	.50	.50	.49

TABLE 7-2-1 PIEZOMETRIC HEAD VALUES FOR FLOW 1

The maximum discrepancy of any calculated piezometric head from the corresponding experimental one is approximately 8 percent and for most points the discrepancy is less than 4 percent. At some points the Darcy solution for piezometric head actually agrees with the experimental measurement more accurately than the nonlinear solution. However, the difference between all calculated values at any point is small and all give acceptable agreement with the experimental measurement.

The most significant advantage of the finite element solution for nonlinear flow is that it enables an accurate calculation of discharge. The difficulty in obtaining a value of the discharge from Darcy's Law has already been noted because of the continuous variation in permeability with velocity. This problem does not arise with the nonlinear flow equations provided the coefficients can be assumed constant throughout the range of velocities encountered.

The discharge was calculated from the nonlinear finite element solutions at a number of vertical sections throughout the bank. The discharge obtained experimentally was .076 cusecs/ft. The average value calculated from the finite element Forchheimer solution was .073 cusecs/ft, while that obtained from the exponential relation was .071

cusecs/ft. Thus both theoretical values agree well with the experimental one.

The numerical analysis was continued until the change in the piezometric head at any point between successive iterations was .00001 ft. The finite element network employed in the solutions is depicted in Fig. 7-2-2. Although the grid size is reasonably coarse, evaluation of discharge at different vertical sections in a continuity check showed that the variation from the mean value was less than $\pm$ 0.3 percent. The discharges calculated at the vertical grid lines designated in Fig. 7-2-2 are listed in Table 7-2-2.

Grid Line as Depicted in Fig. 7-2-2	Total Calculated Discharge (cusecs/ft) from Forchheimer Solution
A-A	.0732
B-B	.0735
C-C	.0735
D-D	.0735
E-E	.0735
F-F	.0735

TABLE 7-2-2
DISCHARGE AT VERTICAL GRID LINES FROM THE FINITE ELEMENT SOLUTION

The table shows that continuity is satisfied to within a total variation of 0.4 percent for the lines given.

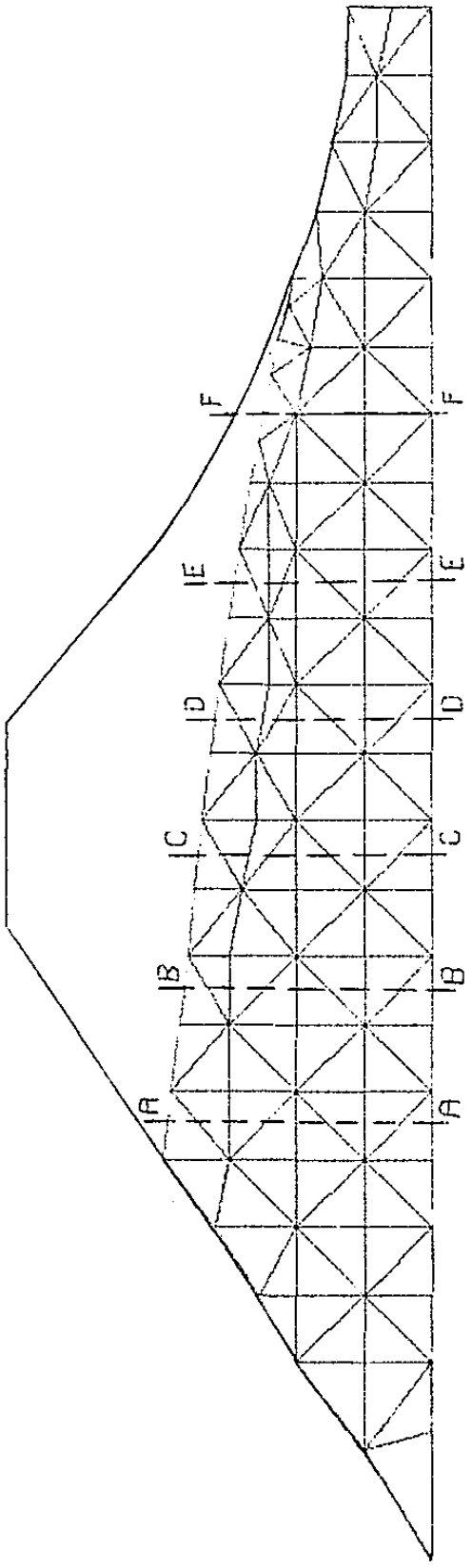

FIG. 7-2-2 FINITE ELEMENT NETWORK FOR FLOW NO.1

Since the discharge quantities are obtained from the velocity and the length of grid by an integration procedure, in which the errors in the numerical results tend to accumulate, the agreement between the quantities at the different sections indicates a satisfactory numerical solution. Analysis of the results from the Darcy and exponential relations leads to similar conclusions regarding the accuracy of the numerical solutions.

Although the piezometric heads calculated from the two nonlinear solutions generally agree to within 1 percent, the difference in discharge values is greater, with the Forchheimer result giving slightly better agreement with the experimental value. Similarly, although there is only a small difference between piezometric heads obtained from the Darcy and nonlinear solutions, the effect on discharge is significant. Thus, if an attempt is made to calculate the discharge by applying one of the nonlinear flow equations to the Darcy head values, it is found that there is a discrepancy of up to 20 percent between discharge values calculated at different sections throughout the bank. It is expected that this discrepancy would be considerably magnified in flow through prototype rockfill banks and in such flows the advantages of the nonlinear solution would also be more significant.

Flow 2 Upstream Water Level = 1.215 ft.

The experimental free surface for this flow is shown in Fig. 7-2-3, together with the theoretical free surface for both Darcy and nonlinear flow. The two nonlinear relations, Forchheimer and exponential, again give virtually coincident results and the equal head lines shown in Fig. 7-2-3 are obtained from the finite element solution for Forchheimer flow.

A comparison of experimental and calculated values of piezometric head was made at the points throughout the flow marked A to N in Fig. 7-2-3 and these are given in Table 7-2-3.

Point	Piezometric Head (ft)			
	Experimental	Forchheimer	Exponential	Darcy
A	1.21	1.21	1.21	1.21
B	1.21	1.20	1.20	1.19
C1	1.16	1.16	1.16	1.14
C2	1.18	1.18	1.18	1.16
D1	1.09	1.10	1.10	1.07
D2	1.11	1.11	1.11	1.08
E1	1.02	1.05	1.05	1.01
E2	1.05	1.06	1.06	1.02
F1	.96	.99	.99	.95
F2	.98	1.01	1.01	.97
G1	.90	.93	.93	.89
G2	.90	.95	.95	.90
L	.80	.83	.83	.78
M	.64	.68	.68	.65
N	.48	.51	.51	.51

TABLE 7-2-3 PIEZOMETRIC HEAD VALUES FOR FLOW 2

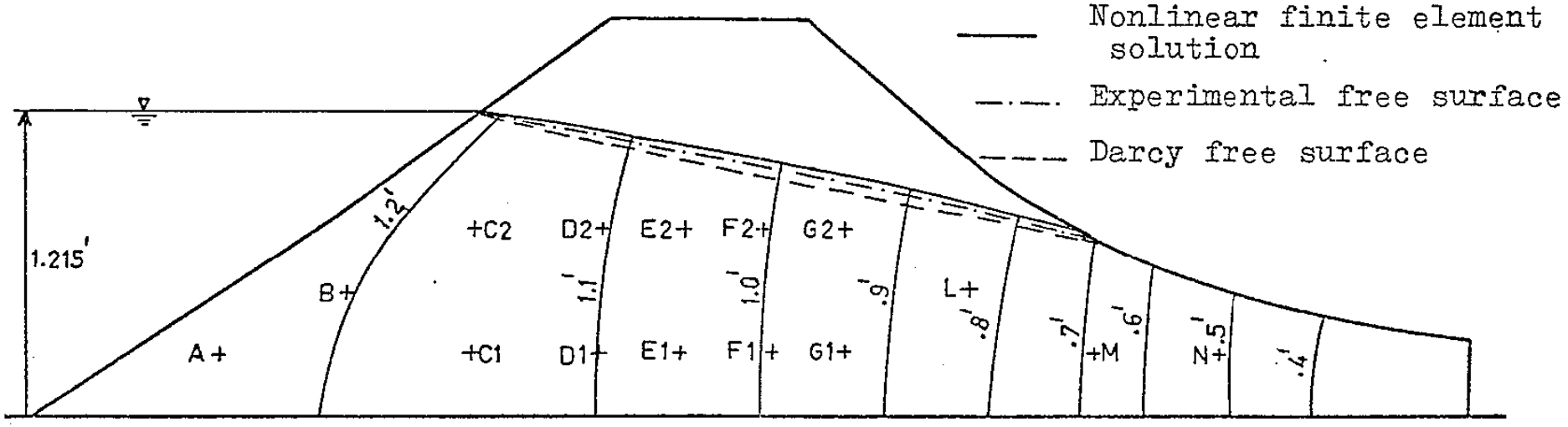

FIG. 7-2-3 FLOW NO. 2 THROUGH DAM WITH NO CUT-OFF WALL

The results show trends similar to those which were evident with flow No.1, the maximum discrepancy of any calculated piezometric head from the corresponding experimental one being approximately 6 percent in this case.

Discharge calculations again yield good agreement with the experimental result:

Experimental discharge = .114 cusecs/ft

Theoretical discharge (Forchheimer) = .110 cusecs/ft

Theoretical discharge (exponential) = .107 cusecs/ft.

The Forchheimer result again shows a small but significant increase in accuracy over the exponential one.

The finite element network used was similar to that for flow No.1 and discharge calculations at various vertical grid lines showed that continuity was satisfied to a similar degree of accuracy as for flow No.1.

7.2.2 Flow through a bank with an impervious cut-off wall

A solution was carried out for two flows through a bank with a sloping impervious cut-off wall. For flow No.1 the headwater height was 1.383 ft. and there was no tailwater. The free surface position obtained from the Forchheimer flow equation and the exponential relation are in close agreement as are the equal head lines. The free surface line and the equal head lines for the Forchheimer solution are plotted in Fig. 7-2-4. The positions of the

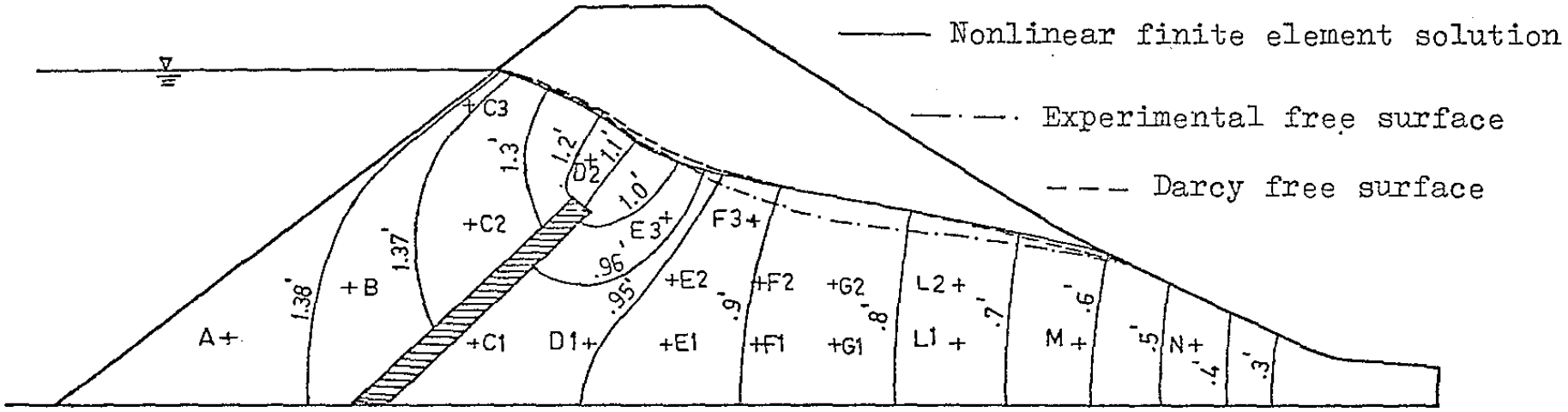

FIG. 7-2-4 FLOW NO.1 WITH AN IMPERVIOUS CUT-OFF WALL

experimental free surface and the Darcy free surface are also shown in Fig. 7-2-4. A comparison of the experimental and calculated values of piezometric head at discrete points (marked A to N in Fig. 7-2-4) is given in Table 7-2-4.

Point	Piezometric Head Value (ft)			
	Experimental	Forchheimer	Exponential	Darcy
A	1.383	1.382	1.382	1.380
B	1.379	1.379	1.379	1.371
C1	.85	.95	.95	.96
C2	1.358	1.356	1.356	1.331
C3	1.379	1.374	1.374	1.371
D1	.85	.95	.95	.98
D2	1.19	1.17	1.17	1.17
E1	.83	.93	.93	.96
E2	.84	.95	.95	.98
E3	.89	.98	.98	1.00
F1	.80	.89	.89	.90
F2	.81	.90	.90	.91
F3	.83	.91	.91	.93
G1	.76	.84	.84	.84
G2	.75	.85	.85	.84
L1	.68	.75	.75	.73
L2	.69	.75	.75	.73
M	.57	.62	.62	.60
N	.41	.45	.45	.44

TABLE 7-2-4
PIEZOMETRIC HEAD VALUES FOR FLOW No.1 WITH CUT-OFF WALL

A consideration of the results shows that good agreement between calculated and observed quantities is obtained upstream of the cut-off wall but that the agreement on the downstream side is less accurate. A problem with numerical

analyses is that it is sometimes difficult to predict the degree of accuracy of the results. Some indication of the accuracy may be determined by solving a given problem with a particular mesh size and solving the same problem with a finer mesh and comparing the results. A solution for this flow problem was therefore obtained using 100 nodes and about 160 elements and then another solution using approximately 300 nodes and 500 elements was carried out. The results of the finer grid solution showed only slightly better agreement with the experimental ones. The difference between the two solutions at various points was usually less than 2 percent. The results given in Fig. 7-2-4 and Table 7-2-4 are for the fine grid solution.

Some idea of the accuracy of the numerical results may also be obtained by carrying out a continuity check. Calculation of discharge from the nonlinear finite element solution at various vertical sections showed that continuity is satisfied to within $\pm$ 3 percent for sections throughout the flow including sections above the cut-off wall.

The finer grid finite element network used in the solutions is depicted in Fig. 7-2-5 and the discharge from the Forchheimer solution at the sections designated in Fig. 7-2-5 are given in Table 7-2-5.

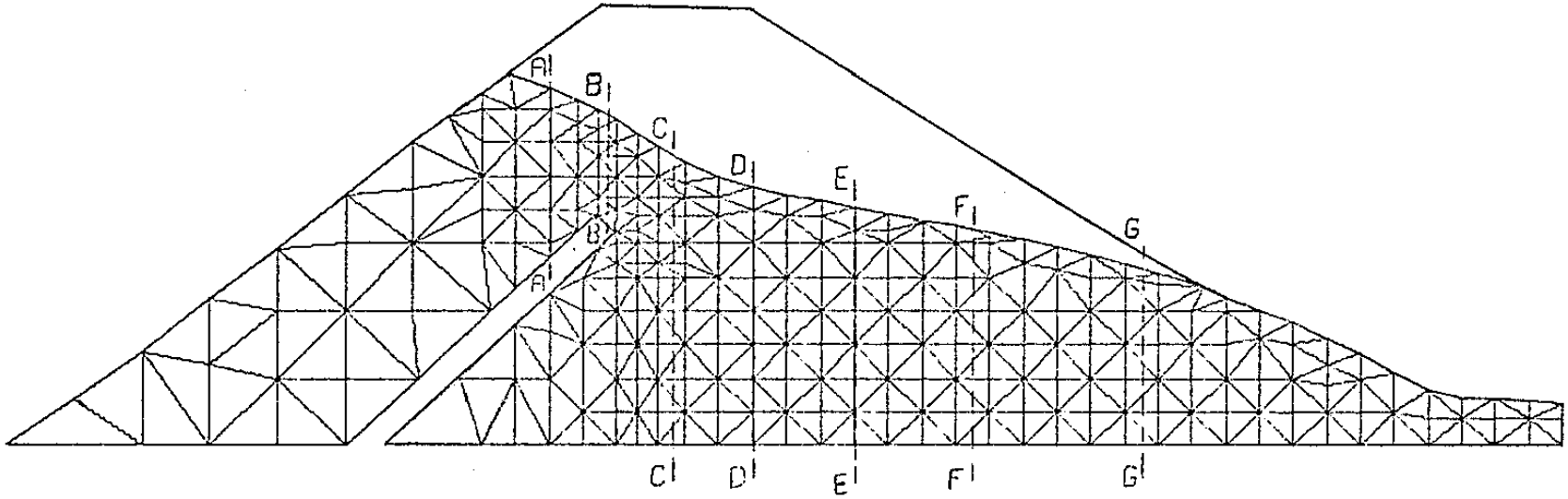

FIG. 7-2-5 FINITE ELEMENT NETWORK FOR FLOW NO.1 WITH CUT-OFF WALL

Grid Line as Depicted in Fig. 7-2-5	Total Calculated Discharge (cusecs/ft) Forchheimer Solution
A-A	.091
B-B	.089
C-C	.088
D-D	.092
E-E	.093
F-F	.093
G-G	.093

TABLE 7-2-5
DISCHARGE AT VERTICAL GRID LINES FOR FLOW WITH CUT-OFF WALL

Although the agreement of values in Table 7-2-5 could be improved by more iterations and by using a finer grid, experience has shown that the final average calculated discharge and the piezometric heads at the nodes would not be significantly affected.

The experimental discharge was observed to be .083 cusecs/ft. The average value calculated from the Forchheimer solution was .091 cusecs/ft. while that from the exponential relation was .090 cusecs/ft. Although values of piezometric head obtained from the Darcy solution agree quite closely with those from the nonlinear solutions, discharge calculations from these Darcy head values are again inaccurate. For the second flow investigated, the upstream water level was 1.18 ft. and the downstream level

was .12 ft. The free surface position and equal head lines from the Forchheimer solution are plotted in Fig. 7-2-6 together with the positions of the free surface obtained experimentally and from the Darcy solution. The results show similar trends to those obtained for the first flow except that the nonlinear Forchheimer solution gives a decidedly more accurate prediction of the free surface line in this case than does the Darcy solution. The piezometric head values obtained from the nonlinear flow solution at points within the flow region also agree more closely with the experimental measurements than do those from the Darcy solution. A calculation of discharges across various vertical grid lines throughout the flow showed that continuity was satisfied to a similar degree of accuracy as for flow No.1.

The experimentally measured discharge for this second flow was .058 cusecs while that obtained from both the Forchheimer and exponential solutions was .065 cusecs.

Although the Forchheimer solution gives more accurate results than the Darcy solution there is still a discrepancy between calculated and observed piezometric heads especially on the downstream side of the cut-off wall. Some of this discrepancy between the calculated and experimental values may be due to the complexity of the

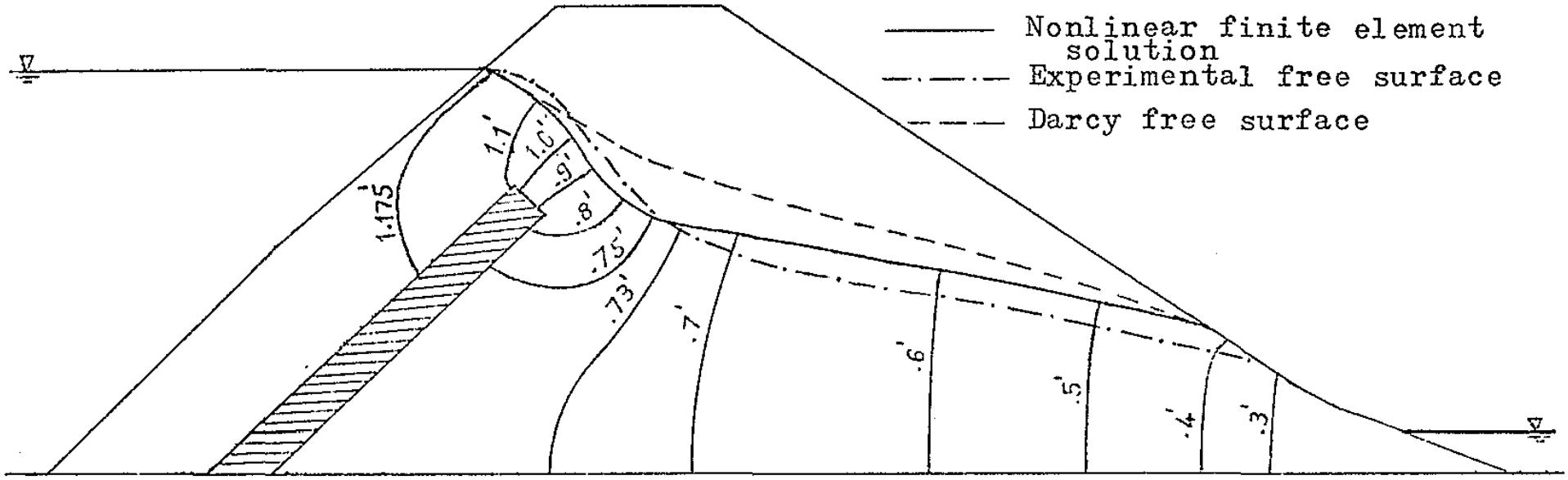

FIG. 7-2-6 FLOW NO.2 WITH AN IMPERVIOUS CUT-OFF WALL

lower impervious boundary. Singularities arise at abrupt changes in direction of the flow boundaries and these cannot be easily allowed for in a numerical solution to nonlinear partial differential equations. The only allowance for singularities made in the analysis was to use a finer grid size around the corners at the top of the cut-off wall.

Part of the discrepancy may also be explained by the actual nature of the flow passing over the wall which probably does not conform well to the continuous saturated flow condition assumed in the analysis. In the experimental tests some aerification of the flow occurred as it passed over the cut-off wall with a result that only a mean position of the free surface could be plotted. Parkin (1963a) has called this the free-fall region.

In view of the difficulties in accounting for this aerified nature of the flow in any analytical solution the calculated values of piezometric head and discharge are acceptable results.

CHAPTER 8

CONCLUSIONS

8.1 Nonlinear Head Loss Relations in Porous Media Flow

The realisation of the limited validity of the Darcy linear law of head loss for flow through porous media at high Reynolds numbers has led researchers to formulate nonlinear relations that will accurately predict the head loss over an extended range of Reynolds numbers. The suggested forms of the appropriate nonlinear relations have varied considerably. Two of the most common forms for flow of water through coarse granular materials are the Forchheimer and exponential equations. The Forchheimer relation is written as:

$$i = aV + bV^2 \qquad \text{.... 8.1-1}$$

while the exponential relation is:

$$i = cV^m \qquad \text{.... 8.1-2}$$

in which i is the hydraulic gradient, V is the average macroscopic velocity and a, b, c and m are terms which depend on the properties of the fluid and medium.

Deductions from the Navier-Stokes equations (Irmay, 1958; Sunada, 1965) have shown that the Forchheimer equation can be derived by a dimensional approach, but further consideration (Stark and Volker, 1967; Stark, 1969) has shown that the coefficients a and b will only be strictly constant

for a constant velocity profile of flow. Numerical solutions of the Navier-Stokes equations (Stark, 1968), for flow through idealised media, have shown that the velocity profile varies with the Reynolds number so that a and b depend on the Reynolds number. However these solutions have also shown that the velocity profile and therefore the values of a and b change slowly with changes in Reynolds number so that constant values of a and b can be applied, with small error, over a range of Reynolds numbers. Experimental measurements of hydraulic gradient and velocity, for flow through coarse grained materials, have been carried out by numerous authors and have supported the above conclusions. To ensure best accuracy of results, the coefficients a and b should be determined by curve fitting to the velocity and hydraulic gradient results over the Reynolds number range under consideration.

The exponential head loss relation has also been supported by many authors and has been applied in the analysis of some practical flow situations. This relation however has been suggested on the basis of experimental results and theoretical justification for it has not been reported as for the Forchheimer relation.

Although the breakdown of Darcy's Law at high Reynolds numbers has been widely recognised, the treatment of

practical situations involving nonlinear flow has been limited. The approach utilised in this thesis has incorporated experimental work with materials sufficiently coarse to render nonlinear effects appreciable. Experiments have been carried out over ranges of Reynolds numbers for situations similar to those likely to be encountered in problems of practical importance. Thus the axisymmetric flow tests were performed to investigate nonlinear effects in the area adjacent to a well where the velocities are high, while the gravel bank experiments in the open flume were designed to simulate flow through rockfill, which is of increasing importance in dam and coffer-dam constructions.

The results of the well flow tests have shown that the position of the top flow line and equal head lines obtained from the Darcy and nonlinear solutions differ appreciably only at large drawdowns. For the confined flow experiments the results indicate that the Darcy solution for the piezometric head line agrees more closely with the experimental than the nonlinear solutions. However at least part of this discrepancy is considered to be due to experimental error in determining the free surface, as permeameter results had shown that Darcy's Law is decidedly inaccurate, over the Reynolds number

range which occurs in the well tests for any particular flow. The unconfined axisymmetric flow analyses showed that both the Forchheimer and exponential relations gave better agreement with the experimentally determined flow nets than the Darcy solution. Especially at the highest flows in the range investigated, the nonlinear solutions give appreciably more accurate results. The two-dimensional flow experiments in the open flume showed that the difference in flow nets obtained from the linear and nonlinear solutions is quite small for small drawdowns. In flow through banks of $\frac{3}{4}$ in. nominal size aggregate the difference in the phreatic surfaces is small for all three head loss relations and it appears that, in this case, the flow net could usually be obtained to sufficient accuracy from a Darcy solution. The reason for this is that, although Darcy's Law does not apply over a wide range of Reynolds numbers for such a coarse grained material, the variation in average velocity from the upstream face to the downstream face of the bank is not great and a Darcy solution will therefore be reasonably accurate. Nevertheless, the material which occurs in actual applications may have a nominal particle size of the order of 2 ft. or greater and for this material the nonlinear effects will be increased so that the error of

the Darcy solution for the free surface may then be more significant than in the experiments reported herein.

It is however, in determinations of discharge that the solutions for nonlinear porous media flow are particularly significant. For the 3/16 in. nominal size gravel employed in the well flow experiments it has been shown that estimations of discharge from Darcy's Law, based on a permeability coefficient determined for any particular flow, will be in error for any other flow. For well tests under field conditions the discharge from the pump used in the test is measured. The drawdown between the pumped well and an observation well located at a known distance away is determined. The Dupuit-Forchheimer expression is then employed to calculate the average permeability coefficient. If the permeability is determined from a flow with a small drawdown, then for the range of flows and the material used in the experiments, this will result in an underestimation of discharge for still smaller drawdowns and an overestimation by as much as 50 percent for highest drawdowns. The nonlinear relations however can accurately predict the discharge to within a few percent over the whole range of drawdowns. It is still necessary to determine the appropriate values of the coefficients in the head loss relations for the

prototype material and for the Reynolds number range encountered in the prototype flows. A satisfactory method of achieving this has been formulated, based on permeameter results at different porosities, and using an approximate solution for horizontal flow to interpolate between the sets of coefficients.

In flow through rockfill dams and banks in actual practice, discharge calculations will usually need to be carried out in the design stage, before construction commences. For this reason it would not be possible to determine the permeability or the nonlinear head loss coefficients from actual flow results. In the gravel bank experiments therefore, coefficients in the nonlinear head loss equations were obtained by fitting curves to permeameter test results for a sample packed similarly to the prototype material. Under these conditions, any determination of discharge from Darcy's Law would be difficult because the permeability varies continuously over all velocity values used in the permeameter. The availability of a nonlinear solution therefore assumes greater importance for such situations and this is likely to be even more important with the coarser materials which occur in practice.

A comparison of the results from the two nonlinear

relations (the Forchheimer and exponential) shows that both give accurate predictions of discharge and of piezometric head values. It was noted in Chapter 2 that the Forchheimer equation was theoretically more sound than the exponential one. The curve fitting results reinforced this conclusion, as a calculation of the standard error of estimate for the fitted curves showed that in every case the Forchheimer equation fitted all permeameter results with greater accuracy than did the exponential equation. However the results obtained from application of the two equations to practical flow situations showed that, while the Forchheimer equation in general gave more accurate results, this increased accuracy was only significant in a limited number of cases. These included axisymmetric flow to a well at large drawdowns and flow through coarse gravel banks.

Again it is possible that the increase in accuracy of the Forchheimer equation may become more appreciable in flow through rockfill with the larger particle size likely to be met in practice.

Thus, although both relations give reasonably accurate results, it is considered that analyses should be based on the Forchheimer relation because it does give some improvement in certain cases and it involves no more

difficulty in the analysis than the exponential relation.

8.2 Finite Difference and Finite Element Solutions

The field differential equations resulting from all three head loss relations considered, are partial differential equations and for unconfined flow situations, the solution of these equations involves a numerical field approach. The two approaches used in this thesis have been the finite difference and finite element methods and each differential equation has been shown to be amenable to solution by both methods. A brief consideration of the relative merits of the finite difference and finite element techniques is therefore pertinent.

The finite element method has advantages over a finite difference approach when the boundaries of the flow area are irregularly shaped. The elements can be varied in size to conform to the boundaries without difficulty and no change in the basic program is necessary for any shape. The variation in element orientation and size is catered for in the input data. The finite difference method, on the other hand, is much less readily adaptable to irregular boundaries, especially when a fixed mesh length is assumed at interior points in the field. Thus the finite element method is better suited to the analysis of flow through dams and banks of placed rockfill where the slopes of the

faces vary and where the lower boundary may not be uniform or horizontal. The finite element method is also easily adapted to flow situations involving a nonhomogeneous flow field because, provided the boundaries separating different materials are known, the elements can be made to conform to these boundaries. The appropriate values of the coefficients for each element can be specified and read in as data for the computer program.

When compared with the finite difference technique, the method of finite elements has some disadvantages in that, for a given number of grid points, it requires more computer storage and may require more computer time to achieve a given accuracy of solution. Thus for a given amount of computer storage and time, a finer grid size will usually be possible with the finite difference method, although it is usually easier, with the finite element method, to incorporate a finer mesh in particular locations where increased accuracy is desired.

With the finite element approach, the preparation of data for large element numbers becomes tedious when this is done manually, whereas the finite difference grid network is often set up in the program itself and no such tedium is encountered. However, programs are being developed (Zienkiewicz, 1967) to produce a finite element network for

general field shapes so that this difficulty will eventually be eliminated for the finite element method.

The problem of unconfined flow to a well results in a flow field in which the equal head lines at the upstream and downstream boundaries can be assumed vertical; and if the medium is homogeneous and is underlain by a horizontal impervious stratum then a finite difference analysis is readily adaptable. The finite element method can, of course, be applied to the analysis of the unconfined axisymmetric flow situation (Taylor and Brown, 1967), if it is advantageous because of nonhomogeneity of the medium or irregularity of the flow boundaries.

The two approaches differ in the treatment of the Neumann boundary conditions. The finite element method automatically allows for no flow across the impervious base and across the free surface, as a "natural" boundary condition, while this condition has to be incorporated in finite difference form in the alternative method. This difference becomes significant in the adjustment of the free surface where the finite difference method is restricted because of the regular nature of the grid lines. Nevertheless, automatic adjustment of the free surface with the finite element method also introduces complexity

in programming because of the need to allow for changes in the element network in the vicinity of the free surface.

With the continued improvement in capabilities of each new generation of computers and with the need to handle more complex flow situations, it is likely that the finite element method will be increasingly employed in solutions of porous media flow problems.

8.3 Applications to Practical Flow Situations

8.3.1 Determination of coefficients for actual media

Problems still arise in applying the nonlinear relations to practical flow situations because of the difficulty in determining values of the coefficients in the equations for naturally occurring materials. Some empirical methods have been formulated for determining the coefficients in terms of particle size, porosity etc. Engelund (1953) proposed equations for the coefficients a and b of the Forchheimer relation while Parkin, Trollope and Lawson (1966) gave a nomogram for obtaining the head loss through marbles and rock at a range of void ratios, from an exponential head loss relation. At their present stage of development such empirical methods cannot account for the wide variations in properties which occur with porous media in practice, as they have been tested for only a very limited range of materials. But it is possible that with continued

determinations of coefficients, information may be accumulated for a more comprehensive range of media so that coefficients will eventually be determined from formulae or charts as functions of material gradings, porosities, mean particle diameter etc.

Another possible avenue for obtaining required coefficients is from solutions to the fundamental Navier-Stokes equations. At present solutions are only available for ~~linear~~ laminar flow and idealised particle shapes, but with the improvement of numerical methods and computer systems, coefficients may eventually be obtained from numerical solutions for 3-dimensional flow through channels which are representative of actual porous media.

For sufficiently fine grained materials and where the results for at least one prototype flow are available, the coefficients may be obtained from permeameter test results in conjunction with an approximate analysis of the flow, as described in Chapter 6. For some rockfill materials the particle size may be too large to allow accurate permeameter tests and in this case it may be possible to obtain coefficients from semi-field type measurements for flow through material in specially constructed flumes, with discharges measured by weirs or flow meters. Although such tests may involve substantial costs, they would provide

the appropriate coefficients for the nonlinear head loss relation and a complete analysis of flow through the rockfill could then be achieved by solutions based on this relation.

8.3.2 Future applications and investigations

In stability analyses of slopes subjected to water flow, the position of the phreatic surface and the distribution of piezometric heads within the slope are required. Although no consideration of the stability of the gravel banks has been undertaken in this thesis, the solutions for piezometric head within the banks would be directly applicable in such considerations. Solutions for the phreatic surface and piezometric heads, from the nonlinear equations, could therefore be used in the design stage for analysing the stability of proposed rockfill structures.

The practice of allowing rockfill coffer dams to be overtopped at peak floods is being utilised to an increasing extent in modern dam constructions, as mentioned in Chapter 2. Under these conditions the analysis of the flow is quite complex because of the different factors governing the flow through, and over, the rockfill. If a finite element approach were devised for analysing the part of the flow over the rockfill, then by combining this

with the finite element solution for nonlinear flow within the rockfill, an overall solution for the problem would be possible as mentioned by Fenton (1968). This would represent a significant improvement in the analysis of the overtopping flow situation.

The existence of nonlinear flow in the area adjacent to a pumping well can be adequately accounted for, by invoking a nonlinear Forchheimer head loss relation with appropriate coefficients, in the solution. Permeameter tests on a sample of sand taken from the Burdekin River area (North Queensland) have shown that nonlinear effects can be expected at high pumping rates in actual aquifer materials but the significance of these effects depends on the type of material, its mean particle diameter, grading, etc. and will decrease with decreasing mean particle diameter. However, even in fine grained aquifers, the incorporation of a gravel bed in the area adjacent to a recharge or discharge well, may be necessary to ensure maximum efficiency. The flow through the gravel bed will follow a nonlinear head loss relation so that an appraisal of the development of the aquifer system will necessitate allowance for the nonlinear effects and this can be achieved in a manner similar to that presented in Chapter 6.

Both the finite element and finite difference methods can be extended to account for nonhomogeneous media provided all the relevant coefficients in the head loss equations are known. However, unless the boundaries separating the strata are parallel to the grid lines of the finite difference network, the finite element method will be better suited to these conditions as discussed in section 8.2.

The availability of numerical methods of solution for nonlinear flow through porous materials enables a thorough investigation of flow conditions to be made in the preliminary or design stage of a project. There is the advantage that the consequences of changes in variables can often be more easily studied than in model tests and, provided the coefficients in the head loss relations can be obtained for the prototype material, the need for scaling of results is eliminated. Flow patterns can be ascertained from the calculated values of piezometric head within the flow and discharges can be estimated for varying boundary conditions of the flow.

ACKNOWLEDGEMENTS

The work described in this thesis was carried out in the Engineering Department of the University College of Townsville while the author was supported by a grant from the Water Research Foundation of Australia.

The author records his appreciation to Professor D.H. Trollope, Head of the Department of Civil Engineering at the College, for his general supervision of, and encouragement in, the work and for his constructive criticisms of the thesis. Appreciation is also expressed to Mr K.P. Stark, Senior Lecturer in Engineering, for detailed supervision of the project, for assistance with many valuable discussions and suggestions and for his helpful comments in the final preparation of the thesis.

The work of Mr R. James, Senior Laboratory Assistant, of the hydraulic laboratory staff is gratefully acknowledged in connection with the experimental work; his assistance with many aspects of the construction of the apparatus proved invaluable. Mr W.A. Tapiolas, Research Student, assisted with some experimental measurements and with suggestions for construction of the circular tank while Mr P. Byrnes, formerly of the laboratory staff also helped with some of the experimental readings.

The contributions of Mr B.S. Best, Lecturer in Engineering, and Mr F.J. Kapitzke, Research Student, are acknowledged for helpful discussions on the finite element method in stress analysis. The staff of the computer centre, and in particular Mr I.M. Hunter, assisted with the computer work. The photographic work was performed by the Photography Section at the College.

The interest of the author's parents throughout his years of study has been appreciated. And finally the author would express his sincere thanks to his wife, Merlyn, who typed the thesis, assisted in the preparation of diagrams and helped in the final compilation of the thesis; and especially for her continued patience, understanding and encouragement throughout the entire project.

BIBLIOGRAPHY

ADZUMI, H. (1939). The flow of gases through metallic capillaries at low pressures. Bull.Chem.Soc.Japan, 14:343-347.

ANANDAKRISHNAN, M. and VARADARAJULU, G.H. (1963). Laminar and turbulent flow of water through sand. J. Soil Mech. Fdns.Div. ASCE, 89,SM5:1-15.

ANANYAN, A.K. (1965). Fluid flow in bends of conduits. Israel Program for Scientific Translations, Jerusalem.

ARAVIN, V.I. and NUMEROV, S.N. (1965). Theory of fluid flow in undeformable porous media. Israel Program for Scientific Translations, Jerusalem, p.35.

BABBITT, H.E. and CALDWELL, D.H. (1948). The free surface around, and interference between, gravity wells. Bull. Series No.374. Engng Exp. Station, University of Illinois.

BAKHMETEFF, B.A. and FEODOROFF, N.V. (1937). Flow through granular media. J. App. Mech., 4A:97-104.

BARENBLATT, G.I., ZHELTOV, In.P. and KOCHINA, I.N. (1960). Basic concepts in the theory of seepage of homogeneous liquids in fissured rocks (strata). J.App.Math. and Mech., 24, 5:1286-1303.

BONDARENKO, N. and NERPIN, S. (1965). Rheological properties of water in porous media. R.I.L.E.M. Bull., 29:13-16.

BORELI, M. (1953). Discussion on McNown, J.S., Hsu, E.Y. and Yih, C.S., Application of the relaxation technique in fluid mechanics, Proc. ASCE, 223:396-3 - 396-9.

BORELLI, M. (1955). Free-surface flow toward partially penetrating wells. Trans. Amer. Geophys.Union, 36:664-672.

BOULTON, N.S. (1951). The flow pattern near a gravity well in a uniform water-bearing medium. Proc. Instn. of Civ. Engrs., 36:534-550.

BROOKER, D.B. (1961). Pressure patterns in grain-drying systems established by numerical methods. Trans. A.S.A.E., 4:72-74.

CASAGRANDE, A. (1949). Soil mechanics in the design and construction of the Logan airport. J. Boston Soc. Civ. Engrs., 36:192-221.

CASSIDY, J.J. (1965). Irrotational flow over spillways of finite height. J. Eng. Mech. Div. ASCE, 91,EM6: 155-174.

CHAUVETEAU, G. and THIRRIOT, Cl. (1967). Régimes d'écoulement en milieu poreux et limite de la loi de Darcy. La Houille Blanche, 2:141-147.

CHILDS, E.C. and COLLIS-GEORGE, N. (1950). The permeability of porous materials. Proc. R. Soc., 201A:392-405.

CHILTON, T.H. and COLBURN, A.P. (1931). Pressure drop in packed tubes. J. of Ind. and Eng. Chem., 23: 913-919.

COURANT, R. and HILBERT, D. (1953). Methods of Mathematical Physics, Vol.1, Interscience Publishers Inc., New York.

CURTIS, R.P. (1965). Flow over and through rockfill banks. Dept. Rep. No.DR8, Civil Engng. Dept., University of Melbourne.

CURTIS, R.P. and LAWSON, J.D. (1967). Flow over and through rockfill banks. J. Hydr. Div. ASCE, 93,HY5: 1-21.

DACHLER, R. (1934). Uber den stromungsvorgang bei hangquellen. Die Wasserwirtschaft, 5-6:p.7.

DALLA VALLE, J.M. (1948). Micromeritics - The Technology of Fine Particles. Pitman, New York.

DARCY, H. (1856). Les fontaines publiques de la ville de Dijon. Victor Dalmont, Paris.

De VEUBEKE, B.F. (1965). Displacement and equilibrium models in the finite element method. Chapter 9 in Stress Analysis, ed. Zienkiewicz, O.C. and Holister, G.S., John Wiley & Sons Inc.

De WIEST, R.J.M. (1965). Geohydrology. John Wiley & Sons Inc.

DUDGEON, C.R. (1964). Flow of water through coarse granular materials. M.Eng.thesis, University of New South Wales.

DUDGEON, C.R. (1966). An experimental study of the flow of water through coarse granular media. La Houille Blanche, 7:785-800.

DUDGEON, C.R. (1967). Wall effects in permeameters. J. Hydr.Div. ASCE, 93, HY4:137-148.

DUDGEON, C.R. (1968). Relationship between porosity and permeability of coarse granular materials. Proc. 3rd Aust. Conf. on Hydr. and Fluid Mech., 76-80.

DUPUIT, J. (1863). Etudes théoriques et pratiques sur le mouvement des eaux dans les canaux découverts et à travers les terrains permeables. 2nd ed., Dunod, Paris.

ENGELUND, F. (1953). On the laminar and turbulent flows of groundwater through homogeneous sand. Bull. No.4 Hydraulic Laboratories, Technical University of Denmark.

ERGUN, S. and ORNING, A A. (1949). Fluid flow through randomly packed columns and fluidised beds. J. of Ind. and Eng. Chem., 41:1179-1184.

ESCANDE, L. (1953). Experiments concerning the infiltration of water through a rock mass. Proc. Minnesota Int. Hydr. Conv.

FENTON, J.D. (1968). Hydraulic and stability analyses of rockfill dams. Dept.Rep.No.DR15. Civil Engng. Dept., University of Melbourne.

FINN, W.D.L. (1967). Finite-element analysis of seepage through dams. J.Soil Mech.Fdns.Div. ASCE, 93,SM6: 41-48.

FORCHHEIMER, P.H. (1886). Uber die ergiebigkeit von brunnen-anlagen und sickerschlitzen. Zeit.Der Arch. Ing.Ver., Hannover, 32:539-564.

FORCHHEIMER, P.H. (1901). Wasserbewegung durch Boden. Z. Ver. dt. Ing., p.1782.

FORCHHEIMER, P.H. (1930). Hydraulik, Teubner, Berlin.

FORSYTHE, G.E. and WASOW, W.R. (1960). Finite-difference methods for partial differential equations. John Wiley & Sons Inc.

FOX, J.A. and ALI, J. (1968). Unsteady unconfined flow to gravity wells. Proc. Instn. of Civ. Engrs., 40:451-469.

FRANZINI, J.B. (1968). Discussion on Dudgeon, C.R. Wall effects in permeameters, J. Hydr.Div. ASCE, 94, HY4: 1148-1150.

FROMM, J.E. (1963). A method for computing nonsteady incompressible, viscous fluid flows. LA-2910 Los Alamos Scien. Lab. Report.

GHEORGHITZA, St. I. (1964). On the nonsteady motion of visco-plastic liquids in porous media. J. of Fluid Mech., 20, Pt.2.

GIESE, J.H. (1958). On the truncation error in a numerical solution of the Neumann problem for a rectangle. J. Math.Phys., 37:169-177.

GIUDICI, S. (1967). Discussion on Parkin, A.K., Trollope, D.H. and Lawson, J.D., Rockfill structures subject to water flow. J. Soil Mech.Fdns.Div. ASCE, 93, SM5: 329-336.

GLOVER, R.E. (1964). Ground-water movement. Engng.Monog. No.31, United States Dept. of the Interior.

GOLDSTEIN, S. (1938). Modern developments in fluid dynamics. Vol.II, Oxford Clarendon Press.

GRCIC, J.A. (1961). Model test of steady flow toward a well. Proc. I.A.H.R. 9th Convention: 591-600.

HALL, H.P. (1954). A historical review of investigations of seepage toward wells. J. Boston Soc.Civ.Engrs., 41:251-311.

HALL, H.P. (1955). An investigation of steady flow toward a gravity well. La Houille Blanche, 10:8-35.

HANSEN, V.E. (1953). Unconfined ground-water flow to multiple wells. Trans. ASCE, 118:1098-1115.

HANTUSH, M.S. (1961). Drawdown around a partially penetrating well. J. Hydr.Div. ASCE, 87, HY4:83-98.

HANTUSH, M.S. (1962a). Hydraulics of gravity wells in sloping sands. J. Hydr.Div. ASCE, 88, HY4:1-15.

HANTUSH, M.S. (1962b). On the validity of the Dupuit-Forchheimer well discharge formula. J. Geophys.Res., 67:2417-2420.

HARLOW, F.H. and WELCH, J.E. (1965). Numerical calculation of time-dependent viscous incompressible flow of fluid with free surface. The Physics of Fluids, 8:2181-2189.

HARR, M.E. (1962). Groundwater and seepage. McGraw-Hill Book Co. Inc., New York.

HAZEN, A. (1893). Some physical properties of sands and gravels with special reference to their use in filtration. 24th Annual Rep., Mass. State Board of Health. Pub. Document 34:539-556.

HENDRICK, K.R. (1965). Membrane analogy as applied to well hydraulics. Dept. Rep. No.DR7, Civil Engng. Dept., University of Melbourne.

HINZE, J.O. (1959). Turbulence. McGraw-Hill Book Co.Inc.

HOW LUM, C. (1966). An investigation into porous media flow. B.E. thesis, University College of Townsville.

HUARD de la MARRE, M.P. (1956). Expressions exactes des debits d' infiltration dans des barrages tridimensionnels a parois verticales. Academic des Sciences Comptes Rendus, 242:1125-1127.

HUBBERT, M.K. (1940). The theory of groundwater motion. J. Geol., 48:785-944.

HUBBERT, M.K. (1956). Darcy's Law and the field equations of the flow of underground fluids. J. Petrol.Tech., 8:222-239.

IRMAY, S. (1958). On the theoretical derivation of Darcy and Forchheimer formulas. Trans.Amer.Geophys.Union, 39:702-707.

JEPPSON, R.W. (1966). Techniques for solving free-streamline, cavity, jet and seepage problems by finite differences. Ph.D. dissertation, Stanford University.

JEPPSON, R.W. (1968a). Seepage from ditches - solution by finite differences. J. Hydr.Div. ASCE, 94, HY1:259-283.

JEPPSON, R.W. (1968b). Seepage through dams in the complex potential plane. J.Irrig. and Drain.Div. ASCE, 94, IR1:23-39.

JOHNSON, Edward E. Inc. (1966). Groundwater and wells: a reference book for the well industry. St.Paul Minnesota, Edward E. Johnson.

JOLLS, K.R. and HANRATTY, T.J. (1966). Transition to turbulence for flow through a dumped bed of spheres. J.Chem.Eng.Sc., 21:1185-1190.

JONES, K.R. (1962). On the differential form of Darcy's Law. J.Geophys.Res., 67:731-732.

KING, F.H. (1899). Principles and conditions of the movements of ground water. U.S.Geol.Survey, 19th Annual Rep., Part II:59-294.

KIRKHAM, D. (1959). Exact theory of flow into a partially penetrating well. J.Geophys.Res., 64:1317-1327.

KIRKHAM, C.E. (1967). Turbulent flow in porous media. Dept.Rep.No.DR11. Civil Engng.Dept., University of Melbourne.

KOZENY, J. (1927). Uber kapillare bitung des wassers in Boden. S.-Ber. Akad.Wiss.Wien, 136A:271-306.

KRISTIANOVICH, S.A. (1940). Movement of groundwaters violating Darcy's Law. J.Appl.Math. and Mech., 4: 33-52.

LAMB, H. (1932). Hydrodynamics. University Press, Cambridge.

LANCZOS, C. (1962). The variational principles of mechanics. Univ. of Toronto Press, Canada.

LANE, R.G.T. (1967). Temporary dam construction under water and overtopped by floods. Trans. Ninth Int. Cong. on Large Dams, 4:59-83.

LAWSON, J.D., TROLLOPE, D.H. and PARKIN, A.K. (1962). Some hydraulic aspects of unconventional rockfill dams. Proc., 1st Aust.Conf. on Hydr. and Fluid Mech., :159-172.

LAWSON, J.D. and HENDRICK, K.R. (1965). Membrane analogy as applied to well hydraulics. Proc., 2nd Aust.Conf. on Hydr. and Fluid Mech., :A231-A250.

LEWIS, J.G. (1955). Shear strength of rockfill. New Zealand Eng., Nov.15:388-389.

LIEBMANN, H. (1918). Die angenäherte ermittlung harmonischer functionen und konformer abbildung (nach Ideen von Boltzmann und Jacobi), Sitzungsberichte der Bayer. Akad.Wiss., Math.-Phys.Kl., 47:385-416.

LINDQUIST, E. (1933). On the flow of water through porous soil. Rep.First Cong. on Large Dams, 5:81-101.

LUTHIN, J.N. and SCOTT, V.H. (1952). Numerical analysis of flow through aquifers toward wells. Agric. Engng., 33:279-282.

MACAWARIS, A.G. (1966). Effect of rivers and impermeable barriers on flow to wells. M.Eng. thesis, SEATO Graduate School of Engineering, Bankok.

MARKLAND, E. (1965). Calculation of flow at a free overfall by relaxation method. Proc.Instn. of Civ.Engrs., 31:71-78.

MARTIN, J.J. (1948). Pressure drop through columns of balls. D.Sc. thesis, Carnegie Institute of Technology.

MENCL, V., BOBKOVA, J. and HANZLOVA, V. (1965). Flow of water in soils at small hydraulic gradients. R.I.L.E.M. Bull., 29:45-46.

MISSBACH, A. (1937). Listy Cukrova, 55:p.293.

MOGG, J.L. (1959). Effect of aquifer turbulence on well drawdown. J.Hydr.Div. ASCE, 85, HY11:99-112.

MOHAR, S.M. (1965). Turbulent flow through porous media. M.Eng. thesis, SEATO Graduate School of Engineering, Bankok.

MORCOM, A.R. (1946). Fluid flow through granular materials. Trans. Instn. of Chem.Engrs., 24:30-43.

MOTT, R.A. (1951). The laws of motion of particles in fluids and their application to the resistance of beds of solids to the passage of fluid. Some Aspects of Fluid Flow, Edward Arnold and Co., London, pp.242-256.

MURRAY, J.A. (1960). Relaxation methods applied to seepage flow problems in earth dams and drainage wells. J. Instn.Engrs., India, 41:149-161.

MUSKAT, M. (1946). The flow of homogeneous fluids through porous media. J.W. Edwards Inc., Ann Arbor, Michigan.

OLIVIER, H. (1967). Through and overflow rockfill dams - new design techniques. Proc.Instn. of Civ.Engrs., 36:433-471.

PARKIN, A.K. (1963a). Rockfill dams with inbuilt spillways, Part 1 - hydraulic characteristics. Bull.No.6, Water Research Foundation of Australia.

PARKIN, A.K. (1963b). Rockfill dams with inbuilt spillways, Part 2 - stability characteristics. Bull.No.7, Water Research Foundation of Australia.

PARKIN, A.K., TROLLOPE, D.H. and LAWSON, J.D. (1966). Rockfill structures subject to water flow. J. Soil Mech.Fdns.Div. ASCE, 92, SM6:135-151.

PARS, L.A. (1962). An introduction to the calculus of variations. Heinemann, London.

PETER, Y. (1955). Model tests of groundwater flow into a tubular well. Civ.Eng. and Pub.Works Rev., 50:1227-1229.

PHILIP, J.R. (1958). Physics of water movement in porous solids. Highway Research Board, Washington, Special Report, 40:147-163.

POLUBARINOVA-KOCHINA, P.Ya. (1962). Theory of the motion of ground water. Translated by J.M. De Wiest, Princeton Univ. Press, Princeton, N.J.

PRICKETT, T.A. (1967). Designing pumped well characteristics into electric analog models. Ground Water, 5, No.4: 10pp.

ROSE, H.E. (1951). Fluid flow through beds of granular material. Some Aspects of Fluid Flow, Edward Arnold & Co., London, pp.136-163.

ROSE, H.E. and RIZK, A.M.A. (1949). Further researches in fluid flow through beds of granular material. Proc. Instn.Mech.Eng., 160:493-503.

RUMER, R.R. and DRINKER, P.A. (1966). Resistance to laminar flow through porous media. J.Hydr.Div. ASCE, 92, HY5:155-163.

RUSSELL, D.B. (1963). On obtaining solutions to the Navier-Stokes equations with automatic digital computers. A.R.C. R. & M., H.M.S.O., London.

SANDIE, R.B. (1961). A laboratory investigation of self spillway rockfill dams. M.Eng.Sc. thesis, University of Melbourne.

SCHEIDEGGER, A.E. (1960a). Flow through porous media. Appl.Mech.Reviews, 13:313-318.

SCHEIDEGGER, A.E. (1960b). The physics of flow through porous media. The Macmillan Co., New York.

SCHNEEBELI, G. (1953). Sur la théorie des écoulements de filtration. La Houille Blanche, Special A: 136-192.

SCHNEEBELI, G. (1955). Expériences sur la limite de validité de la loi de Darcy et l'apparition de la turbulence dans un écoulement de filtration. La Houille Blanche, 2:141-149.

SHARP, B.B. (1961). Flow in a rockfill dam with in-built spillway. Civ.Eng. and Pub. Works Rev., 56:1589-1590.

SHAW, F.S. and SOUTHWELL, R.V. (1941). Relaxation methods applied to engineering problems; VII Problems relating to the percolation of fluids through porous materials. Proc. R.Soc., Series A, 178:1-17.

SLEPICKA, F. (1961). The laws of filtration and limits of their validity. Proc. I.A.H.R. 9th Convention: 383-394.

SLICHTER, C.S. (1897). Theoretical investigation of the motion of groundwaters. 19th Annual Report, U.S. Geol. Survey, Part 2, p.329.

SNOW, D.T. (1965). A parallel plate model of fractured permeable media. Ph.D. thesis, University of California.

SOUTHWELL, R.V. (1940). Relaxation methods in engineering science. Oxford Univ. Press, London.

SOUTHWELL, R.V. (1946). Relaxation methods in theoretical physics. Oxford Univ. Press, London.

SPARKS, A.D.W. (1967). The sloughing, overtopping and reinforcement of rockfill and earth dams. Trans. Ninth Int.Cong. on Large Dams, 4:327-349.

SPEEDIE, M.G., TADGELL, J.F. and CARR, S.R. (1967). Use of hydraulic models in planning flood diversion through rockfill. Trans. Ninth Int.Cong. on Large Dams, 4: 471-484.

STARK, K.P. (1968). Some aspects of the nonlinear laminar regime of flow in porous media. Ph.D. thesis, University of Queensland.

STARK, K.P. (1969). A numerical study of the nonlinear laminar regime of flow in an idealised porous medium. Proc. I.A.H.R. Haifa, Israel.

STARK, K.P. and VOLKER, R.E. (1967). Nonlinear flow through porous materials - some theoretical aspects. Res. Bull. No.1, Department of Engineering, University College of Townsville.

SUNADA, D.K. (1965). Laminar and turbulent flow of water through homogeneous porous media. Ph.D. dissertation, University of California.

TAMADA, K. and FUJIKAWA, H. (1957). The steady two-dimensional flow of viscous fluid at low Reynolds numbers passing through an infinite row of equal parallel circular cylinders. Quart.Jour.Mech.Appl. Math. 10:425-432.

TAPIOLAS, W.A. (1967). A study of steady flow through an artesian aquifer. B.E. thesis, University College of Townsville.

TAYLOR, R.L. and BROWN, C.B. (1967). Darcy flow solutions with a free surface. J.Hydr.Div. ASCE, 93, HY2:25-33.

TEK, M.R. (1957). Development of a generalised Darcy equation. Trans.Amer.Inst.Min.Met.Engrs., 210:376-378.

THEIS, C.V. (1935). The relation between the lowering of the piezometric surface and the rate and duration of discharge of a well using groundwater storage. Trans. Amer.Geophys.Union, 16:519-524.

THIEM, G. (1906). Hydrologische Methoden, Gebhardt, Leipzig, 1906.

THOM, A. (1928a). The boundary layer of the front portion of a cylinder. A.R.C., R & M 1176, H.M.S.O., London.

THOM, A. (1928b). An investigation of fluid flow in two dimensions. A.R.C., R & M 1194, H.M.S.O., London.

THOM, A. and APELT, C.J. (1961). Field computations in engineering and physics. D. van Nostrand Co.Ltd., London.

TROLLOPE, D.H. (1957). The systematic arching theory applied to the stability analysis of embankments. Proc. 4th Int.Conf.Soil Mech. and Fndn.Engg., 2:382.

VAN DER TUIN, H. (1960). La permeabilitié et les applications practiques des materiaux gros. Compte Rendu des Sixièmes Journées de L'Hydraulique, Société Hydrotechnique de France, 1:17-23.

WARD, J.C. (1964). Turbulent flow in porous media. J.Hydr. Div. ASCE, 90, HY5:1-13.

WATSON, K.K. (1963). The permeability of an idealised two-dimensional porous medium using the Navier-Stokes equations. Proc. 4th Aust. N.Z. Conf. on Soil Mech. and Found.Eng. :37-40.

WEISS, A. (1951). Construction technique of passing floods over earth dams. Trans. ASCE, 116:1158-1173.

WHITE, A.M. (1935). Pressure drop and loading velocities in packed towers. Chem.Eng.Prog., 31:390-408.

WILKINS, J.K. (1956). The flow of water through rockfill and its application to the design of dams. Proc. 2nd Aust. N.Z. Conf. on Soil Mech. and Found.Eng. : 141-147.

WILKINS, J.K. (1963). The stability of overtopped rockfill dams. Proc. 4th Aust. N.Z. Conf. on Soil Mech. and Found.Eng.:1-7.

WITTKE, W. and LOUIS, C. (1966). Zur berechnung des einflusses der bergwasserstromung auf die standsicherheit von boschungen und bauwerken in zerkluftetem fels. Proc. First Int.Cong. Rock Mech., Lisbon, 2:201-206.

WRIGHT, D.E. (1968). Nonlinear flow through granular media. J. Hydr.Div. ASCE, 94, HY4:851-872.

WYCKOFF, R.D., BOTSET, H.G. and MUSKAT, M. (1932). Flow of liquids through porous media under the action of gravity. J. App. Physics, 3:90-113.

YANG, S.T. (1949). Seepage toward a well analysed by the relaxation method. Ph.D. dissertation, Harvard University.

YOUNG, D. (1954). Iterative methods for solving partial difference equations of elliptic type. Trans.Amer. Math.Soc., 76:92-111.

YOUNGS, E.G. (1965). Horizontal seepage through unconfined aquifers with hydraulic conductivity varying with depth. J. of Hydrology, 8:283-296.

YOUNGS, E.G. (1966). Horizontal seepage through unconfined aquifers with non-uniform hydraulic conductivity. J. of Hydrology, 4:91-97.

ZABRODSKY, S.S. (1966). Hydrodynamics and heat transfer in fluidised beds. The M.I.T. Press, Massachusetts Institute of Technology.

ZIENKIEWICZ, O.C. and CHEUNG, Y.K. (1965). Finite elements in the solution of field problems. The Engineer, Sept.: 507-510.

ZIENKIEWICZ, O.C., MAYER, P. and CHEUNG, Y.K. (1966). Solution of anisotropic seepage problems by finite elements. J. Eng.Mech.Div. ASCE, 92, EM1:111-120.

ZIENKIEWICZ, O.C. (1967). The finite element method in structural and continuum mechanics. McGraw-Hill Pub. Co. Ltd., London.

APPENDIX I

Results for Confined Flow Experiments.

Flow Nos. 1, 2 and 4.

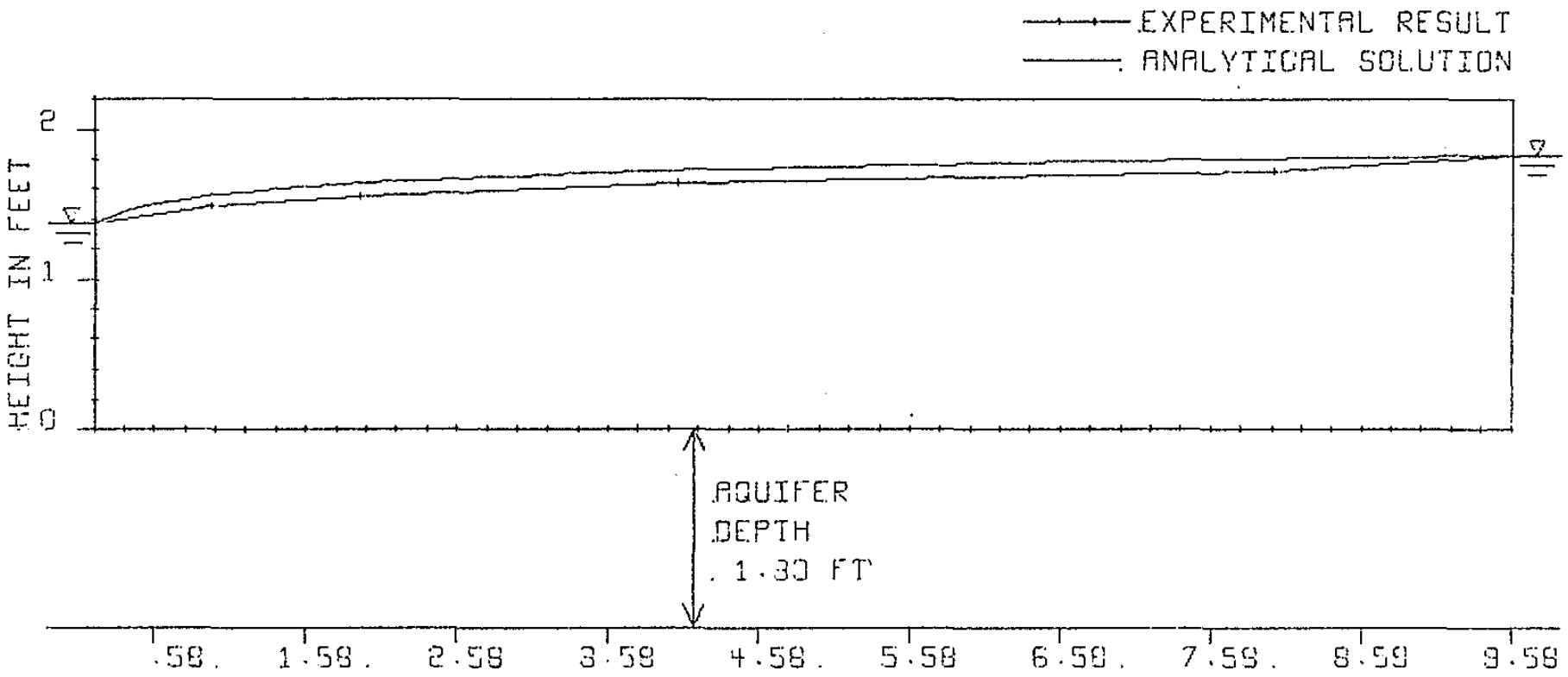

CONFINED FLOW EXPERIMENT
FLOW NO 1
RESULTS FOR DARCY FLOW

RW= .187 RE= 9.587
HW= 2.696 HE= 3.156
Q(CALC) = .177 Q(EXPER) = .177 CUSEC

FIG. A-I-1

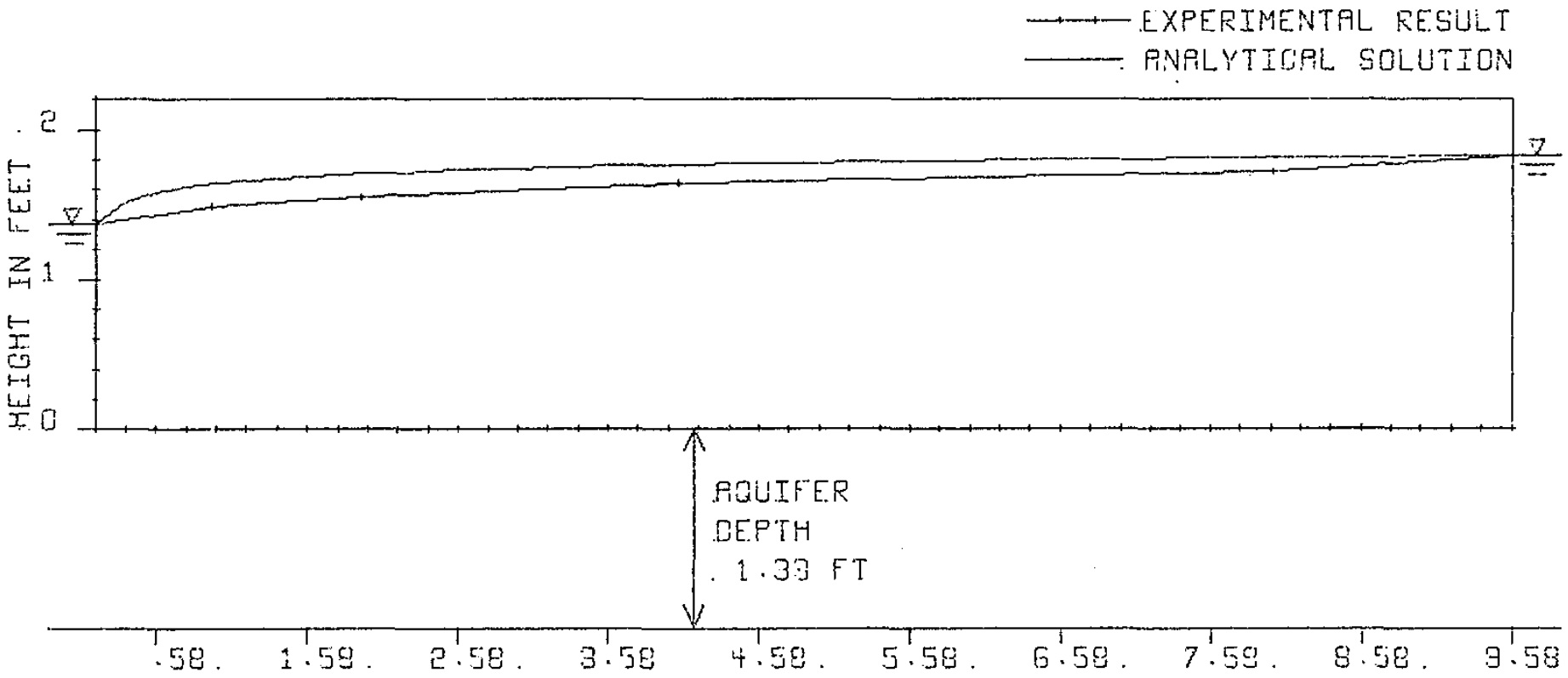
EXPERIMENTAL RESULT
ANALYTICAL SOLUTION
HEIGHT IN FEET
2
1
0
AQUIFER
DEPTH
1.33 FT
.58
1.59
2.58
3.58
4.58
5.58
6.58
7.59
8.58
9.58
RADIUS IN FEET
CONFINED FLOW EXPERIMENT
FLOW NO 1
RESULTS FOR FORCHHEIMER FLOW
RW= .187
HW= 2.696
Q(CALC) = .179
RE= 9.587
HE= 3.156
Q(EXPER) = .177 CUSEC

FIG. A-I-2

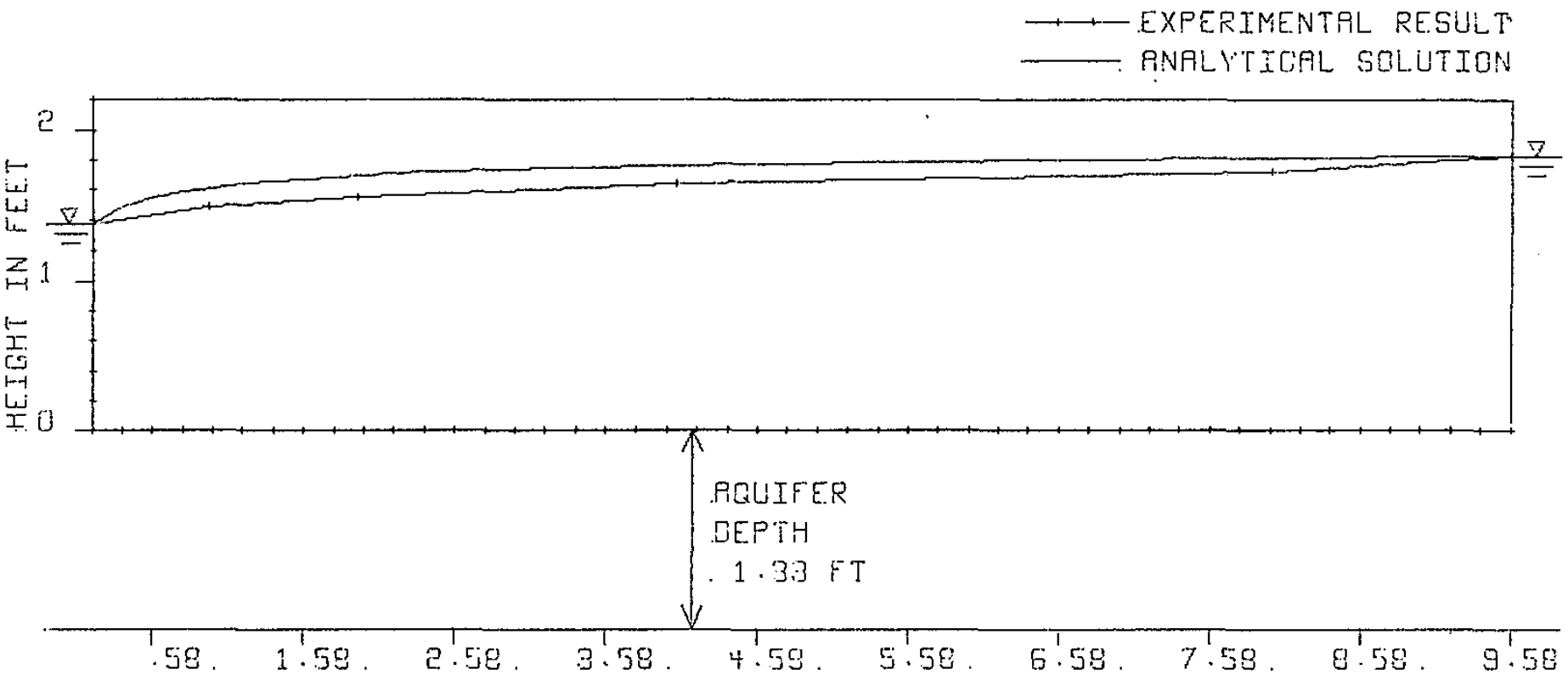

CONFINED FLOW EXPERIMENT RW= .187 RE= 9.587
FLOW NO 1 HW= 2.696 HE= 3.156
RESULTS FOR EXPONENTIAL FLOW Q(CALC) = .191 Q(EXPER) = .177 CUSEC

FIG. A-I-3

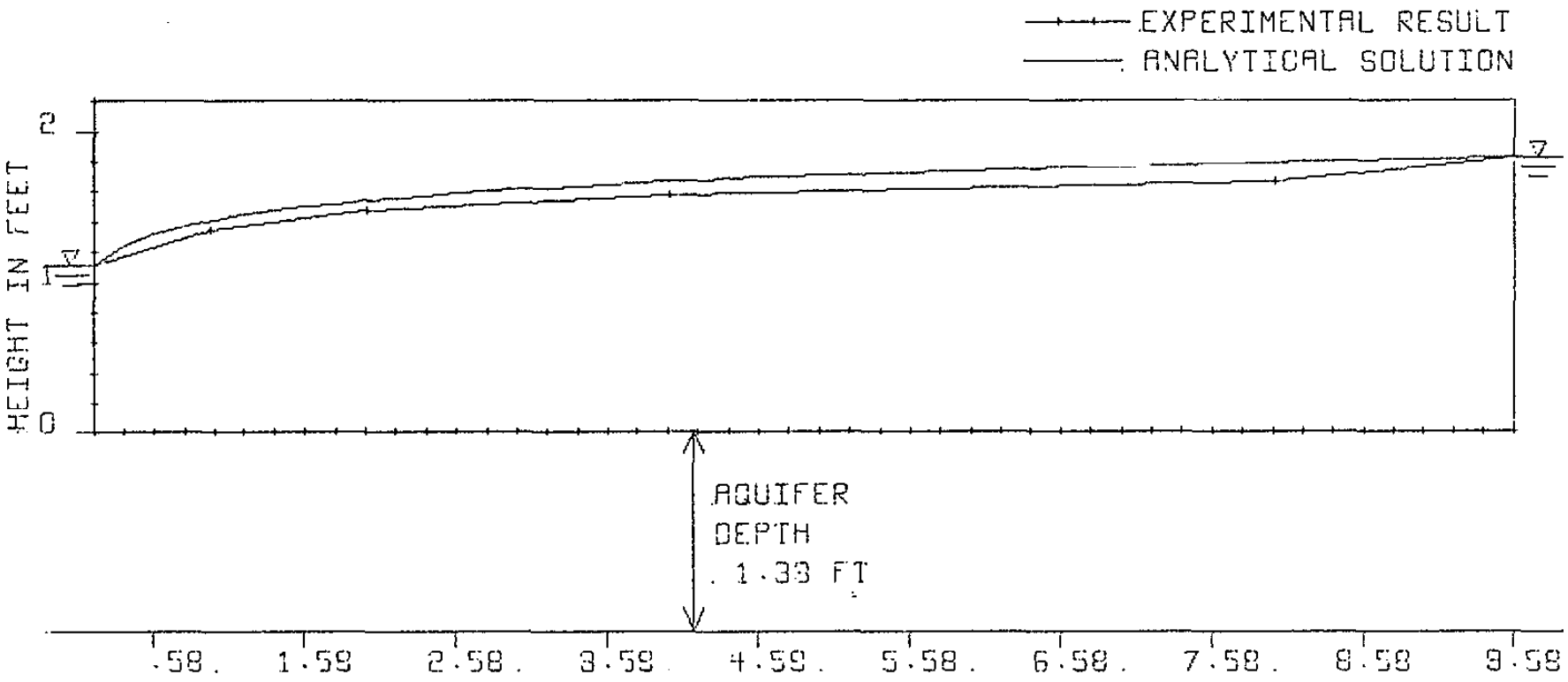

CONFINED FLOW EXPERIMENT
FLOW NO 2
RESULTS FOR DARCY FLOW

RW= .187 RE= 9.587
HW= 2.441 HE= 3.154
Q(CALC) = .274 Q(EXPER) = .240 CUSEC

FIG. A-I-4

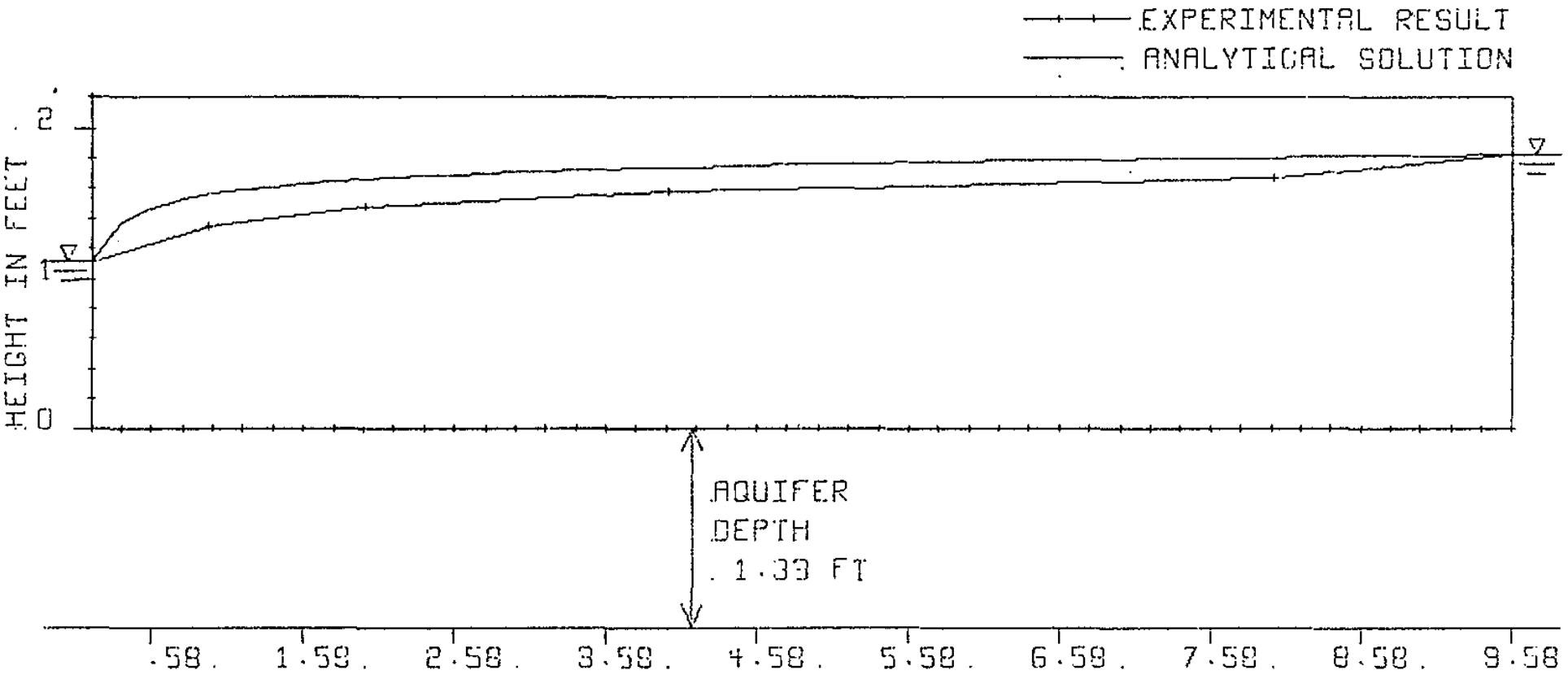

CONFINED FLOW EXPERIMENT
. FLOW NO 2
RESULTS FOR FORCHHEIMER FLOW

. RW= .187 RE= 9.587
. HW= 2.441. HE= 3.154
Q(CALC) = .241 Q(EXPER) = .240 CUSEC

FIG. A-I-5

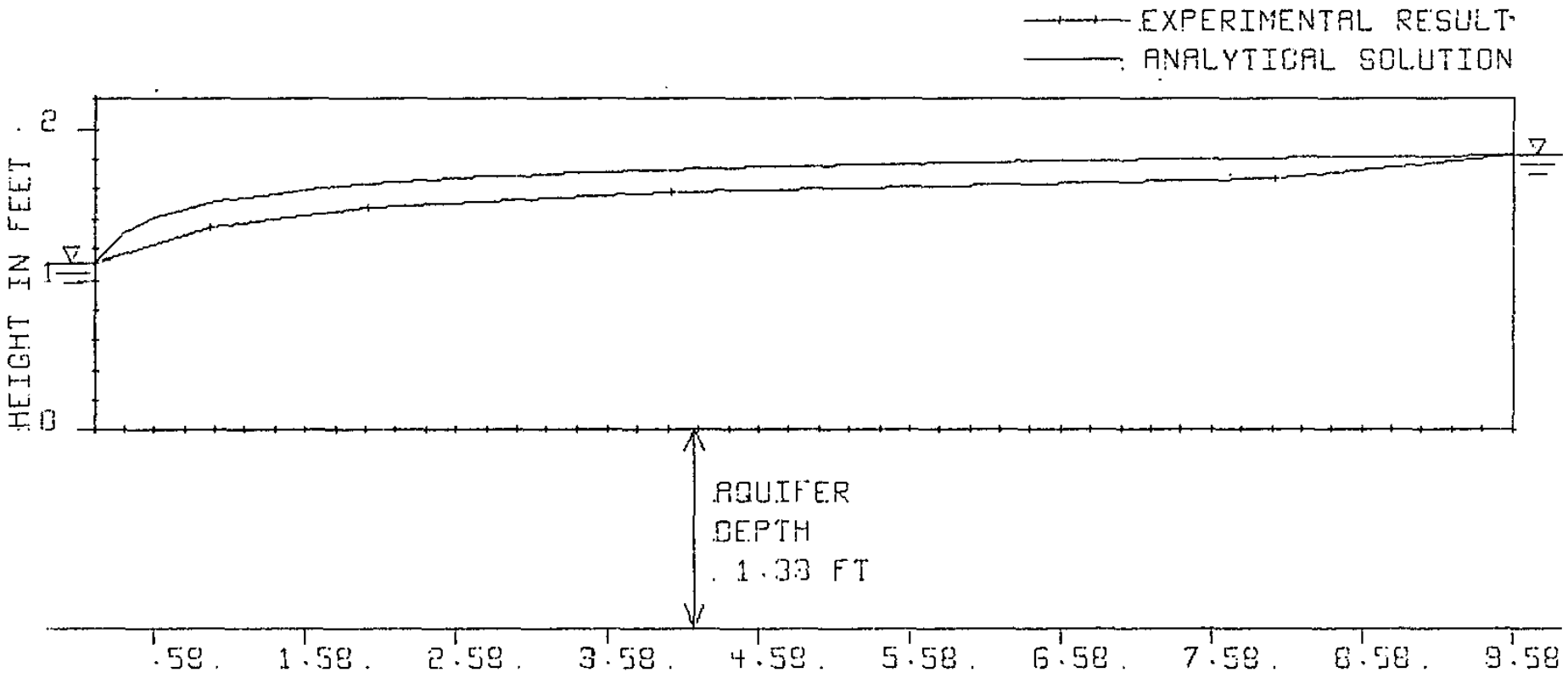

CONFINED FLOW EXPERIMENT
FLOW NO 2
RESULTS FOR EXPONENTIAL FLOW

RW= .187 RE= 9.587
HW= 2.441 HE= 3.154
Q(CALC) = .268 Q(EXPER) = .240 CUSEC

FIG. A-I-6

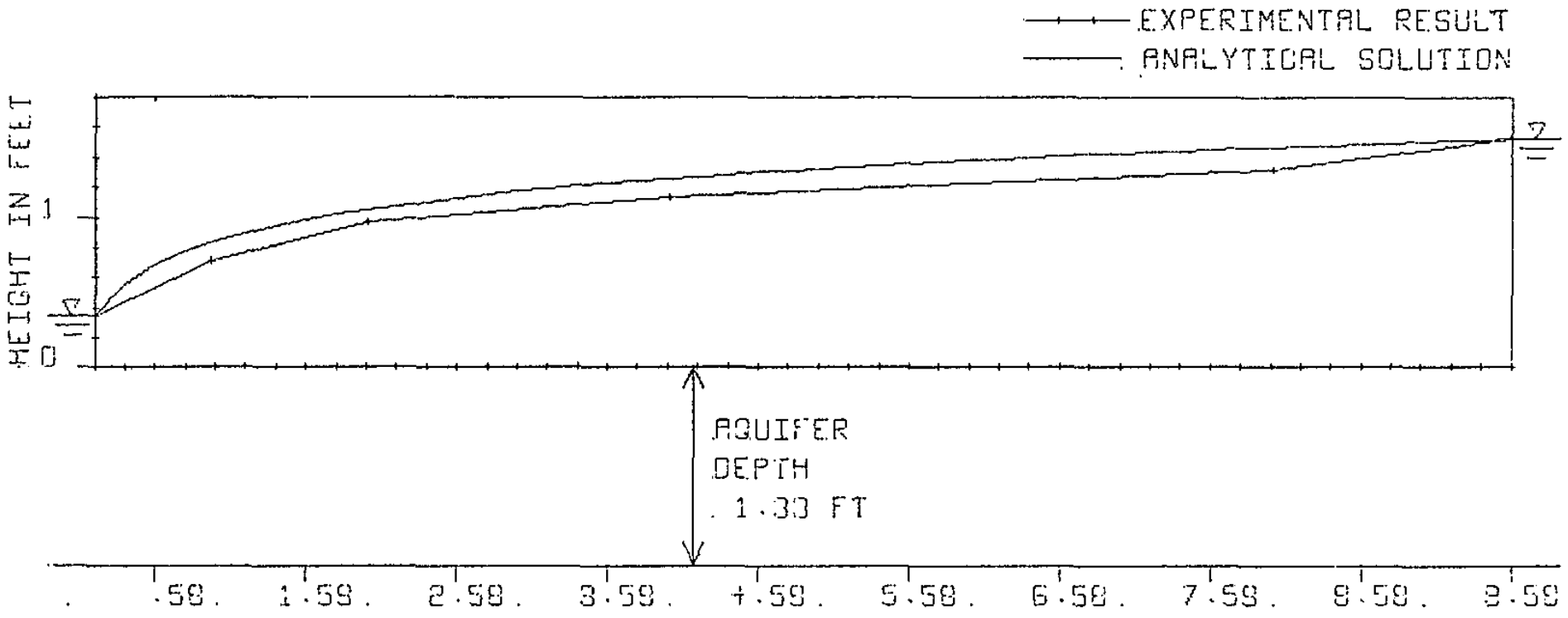

CONFINED FLOW EXPERIMENT
FLOW NO 4
RESULTS FOR DARCY FLOW

RW= .187 RE= 9.587
HW= 1.671 HE= 2.851
Q(CALC) = .454 Q(EXPER) = .370 CUSEC

FIG. A-I-7

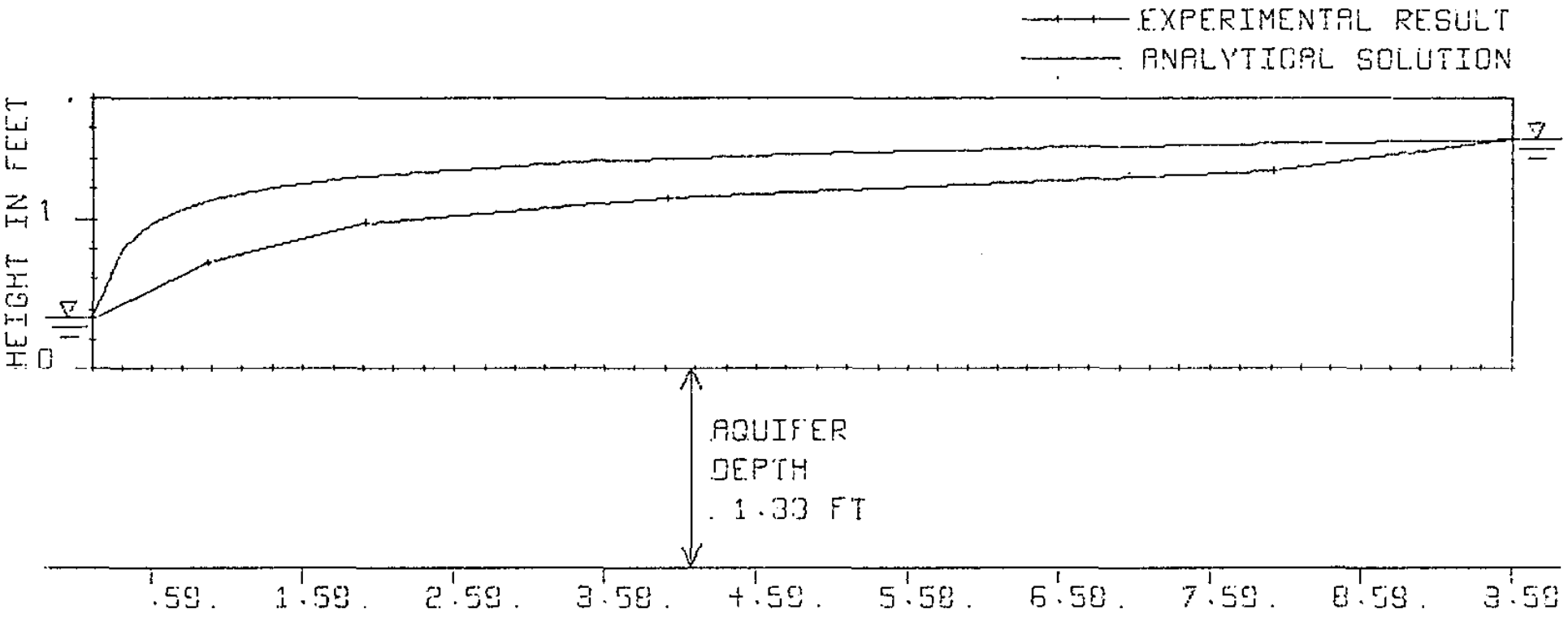
EXPERIMENTAL RESULT
ANALYTICAL SOLUTION
HEIGHT IN FEET
1
0
AQUIFER
DEPTH
1.33 FT
.59
1.59
2.59
3.58
4.59
5.58
6.58
7.59
8.59
9.59
RADIUS IN FEET
CONFINED FLOW EXPERIMENT
. FLOW NO 4
RESULTS FOR FORCHHEIMER FLOW
. RW= .187
. HW= 1.671
RE= 9.587
HE= 2.851
Q(CALC) = .333
Q(EXPER) = .370 CUSEC

FIG. A-I-8

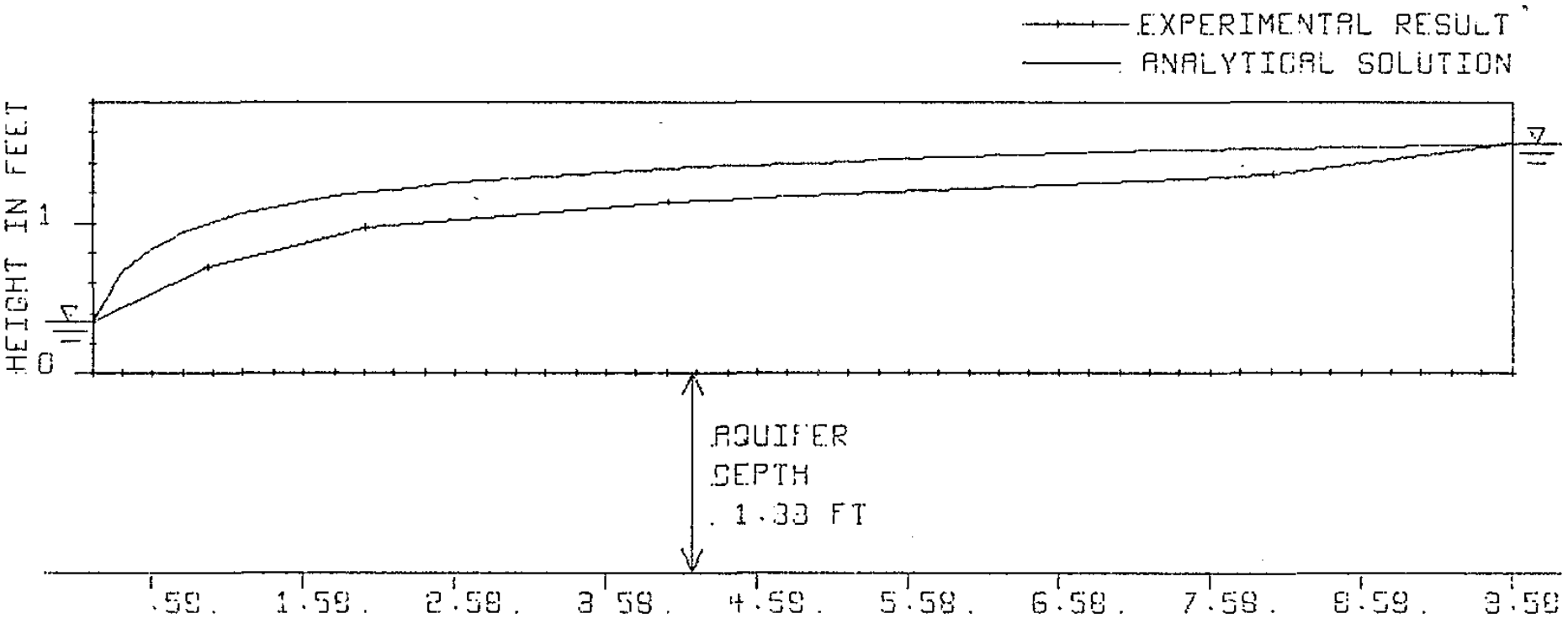

CONFINED FLOW EXPERIMENT
. FLOW NO 4
RESULTS FOR EXPONENTIAL FLOW

. RW= .187 RE= 9.587
. HW= 1.671 HE= 2.851
Q(CALC) = .398 Q(EXPER) = .370 CUSEC

FIG. A-I-9

APPENDIX II

Flow Net Results for Unconfined Axisymmetric Experiments with Complete Circle.

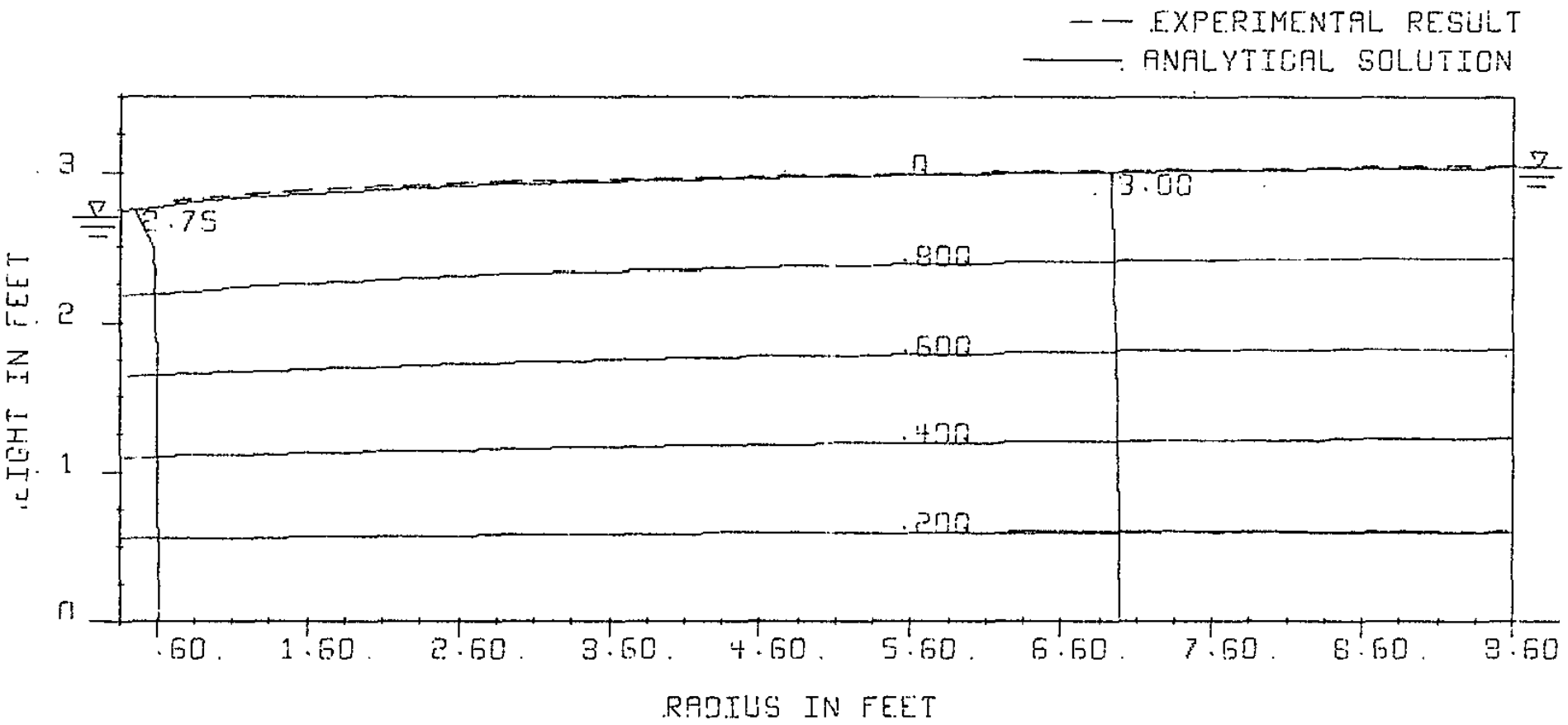

EXPERIMENT WITH COMPLETE CIRCLE . RW= .354 RE= 9.604
. FLOW NO 1 . HW= 2.693 HE= 3.030
RESULTS FOR DARCY FLOW Q(CALC) = .282 Q(EXP) = .341 CUSEC

FIG. A-II-1

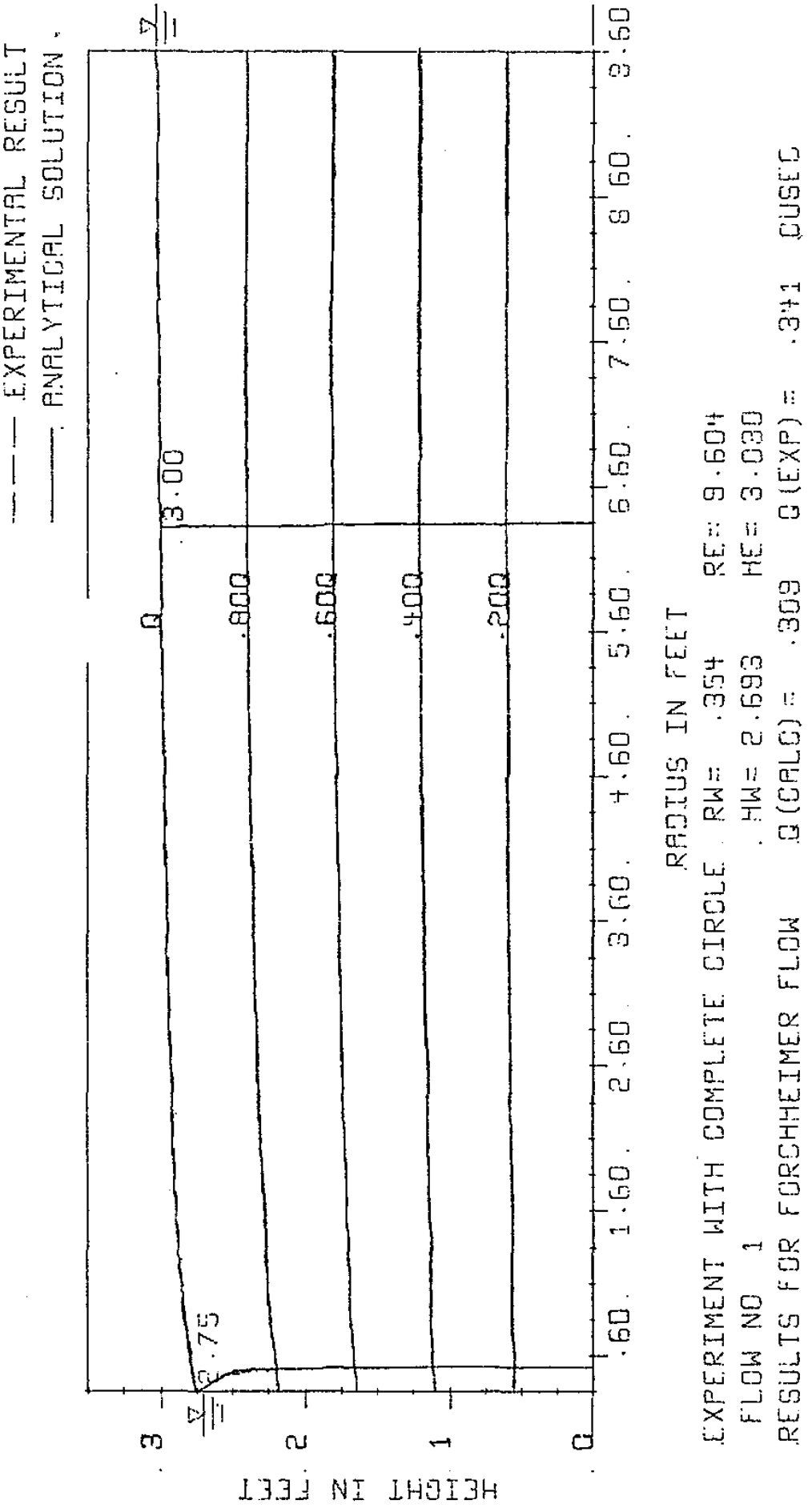
EXPERIMENTAL RESULT
ANALYTICAL SOLUTION
Z/H
3.00
Q
.800
.600
.400
.200
.75
Z/H
3
2
1
0
HEIGHT IN FEET
.60
1.60
2.60
3.60
4.60
5.60
6.60
7.60
8.60
RADIUS IN FEET
EXPERIMENT WITH COMPLETE CIRCLE RW= .354 RE= 9.604
FLOW NO 1 HW= 2.693 HE= 3.030
RESULTS FOR FORCHHEIMER FLOW Q(CALC)= .309 Q(EXP)= .341 CUSEC

FIG. A-II-2

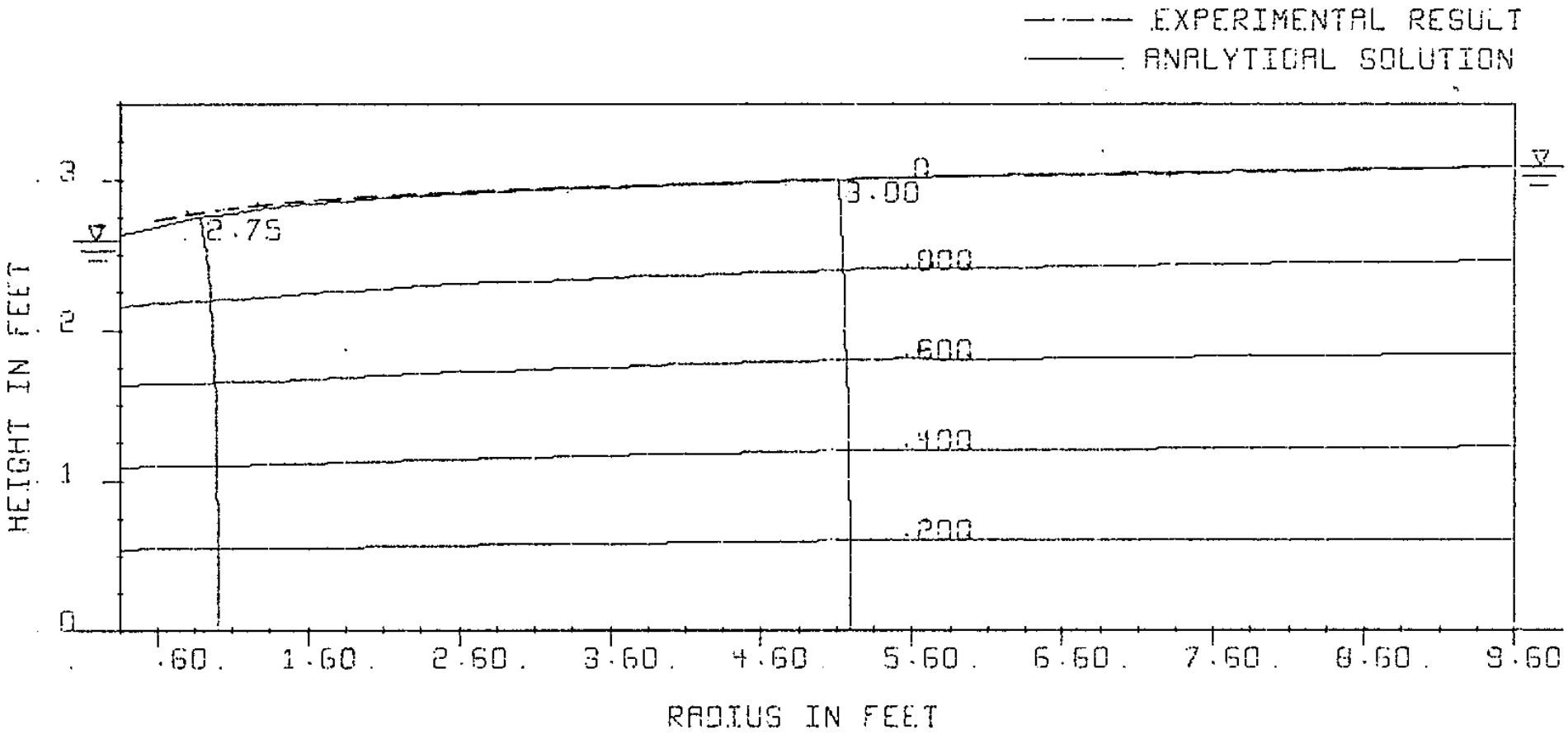

EXPERIMENT WITH COMPLETE CIRCLE RW= .354 RE= 9.604
FLOW NO 2 HW= 2.589 HE= 3.065
RESULTS FOR DARCY FLOW Q(CALC) = .414 Q(EXP) = .414 QUSED

FIG. A-II-3

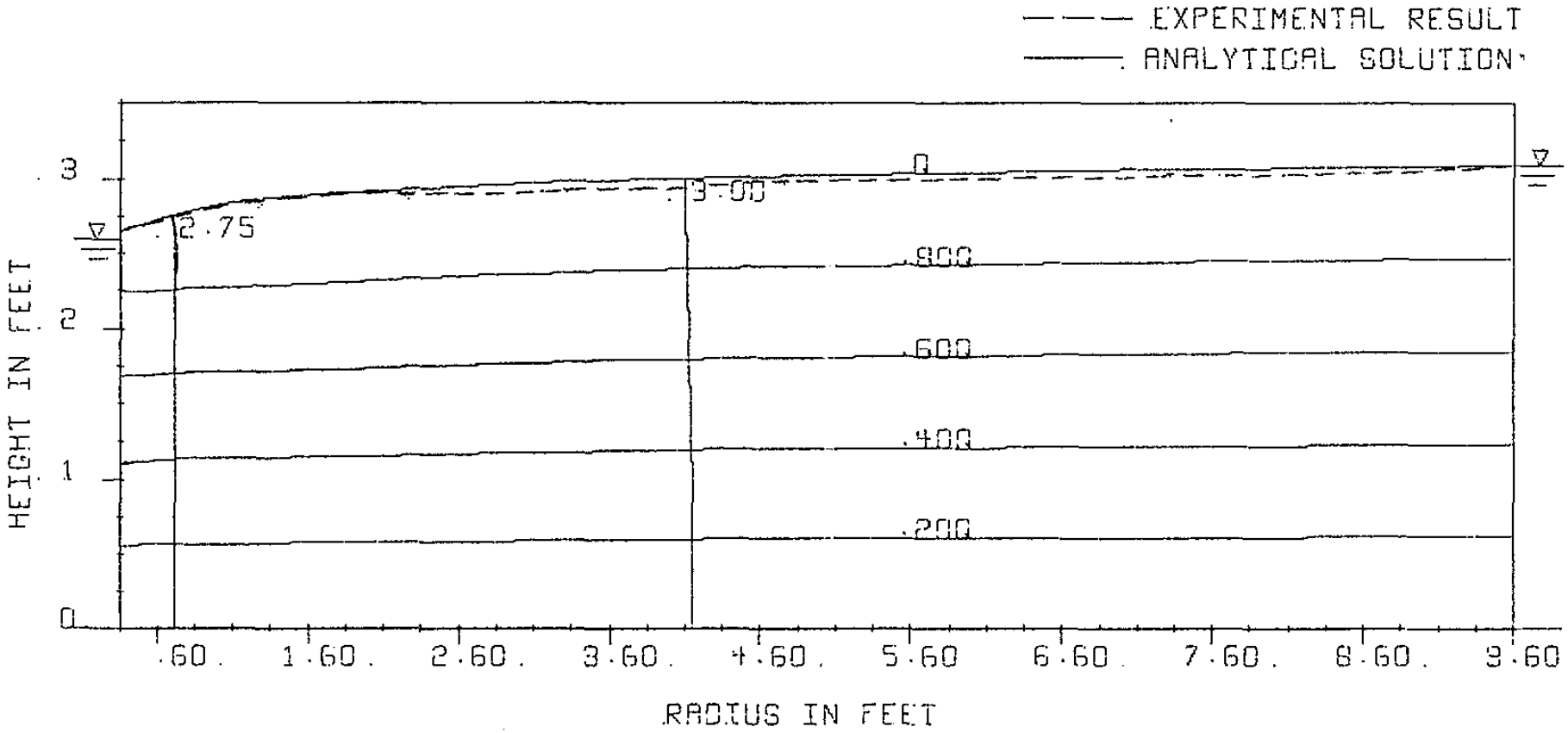

EXPERIMENT WITH COMPLETE CIRCLE . RW= .354 RE= 9.604
FLOW NO 2 . HW= 2.583 HE= 3.085
RESULTS FOR FORCHHEIMER FLOW Q(CALC)= .417 Q(EXP)= .414 CUSEC

FIG. A-II-4

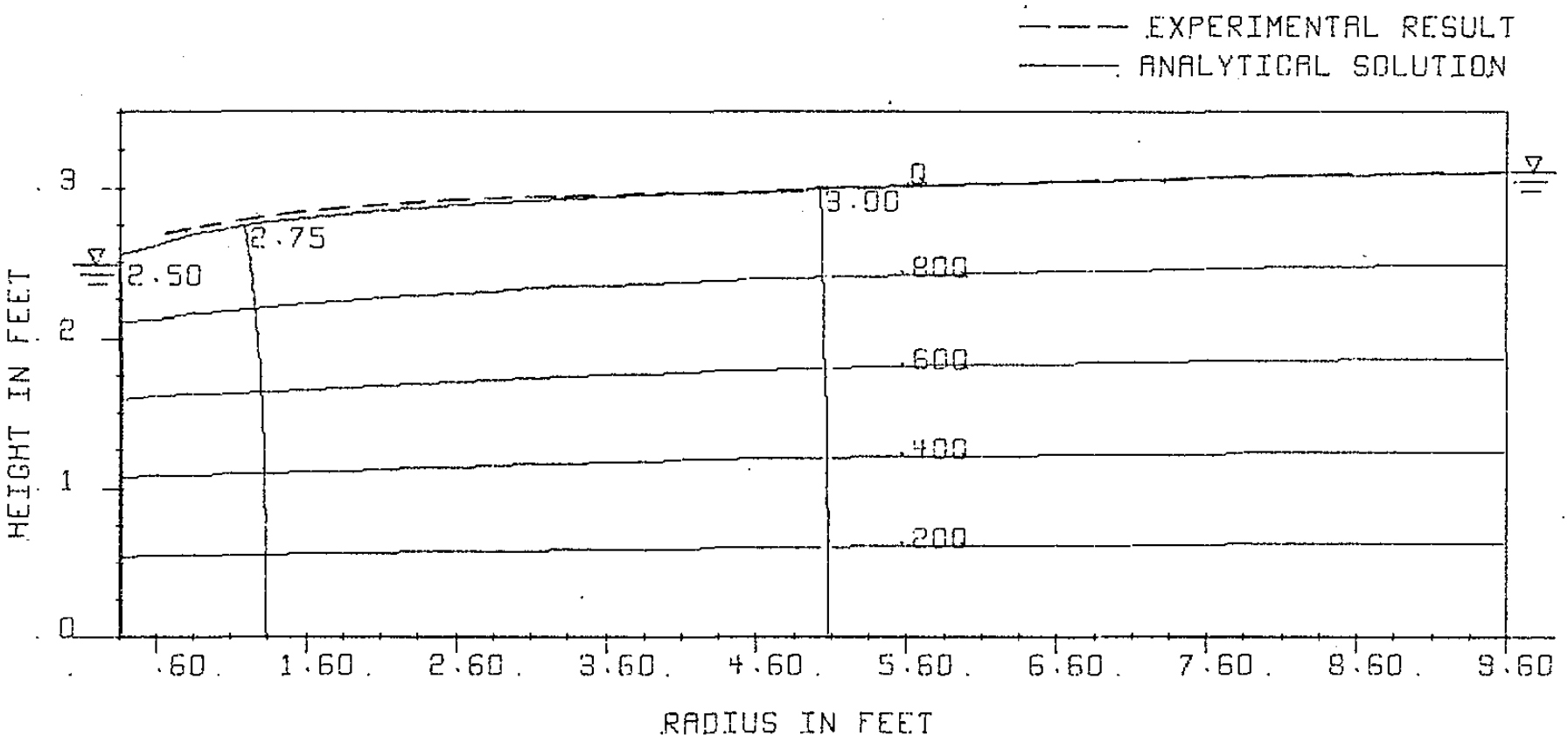

EXPERIMENT WITH COMPLETE CIRCLE . RW= .354 RE= 9.604
. FLOW NO 3 . HW= 2.494 HE= 3.110
RESULTS FOR DARCY FLOW Q(CALC) = .513 Q(EXP) = .510 CUSEC

FIG. A-II-5

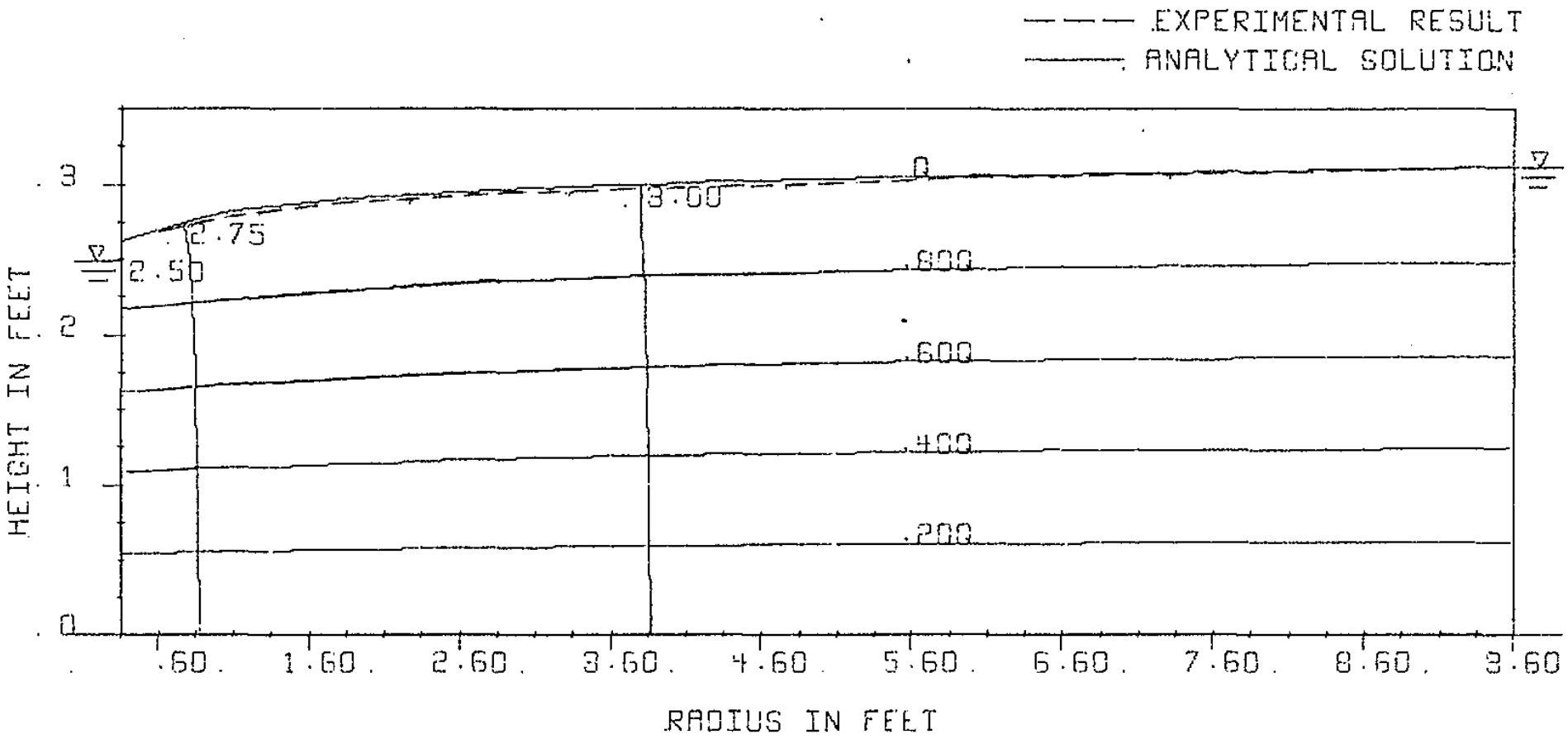

EXPERIMENT WITH COMPLETE CIRCLE . RW= .354 RE= 9.604
. FLOW NO 3 . HW= 2.494 HE= 3.110
RESULTS FOR FORCHHEIMER FLOW Q(CALC)= .485 Q(EXP)= .510 CUSEC

FIG. A-II-6

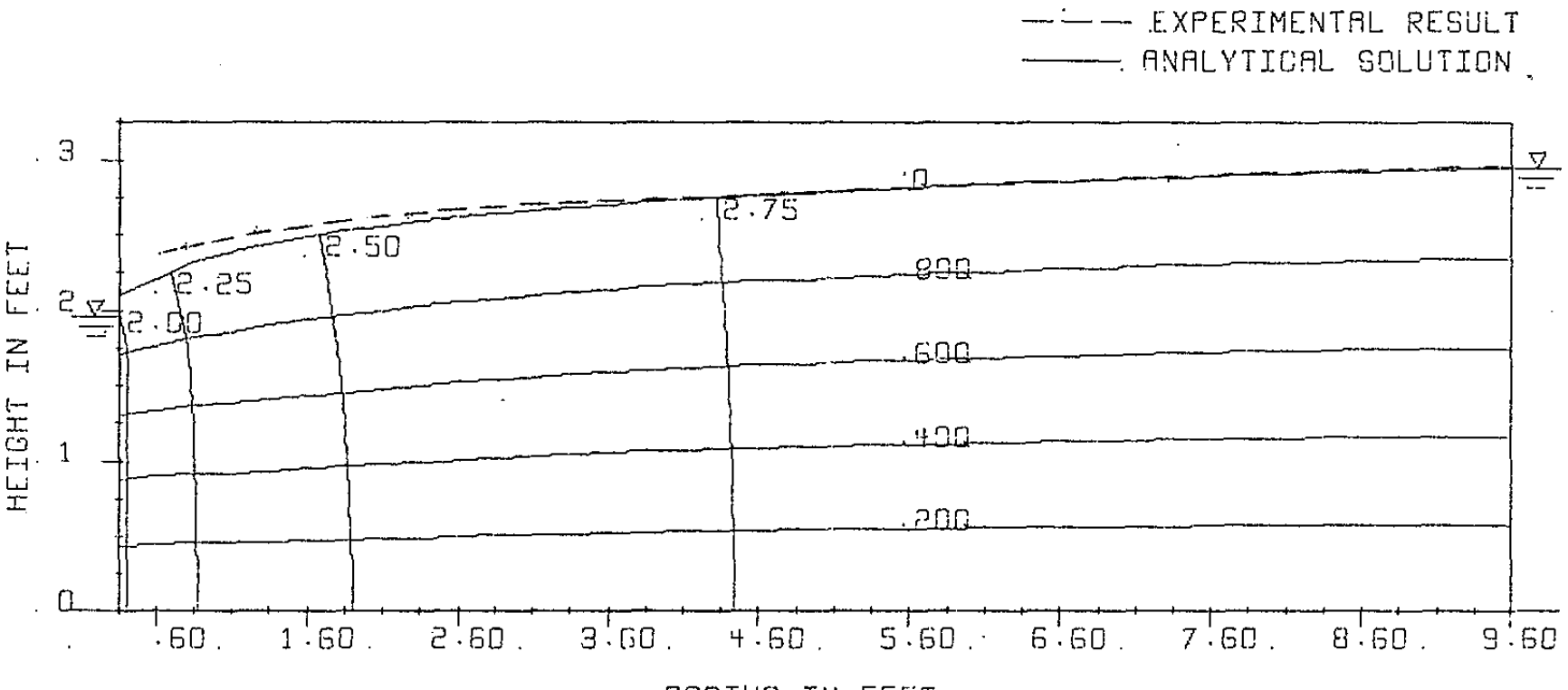

EXPERIMENT WITH COMPLETE CIRCLE RW= .354 RE= 9.604
FLOW NO 4 HW= 1.956 HE= 2.950
RESULTS FOR DARCY FLOW Q(CALC) = .720 Q(EXP) = .625 CUSEC

FIG. A-II-7

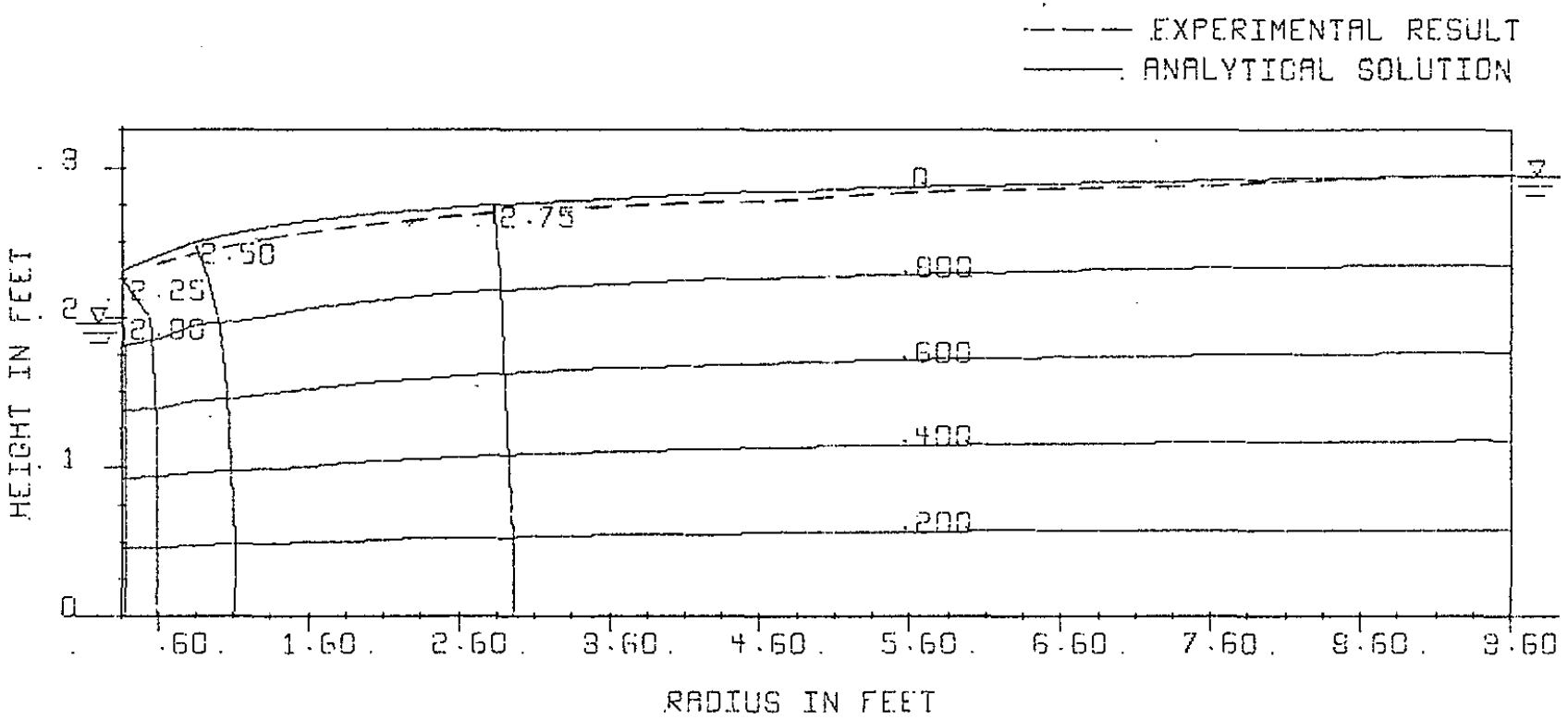

EXPERIMENT WITH COMPLETE CIRCLE . RW= .354 RE= 9.604
. FLOW NO 4 . HW= 1.956 HE= 2.350
RESULTS FOR FORCHHEIMER FLOW Q(CALC)= .595 Q(EXP)= .625 CUSEC

FIG. A-II-8

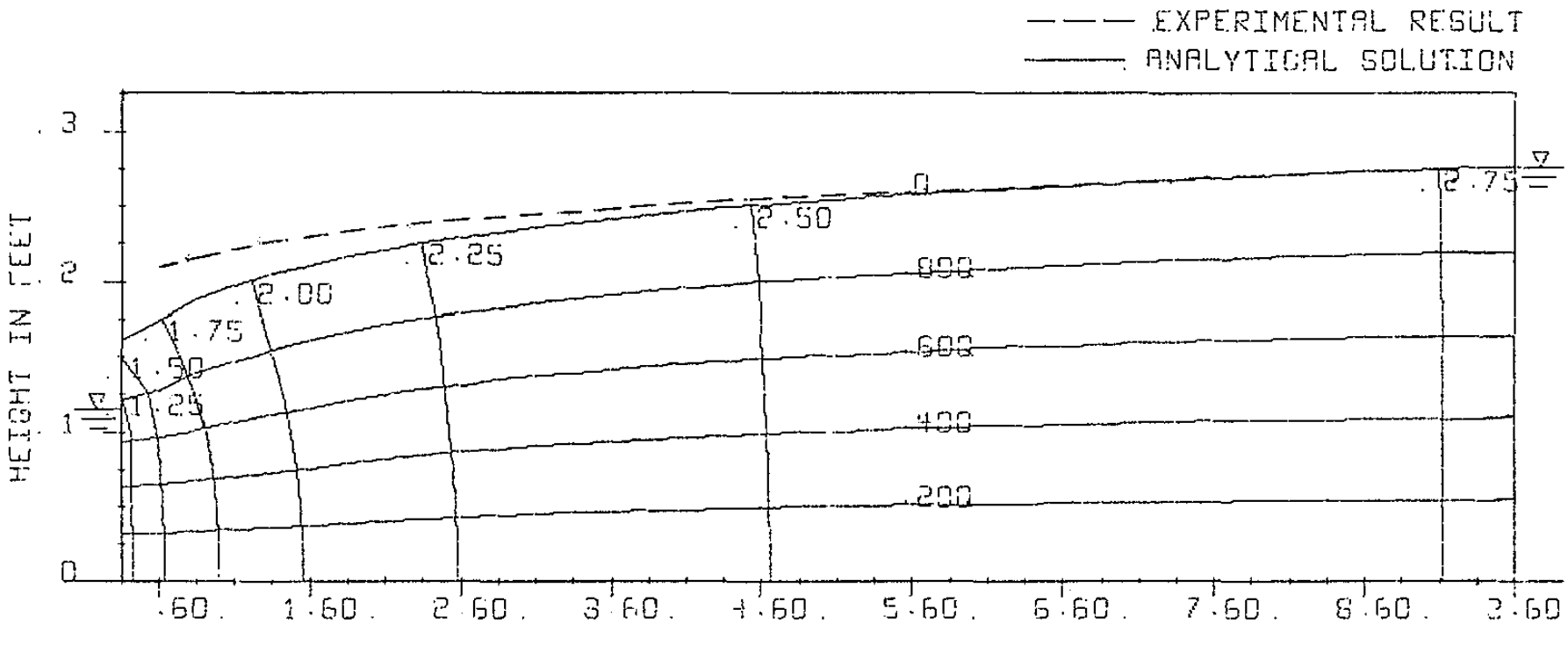

EXPERIMENT WITH COMPLETE CIRCLE RW= .354 RE= 9.604
FLOW NO 5 HW= 1.151 HE= 2.768
RESULTS FOR DARCY FLOW Q(CALC)= .945 Q(EXP)= .680 CUSEC

FIG. A-II-9

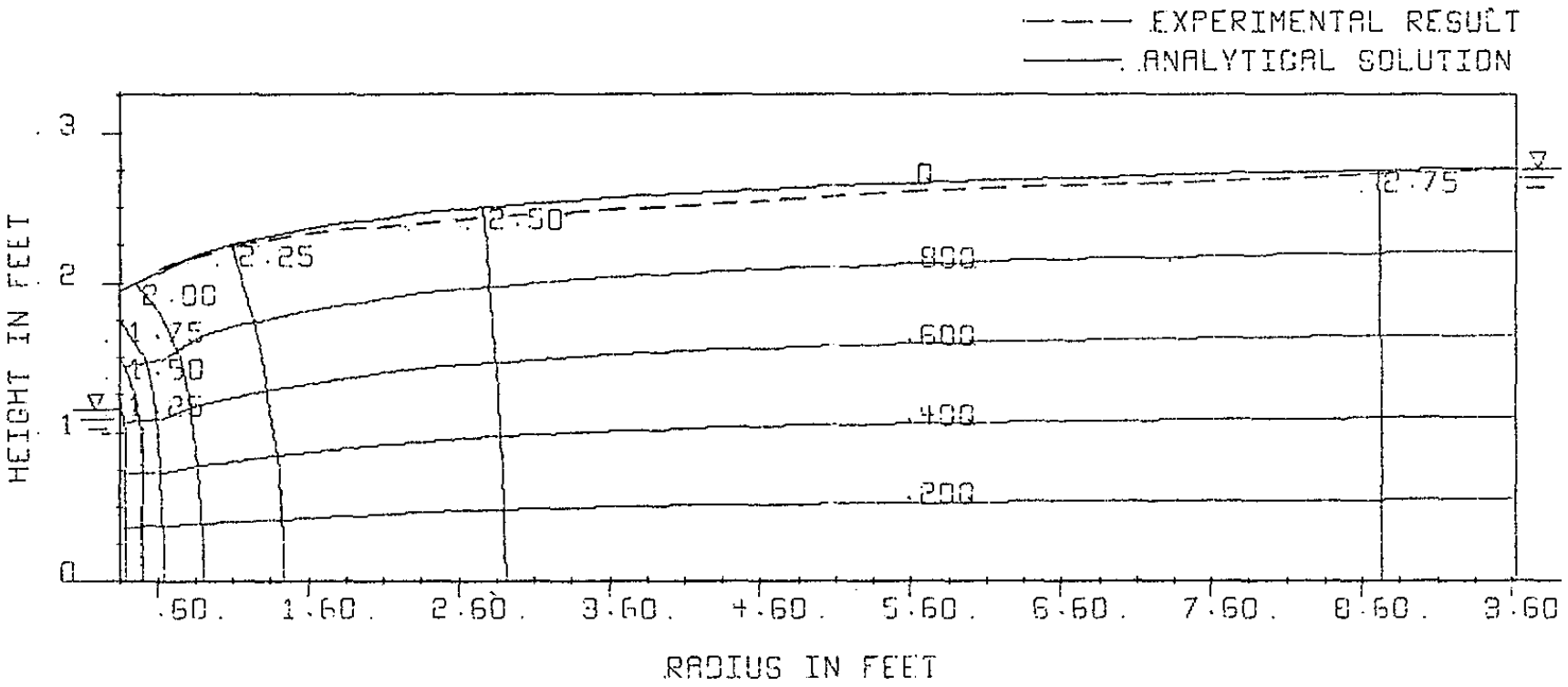

EXPERIMENT WITH COMPLETE CIRCLE . RW= .354 RE= 9.604
. FLOW NO 5 . HW= 1.151 HE= 2.768
RESULTS FOR FORCHHEIMER FLOW Q(CALC) = .691 Q(EXP) = .680 CUSEC

FIG. A-II-10

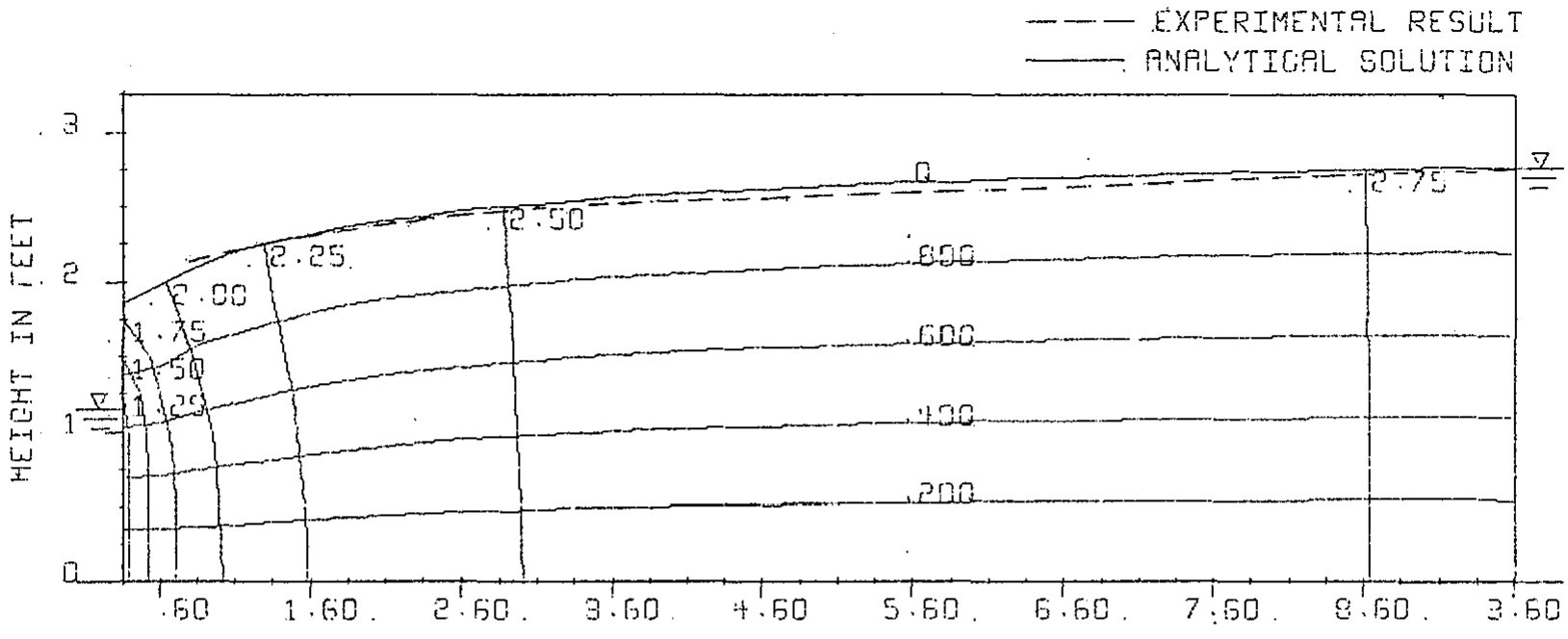

EXPERIMENT WITH COMPLETE CIRCLE . RW= .354 RE= 9.604
. FLOW NO 5 . HW= 1.151 HE= 2.768
RESULTS FOR EXPONENTIAL FLOW Q(CALC)= .723 Q(EXP)= .680 CUSEC

FIG. A-II-11

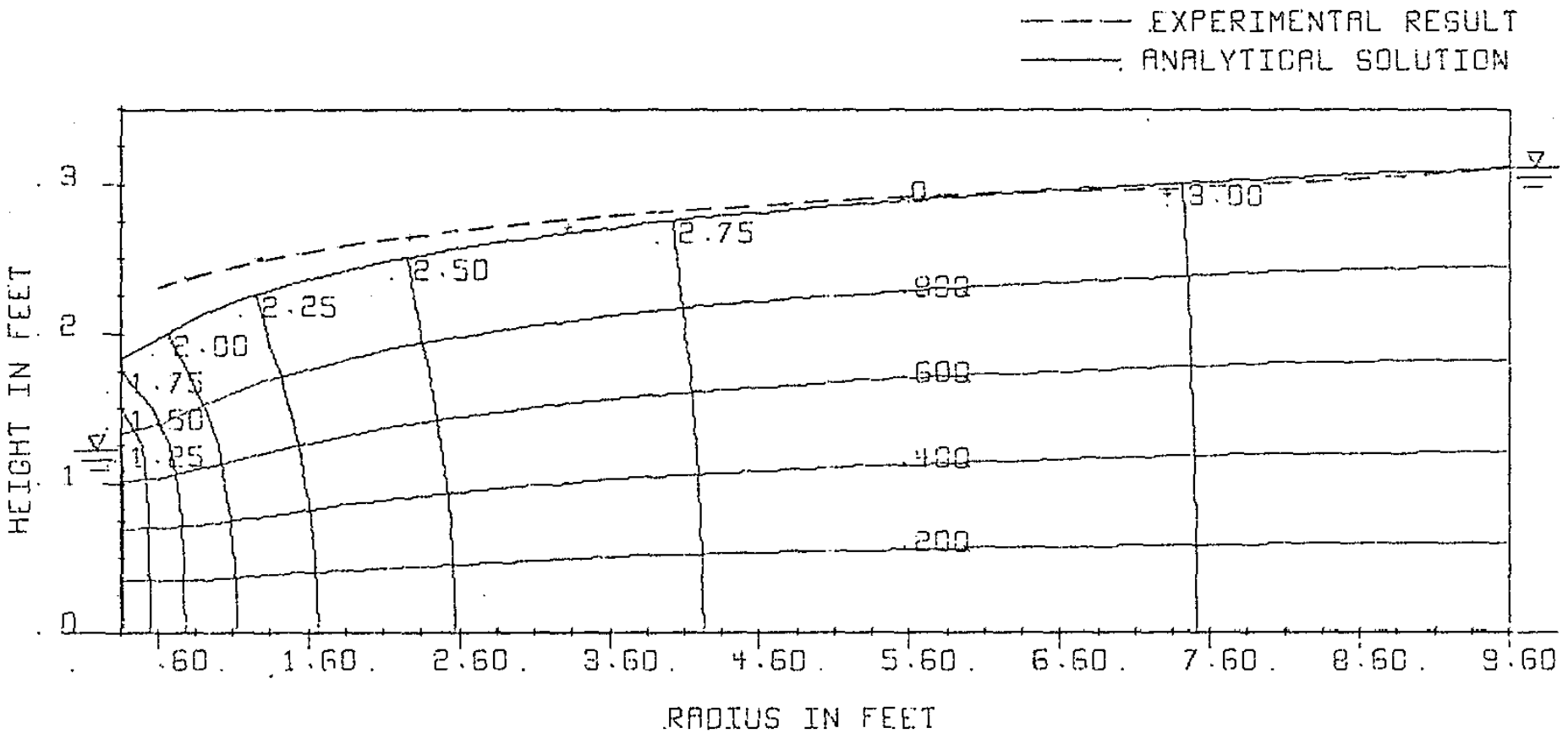

EXPERIMENT WITH COMPLETE CIRCLE . RW= .354 RE= 9.604
. FLOW NO 7 . HW= 1.214 HE= 3.098
RESULTS FOR DARCY FLOW Q(CALC) = 1.200 Q(EXP) = .870 CUSEC

FIG. A-II-12

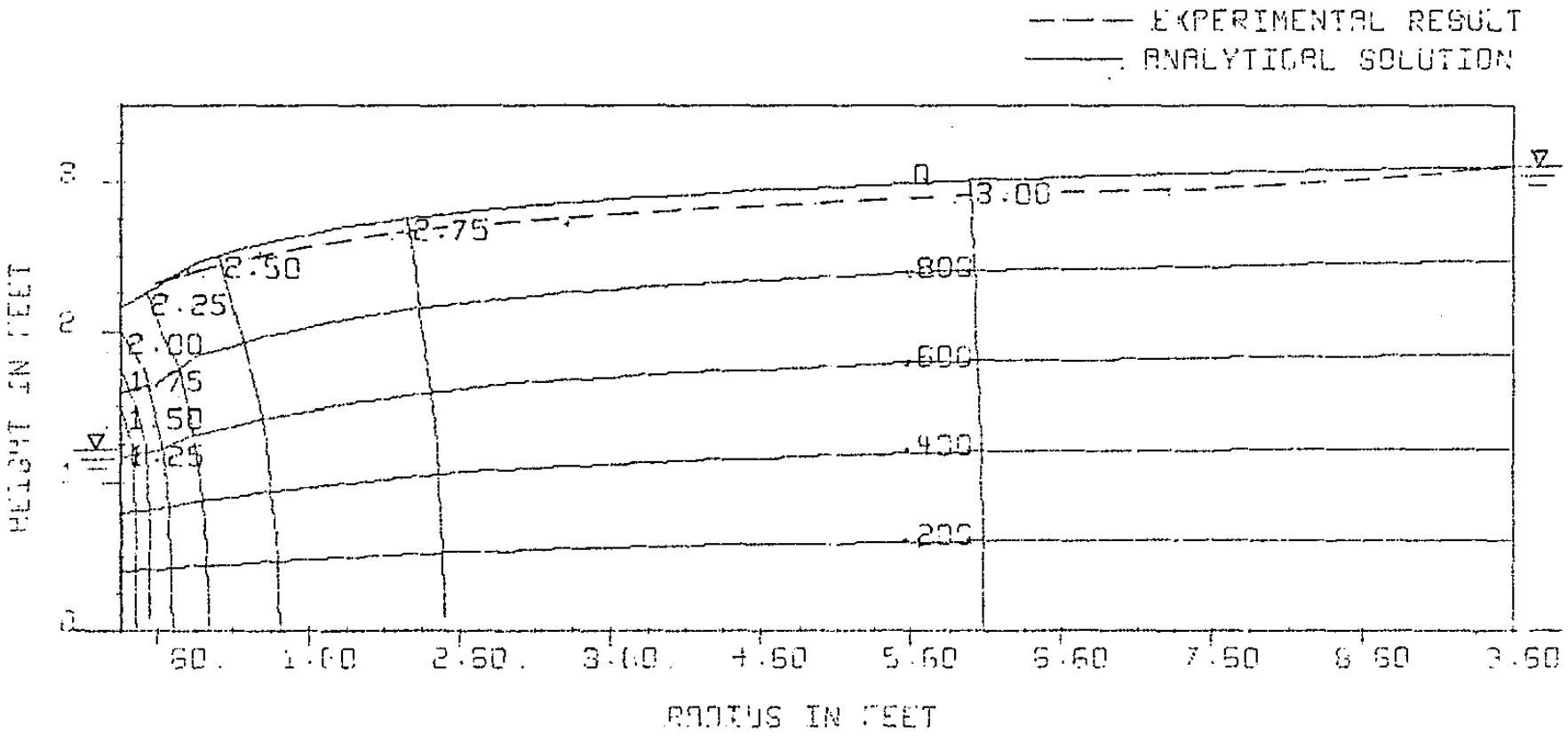

EXPERIMENT WITH COMPLETE CIRCLE PW= .354 RE= 9.604
FLOW NO 7 HW= 1.214 HE= 3.098
RESULTS FOR FORCHHEIMER FLOW Q(CALC)= .839 Q(EXP)= .870 CUSEC

FIG. A-II-13

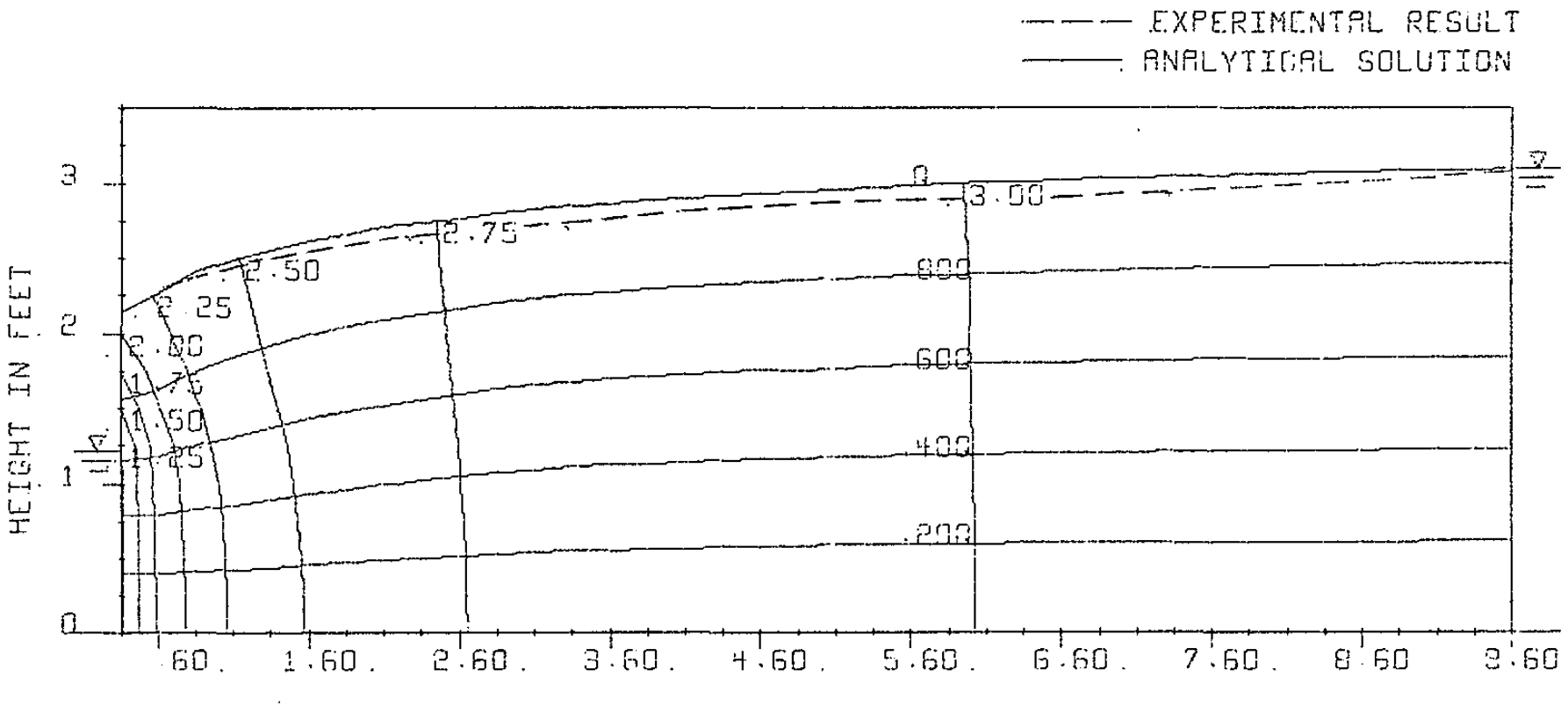

EXPERIMENT WITH COMPLETE CIRCLE RW= .354 RE= 9.604
FLOW NO 7 HW= 1.214 HE= 3.098
RESULTS FOR EXPONENTIAL FLOW Q(CALC)= .878 Q(EXP)= .870 CUSEC

FIG. A-II-14

APPENDIX III

Flow Net Results for Unconfined Axisymmetric Experiments with Sector.

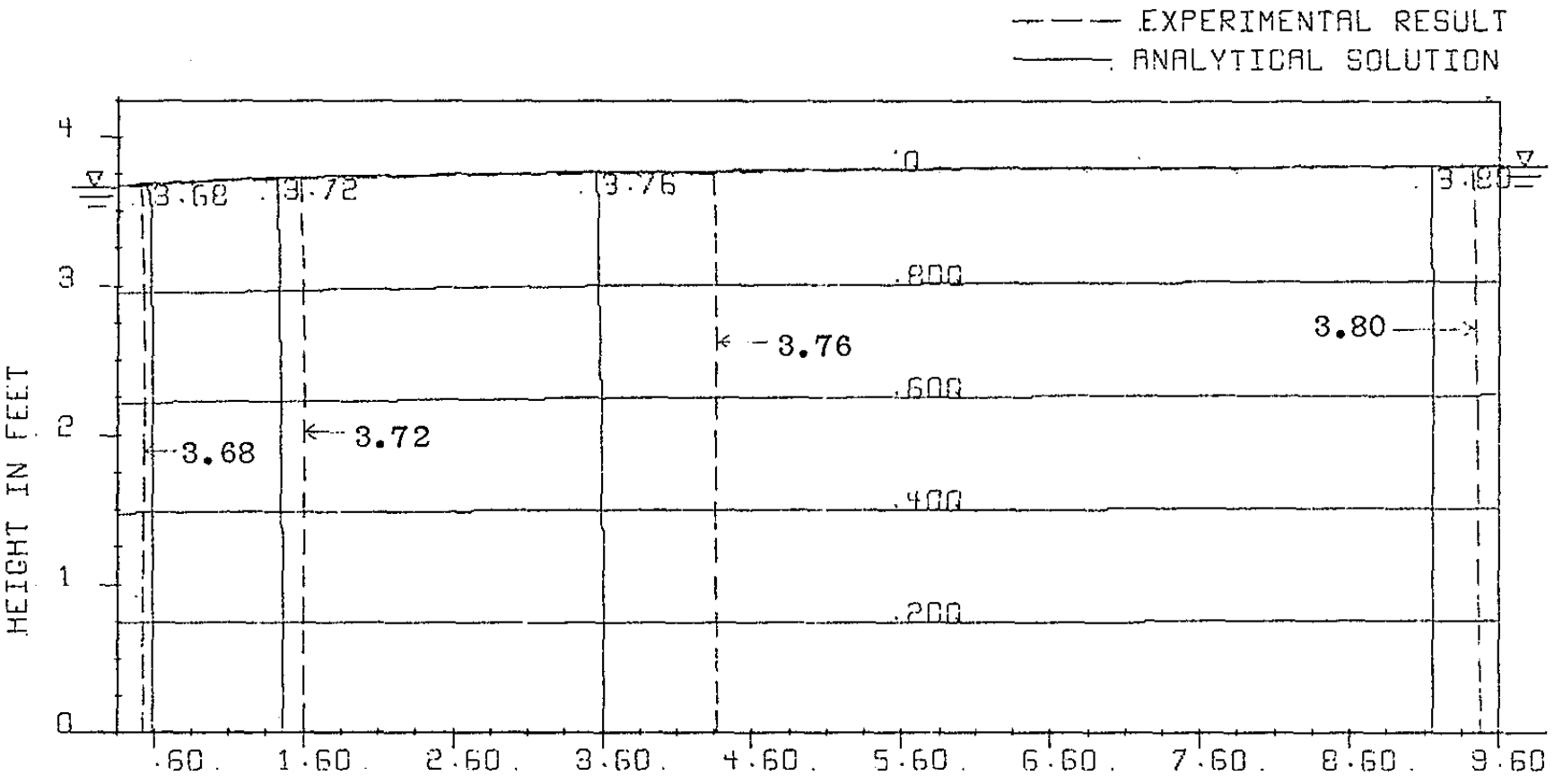

EXPERIMENT WITH SECTOR
FLOW NO 1
RESULTS FOR DARCY FLOW

RW= .354 RE= 9.604
HW= 3.658 HE= 3.802
Q(CALC)= .129 Q(EXP)= .157 CUSEC

FIG. A-III-1

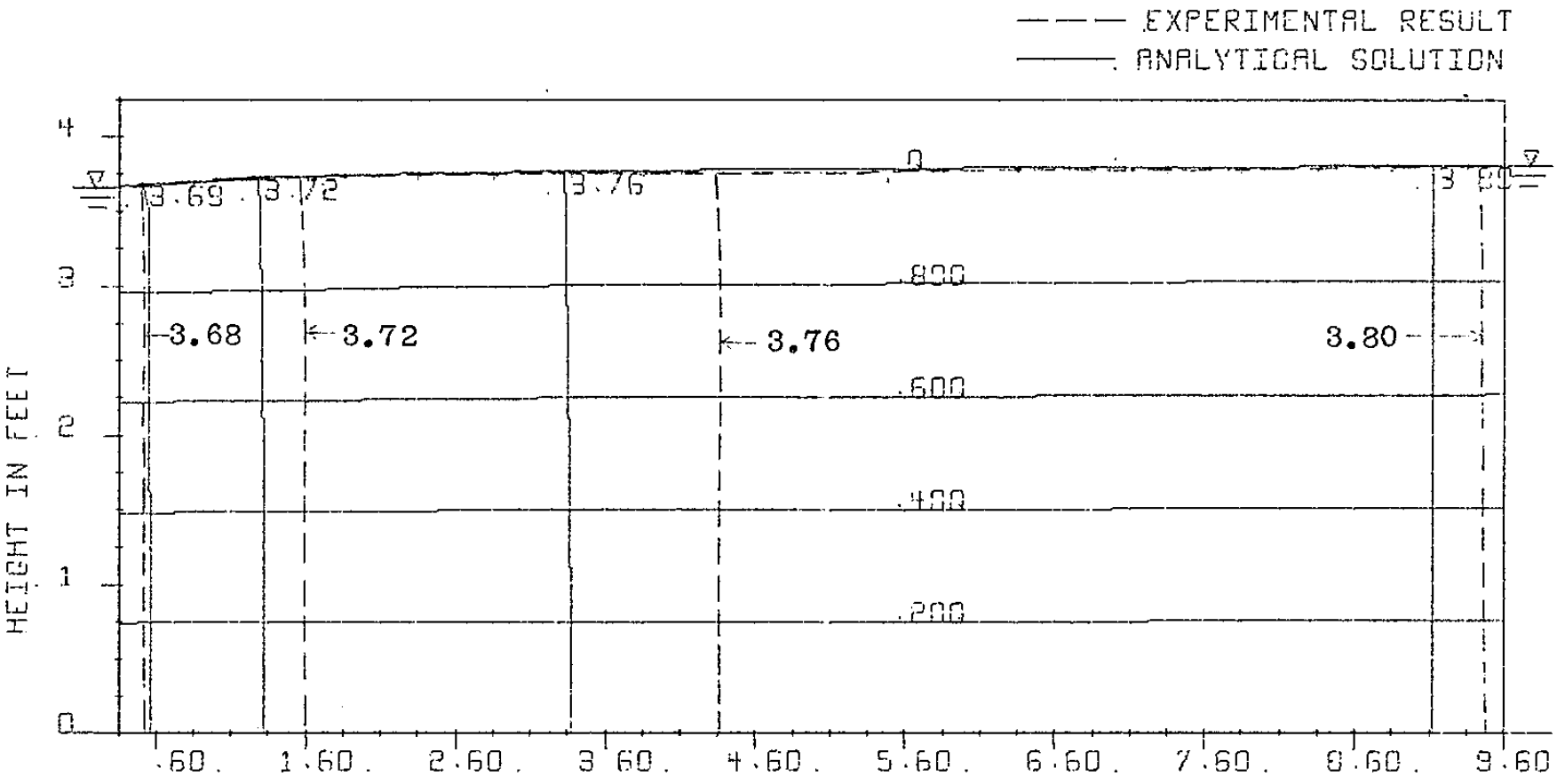

EXPERIMENT WITH SECTOR . RW= .354 RE= 9.604
. FLOW NO 1 . HW= 3.658 HE= 3.802
RESULTS FOR FORCHHEIMER FLOW Q(CALC) = .147 Q(EXP) = .157 CUSEC

FIG. A-III-2

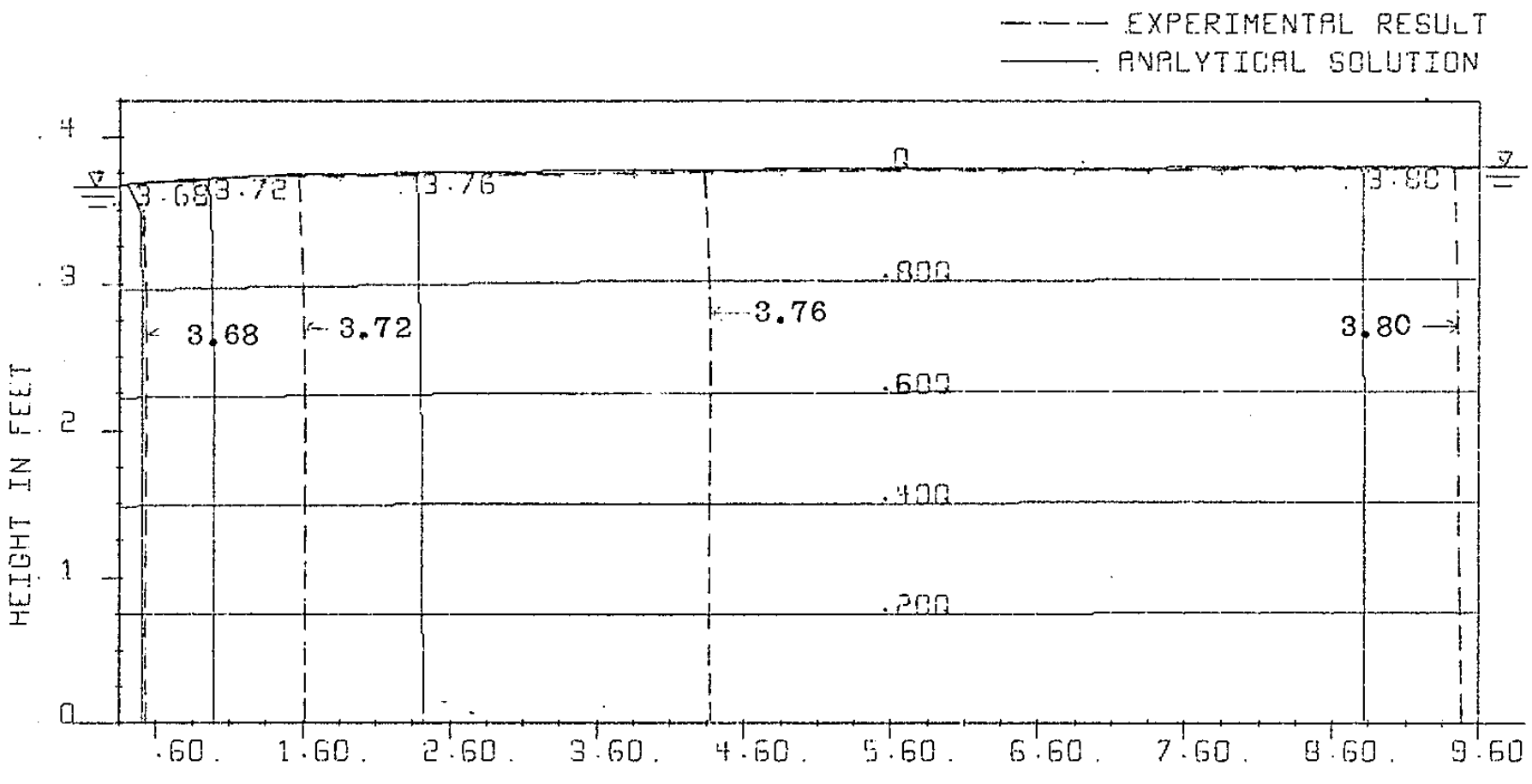

EXPERIMENT WITH SECTOR
. FLOW NO 1
RESULTS FOR EXPONENTIAL FLOW

RW= .354 RE= 9.604
. HW= 3.658 HE= 3.802
Q(CALC) = .169 Q(EXP) = .157 CUSEC

FIG. A-III-3

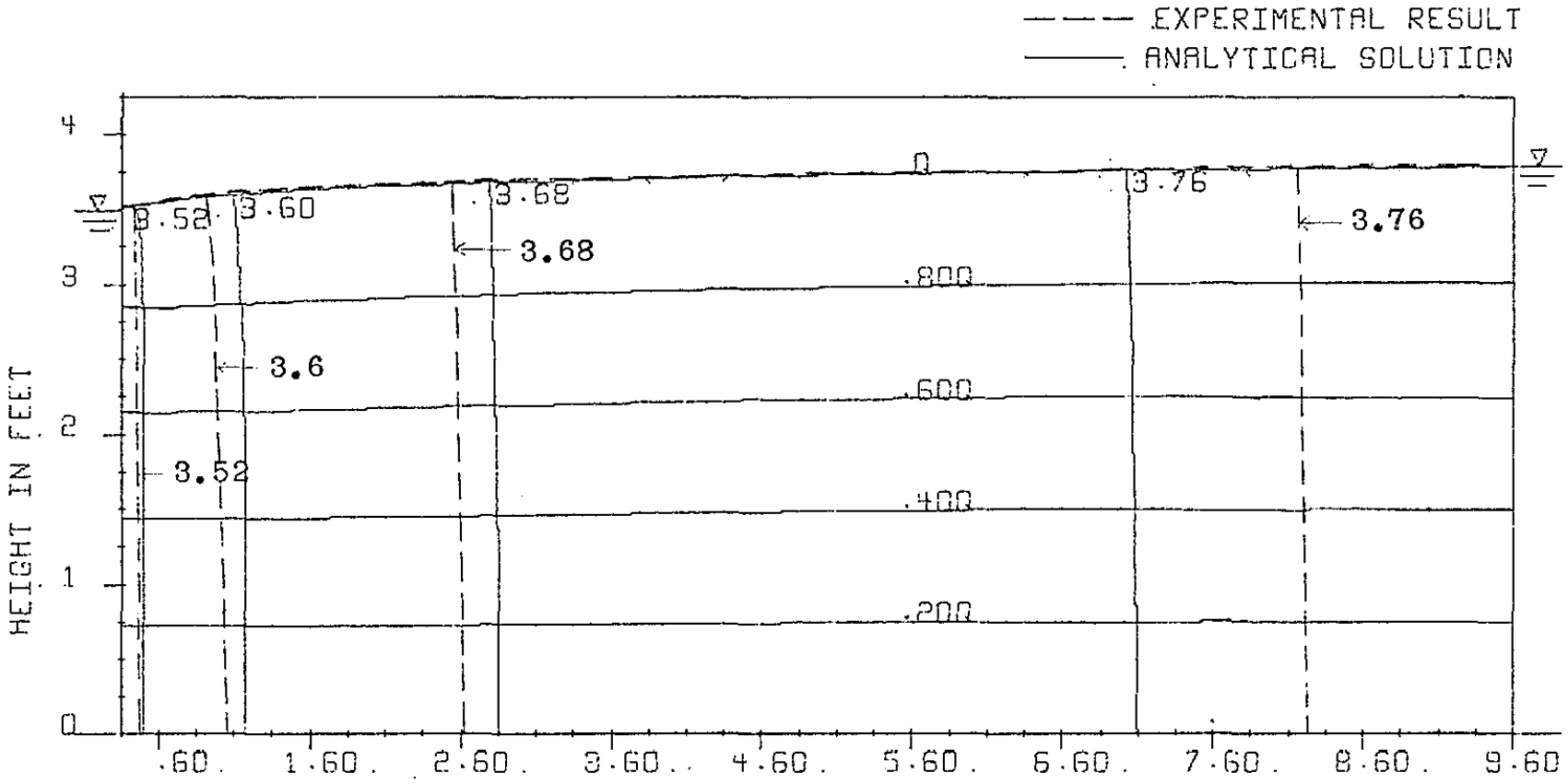

EXPERIMENT WITH SECTOR
. FLOW NO 2
RESULTS FOR DARCY FLOW

. RW= .354 RE= 9.604
. HW= 3.492 HE= 3.786
Q(CALC) = .258 Q(EXP) = .280 CUSEC

FIG. A-III-4

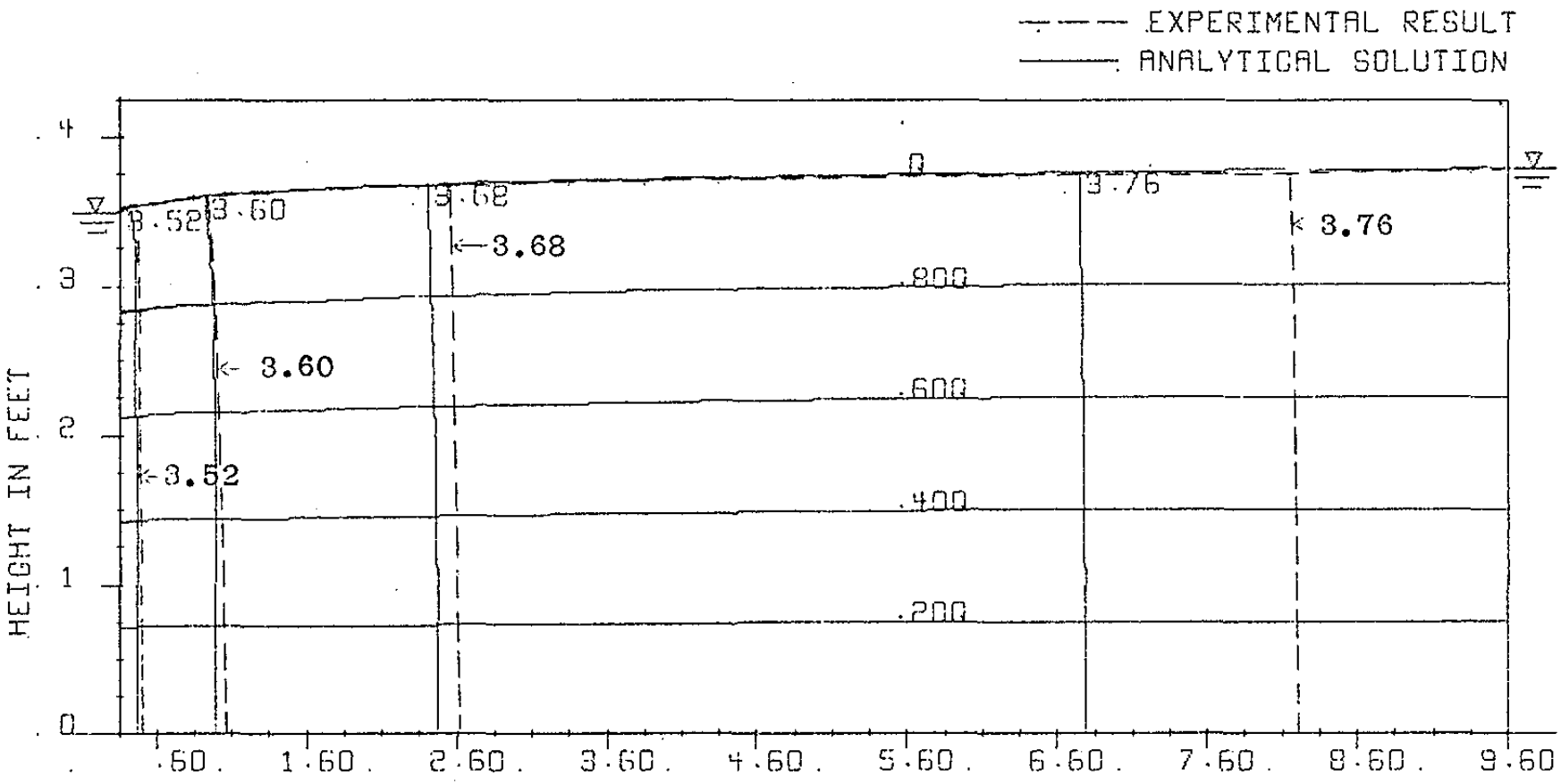

EXPERIMENT WITH SECTOR . RW= .354 RE= 9.604
. FLOW NO 2 . HW= 3.492 HE= 3.786
RESULTS FOR FORCHHEIMER FLOW Q(CALC) = .274 Q(EXP) = .280 CUSEC

FIG. A-III-5

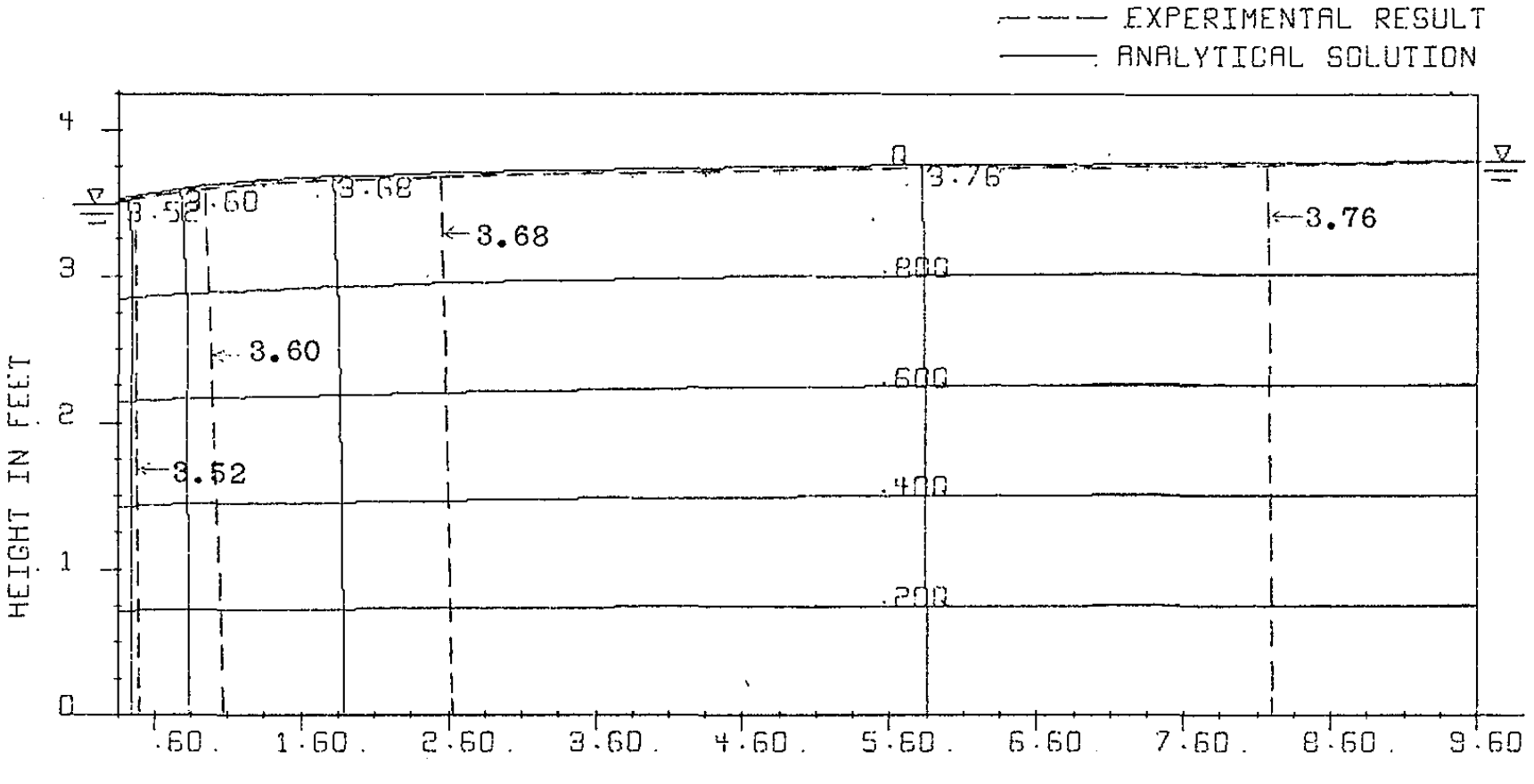

EXPERIMENT WITH SECTOR . RW= .354 RE= 9.604
. FLOW NO 2 . HW= 3.492 HE= 3.786
RESULTS FOR EXPONENTIAL FLOW Q(CALC) = .288 Q(EXP) = .280 CUSEC

FIG. A-III-6

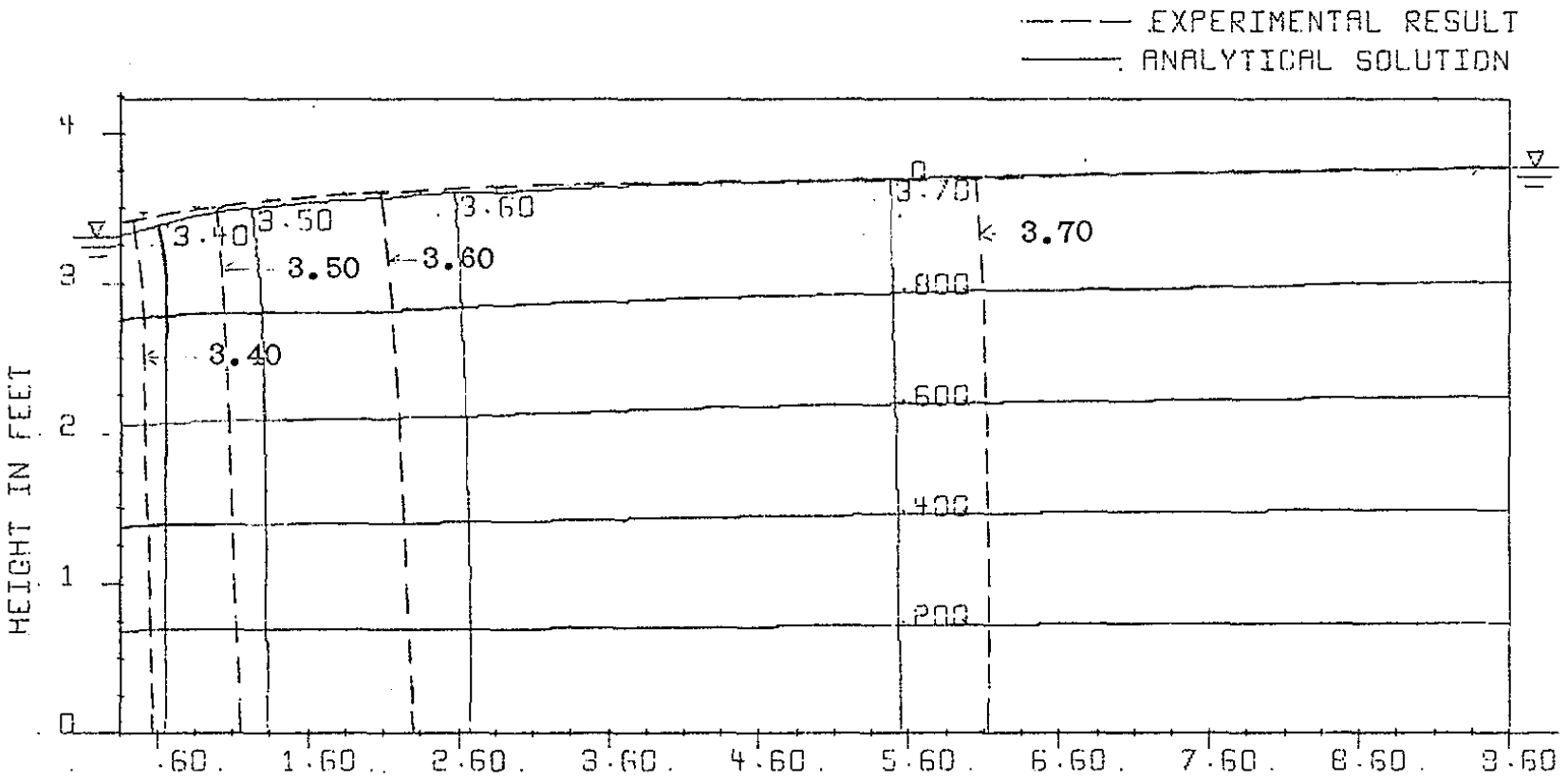

EXPERIMENT WITH SECTOR
. FLOW NO 3
RESULTS FOR DARCY FLOW

. RW= .354 RE= 9.604
. HW= 3.313 HE= 3.773
Q(CALC) = .396 Q(EXP) = .395 CUSEC

FIG. A-III-7

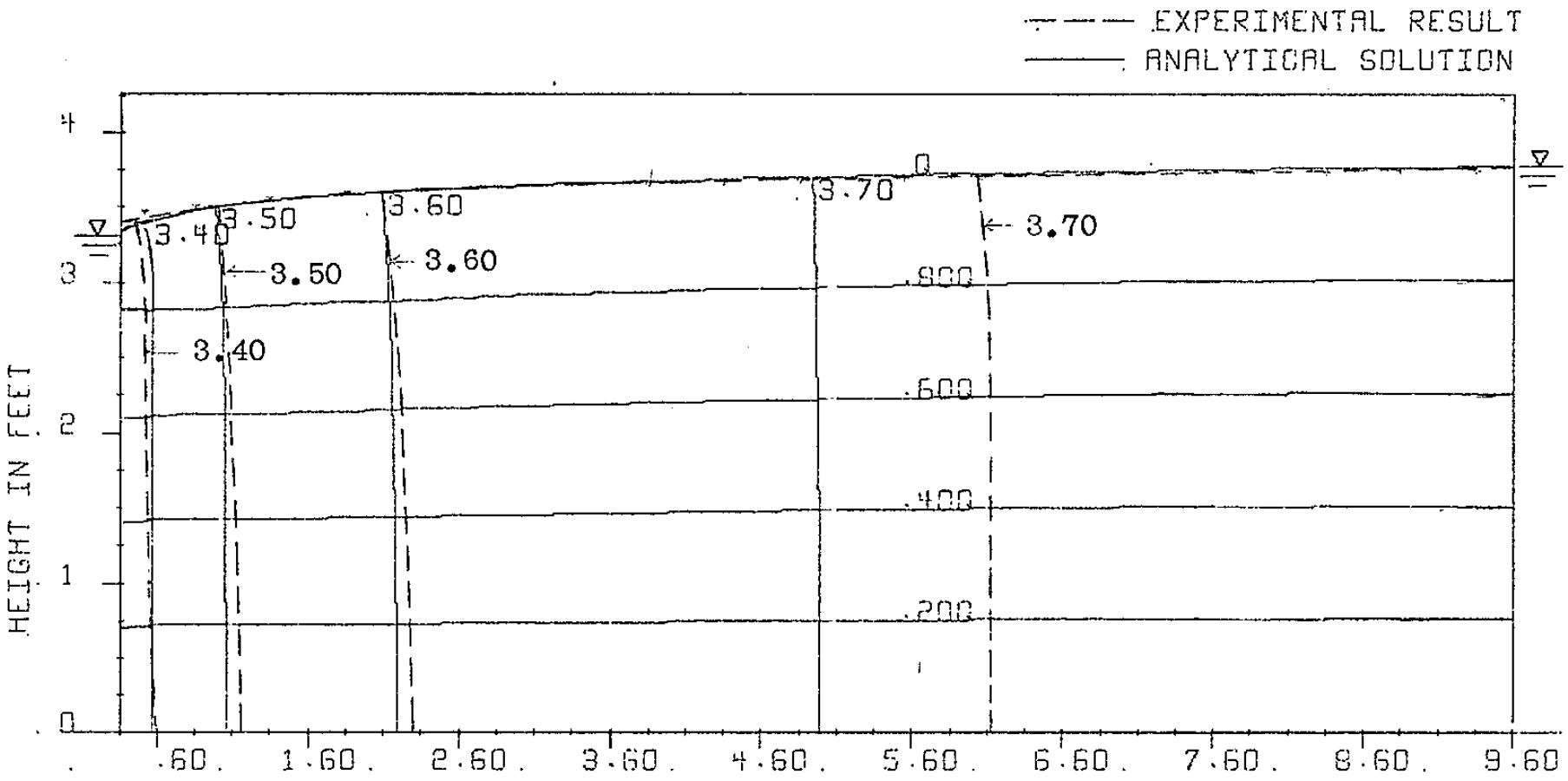

EXPERIMENT WITH SECTOR . RW= .354 RE= 9.604
. FLOW NO 3 . HW= 3.313 HE= 3.773
RESULTS FOR FORCHHEIMER FLOW Q(CALC) = .394 Q(EXP) = .395 CUSEC

FIG. A-III-8

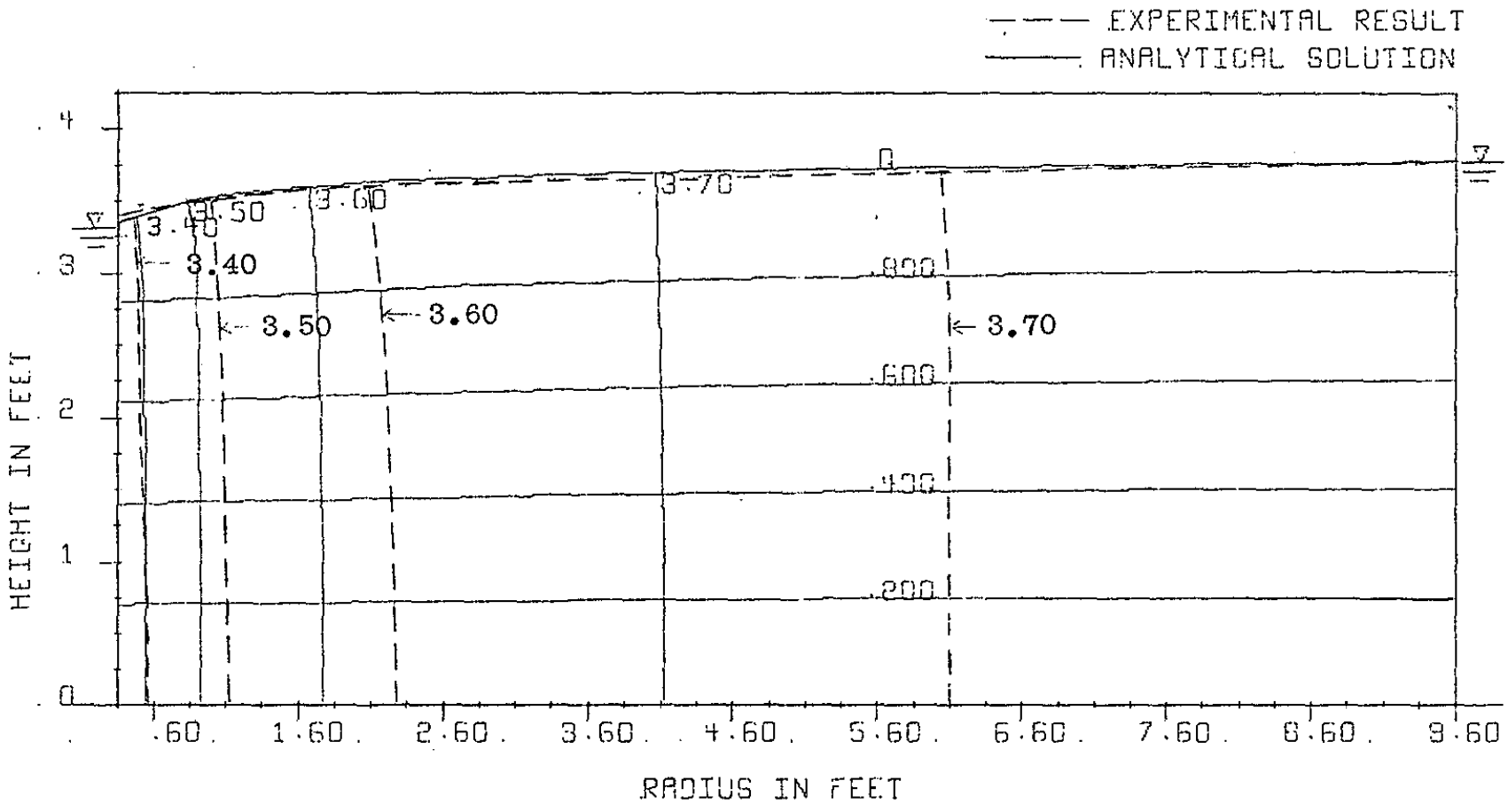

EXPERIMENT WITH SECTOR . RW= .354 RE= 9.604
. FLOW NO 3 . HW= 3.313 HE= 3.773
RESULTS FOR EXPONENTIAL FLOW Q(CALC) = .397 Q(EXP) = .395 CUSEC

FIG. A-III-9

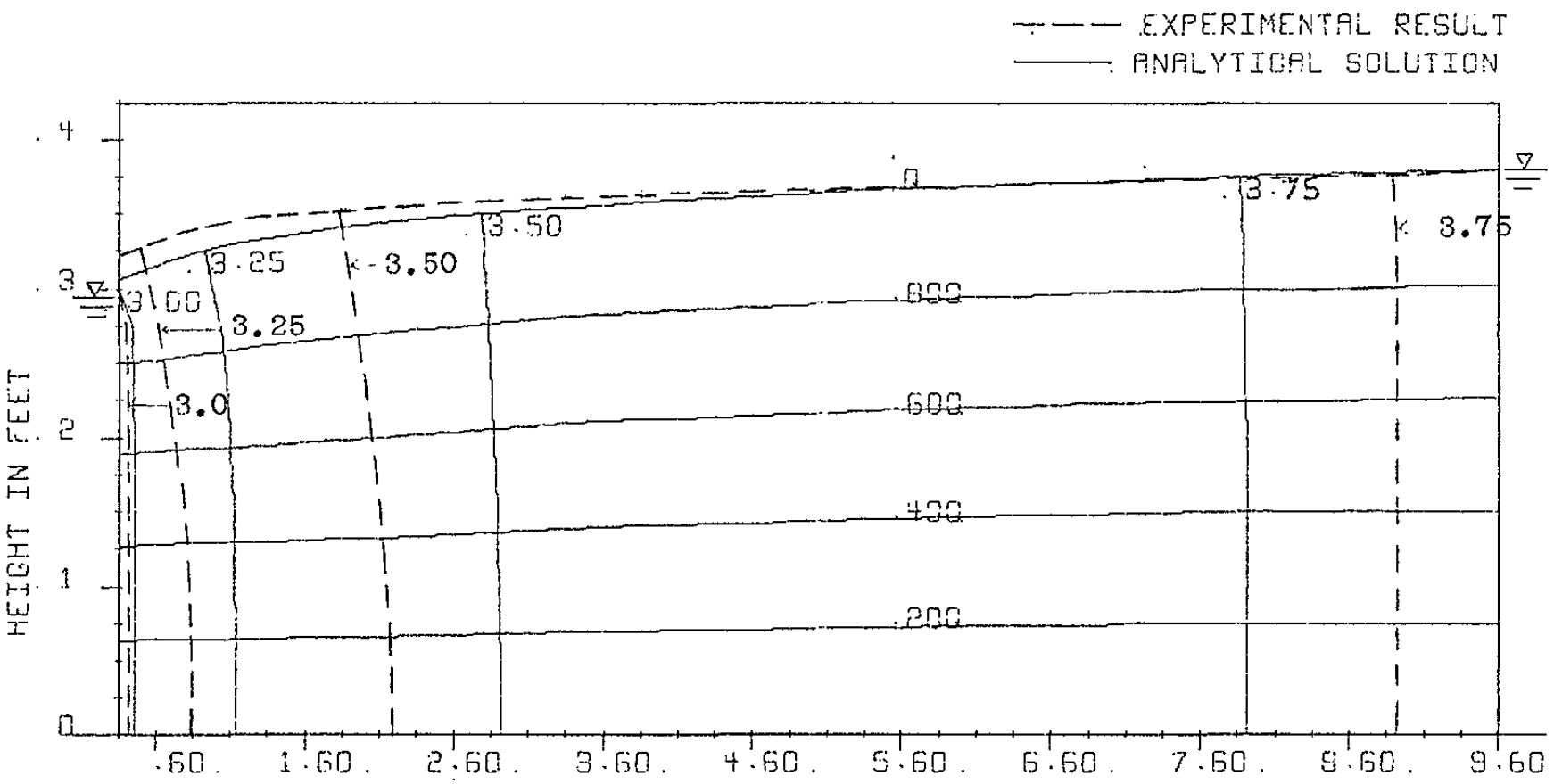

EXPERIMENT WITH SECTOR
. FLOW NO 4
RESULTS FOR DARCY FLOW

. RW= .354 RE= 9.604
. HW= 2.930 HE= 3.797
Q(CALC) = .712 Q(EXP) = .612 CUSEC

FIG. A-III-10

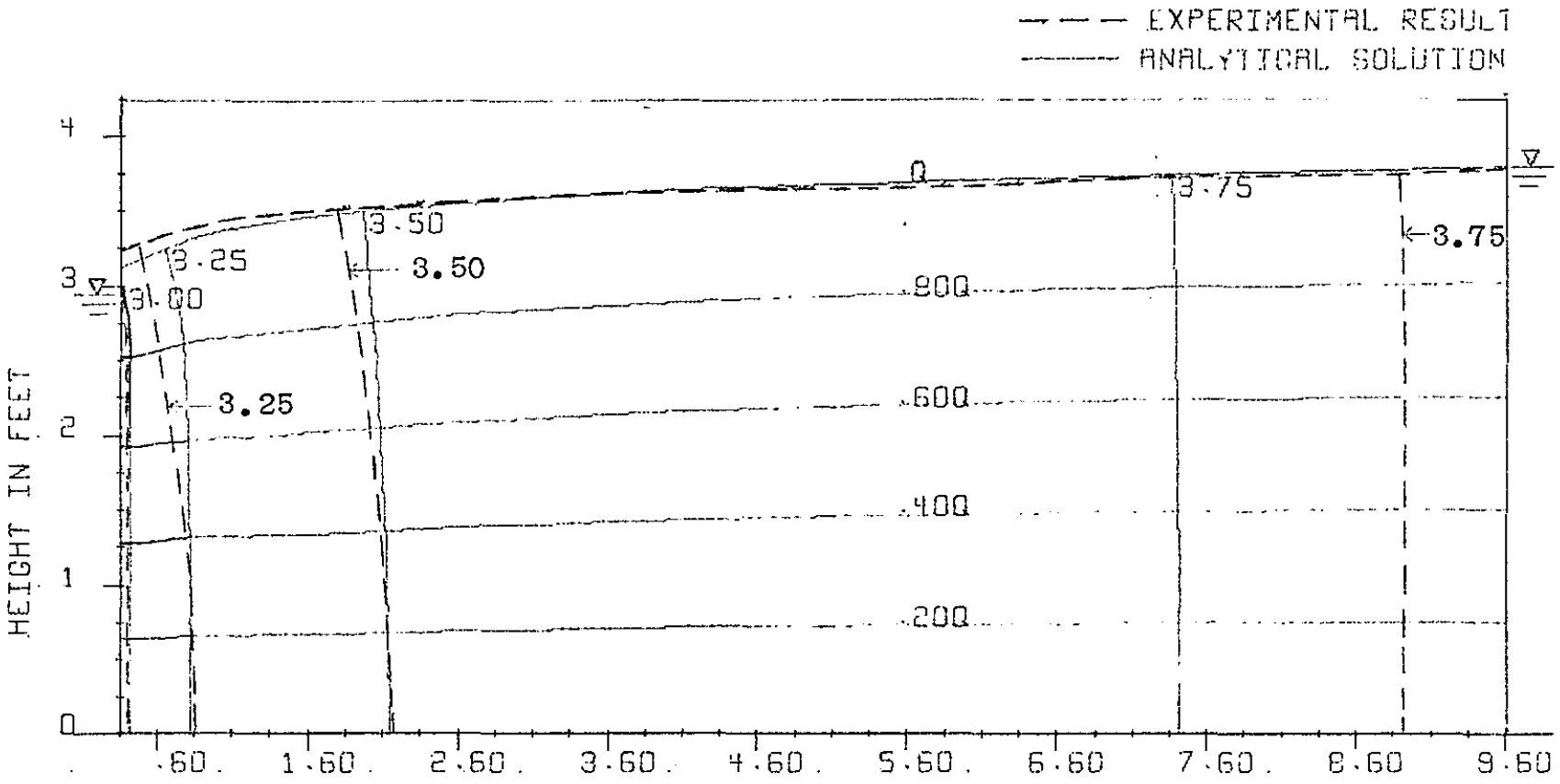

EXPERIMENT WITH SECTOR RW= .354 RE= 9.604
FLOW NO 4 HW= 2.938 HE= 3.797
RESULTS FOR FORCHHEIMER FLOW Q(CALC) = .629 Q(EXP) = .612 CUSEC

FIG. A-III-11

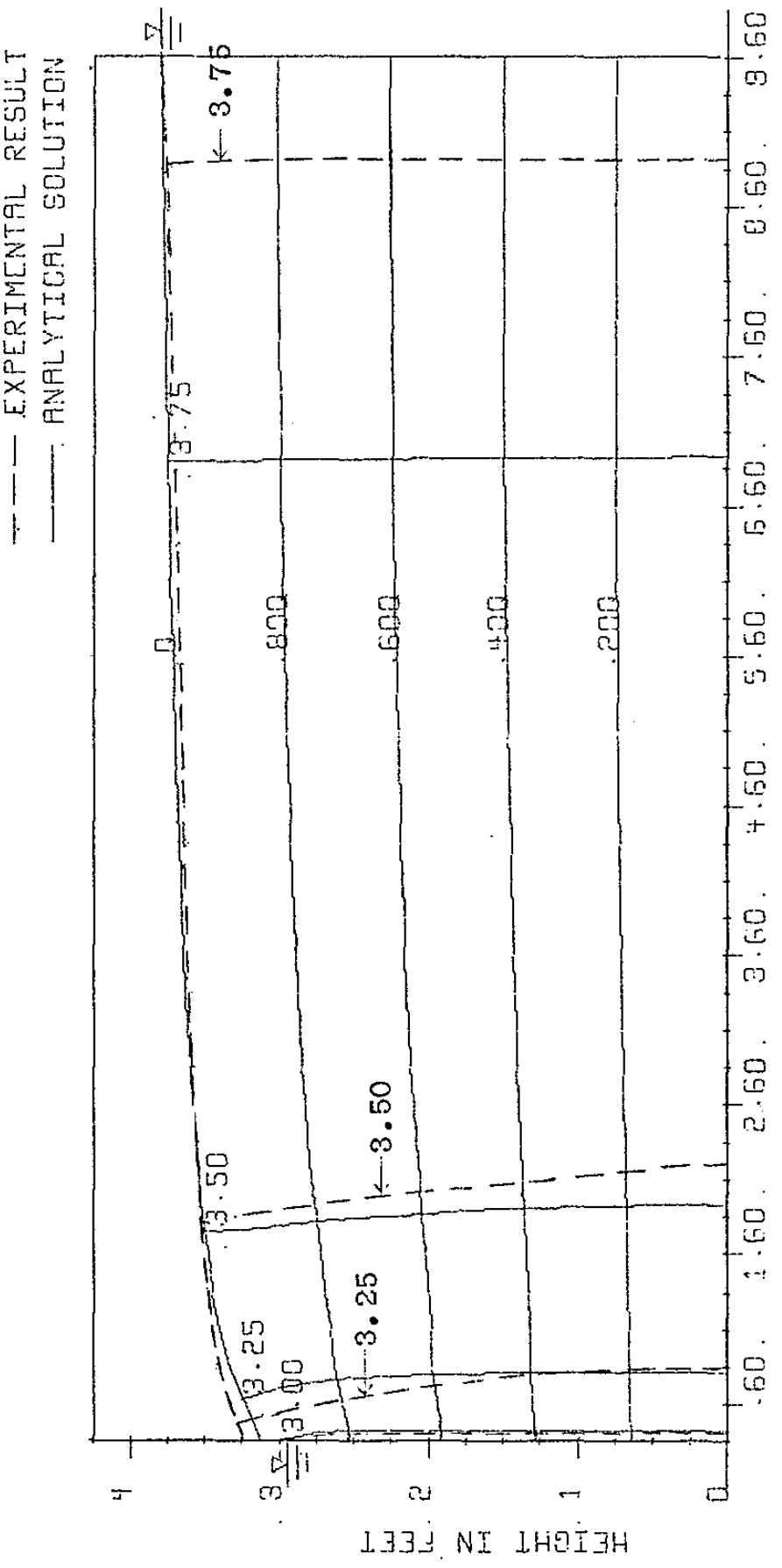
EXPERIMENTAL RESULT
ANALYTICAL SOLUTION
HEIGHT IN FEET
RADIUS IN FEET
3.75
3.50
3.25
3.00
.800
.600
.400
.200
0
EXPERIMENT WITH SECTOR
FLOW NO 4
RESULTS FOR EXPONENTIAL FLOW
RW= .354
HW= 2.938
Q(CALC) = .619
RE= 9.604
HE= 3.797
Q(EXP) = .612 CUSEC

FIG. A-II-12

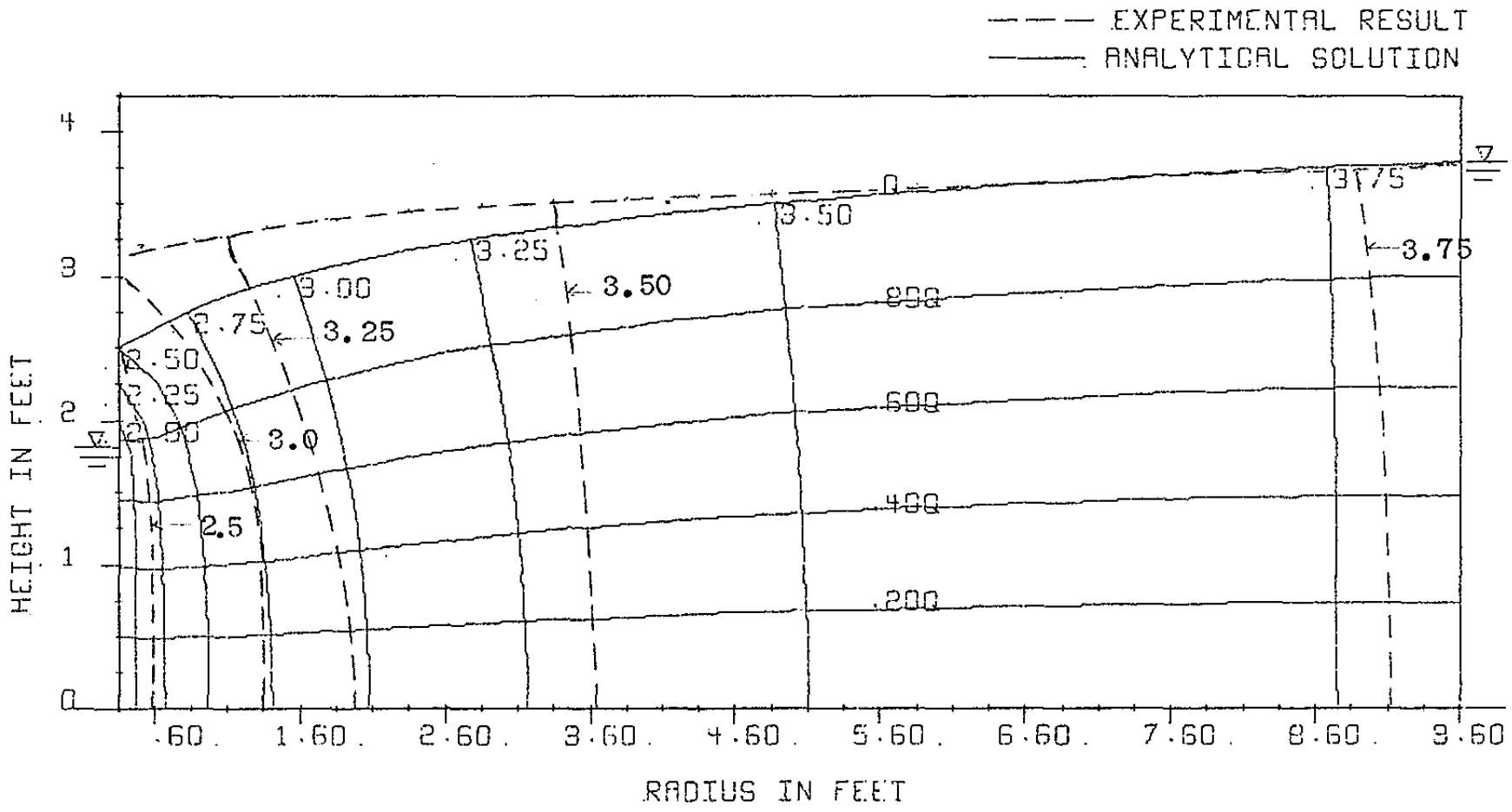

EXPERIMENT WITH SECTOR
. FLOW NO 6
RESULTS FOR DARCY FLOW

. RW= .354 RE= 9.604
. HW= 1.817 HE= 3.791
Q(CALC) = 1.326 Q(EXP) = .951 CUSEC

FIG. A-III-13

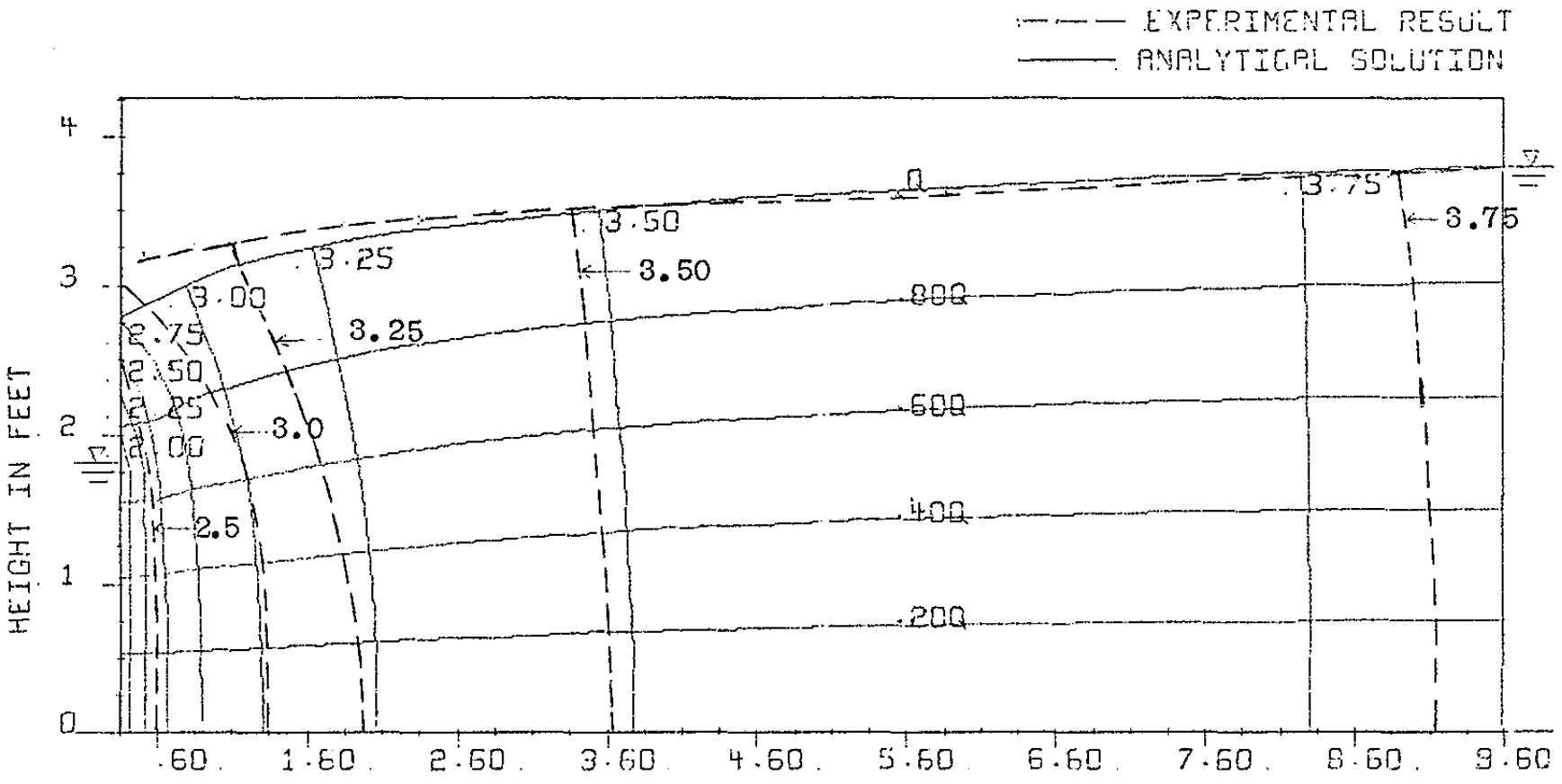

EXPERIMENT WITH SECTOR . RW= .354 RE= 9.604
. FLOW NO 6 . HW= 1.817 HE= 3.791
RESULTS FOR FORCHHEIMER FLOW Q(CALC) = .972 Q(EXP) = .951 CUSEC

FIG. A-III-14

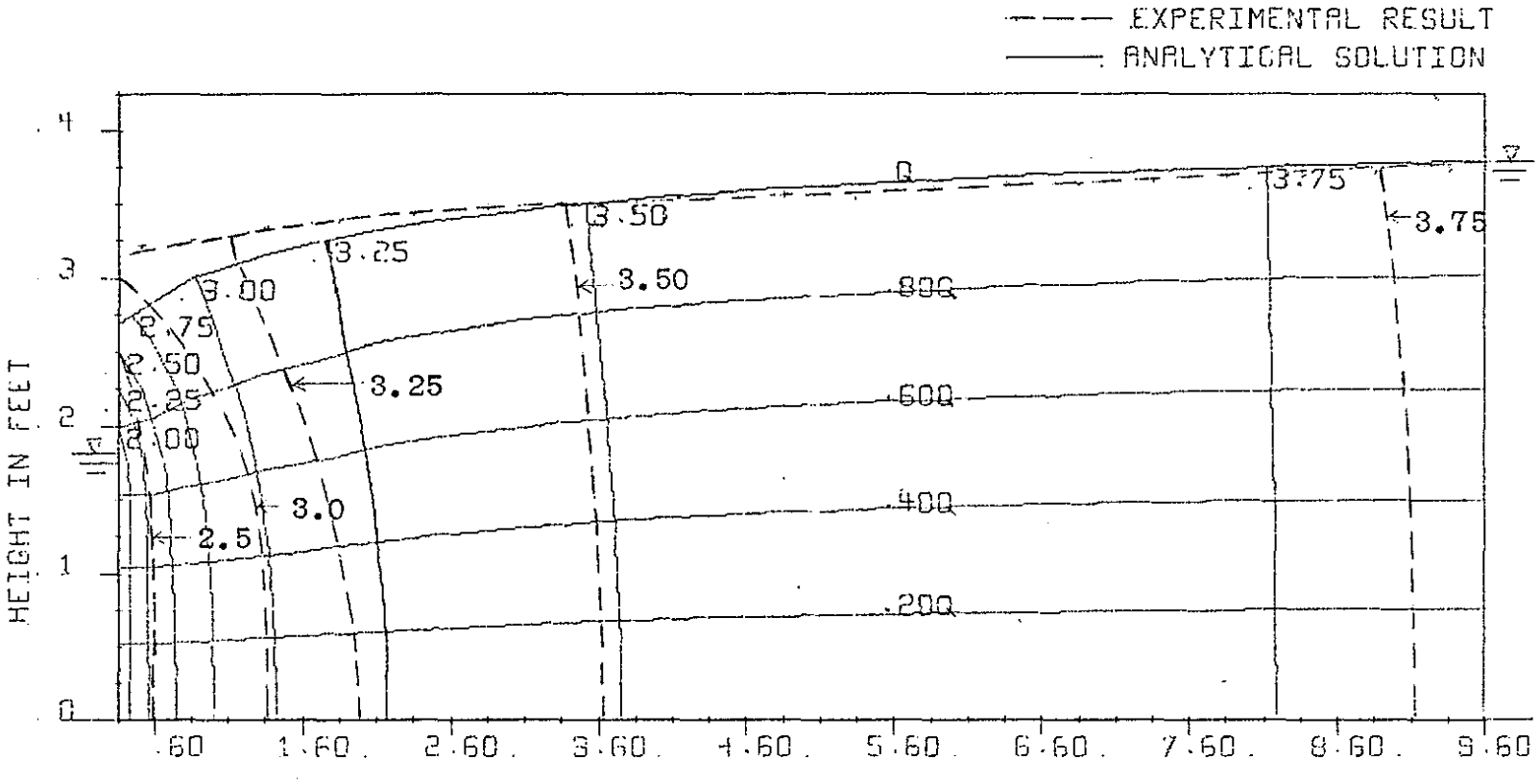

EXPERIMENT WITH SECTOR . RW= .354 RE= 9.60'
. FLOW NO 6 . HW= 1.817 HE= 3.791
RESULTS FOR EXPONENTIAL FLOW Q(CALC)= .981 Q(EXP)= .951 CUSEC

FIG. A-III-15

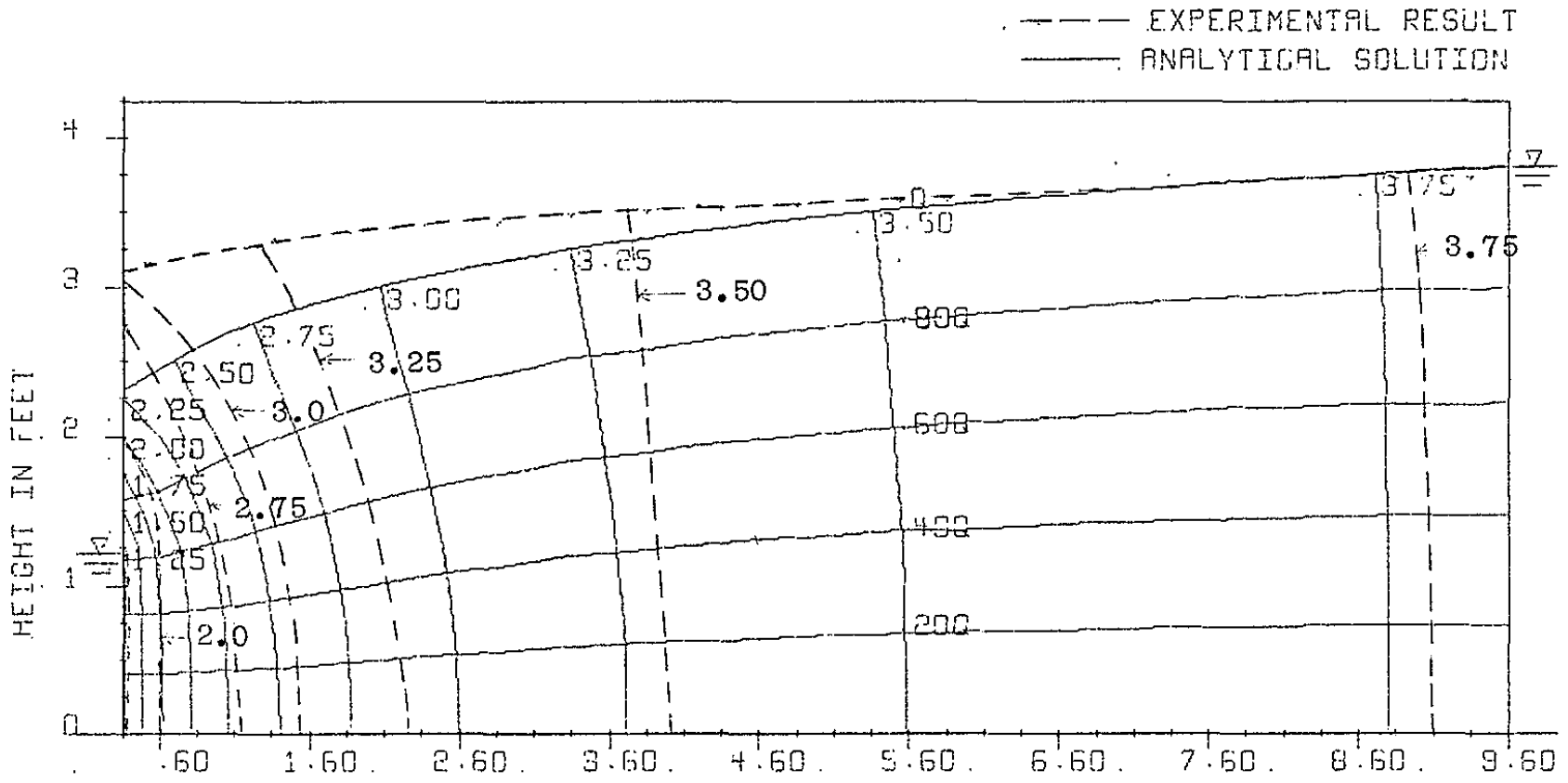

EXPERIMENT WITH SECTOR
. FLOW NO 7
RESULTS FOR DARCY FLOW

. RW= .354 RE= 9.604
. HW= 1.213 HE= 3.796
Q(CALC) = 1.564 Q(EXP) = 1.030 CUSEC

FIG. A-III-16

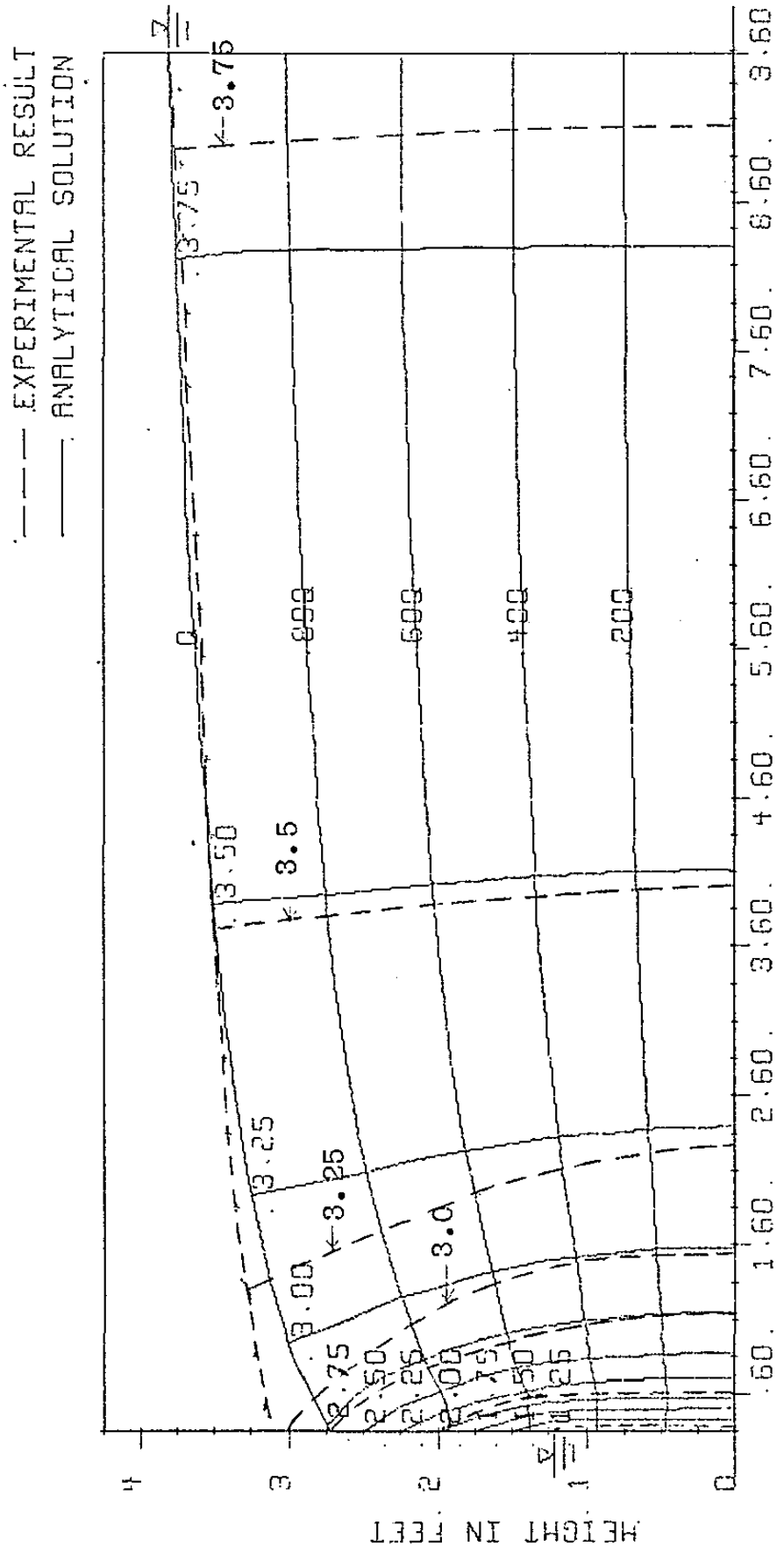

EXPERIMENT WITH SECTOR . RW= .354 RE= 9.604
. FLOW NO 7 . HW= 1.213 HE= 3.736
RESULTS FOR FORCHHEIMER FLOW Q(CALC) = 1.078 Q(EXP) = 1.030 CUSEC

FIG. A-III-17

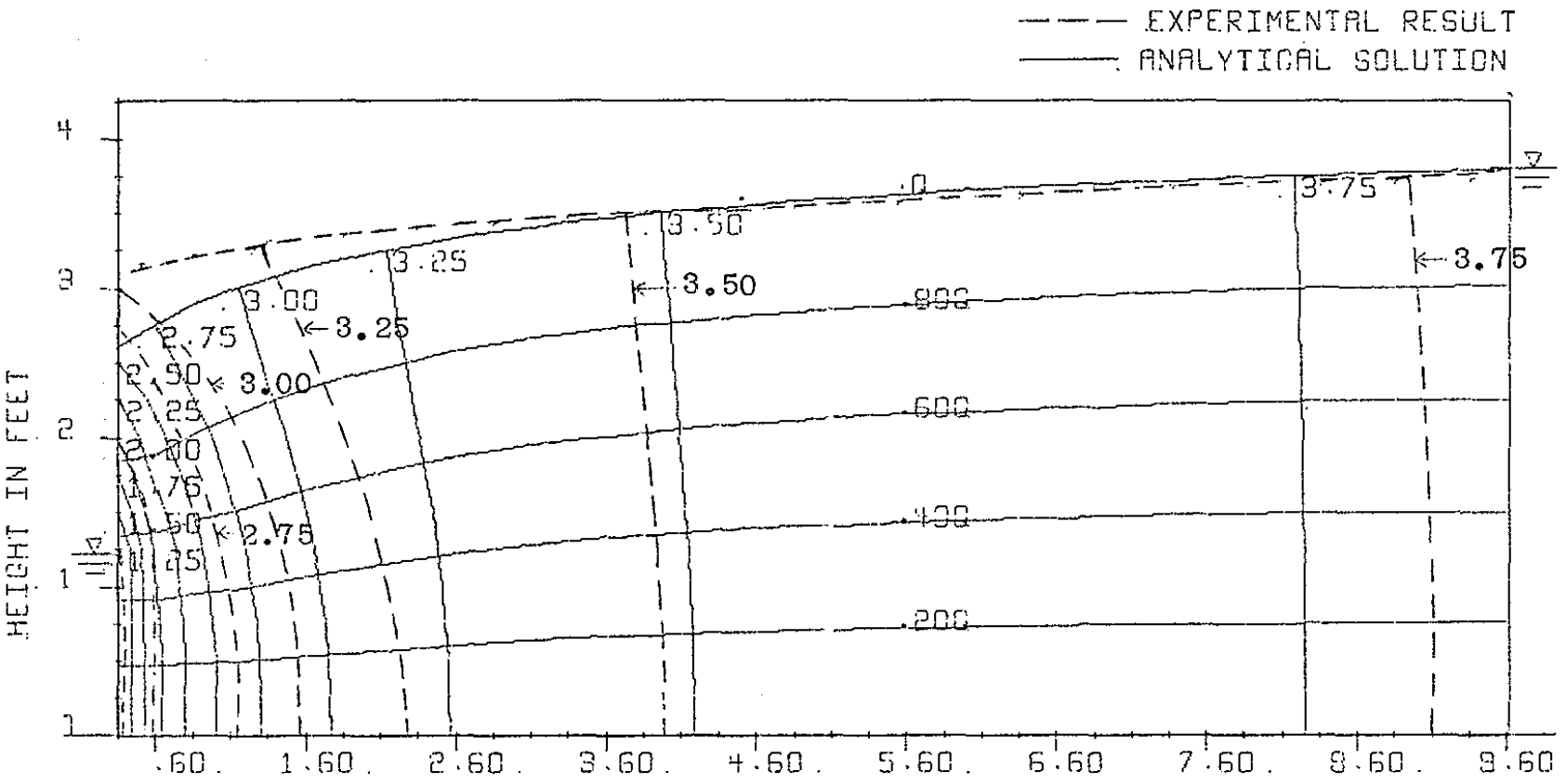

EXPERIMENT WITH SECTOR . RW= .354 RE= 9.604
. FLOW NO 7 . HW= 1.213 HE= 3.796
RESULTS FOR EXPONENTIAL FLOW Q(CALC) = 1.104 Q(EXP) = 1.030 CUSEC

FIG. A-III-18

APPENDIX IV

Flow Net Results for Unconfined Two-Dimensional Flow Through a Permeable Wall.

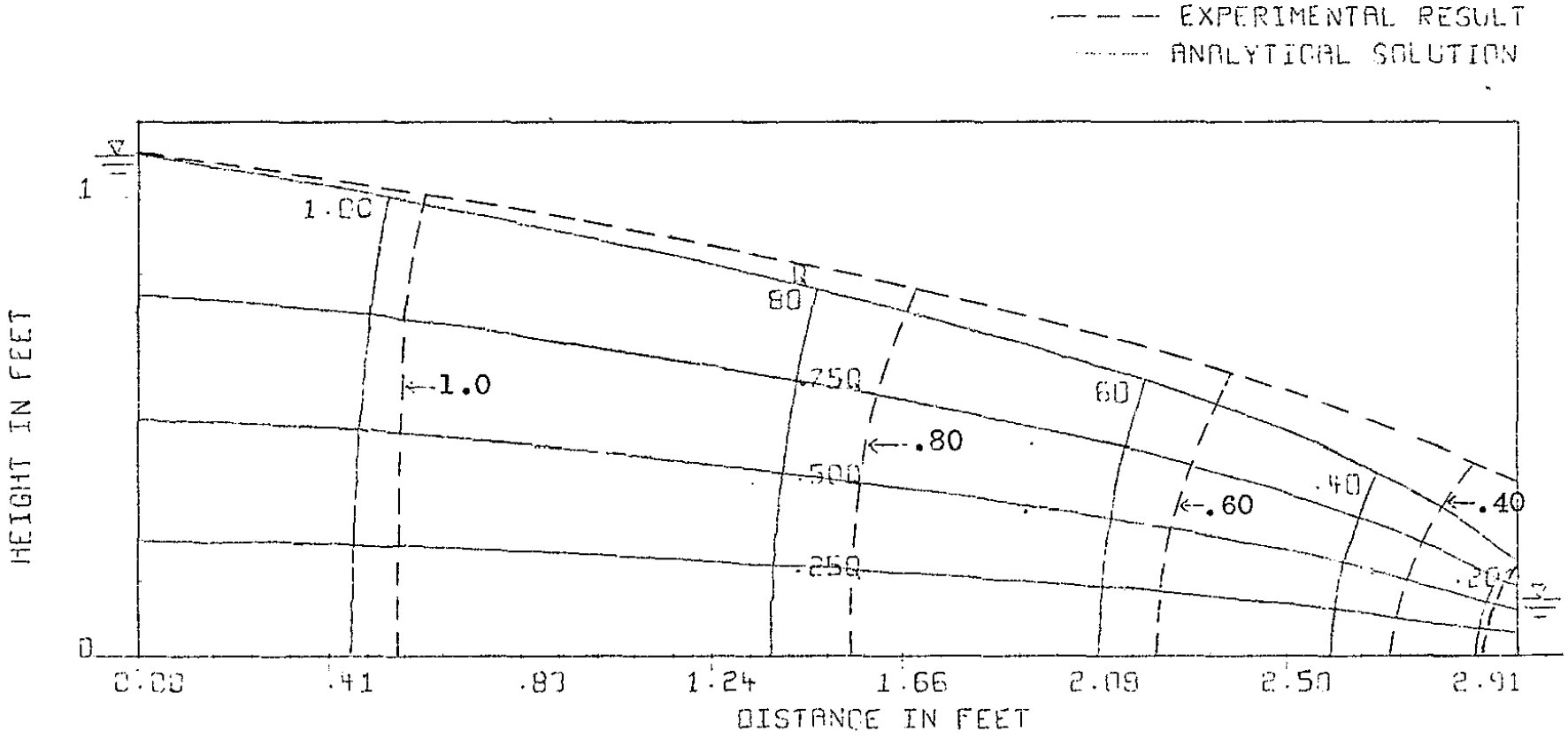

PERMEABLE WALL PROBLEM
FLOW NO 2
RESULTS FOR DARCY FLOW

LENGTH OF WALL= 3.000
HD= .125 HU= 1.092
Q(CALC)= .034 Q(EXP)= .027 CUSEC

FIG. A-IV-1

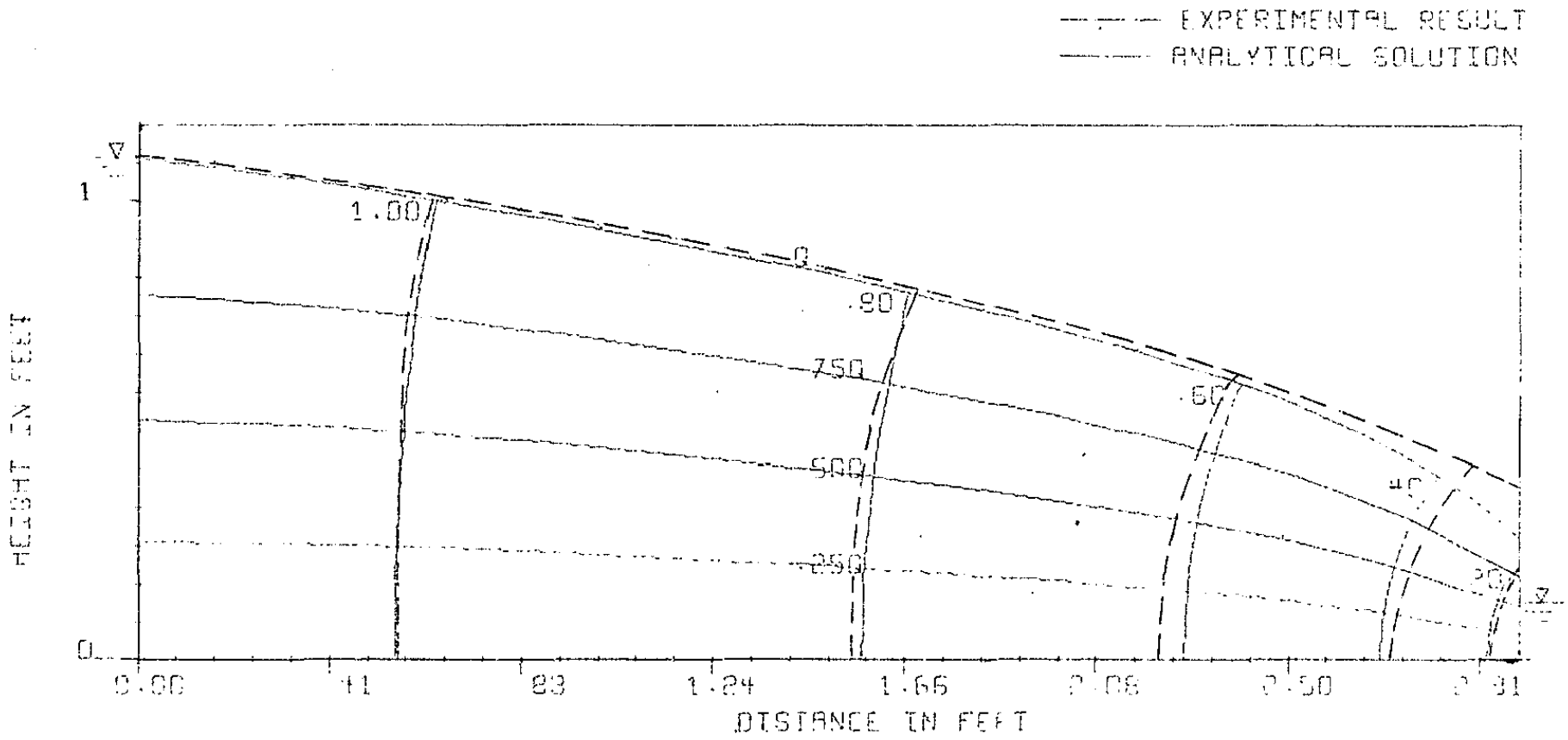
EXPERIMENTAL RESULT
ANALYTICAL SOLUTION
HEIGHT IN FEET
1
0
1.00
.90
.75
.60
.50
.25
0.00
.41
.83
1.24
1.66
2.08
2.50
2.91
DISTANCE IN FEET
PERMEABLE WALL PROBLEM
FLOW NO 2
RESULTS FOR FORCHHEIMER FLOW
LENGTH OF WALL= 3.000
HO= .125' HU= 1.092
Q(CALC)= .026 Q(EXP)= .027 CUSEC

FIG. A-IV-2

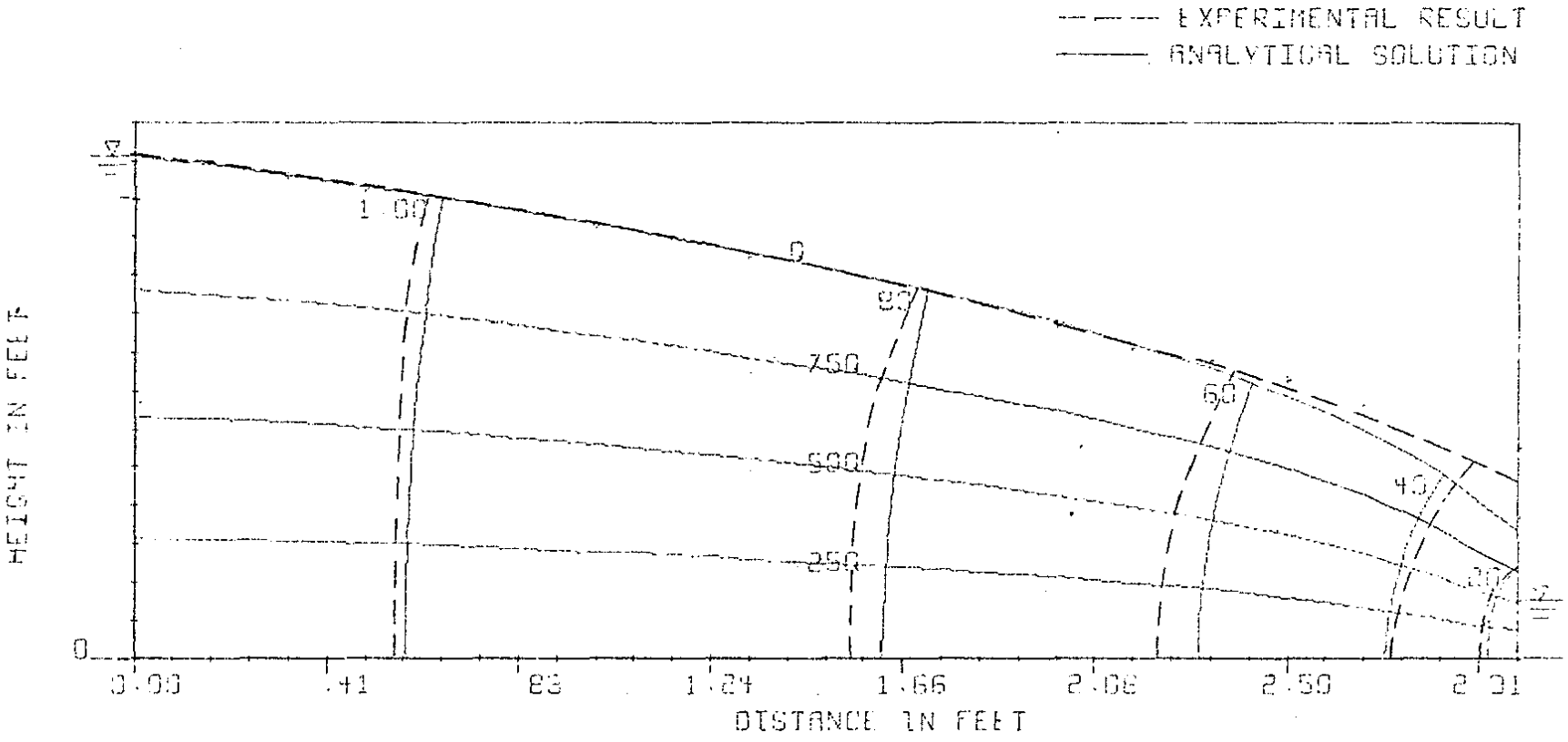

PERMEABLE WALL PROBLEM — LENGTH OF WALL= 3.000
FLOW NO 2 — HD= .125' HU= 1.032
RESULTS FOR EXPONENTIAL FLOW — Q(CALC)= .024 Q(EXP)= .027 CUSEC

FIG. A-IV-3